

Experimental Modeling of Heat Transfer in Taylor Flow in Mini-Scale Tubing

BY

© KHALIFA B. ALRBEE

A Thesis submitted to the School of Graduate Studies in partial fulfillment of the
requirements for the degree of
Doctor of Philosophy

Department of Mechanical Engineering
Faculty of Engineering and Applied Science

Memorial University of Newfoundland

March 2020

St. John's, NL

Canada

Abstract

Heat transfer enhancement in mini / micro scale channels is desired in most compacted devices. Typically, these devices experience a high heat generation. In this regard several approaches were invented to increase heat dissipation rates. Taylor flow provides a promising technique to enhance heat transfer within mini / micro scale channels.

Taylor flow parameters and channel geometries are experimentally and theoretically studied to improve the thermal performance of mini / micro channels. The present dissertation aims to investigate heat transfer enhancement using the Taylor flows of gas-liquid and liquid-liquid flows in straight and curved tubes. The influence of the liquid slug length on heat transfer is examined when the isothermal boundary condition is applied to the heat transfer surface. This study also examines the effect of nanoparticle inclusion in the continuous and Taylor flows as new achievement in this regard. This dissertation will address heat transfer enhancement in the mini scale tubes over eight chapters as follows.

The first chapter provides a brief introduction and shows the originality, novelty, and importance of using the Taylor flows in the heat transfer enhancement. The second chapter summarizes a survey on the past attempts to investigate heat transfer of Taylor flows. The third and fourth chapters are devoted to study heat transfer in Taylor flows of gas-liquid and liquid-liquid in mini scale straight tubes. These experiments examine the effect of the liquid slug length on the thermal behavior of the Taylor / slug flows. In the fifth and sixth chapters, the thermal behavior of Taylor flows inside curved / coiled geometry are experimentally studied, and new empirical models were developed using the experimental data. The experiments considered the effects of three parameters, tube curvatures, liquid slug ratios, and Prandtl numbers. The seventh chapter addresses the heat transfer enhancement of nanofluids and compares with the conventional liquids. The study demonstrated the effect of nanoparticle concentration on heat transfer in continuous and Taylor flows.

The last chapter provides a summary and conclusion of the present study. Recommendations for the future studies are also stated to highlight the important aspects for further investigation.

Acknowledgements

K. Alrbee, would like to express his deepest gratitude to all people and institutions who helped and supported this study. First, my supervisors, Dr. Yuri S. Muzychka, and Dr. X. Duan for their continuous support and guidance.

Institutions to be highly appreciated, Libyan Ministry of High educations, Natural Sciences and Engineering Research Council (NSERC) of Canada, and all Memorial University faculty and staff. Also, I would like to thank University of Elmerghib for the follow up and encouragement. Last but not the least, my family, parents, wife, and children and all my friends for the continuous support.

Table of Contents

Abstract	ii
Acknowledgments	iv
Table of Contents	ix
List of Tables	xi
List of Figures	xvi
Nomenclature	xvii
 1.INTRODUCTION	 1
1.1 Overview	1
1.2 Heat Transfer in Taylor Flow	2
1.3 Heat Transfer in Curved Tube	4
1.4 Performance and Preparation of nanofluid	5
1.5 Scanning electron microscope (SEM)	7
1.6 Conductivity of Nanofluid	7
1.8 Research Methodology	8
1.9 Lab facilities and Experimental Setup	9
1.10 Uncertainty and Error Analysis	12
1.11 Benchmark Test of The Assembled Setup.....	13
1.11.1 Heat Transfer Benchmark Tests.....	13
1.12 Pressure Drop Benchmark Test	17
<u>1.13</u> References.....	19
 2. A REVIEW ON HEAT TRANSFER ENHANCEMENT IN MINI / MICRO CHANNELS..	 22
2.1 Introduction.....	22
2.2 Continuous Flow in Mini / Micro Scale Tubes.....	23
2.3 Segmented / Taylor Flow.....	24
2.3.1 Gas Liquid Taylor Flow	25

2.3.2 Liquid- Liquid Taylor Flow	28
2.4 Nanofluid	32
2.4.1 Thermal Conductivity of Nanofluids	33
2.4.2 PERFORMANCE OF NANOFLUIDS	34
2.5 Research Objectives	34
2.6 References	38
3. LAMINAR HEAT TRANSFER OF GAS-LIQUID SEGMENTED FLOWS IN CIRCULAR DUCTS WITH CONSTANT WALL TEMPERATURE	43
3.1 Introduction	43
3.3 Theory of Data Analysis	48
3.4 Experimental Setup	50
3.5 Results and Discussion	53
3.6 References	59
4. HEAT TRANSFER OF GAS-LIQUID TAYLOR FLOW IN COILED TUBE WITH CONSTANT WALL TEMPERATURE	64
4.1 Introduction	64
4.2 Theory of Data Analysis	68
4.3 Experimental Setup and Procedure	70
4.6 Result and Discussion	73
Modeling of Experimental Data	80
4.8 Conclusion	86
4.9 References	87
5. AN APPROXIMATE METHOD OF ANALYSIS FOR LAMINAR HEAT TRANSFER IN LIQUID-LIQUID TAYLOR FLOWS IN MINI SCALE TUBING	91
5.1 Introduction	91
5.2 Separated Phase Modeling of Taylor Flow	95
5.3 Experimental Setup and Procedure	97
5.4 Results and Discussion	100
5.6 Conclusion	108

5.7 References	109
6. HEAT TRANSFER IN LIQUID-LIQUID TAYLOR FLOW IN MINI SCALE COILED TUBES	113
6.1 Introduction	113
6.2 Taylor flow Modeling	117
6.3 Methodology of Experimental Study	121
6.4 Result and Discussion	123
6.5 Modeling of Experimental Data	129
6.6 Conclusion	136
6.7 References	137
7. HEAT TRANSFER ENHANCEMENT IN LAMINAR GRAETZ AND TAYLOR FLOWS USING NANOFLUIDS	140
7.1 Introduction	140
7.2 Literature Review	141
7.3 Fundamental of Graetz Theory	143
7.4 Experimental Setup	145
7.5 Nanofluid Preparation and Modeling	148
7.6 Result and Discussion	151
7.7 Summery and Conclusion	158
7.8 References	159
8. CONCLUSIONS AND RECOMMENDATIONS	164
8.1 Summary and Conclusions	163
8.2 Recommendation for Future studies	164
8.2.1 Particle Motion in Taylor Flow	164
8.2.2 Micro Scale Geometries	165
8.2.3 Fluid Engineering	165
8.2.4 Film Thickness	165
8.3 References	166

LIST OF TABLES

Table 2. 2	summery of liquid-liquid Taylor flow studies in mini scale channels.....	32
Table 2. 3	Common theoretical models of thermal conductivity of solid-liquid mixture	34
Table 2. 4	Preparation and thermal performance of Nano fluids in mini- micro channels.....	35
Table 3. 1	Summery of Published Experimental Data Compared with Present Data.....	52
Table 4. 1	summery of gas-liquid experiments in coiled tube	73
Table 4. 2	summery of single phase experiments	75
Table 4. 3	contains gas-liquid flow limits of present study	78
Table 5. 1	Thermophysical Properties of Used Liquids	98
Table 6. 1	contains thermophysical properties of used liquids	121
Table 7. 1	Heat transfer enhancement in different flow regimes with/without nanoparticles	156

List of Figures

Figure 1. 1	instantaneous velocity vectors in liquid-liquid slugs for straight and curved tubes [26]	3
Figure 1. 2	Taylor / Slug flow in mini / micro channels with different fractions.....	3
Figure 1. 3	effect of Dean number on velocity profiles (right) vertical plane, (lift) horizontal plan [24].....	4
Figure 1. 4	fluid motion and radial mixing in curved tube [24]	4
Figure 1. 5	secondary flow field at low and high Dean numbers, [25].....	5
Figure 1. 6	the lab facilities (a-b &c) required for nanofluid preparation using two step method .	5
Figure 1. 7	transmission electron microscopy (TEM) images of 1 μ m scale for dried up nanofluids CNT, Cu and Graphene.....	6
Figure 1. 8	scanning Electronic Microscopy (SEM) used for measuring nanoparticle size and sample composition analysis.....	7
Figure 1. 9	KD2 thermal conductivity analyzer available for thermal conductivity measurements	8
Figure 1. 10	demonstration of present study in mini scale tubes.....	9
Figure 1. 11	microfluidic lab facilities used for collecting experimental data	9

Figure 1. 12 diagram of conducted benchmark tests of heat transfer and pressure drop.....	10
Figure 1. 13 heat transfer and pressure drop measurements at inlet and outlet of the test section	11
Figure 1. 14 high speed Phantom Camera Images.....	12
Figure 1. 15 effect of channel length variation on dimensionless heat transfer in mini scale tube	15
Figure 1. 16 benchmarking results of pressure drop for mini scale straight tube with 10 % maximum error bar.	15
Figure 1. 17 effect of bath temperature variation on dimensionless heat transfer in mini scale tube 200 mm long	16
Figure 1. 18 effect of channel diameter variation on dimensionless heat transfer in mini scale tube 150 mm long	16
Figure 1. 19 pressure drop benchmark tests using pure liquids of single phase flows with less than 10 % error	18
Figure 1. 20 effect of bath temperature variation on friction factor in mini scale tube 200 mm long	18
Figure 2. 1 compacted heat sink incorporated into integrated circuit IC, for 1 cm ² using water coolant [1].	23
Figure 2. 2 effect of tube curvature on heat transfer of single phase in mini scale channel [3] ...	24
Figure 2. 3 experimental setup of heat transfer in mini scale curved tubes [3]	23
Figure 2. 4 experimental setup of segmented Taylor flow [10].....	25
Figure 2. 5 effect of liquid slugs of gas-liquid flow on local Nusselt number plotted versus Graetz number [10].....	26
Figure 2. 6 microencapsulated phase change material (MPCM) suspension [15].....	27
Figure 2. 7 experimental setup [15]	27
Figure 2. 8 effect of slug lengths of liquid-liquid Taylor flow on local Nusselt number [18]	30
Figure 2. 9 experimental setup of liquid-liquid Taylor flow [18].....	29
Figure 2. 10 assembled experimental setup of liquid-liquid Taylor flow [19]	31
Figure 2. 11 local temperature distribution between two slugs (water flow rate: 100 μ l/min, oil flow rate: 30 μ l/min) [19].	31

Figure 2. 12 thermal conductivity values of materials [26]	33
Figure 2. 13 schematic of the experimental setup [35]	36
Figure 3. 1 gas-liquid flow cell in a mini-scale tube.....	50
Figure 3. 2 experimental setup for gas-liquid Taylor flow in straight tube subjected to isothermal condition	51
Figure 3. 3 high speed camera images for gas-liquid Taylor flow of void fraction $\alpha = 0.5$	52
Figure 3. 4 effect of slug length on dimensionless heat flux in a 50 mm tube length and varying Reynolds numbers.....	53
Figure 3. 5 effect of slug lengths on dimensionless heat flux in a 100 mm tube length and varying Reynolds numbers.....	54
Figure 3. 6 dimensionless heat flux data compared with published data [3,4] for varying Reynolds numbers.....	54
Figure 3. 7 Nusselt number data of gas-liquid flow of various slug lengths plotted versus Reynolds number.	55
Figure 3. 8 effect of slug lengths on Nusselt number data for a 50 mm tube length and constant Reynolds number.	55
Figure 3. 9 effect of slug length on Nusselt number data for a 100 mm tube length and constant Reynolds number for each set.....	56
Figure 3. 10 effect of slug length on dimensionless heat flux in a 100 mm tube length and constant Reynolds number.	57
Figure 3. 11 effect of slug length on dimensionless heat flux in a 50 mm tube length and constant Reynolds number.	57
Figure 3. 12 effect of slug length on dimensionless heat flux data in a 50 mm tube length and constant Reynolds number.....	58
Figure 3. 13 experimental data compared with published data from [3,4] for constant Reynolds numbers.....	58
Figure 3. 14 Dimensionless mean wall heat flux data for various dimensionless slug lengths for a tube length of 50 mm compared with the model of Muzychka [1].	59
Figure 3. 15 dimensionless mean wall heat flux data for various dimensionless slug lengths for a tube length of 100 mm compared with the model of Muzychka [1].	59

Figure 4. 1 Shows flow segmentation of gas-liquid using 1 cSt oil and air bubbles. $\alpha L = 0.5$ mm, and constant Reynolds number $Re_D = 104$ with liquid flow rate $Q = 8$ ml/min for tube radius 2cm.	69
Figure 4. 2 Experimental set up of gas-liquid Taylor flow in mini scale curved tube.....	69
Figure 4. 3 Test sections of same length (250 mm) and three curvatures ($R = 10, 20$ and 40 mm)	69
Figure 4. 4 Test sections of same length (250 mm) and three curvatures ($R = 10, 20$ and 40 mm)	71
Figure 4. 5 experimental set up of gas-liquid Taylor flow in mini scale curved tube	71
Figure 4. 6 single phase data of 1 cSt oil compared with straight tube Graetz Poiseuille flow model to show the secondary flow effect.	75
Figure 4. 7 Single phase data of 1 cSt oil compared with a model of Nusselt number for coiled tube developed by Ghobadi and Muzychka [2]	75
Figure 4. 8 effect of tube curvatures on Nusselt number data of single phase using 1 cSt silicone oil, $L = 250$ mm, $260 < Re_D < 2400$	75
Figure 4. 9 dimensionless heat transfer data of single phase flow with varied tube curvatures and fixed Prandtl number $Pr = 16.2$	76
Figure 4. 10 effect of liquid slug ratio γ and Prandtl number on Nusselt number data of gas-liquid flow with, $R = 40$ mm.	79
Figure 4. 11 gas-liquid flow modeling based on liquid slug ratio γ for liquid fraction $\alpha = 0.5$ and $Pr = 16.2$	81
Figure 4. 10 Nusselt number Nu_D data of different curvatures 10, 20 and 40 mm and fixed slug ratio $\gamma = 0.008$, $Pr = 16.2$	82
Figure 4. 12 Nusselt number Nu_D data created with different curvatures 10, 20 and 40 mm and fixed slug ratio $\gamma = 0.032$, $Pr = 9.9$	83
Figure 4. 13 Nusselt number $Nu_{C,D}$ data created with different curvatures 10, 20 and 40 mm and fixed slug ratio $\gamma = 0.060$, $Pr = 9.9$	84
Figure 4. 14 the proposed correlation when compared with Nusselt number Nu_D data created with different Prandtl numbers and fixed slug ratio $\gamma = 0.032$	84

Figure 4. 15 predictable behaviour of gas-liquid Taylor flow using 0.65 cSt silicone oil with varied flow segmentation γ and over range of Dean number $De \cong (20 \text{ to } 70)$	85
Figure 4. 16 predictable behaviour of gas-liquid Taylor flow using 1 cSt silicone oil with varied flow segmentation γ and over range of Dean number $De \cong (10 \text{ to } 40)$	85
Figure 5. 1 liquid-liquid Taylor flow cell with a liquid fraction $\alpha_n = 0.5$	98
Figure 5. 2 experimental setup was assembled to measure heat transfer of slug flow in mini scale tubes under constant wall temperature.....	99
Figure 5. 4 experimental data of homogeneous analysis using 5 cSt silicone oils were segmented by water at $\alpha_A = 0.25$ and 0.5	101
Figure 5. 5 experimental data of homogeneous analysis using silicone oils segmented by water at same oil fraction $\alpha_A = 0.25$	102
Figure 5. 6 Experimental data of water component plotted using superficial duct length and flow velocity at five values of Reynolds number with varying slug length.....	103
Figure 5. 7 Experimental data for 1 cSt silicone oil component plotted using superficial duct length and flow velocity at five values of Reynolds number with varying slug length.....	105
Figure 5. 8 experimental data using actual wetted duct area of (for 1 cSt oil) component when applying separated phase modeling	106
Figure 5. 9 experimental data using actual wetted duct area of water component when applying separated phase modeling.	105
Figure 5. 10 dimensionless heat flux data for the both components of segmented flow as compared with model predictions for three values of (LS/L)	106
Figure 5. 11 effect of liquid slug length ratio (Ls/L) on q^* for three silicone oil components in Taylor flow for $\alpha = 0.25$. RMSPE=6.8%	106
Figure 5. 12 Effect of liquid slug length ratio (Ls/L) on q^* for three silicone oil components in Taylor flow for $\alpha = 0.75$. RMSPE=11.4%	107
Figure 5. 13 Effect of liquid slug length ratio (Ls/L) on heat transfer for three silicone oil components in Taylor flow for $\alpha = 0.5$. RMSPE=7.3%	106
Figure 5. 14 dimensionless heat flux data for all oil combinations as compared with model predictions for three values of (LS/L)	107

Figure 6. 1 liquid-liquid Taylor flow cell configuration.....	118
Figure 6. 2 intensity of secondary flow of high and low Dean number (Dravid and., Smith, [8])	119
Figure 6. 3 liquid-liquid Taylor flow segmentations of fraction $\alpha_n = 0.5$	122
Figure 6. 4 heat transfer experimental setup of liquid-liquid Taylor flow in curved/ coiled tube and under constant wall temperature.	123
Figure 6. 5 Benchmarking results of heat transfer in single phase flow using distilled water. ..	123
Figure 6. 6 effect of slug ratio γ on dimensionless heat transfer data of silicone oils plotted as function of Reynolds number Re_D	125
Figure 6. 7 effect of slug ratio γ on dimensionless heat transfer data q^* plotted as function of Reynolds number Re_D	125
Figure 6. 8 effect of flow slug ratio γ on dimensionless heat transfer q^* plotted as function of dimensionless tube length L^*	125
Figure 6. 9 effect of slug ratio γ on Nusselt number Nu_D of Taylor flow plotted versus dimensionless tube length L^* ($R = 10$ mm).....	127
Figure 6. 10 effect of Prandtl number Pr change on Nusselt number data Nu_D of Taylor flow as a function of dimensionless tube length L^* ($D = 10$ mm).....	126
Figure 6. 11 effect of tube curvature radius R on Nusselt number Nu_D , of liquid-liquid Taylor flow versus dimensionless tube length L^*	128
Figure 6. 12 effect of slug ratio γ on dimensionless heat transfer of Taylor flow as function of Dean number De for ($R = 10$ mm).	129
Figure 6. 13 effect of slug ratio γ on Nusselt number data Nu_D of Taylor flow as function of Dean number De ($R = 10$ mm).....	128
Figure 6. 14 effect of liquid slug ratio γ (L_s / L) on proposed model of Nusselt number Nu_D	131
Figure 6. 15 heat transfer of liquid-liquid flow with varied curvatures plotted versus De and compared with proposed model.	131
Figure 6. 16 Taylor flow data (1 cSt oil + water) of varied slug ratio LS / L compared with homogenous model [6].	132
Figure 6. 17 heat transfer of liquid-liquid flow with varied Prandtl number plotted against De and compared with proposed model.	132

Figure 6. 18 Nusselt Number of Taylor flow with varied Prandtl number Pr compared with the proposed model.....	134
Figure 6. 19 Nusselt Number of Taylor flow of various Prandtl number Pr compared with the proposed model.....	134
Figure 6. 20 Nusselt Number of Taylor flow with various γ compared with proposed model.	135
Figure 6. 21 Nusselt number of liquid-liquid Taylor flow of various γ compared with the proposed model.....	135
Figure 6. 22 Nusselt Number of liquid-liquid Taylor flow of various γ compared with the proposed model.....	136
Figure 7. 1 Schematic of experimental setup of segmented flow	146
Figure 7. 2 Laminar friction factor benchmark test for a straight tube using different fluids with maximum error of 5 -7 percent	147
Figure 7. 3 benchmarking results of heat transfer using distilled water in 150 mm tube length	148
Figure 7. 4 segmented flow of gas-liquid in mini scale tube with $\alpha L = 0.5$	148
Figure 7. 5 shows three samples of Al_2O_3 with different concentrations, second row shows stability of samples after a week.....	149
Figure 7. 6 SEM image shows the microstructure of Al_2O_3 Nano powders with micro scale ..	149
Figure 7. 7 shows composition and purity analysis of Al_2O_3 Nano powders using (SEM)	150
Figure 7. 8 thermal conductivity measurements compared with published predictive models ..	151
Figure 7. 9 effect of nanofluid concentration on Nusselt number plotted versus inverse Graetz number	153
Figure 7. 10 Figure effect of nanofluid concentration on dimensionless heat flux plotted versus inverse Graetz number.	152
Figure 7. 11 Nusselt number data of water and three nanofluid concentrations plotted versus Reynolds number	153
Figure 7. 12 effect of nanofluid concentration on friction factor versus Reynolds number	154
Figure 7. 13 Performance analysis of Aluminum oxide nanofluid concentrations.....	155
Figure 7. 14 dimensionless heat flux data of gas-liquid flow with liquid fraction 0.5 and 0.75 plotted versus invers Graetz number.....	155
Figure 7. 15 effect of nanofluid concentration on heat transfer of segmented flow	157

Figure 7. 16 Segmented nanofluid data of 1 vol. % concentration plotted versus invers Graetz number.	157
Figure 7. 17 Nusselt number of dispersed gas-liquid Taylor flows with different concentrations plotted versus Reynolds number	158

NOMENCLATURE

A_w	= tube surface area, m^2
Al_2O_3	= aluminum oxide
Ca	= capillary number = $\mu U/\sigma$
CNT	= Carbon nano tube
C_p	= specific heat, J/kg K
D	= diameter of circular tube, m
De	= Dean number, = $Re\sqrt{D/2R}$
TEM	= transmission electron microscopy
Er	= experimental error
f	= Friction factor
k	= thermal conductivity, W/mK
L	= Tube length, m
L_s	= slug length, m
L^*	= dimensionless of tube length = $(L/D)/Pe_D$
L_s^*	= dimensionless length of slug, = $(L_s/D)/Pe_D$
m	= measured data point
MPCM	= microencapsulated phase change materials
\dot{m}	= mass flow rate kg/s
N	= Number of data points
Nu_D	= Nusselt number, = $h D/k$
p	= predicted data point
P	= Pressure value, N/m ²
PEC	= performance evaluation criteria
Pe_D	= Peclet number, = UD/α
Pr	= Prandtl number, = ν/α
Q	= bulk heat transfer, W
\bar{q}	= mean wall heat flux, W/m^2
q^*	= dimensionless wall heat flux, $\bar{q}D/k(T_w - T_i)$

R	= radius of curvature, m
$RMSPE$	= Root mean square percentage error
Re_D	= Reynolds number = UD/ν
T	= temperature, K
U	= Taylor flow velocity, m/s
W_R	= total uncertainty
x_n	= variable
z	= local axial coordinate, m

Greek Symbols

α	= thermal diffusivity, m^2/s
ν	= kinematic viscosity, m^2/s
ρ	= fluid density, kg/m^3
α_n	= fraction of component
β	= slug aspect ratio, = L_s/D
μ	= fluid dynamic viscosity, Ns/m^2
γ	= slug ratio.= L_s/L
\emptyset	= volume concentration ratio
Δ	= difference

Subscript

A, B	= Taylor flow phases
bf	= base fluid
e	= effective
G	= gas
L	= liquid
nf	= nanofluid
nP	= nano particle
s	= slug
w	= wall
$\overline{(\cdot)}$	= mean value

Superscripts

* = dimensionless notation

\bar{x} = average value

CHAPTER 1

1.Introduction

1.1 Overview

Our daily life is surrounded by heat transfer phenomena. Thermal management systems in many applications is important to achieve effective solutions for heat dissipation in compact devices. Increasing the demand of heat dissipation in multiple engineering applications which require efficient thermal management to ensure performance stability with minimum manufacturing costs and complexity. This issue becomes challenging for cooling systems scaled to mini / micro size which suffer high thermal generation rates. Passive and active techniques were developed to improve heat transfer coefficients. Decreasing the size of electronics led to a corresponding interest in mini and micro cooling systems to be attached in a limited space. Typically, air-cooled systems do not meet the requirements in cases of higher heat flux. Thus, liquids appeared to be recommended because their thermal conductivity and heat capacity are greater.

Most of the prevailing trends aim to prevent excessive heat accumulation by adopting passive cooling techniques in electronic devices for greater ease, simplicity, and cost effectiveness. Mini and micro channel heat sinks attached to heat sources show competitive heat removal for compact microelectronics that experience high heat generation. An intensive interest in mini / micro liquid cooling systems is aligned with the increasing demands of microfabrication technology in a wide range of applications. Although, single phase flow in mini / micro scale heat sinks provides a comparative amount of heat removal. Several techniques were employed to enhance removing

additional heat using additives to the conventional flow of liquids or by creating flow regimes of multi components. The channels of small scale geometry aim to further increase heat transfer enhancement. Taylor flows (either gas-liquid or liquid- liquid) show a promising result to increase heat transfer rates in mini / micro channels . Fairbrother and Stubbs [1] and Taylor [2] studied two phase flow in the gas-liquid slug flow regime. Later, Maddox and Mudawar, [3] investigated the single and two-phase forced convection of a simulated microelectronic heat source to assess the feasibility of cooling. Similarly, Betz and Attinger, [4] performed experiments on compact micro cooling systems with both single and two phase flows and highlighted that segmented flow significantly enhances heat transfer by up to 140 % in a microchannel heat sink when compared with single-phase flow at the same liquid flow rate. The inclusion of nanoparticles in conventional liquids as an advanced technology showed the ability to improve the thermal properties of liquids and enhance heat transfer rates. Additional significant studies were conducted on Taylor / segmented flows to investigate the potential of heat transfer enhancement [6-10].

Numerous studies have investigated characteristics and challenges of nanofluids. Manaya and Sahin [11] experimentally investigated the upper limitations of particle volume fraction on the heat transfer and pressure drop of TiO_2 water nanofluids in microchannel. The study covered a considerable range of concentrations (0.25 %, 0.5%, 1.0%, 1.5%, and 2.0%) under laminar flow conditions with Reynolds numbers between (100-750). These results highlighted heat transfer enhancement with no significant increase in pressure drop when compared with pure water. Several studies on nanofluid performance and applications can be found in the published literature [12-16]. Additional studies on nanofluid stability and preparation are also available [17-20].

1.2 Heat Transfer in Taylor Flow

Taylor flows appear as a series of immiscible substances with a uniform spacing. Taylor flow can be produced in mini / micro scale channels in different ways: gas-liquid, solid-liquid, or liquid-liquid flows. The experimental observations showed the potential of heat transfer enhancement using Taylor flows. The heat transfer enhancement of segmented flows is a result of the increased radial transport within liquid slugs. Horvath [5] and Verntas [7] reported that flow segmentation significantly increased the heat transfer. Later studies examined and developed experimental and theoretical models to predict thermal behaviour of the Taylor flows [21-23].

The present study demonstrated the unique attempts of experimental modeling of heat transfer enhancement based flow segmentation as shown in Fig.1.1. Mini scale straight and curved tubes were employed for laminar gas-liquid and liquid-liquid Taylor flows.

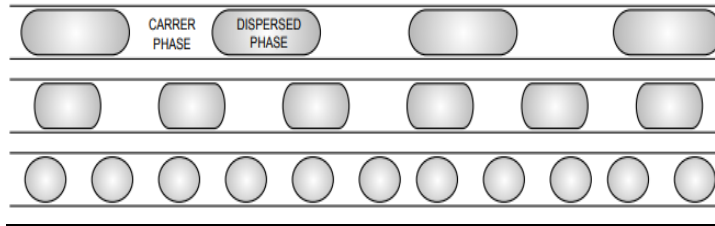


Figure 1.1 Taylor / Slug flow in mini / micro channels with different fractions

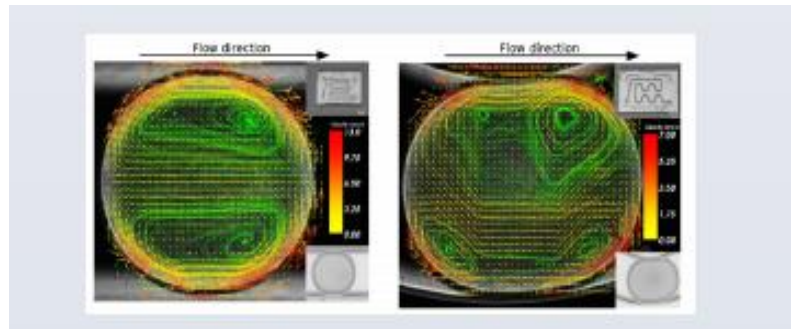


Figure 1.2 instantaneous velocity vectors in liquid-liquid slugs for straight and curved tubes [26]

The viability of heat transfer enhancement in Taylor flow has been explained because of internal circulations within liquid phases of flow resulting in increase of heat transfer [6,22,23]. Fig.1.2 shows the velocity distribution of liquid which is circulating continuously in a radial direction while moving down stream, causing heat to be transferred extensively from the heated wall to the centerline of flow in small scale channels.

1.3 Heat Transfer in Curved Tubes

When fluid flows through a straight tube, velocity distribution up to the wall reaches the maximum at the centre point of the tube cross section and zero at the tube wall with a symmetric gradient around the center line of flow. Unlike when a fluid flows through a curved tube, the presence of secondary flow influences the radial transport of heat and mass Fig. 1.3 shows fluid motion because of the secondary flow.

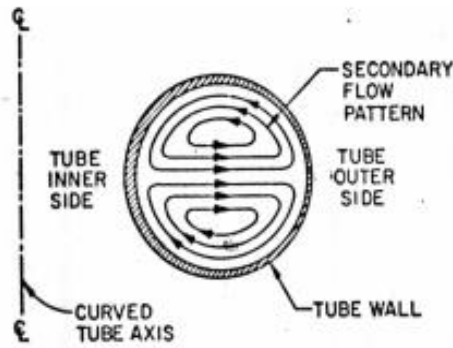


Figure 1.1 fluid motion and radial mixing in curved tube [24]

The secondary flow arises in curved tubes because of the centrifugal force which acts in radial direction and vertical to the flow direction. The maximum velocity at the centreline is affected by centrifugal action, causing the fluid to move towards the outer wall. On the other hand, the fluid at the outer wall will move inwards and thus decreases the radial mixing. Fig1.3 shows secondary flow influences on single phase flow in curved tubes.

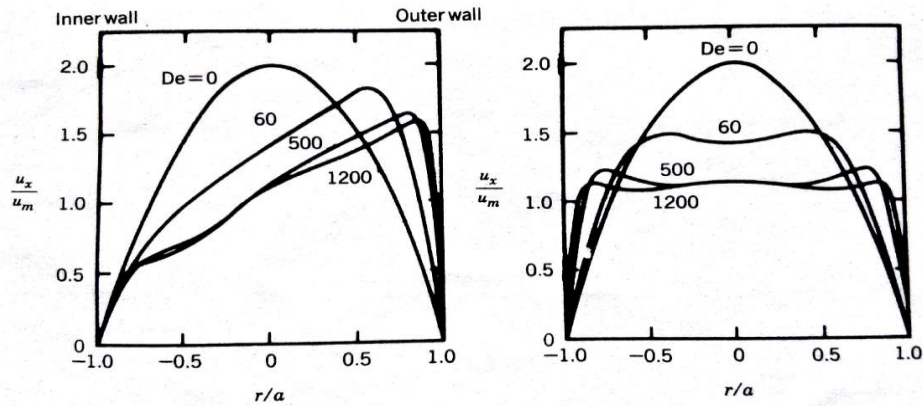


Figure 1.2 effect of Dean number on velocity profiles (right) vertical plane, (left) horizontal plan [24]

The secondary flow in curved tubes enhances heat and mass transfer rates [33]. Published studies using single phase flows verify that heat transfer in a curved tube are dependent upon several parameters: Reynolds number, Prandtl number, and tube diameter-to-curve radius ratio. The present study is experimentally investigating the impact of these parameters on heat transfer in small scale curved tubes using continuous and segmented Taylor flows. Fig. 1.5 shows the influence Dean number on the radial transport within single phase flow in curved tubes.

Both secondary flow and internal circulations within liquid slugs make radial mixing more pronounced in curved tubes. The thermal enhancement is well established in segmented / Taylor flows when introduced to straight and coiled mini scale tubes [8,13,26-31]. Fig. 1.2 demonstrates the velocity fields of straight and curved tubes. Thus, the heat transfer enhancement within liquid slugs will be increased further.

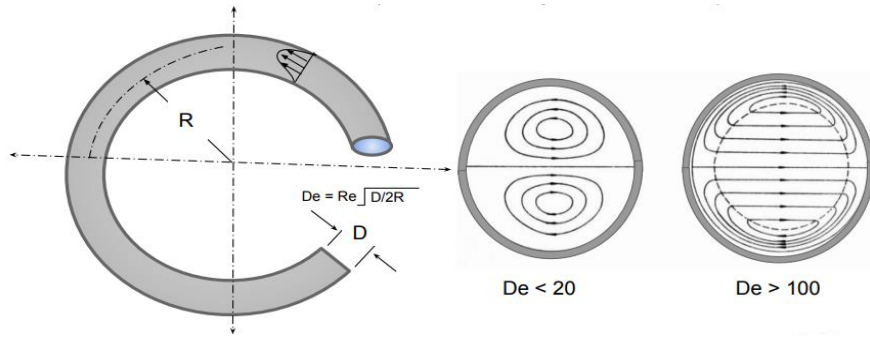


Figure 1.3 secondary flow field at low and high Dean numbers, [25]

1.4 Performance and Preparation of Nanofluid

Nanofluids are advanced classes of solid-liquid mixtures containing suspended additives of nanometer-sized particles (<100 nm). These additives are a higher thermal conductivity material which are called nanoparticles. These fluids are engineered colloidal suspensions of metallic or non-metallic nanoparticles in base fluids. Sukarno [17], Meibo [34] mentioned that commonly used nanoparticles are metals (Cu, Au), oxide metals (Al_2O_3 , TiO_2 , CuO , Fe_3O_4), and non-metallic element (carbon). Typically, the base fluids could be: water, glycol, oils, etc.

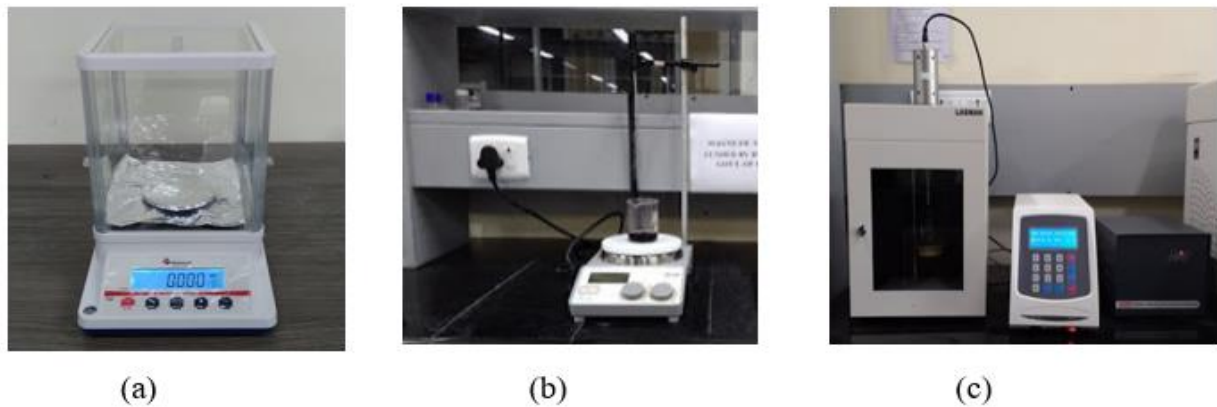


Figure 1.4 lab facilities (a-b &c) required for nanofluid preparation using the two step method

The thermal conductivity of nanoparticles make them potentially useful in many heat transfer applications such as mini-micro channels and heat exchangers.

The preparation of nanofluids requires applying forces within a base fluid while dispersing nanoparticles. This procedure is important to ensure a long term uniform suspension and to prevent nanoparticle aggregation.

The two step method is the most economic and the easiest method to produce nanofluids in large scale. Fig. 1.6 shows the lab facilities required for nanoparticle dispersion. Typically, the two step method starts with specifying the nanofluid concentration and then use the balance to weight the nano powder samples as in Fig. 1.6.a. The dispersion process includes applying mechanical stirring Fig.1.6.b followed by ultrasonication Fig.1.6.c. Stability of the nanofluids is related to several parameters: sonication time, nanoparticle physical properties, and base fluid type [17],[19-20]. Several types of surfactants are used to produce stabilized nanofluids such as: sodium dodecyl benzene sulfonate (SDBS), Sodium Dodecyl Sulfate (SDS), sodium lauryl sulfate (SLS) and emulsifier [34]. In contrast, Meibo, et al [35] reported that adding surfactants to nanofluid to achieve acceptable stability should be as little as possible to avoid affecting thermal conductivity of nanofluid.

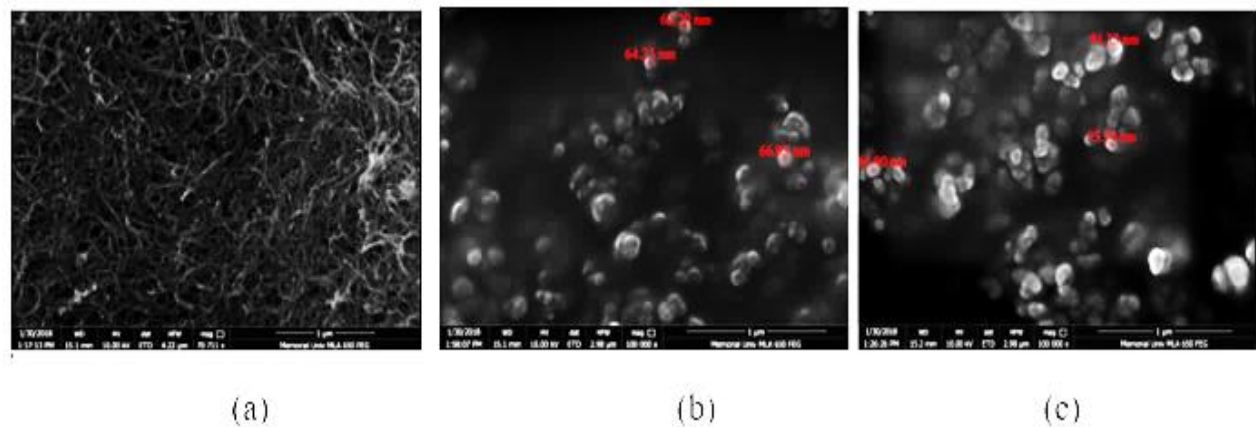


Figure 1.7 transmission electron microscopy (TEM) images of 1 μ m scale for dried up nanofluids CNT, Cu and Graphene

Fig. 1.7 shows TEM images of nanofluids prepared in the present study using the two step method. The sonicator generates sound energy to agitate the particles in the nanofluid on specified amplitude and duration. Typically, the sonication procedure is configured based on the nanoparticle size and concentration. The sonication path is usually used before running the experiments to refresh the nanoparticle distribution.

1.5 Scanning Electron Microscope (SEM)

The scanning electron microscope (SEM) is a type of electron microscope that produces images of the sample surface by scanning it with a high-energy beam of electrons in a raster scan pattern. The electrons interact with the atoms that make up the sample producing signals which contain information about the sample's surface topography, composition, and other properties. Fig 1.8 shows the components of the Scanning Electronic Microscopy.



Figure 1.8 scanning Electronic Microscopy (SEM) used for measuring nanoparticle size and sample composition analysis

The nanoparticles distribution within the base fluid was checked using Scanning Electronic Microscopy. Fig. 1.8 shows a scanning Electronic Microscopy (SEM) Lab which is used to measure nanoparticle size and sample composition. Four types of nanofluids of 0.5 vol %: aluminum oxide Al_2O_3 , Carbon nanotubes CNT, copper oxide CuO , and Graphene were dispersed in distilled water. The samples have been dried up in order to obtain clear images and avoid reflection of the electrons beam, Fig 1.7 shows three images of 1 μm magnification scale were taken to measure size and distribution of the nanoparticles.

1.6 Conductivity of Nanofluid

The main objectives of nanoparticles inclusion into the conventional cooling liquids is to improve the thermal performance and prevent heat accumulation within the compacted devices. Fluids with higher values of thermal conductivity will provide higher heat transfer rates in radial direction. Increasing the thermal conductivity of a liquid is attainable when the right procedure

and substances are properly configured. The transient hot wire is the most popular technique to measure the thermal conductivity of nanofluids with more accuracy and reliability. Fig. 1.9 shows the thermal conductivity analyzer. The analyzer uses the principle of transient temperature rise of high resistive probe initially in thermal equilibrium with measured fluid sample. Similar procedures of the nanofluid preparation were reported in the literature [17-19]. In addition,



Figure 1.9 KD2 thermal conductivity analyzer available for thermal conductivity measurements

multiple studies were devoted to developing experimental and theoretical models to predict the thermal conductivity of mixtures [16,19].

The novel thermal performance of nanofluids allowed for the development of several engineering applications of small scales to become more compacted and thermally efficient [17]. Reducing size and improving functionality of the microelectronics requires high heat flux removal. Optimal performance can be attained when feeding mini and micro channels which offer minimum hydraulic diameter and maximum surface area per unit flow volume [12].

1.7 Research Methodology

This dissertation is interested in investigating laminar heat transfer enhancement in mini scale channels. Taylor / segmented flows are created to show the potential of heat transfer enhancement. Many aspects were investigated using straight tubes, for instance in straight tubes: liquid slug length, Prandtl number and the nanofluid concentration. For coiled / curved geometry, another parameter is considered to achieve additional heat transfer enhancement due to secondary flow. The dissertation also aims to develop new correlations to predict Nusselt numbers using gas –

liquid and liquid – liquid Taylor flows in curved / coiled tubes. An experimental setup was assembled and tested using a single phase flow. Table 1.1 lists the conducted experiments in the present study. In the next section we will address how the quantitative analysis was preformed to estimate the uncertainty and the errors within the collected data.

Table 1.1 conducted experiments in the present study

Flow regime	Working fluid	Straight tube	Coiled tube	Parameters				
				L	L _S	R	Pr	Re _D
Continuous flow	Conventional	✓	✓	✓		✓	✓	✓
	Nanofluid	✓			✓		✓	✓
Taylor flow	Gas - liquid	✓	✓	✓	✓	✓	✓	✓
	Liquid - liquid	✓	✓	✓	✓	✓	✓	✓
	Gas - nanofluid	✓	✓		✓		✓	✓

1.8 Lab Facilities and Experimental Setup

The lab facilities required to study heat transfer or pressure drop in the Taylor flows at mini / micro scale size are available as demonstrated in Fig. 1.10. The assembled setup includes accurate pumping system, heat source to provide an isothermal boundary condition, and a data acquisition system. For flow regime monitoring, the setup is equipped with a high speed camera (Phantom Camera) to capture Taylor flow patterns for the slug length measurements. system.



Figure 1.10 microfluidic lab facilities used for collecting experimental data

For flow regime monitoring, the setup is equipped with a high speed camera (Phantom Camera) to capture Taylor flow patterns for the slug length measurements.

An experimental setup has been assembled in the microfluidic lab at Memorial University of Newfoundland (MUN). Fig. 1.11 demonstrates the schematics of the experimental setup of heat transfer and pressure drop.

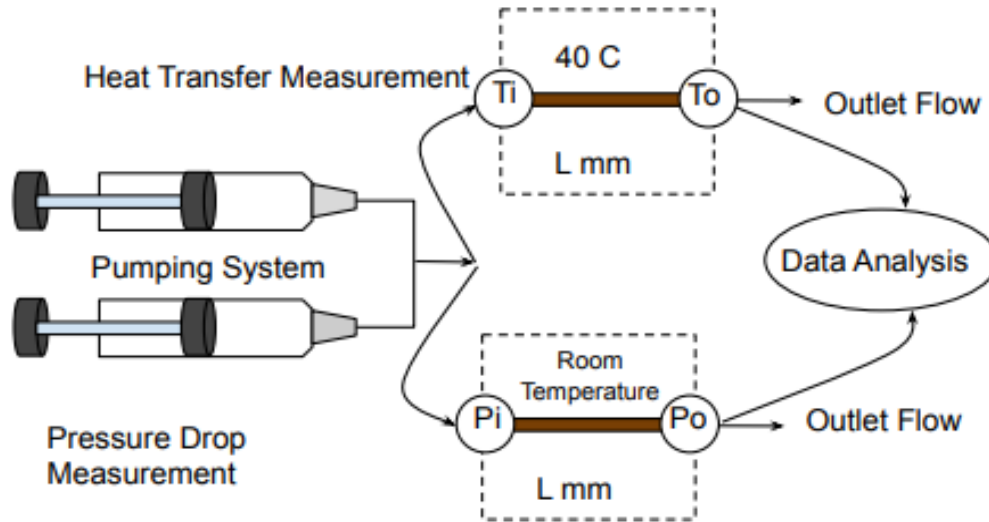


Figure 1.11 diagram of conducted benchmark tests of heat transfer and pressure drop.

The pumping system is equipped with two syringe pumps (Harvard apparatus) with a total capacity of 200 ml each. Harvard pumps are engineered to provide flow accuracy within 0.25 % thus, the maximum volumetric flow rate is proportional to hydrodynamic resistance of the assembled system.

As mentioned earlier the study aims to perform heat transfer experiments to assess the enhancement in mini scale tubes. The experiments are conducted under isothermal boundary conditions. A 3013 Isotemp thermal bath which is PID controlled, as shown in Fig. 1.10 which is designed to provide a temperature stability of $\pm 1\%$ °C over the range of -30 to 200 °C. The flow from four syringes merged and flow into the copper tube test section. The isothermal boundary condition is applied to tube wall. The test section is made of a thermally conductive material to ensure steady state is achieved within a few minutes before running the experiments. The copper tubes were cut with smooth edges so that the flow was not disturbed while entering the tubing.

Fig.1.11 demonstrates schematic of the heat transfer experiment setup. Two Omega T-type thermocouples are used to measure the inlet and outlet bulk temperatures of flow as in Fig.1.12-a. Simple T-junctions with thermocouples imbedded in the flow stream are installed.

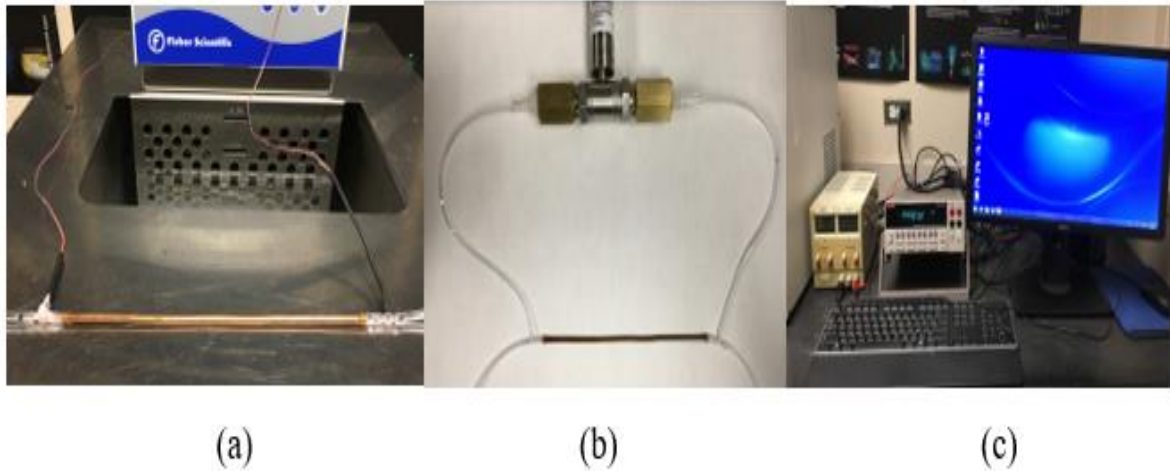


Figure 1.12 heat transfer and pressure drop measurements at inlet and outlet of the test section

Pressure drop was measured for the same tube geometries as shown in Fig. 1.11 to assess the drag force of the laminar flow in smooth pipe. Differential pressure sensors were connected into the inlet and outlet of the test section as demonstrated in Fig. 1.12-b. The pressure sensor was picked to be suitable for the pressure drop range of laminar flow in mini scale tubes from 0 to 1 psi. For pressure drop and heat transfer measurements a Keithley Data Acquisition system was employed as shown in Fig. 1.12-c. The measurements were collected during the experiments and saved to Excel sheets.

Flow patterns of Taylor flow were captured using a high speed camera (Phantom v611), with high professional functionality as demonstrated in Fig. 1-13. Micro Nikon lens was attached to the camera to be able to work at mini-sized scale. Slug length of Taylor flows was precisely measured using Image processing software (ImageJ) instead of using the manual measurements.

1.9 Uncertainty and Error Analysis

Uncertainties of measuring equipment were specified by the manufacturers. Table 1.2 includes values of uncertainties of the measuring equipment, such as temperature, mass flow rate, pressure, etc.



Figure 1.13 high speed Phantom Camera Images

Table 1.1 uncertainty of measuring equipment

Flow Property	Uncertainty
Temperature, T (°C)	± 0.1 °C
Flow rate, Q (L/min)	± 0.25 %
Differential Pressure, ΔP (psi)	± 1 %
Dimension Tolerance, L, D (mm)	± 0.02 mm

The well-known method of Kline and McClintock [32] was employed as a quantitative analysis to estimate potential errors. The total uncertainty represents the contribution of all uncertainties of the used equipment in the experimental setup.

$$W_R = \sqrt{\left(\frac{\partial R}{\partial x_1} w_1\right)^2 + \left(\frac{\partial R}{\partial x_2} w_2\right)^2 + \left(\frac{\partial R}{\partial x_n} w_n\right)^2} \quad (1-1)$$

where w_n is the uncertainty of each single equipment as shown in Table 1.2, R represents the dimensionless groups: Nu_D , q^* and L^* and x_n represents the variables (temperature a pressure, etc).

Root mean squared percentage error (RMSPE) has been employed to measure how well the experimental data agree with theory. The commonly used formula [33] has the form:

$$RMSPE = \sqrt{\left(\sum_1^N \left(\frac{P-M}{P}\right)^2\right) / N} \times 100 \quad (1-2)$$

Where, P and M variables represent the predicted and measured experimental values, and N is the number of data points.

1.10 Benchmark Tests of the Assembled Setup

This section will present the benchmarking results for both, heat transfer and pressure drop using the single phase flows. The experiments were conducted in a mini scale straight tubes are subjected to the isothermal boundary condition. Obtaining good experimental results using single phase flows will give an indication to the reliability of the Taylor flows experiments which will be conducted using the same experimental setup.

1.10.1 Heat Transfer Benchmark Tests

Heat transfer benchmarking tests were performed using the single phase flows in straight tubes. The tests examined the effect of the tube geometries using various tube lengths and diameters. The effect of operating conditions was tested by changing the wall temperature as further investigations which aims to ensure the reliability of collected data. The heat transfer results of single phase are non dimensionlized using mean Nusselt number and dimensionless heat flux as:

$$\overline{Nu}_D = \frac{\overline{q}D}{\bar{k}\Delta T_{LMTD}} \quad (1.3)$$

where

$$\Delta T = \frac{(T_w - T_i) - (T_w - T_o)}{\ln\left(\frac{(T_w - T_i)}{(T_w - T_o)}\right)} \quad (1.4)$$

where T_i and T_o are the measured inlet and outlet temperatures, respectively, and T_w is the constant wall temperature. The dimensionless mean wall heat flux is defined as:

$$q^* = \frac{\overline{q}D}{\bar{k}(T_w - T_i)} \quad (1.5)$$

In both cases, each parameter is a function of $L^* = (L/D) / PeD$.

The Nusselt number data were compared with Greatz Poiseuille theories as:

$$\overline{Nu}_D = \left(\left(\frac{1.614}{L^{*1/3}} \right)^5 + (3.65)^5 \right)^{1/5} \quad (1.6)$$

$$q_{Pois}^* = \left(\left(\frac{1.614}{L^{*1/3}} \right)^{-3/2} + \left(\frac{1}{4L^*} \right)^{-3/2} \right)^{-2/3} \quad (1.7)$$

Fig. 1.15 shows the benchmark test results of the dimensionless heat flux q^* and the Nusselt number Nu_D were plotted as functions of the dimensionless thermal length L^* . These results reveal a good agreement with Poiseuille flow model and were obtained over a wide range of Reynolds number ($100 < Re_D < 1200$) with less than 10 % error compared with theory.

Fig. 1.16 shows the effect of tube length on the heat transfer in mini-scale tubes using three tube lengths: 100, 200, and 300 mm. The experiments were conducted over the same range of flow rates using distilled water. Specifically, the test section was a copper tube of inner diameter 1.65 mm maintained isothermally at 40 °C in the thermal bath. The experimental results show the effect of entrance length on heat transfer. Thus, the flow in the short tube was predominantly characterized as entrance region while long tubes still controlled by a fully developed flow region.

8.

Fig. 1.17 shows experimental results were obtained using two copper tubes with two different inner diameters 1.63 mm and 4.5 mm. The tube length was fixed with length of 200 mm, subjected to the isothermal boundary condition of 40°C. The nondimensionalized experimental results over the same range of Reynolds number Re_D did not show any noticeable change in heat transfer rates.

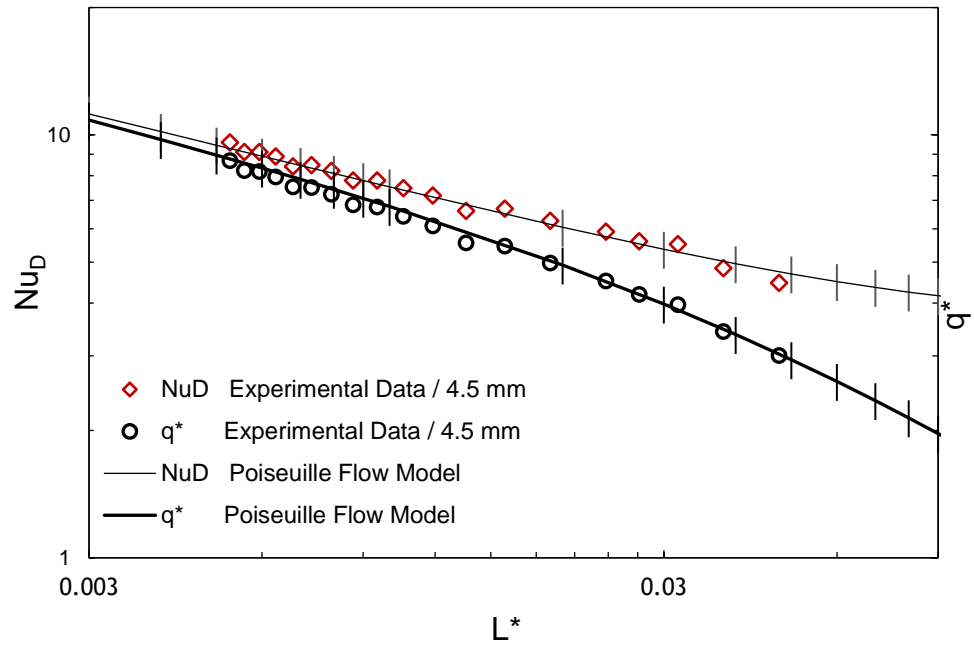


Figure 1.15 benchmarking results of Nusselt number for mini scale straight tube with 10 % maximum error bar.

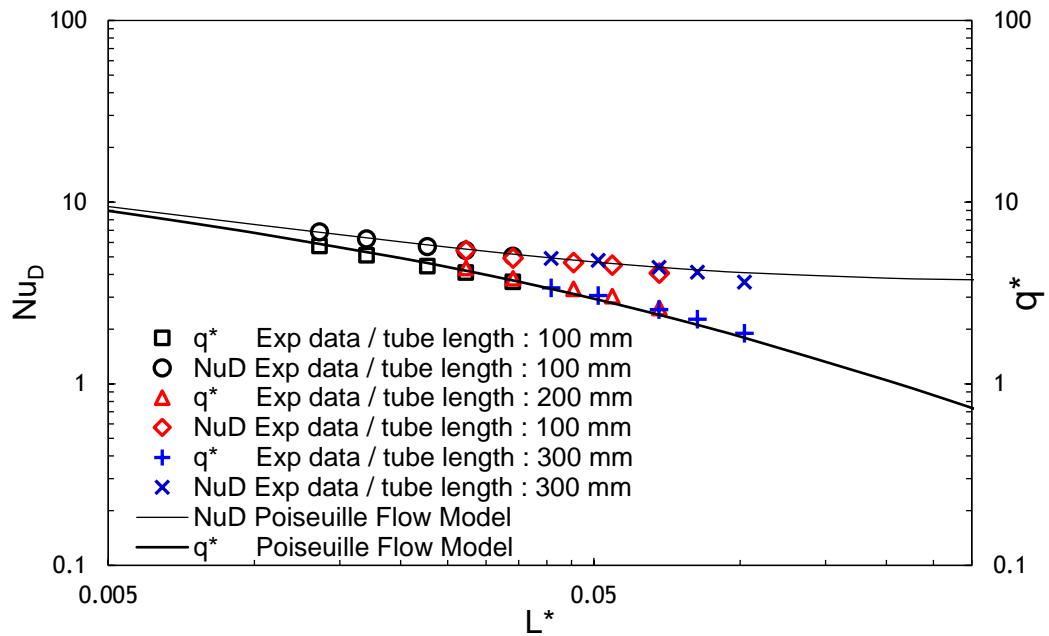


Figure 1.16 effect of channel length variation on dimensionless heat transfer in mini scale tube.

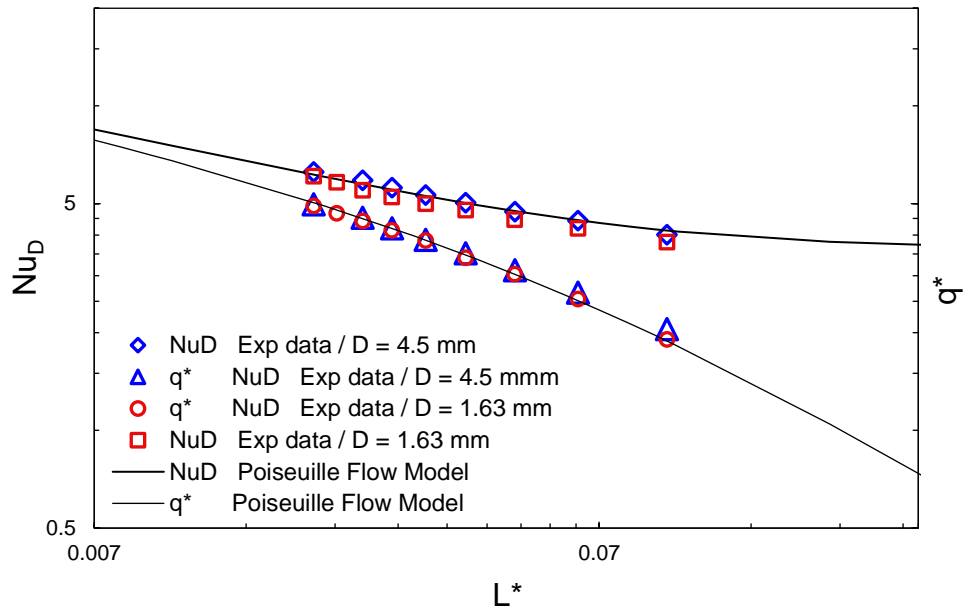


Figure 1.17 effect of channel diameter variation on dimensionless heat transfer in mini scale tube 150 mm long.

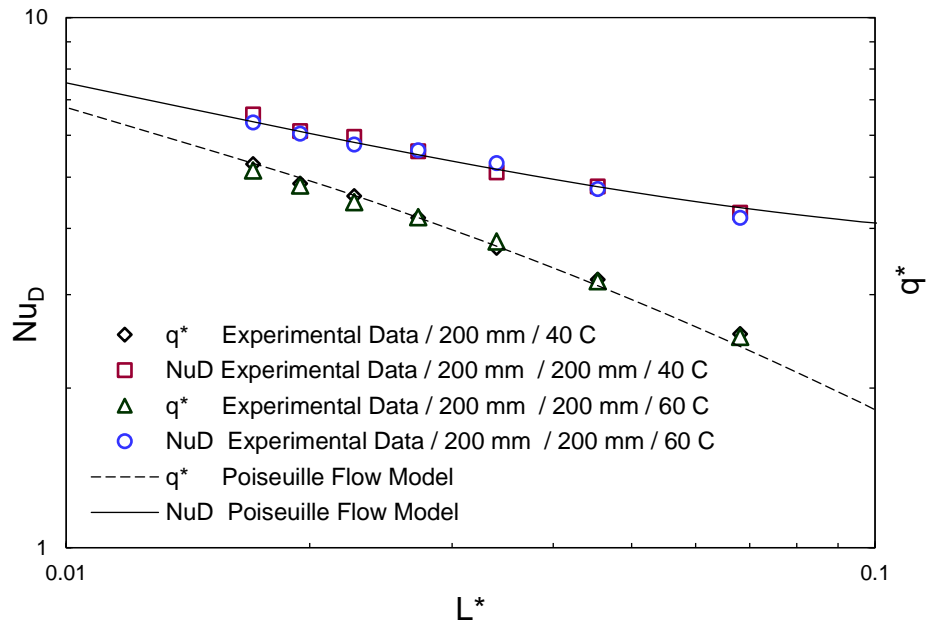


Figure 1.18 effect of bath temperature variation on dimensionless heat transfer in mini scale tube 200 mm long.

Finally, effect of wall temperature on heat transfer rates was examined. Fig. 1.18 show results were collected to investigate effect of the isothermal boundary conditions T_s on the heat transfer rates. The experiments were performed at different wall temperatures of 40 °C and 60 °C. The results show effect of the boundary conditions on the heat transfer rates.

1.11 Pressure Drop Benchmark Test

Pressure drop benchmarking tests using pure single phase flow were performed to validate the collected experimental data. The experimental tests were prescribed under laminar flow conditions in smooth pipe using three liquids, water, and silicone oils (3 and 5 cSt). The friction factor is measured as a function of the mean fluid velocity, fluid properties and tube geometries as:

$$\Delta p = f \frac{\rho \bar{u}^2 LP}{2A} \quad (1.8)$$

Where P is perimeter of the cross section. As shown in Fig. 1.19 the results for the three liquids agreed well with the theoretical Fanning friction model which is defined as:

$$f = \frac{16}{Re_D} \quad (1.9)$$

The agreement within laminar flow range shows a negligible effect is expected on the experimental data due to surface roughness. The Reynolds numbers in our experiments were between 50 to 250 in a tube of length 200 mm and diameter 1.63 mm, which indicates that the hydrodynamic entrance length in used tubes is of the order of 10 mm ensuring hydrodynamic fully developed flow over 90 percent of the tube thus ensuring that thermally developing Graetz flow is the base line for our comparison.

The effect of the inlet temperature was also examined. Fig. 1.20 shows that the results were collected to investigate the effect of thermal conditions on the friction factor in mini scale straight tubes of an inner diameter 1.63 mm and tube length of 200 mm.

Further experimental investigation using the laminar flows were performed by changing the operating conditions. The effect of wall temperature was examined by changing the thermal path temperatures 40 °C and 60 °C. The results revealed that no noticeable effect was observed. The effect of bulk fluid temperature T_m on the friction factor was examined by feeding liquids at different temperatures T_i as presented in Fig. 1.20. These findings agree with the fundamentals of dimensionless analysis.

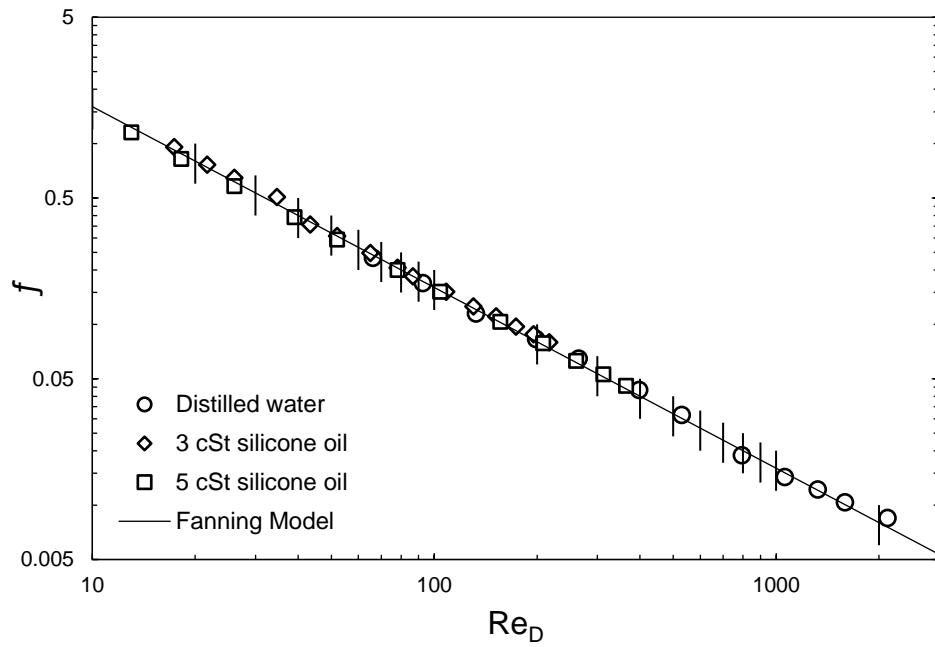


Figure 1.19 pressure drop benchmark tests using pure liquids of single phase flows with less than 10 % error.

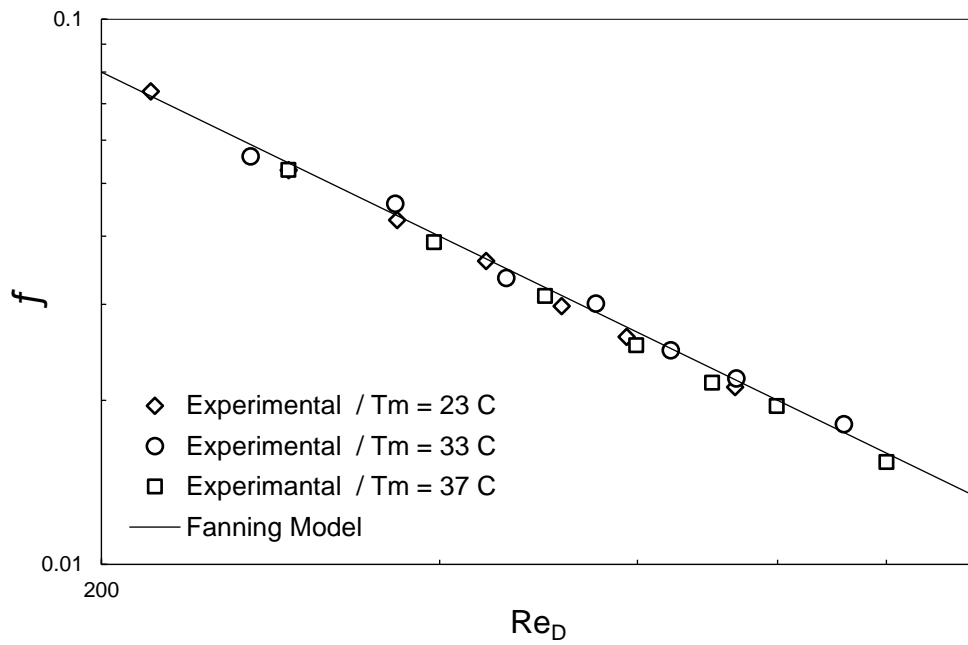


Figure 1.20 effect of bath temperature variation on friction factor in mini scale tube 200 mm long.

1.12 References

- [1] Fairbrother F, Stubbs AE (1935) Studies in electro-endosmosis. Part VI. The “Bubble-Tube” Method of Measurement”, *Journal of Chemical Society* 1:527–529.
- [2] Taylor, “Deposition of a Viscous Fluid on the Wall of a Tube”, *Journal of Fluid Mechanics*. 10(1961) 161–165.
- [3] Maddox D. E., Mudawar I., “Single- and Two-Phase Convective Heat Transfer from Smooth and Enhanced Microelectronic Heat Sources in a Rectangular Channel”, *Journal of Heat Transfer*, ASME NOVEMBER 1989, Vol. 111 p. 1045.
- [4] A. Rachel Betz, D. Attinger, “Can Segmented Flow Enhance Heat Transfer in Microchannel Heat Sinks” *International Journal of Heat and Mass Transfer*, 53 (2010) 3683–3691.
- [5] Horvath C., Solomon, B.A., Engasser, J.M., “Measurement of Radial Transport in Slug Flow Using Enzyme Tubes”, *Industrial and Engineering Chemistry, Fundamentals*, Vol. 12, no. 4, pp. 431-439, 1973.
- [6] Oliver, D.R. and Young Hoon, A., ”Two Phase Non-Newtonian Flow: Part 2 Heat Transfer”, *Transactions of the Institution of Chem. Engineers*, Vol. 46, pp. 116-122, 1968.
- [7] Vrentas, J.S., Duda, J.L, and Lehmkuhl, G.D., “Characteristics of Radial Transport in Solid-Liquid Slug Flow”, *Industrial and Engineering Chemistry, Fundamentals*, Vol. 17, no. 1, pp. 39-45, 1978.
- [8] Adrugi, W., Muzychka, Y.S., and Pope, K., “Heat Transfer in Liquid-Liquid Taylor Flow in Mini-scale Curved Tubing for Constant Wall Temperature,” ASME-IMECE-2015-67700, 2016.
- [9] Muzychka Y. S., Walsh E. Walsh P. “Heat Transfer Enhancement Using Laminar Gas-Liquid Segmented Plug Flows” *Journal of Heat Transfer*, 2011 by ASME, APRIL 2011, Vol. 133 / 041902-1.
- [10] Adrugi, W., Muzychka, Y.S., and Pope, K.,” Heat Transfer Model for Liquid-liquid Taylor flow”, ASME 2018 16th.
- [11] Eyuphan Manaya, Bayram Sahin “Heat Transfer and Pressure Drop of Nanofluids in a Microchannel Heat Sink”, *Heat Transfer Engineering*, 2017, volume, 38. No. 5, 510- 522.

- [12] Hossein S., Mohammad G., “Performance Analysis of Using Nanofluids in Microchannel Heat Sink in different Flow Regimes and its simulation using Artificial Neural Network”, Proceedings of the World Congress on Engineering, 2008, Vol III WCE 2008, July 2 - 4, 2008, London.
- [13] A. Sivakumar, N. Alagumurthi, T. Senthilvelan, “Experimental investigation of forced convective heat transfer performance in nanofluids of Al₂O₃/water and CuO /water in a serpentine shaped micro channel heat sink”, *Heat and Mass Transfer*, (2016) 52:1265-1274, DOI 10.1007/s00231-015-1649-5.
- [14] Anbumeenakshi, Thansekhar, “The Effectiveness of a Nanofluid Cooled Microchannel Heat Sink Under Non uniform Heating Condition”, *Applied Thermal Engineering*, 113 (2017) 1437-1443.
- [15] M. Karimzadehkhoei, S. Yalcin, ” Pressure Drop and Heat Transfer Characteristics of Nanofluids in Horizontal Microtubes Under Thermally Developing Fflow Conditions”, *Experimental Thermal and Fluid Science*, 67(2015) 37-47.
- [16] P. EstellŽ, S. Halelfadl ,”Thermal Conductivity of CNT Water Based Nanofluid: Experimental Trend and Models Overview”, *Journal of Thermal Engineering*, Yildiz Technical University Press, Istanbul, Turkey, Vol. 1, Issue No. 2, pp. 381-390, April 2015.
- [17] D. H. Sukarno “Challenges for Nanofluid Applications in Heat Transfer Technology” IOP Conf. Series: *Journal of Physics: Conf. Series* 795 (2017) 012020.
- [18] A.L.Subramaniyan, A. Kumar, “Preparation and Stability Characterization of Copper Oxide Nanofluid by Two Step Method”, *Material Science Forum*, Vol. 832 (2015) pp 139-143(2015) Trans Tech Publications, Switzerland.
- [19] K. Y. Leong, N. M. Hanafi, “Thermal Effect of Surfactant on Stability and Thermal Conductivity of Carbon Nanotube Based Nanofluids” *Thermal Science*, Year 2016, Vol. 20, No. 2, pp. 429.
- [20] I. M. Mahbulul, Tet Hien Chong,” Effective Ultrasonication Process for Better Colloidal Dispersion of Nanofluid”, *Ultrasonics Sonochemistry* 26 (2015) 361-369.
- [21] Giolla M. M. Eain A., Vanessa E., Punch J., “Local Nusselt Number Enhancements in Liquid–liquid Taylor Flows” *International Journal of Heat and Mass Transfer*, 80 (2015) 85–97.

- [22] Muzychka, Y.S., “Laminar Heat Transfer for Gas-Liquid Segmented Flows in Circular and Non-circular Ducts with Constant Wall Temperature” ASME, 2014.
- [23] J. Howard A. and Walsh P. A., “Heat Transfer Characteristics of Liquid-Gas Taylor Flows incorporating Microencapsulated Phase Change Materials” *Journal of Physics: Conference Series* 525 (2014) 012022.
- [24] Kakac, S., Shah, R. K., Aung, W., “Handbook of Single-Phase Convective Heat Transfer”, *Wiley-Inter-science*, Hoboken, New Jersey, U.S.A., 1987.
- [25] Dravid A. N., Smith K. A., Merrill E. W., Brian P. L. T., Effect of Secondary Fluid Motion on Laminar Flow Heat Transfer in Helically Coiled Tubes, *American Institution of Chemical Engineers*, vol. 17, no. 5, pp. 1114-1122, 1971.
- [26] Malsch, D., Kielpinski, M., Merthan, R., Albert, J., Mayer, G., Köhler, J. M., Süße, H., Stahl, M., and Henkel, T., 2008, “MPIV-Analysis of Taylor Flow in Micro Channels”, *Chemical Engineering. J.*, 135(SUPPL. 1), pp. 166–172.
- [27] W. R. Dean, “Note on the Motion of Fluid in a Curved Pipe”, *London Edinburgh Dublin Philosophy Mag. J. Sci.*, vol. 4, pp. 208–223, 1927.
- [28] W. R. Dean, “The Streamline Flow Through Curved Pipes”, *London Edinburgh Dublin Philosophy Mag. J. Sci.*, vol. 5, pp. 673–695, 1928.
- [29] Ghobadi M., Muzychka Y. S., 2014, “Fully Developed Heat Transfer in Mini Scale Coiled Tubing for Constant Wall Temperature”, *Int. J. of Heat and Mass Transfer*, 72, pp. 87–97.
- [30] Ghobadi M., Muzychka Y. S., “Heat Transfer and Pressure Drop in a Spiral Square Channel”, *Experimental Heat Transfer*, 28:546–563, 2015.
- [31] Ghobadi M., Muzychka Y. S., “Heat Transfer in Spiral Channel Heat Sink”, ASME 2011 9th International Conference on Nanochannels, Microchannels, and Mini channels.
- [32] Kline, S. J., and F. A. McClintock. “Describing Uncertainties in Single-Sample Experiments” *Chemical Engineering*, Vol. 75, No. 1, January 1953: 3-8.
- [33] Eduardo D. Glandt, T. Klein and E Edgar, “Optimization of Chemical Processes”, Second edition, *McGraw-Hill Chemical Engineering Series*, 2001.
- [34] Y. L. Kin, N. M. Hanafi, R. M. SOHAIMI, and N. H. AMER, “The Effect of Surfactant on Stability and Conductivity of Carbon Nanotubes Based Nanofluid”, *Thermal Science*, Year 2016, Vol. 20, No. 2, 429-436.

- [35] Meibo Xing, “Experimental study on the thermal Conductivity Enhancement of Water Based Nanofluids Using Different types of carbon nanotubes” *International Journal of Heat and Mass Transfer*, 88 (2015) 609–616.

CHAPTER 2

A REVIEW ON HEAT TRANSFER ENHANCEMENT IN MINI / MICRO CHANNELS

2.1 Introduction

The reduction in size of electronic devices and increasing the functionality requires further development in mini / micro scale heat sinks. Heat removal within these devices became the priority of the manufacturers and researchers. Typically, mini, and micro channels provide a desired surface area for heat transfer within microelectronics. On the other hand, conventional fluid flows have a limited ability for heat convection. Several options were considered to enhance heat transfer by feeding multi phase flows either gas – liquid or liquid -liquid. Nanofluids were also used as a new approach to provide further enhancement.

The literature of nonboiling flows in mini / micro channels shows considerable attempts to improve heat transfer. For instance, using Taylor flows and the inclusion of high thermal conductive materials demonstrates a promising accomplishment to optimize heat transfer. Heat transfer enhancement within small scale channels can be optimized when using coiled / spiral channels instead of straight flow paths.

Heat transfer in mini / micro channels using Taylor flow is currently receiving more attention. This is because of the increased demand of heat dissipation in compact electronic devices. This chapter is devoted to address the related publications, for experimental and theoretical studies. The

survey is comprised of continuous and Taylor flows in straight and coiled / curved tubes. Inclusion of the nanoparticles into the conventional liquids was also presented in the literature.

2.2 Continuous Flow in Mini / Micro Scale Tubes

The increase of heat transfer and the reduced thermal resistance are advantages of using small scale channels in compact high thermal generation equipment. Tuckerman and Pease [1] experimentally tested a very compacted design of heat sink under constant heat flux boundary conditions of 790 W/cm^2 . The heat sink was attached into the integrated circuit with a total area of 1 cm^2 .

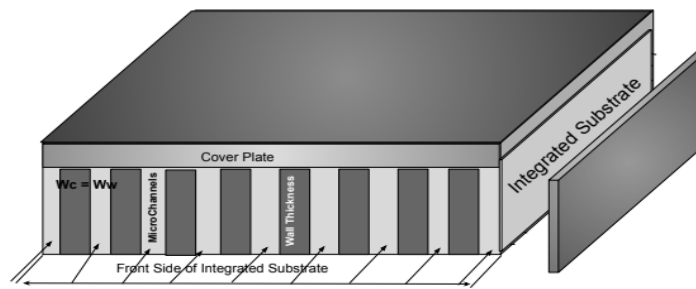


Figure 2.1 compact heat sink incorporated into integrated circuit IC, for 1 cm^2 using water coolant [1].

A new compact, water-cooled integral heat sink for silicon integrated circuits has been designed as shown in Fig. 2.1. By allowing such high power densities, the heat sink may greatly enhance the feasibility of ultrahigh-speed VLSI circuits. The results demonstrated a potential for

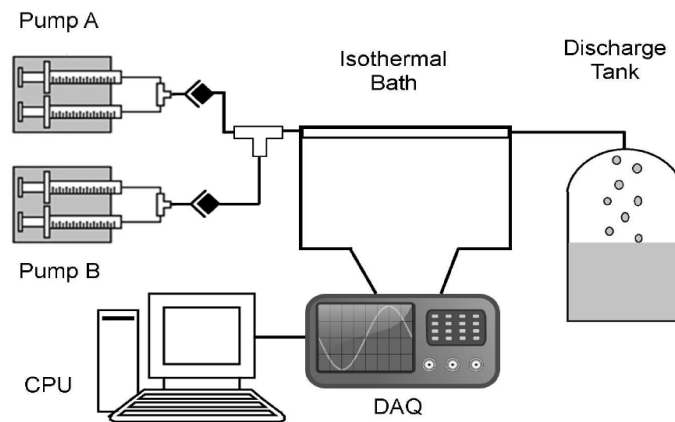


Figure 2.2 experimental setup of heat transfer in mini scale curved tubes [3]

heat transfer enhancement which maintained a measured temperature of the integrated circuit IC around 70 °C. This was close to the operating conditions of the microelectronics. Their results also showed that the increase of heat removal came with penalty of increasing pressure drop.

Ghobadi and Muzychka [3] used single phase flow in mini scale curved tubes to examine the influence of radii of curvature on heat transfer rates. Four tubes of identical lengths were bent to form curved paths of : 1, 2, 4, and 8 cm radii of curvatures. Their experimental results have been compared with the Graetz model. Fig. 2.2 shows the experimental setup subjected to isothermal boundary conditions.

The observations regarding heat transfer rates revealed that heat transfer rates increased by increasing the Dean number De (increasing the curvature, $1/R$). The results showed that short mini-scale curved tubes are capable of a greater heat transfer enhancement. The augmentation is constant for a constant length and Dean number. However, a higher Reynolds number is required when the curvature is smaller to keep a constant Dean number ($De = Re_D \sqrt{D/2R}$).

2.3 Taylor Flow

Taylor flows were considered a significant research area by Fairbrother and Stubbs [5], followed by Taylor [6]. Later, Maddox and Mudawar [7] studied the forced convection of single and two-phase of a simulated microelectronic heat source to assess the potential of enhancing heat

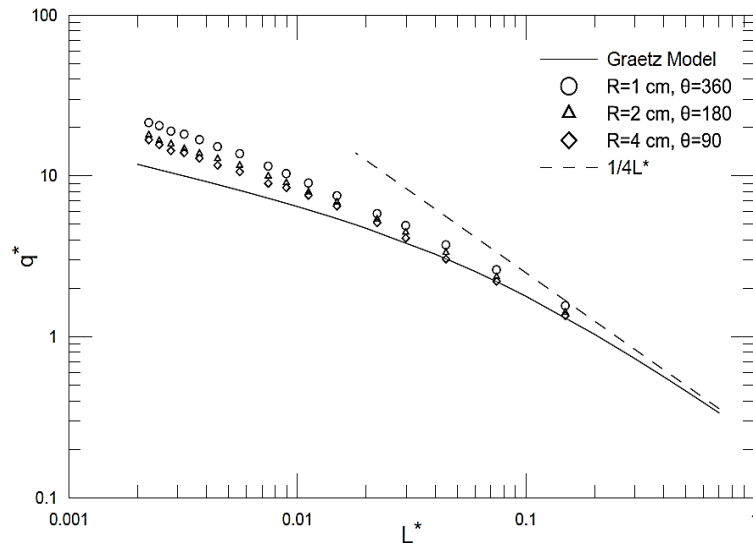


Figure 2.3 effect of tube curvature on heat transfer of single phase in mini scale channel [3]

transfer rates of cooling. Betz and Attinger [8] performed experiments on the compact micro cooling system using single and two phase flows. They found that, the segmented flows have an ability to improve the functionality of compact cooling systems by up to 140 % in a microchannel heat sink when compared with conventional flow for the same Reynolds number. Typically, Taylor flows are created by introducing two immiscible components, gas-liquid or liquid-liquid into a flow channel. Also, solid-liquid phase segmentation is used in some cases to enhance heat transfer [14].

2.3.1 Gas Liquid Taylor Flow

Gas-liquid Taylor flow has been extensively studied both theoretically and experimentally. The flow showed potential of increasing heat transfer rates in small scale applications within compact cooling systems. Haase [9] studied Taylor flow characterizations in mini scale channels using industrial fluids. The gas phase was introduced into the flow stream by injecting the gas through a capillary injector of varied inner diameter. Published experimental data along with his own experimental data were used to develop a new model to predict bubble and slug lengths of both phases.

Walsh et al [10] investigated the potential of heat transfer enhancement in two phase gas-liquid Taylor flows. The case was analyzed in a straight mini scale geometry which is subjected to isothermal boundary conditions. Local Nusselt numbers, obtained using Infrared thermography are analyzed in both entrance and fully developed flow regions.

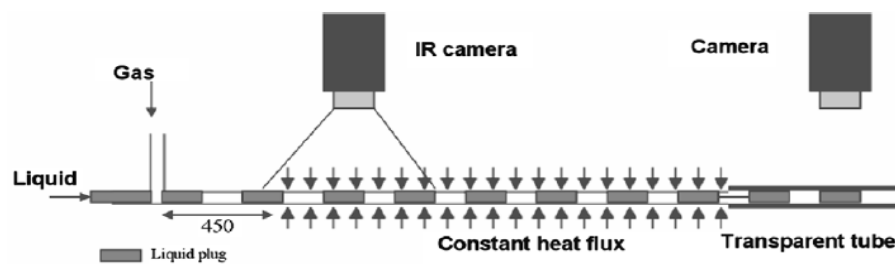


Figure 2.4 experimental setup of segmented Taylor flow [10]

Their results indicated that optimized slug geometries can yield heat transfer enhancement up to an order of magnitude. They concluded that heat transfer in the entrance region of slug flows presents a combination of conventional single phase and plug flow behaviors with short slugs

approaching the theoretical plug flow limit and long slugs approaching the single phase flow limit. The obtained results were employed to propose a model which can be used for predictive purposes in either heat or mass transfer applications.

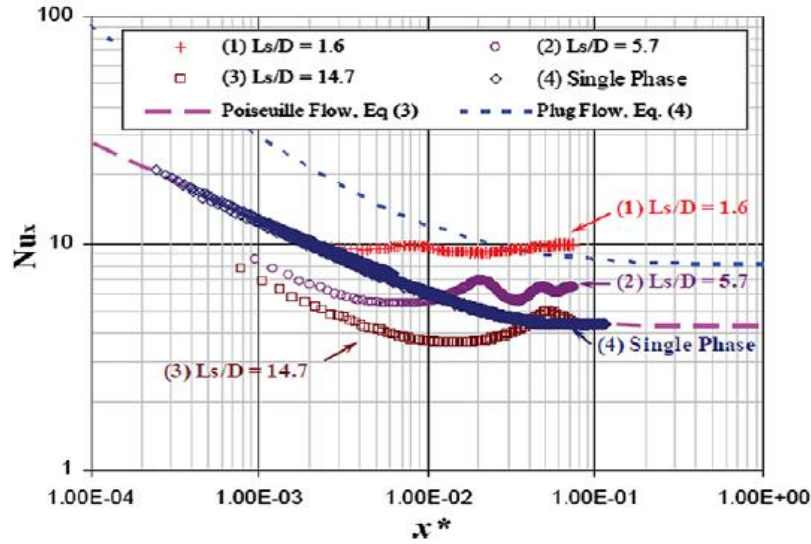


Figure 2.5 effect of liquid slugs of gas-liquid flow on local Nusselt number plotted versus Graetz number [10]

Farzad and Peles [11] conducted an experimental study using Taylor flow of gas-liquid in micro channels. The mixing effect of bubbles and the interaction with a thermal boundary layer were studied over a range of flow rates. They revealed that, heat transfer was increased up to 100 % when compared with single-phase flow.

Howard and Walsh [15] examined the influence of incorporating microencapsulated phase change materials (MPCM) on the heat transfer of Taylor flows in mini scale straight channels. Taylor flows showed heat transfer enhancements due to the internal circulations within liquid slugs. On the other hand, microencapsulated phase change materials (MPCM) offered a significant

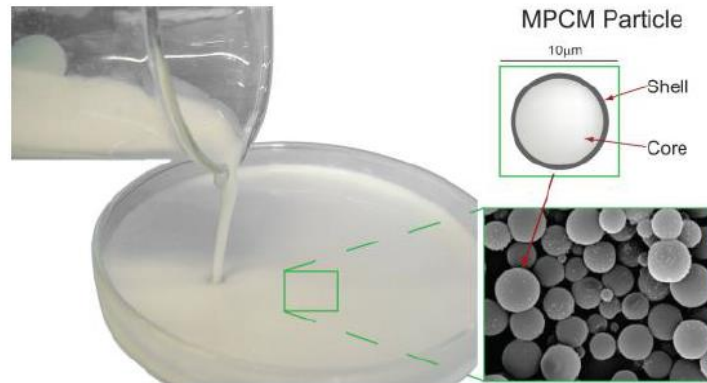


Figure 2.6 microencapsulated phase change material (MPCM) suspension [15]

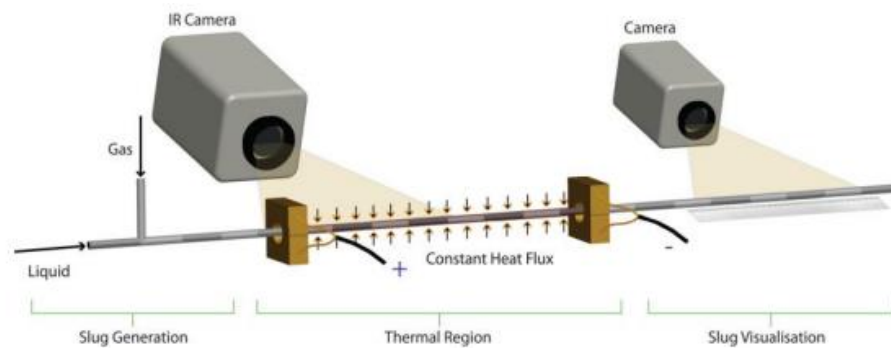


Figure 2.7 experimental setup of Howard and Walsh [15]

increase of the thermal capacity.

The experimental test facility in Fig. 2. 7 allowed the incorporated MPCM Taylor flows to be subjected to a constant heat flux boundary condition. The local temperature of the wall was measured using Infrared thermography to determine the local Nusselt number. A mass concentration of 30.2 % of the MPCM as in Fig. 2.6 was examined. Reported results revealed a significant reduction in experimental wall temperatures associated with MPCM-air Taylor / slug flows when compared with the Graetz theory. Their study verified the potential of heat transfer enhancement using MPCM Taylor flows.

2.3.2 Liquid- Liquid Taylor Flow

Liquid-liquid Taylor flow is considered as two phase flow although both components are liquid phases. The flow can be created by introducing two liquids into the same channel flow to

Table 2.1 gas-liquid Taylor flow studies using mini and micro scale tube.

Author	Condition	Geometries	findings
Pele [11]	Constant heat flux	Mini scale straight tube, L=500 mm, D=1.5 mm	Mini scale channel subjected to isoflux conditions to optimize slug geometries for better heat transfer enhancement.
Oliver [50]	Constant wall temperature	Mini scale straight tube, L=914.4 mm, D=6.35 mm	Witted tube area and actual flow velocity was considered.
Horfath [13]	Constant wall temperature	Mini scale straight channel, L=600 mm D=2.32 mm	Liquid slugs become thermally saturated at lower (Ls/D). That was result of the high radial mixing of segmented flow within short slugs.
Betz [51]	Constant heat flux	Mini scale straight tube, L = 0.025 m $w_w = w_c = 0.0075$ m	Heat transfer was enhanced by up to 140% with reasonable penalty of pumping power
Haas [9]	Flow formation	Square mini channel, Dh=1.0 mm, variable D= (0.184, 0.317, 0.490 mm).	Bubble forming mechanisms were identified leading to a complex interaction between physical properties of the fluids, and geometrical parameters.

form a train of immiscible liquid slugs. Thermal behavior of the flow in mini / micro channels have been investigated and the enhancement was verified when compared with a single phase flow. Considerable publications addressed many aspects under isothermal and isoflux boundary conditions [17 – 20].

Eain et al [18] conducted an experimental study to examine the potential of heat transfer enhancement using liquid–liquid Taylor flow regime in a mini scale channel. They aimed to

investigate the thermal effects of slug length variation for both phases on the local Nusselt numbers. The isoflux boundary condition was applied to the test section. High resolution infrared thermography system was employed to measure local wall temperature as shown in Fig. 2.7. The experiments were carried out over a carrier slug to dispersed length ratios (L_S / L_d) : 3.77, 0.65 and 0.148. They observed higher heat transfer rates and lower wall temperature for smaller segmentation ratios as can be seen in Fig. 2.8.

Thus, performance of the designed system reached the maximum when carrier slug lengths approached the channel diameter. Their results were presented as a local Nusselt number versus inverse Graetz number x^* . They also reported that using dispersed phase of PCM resulted in heat

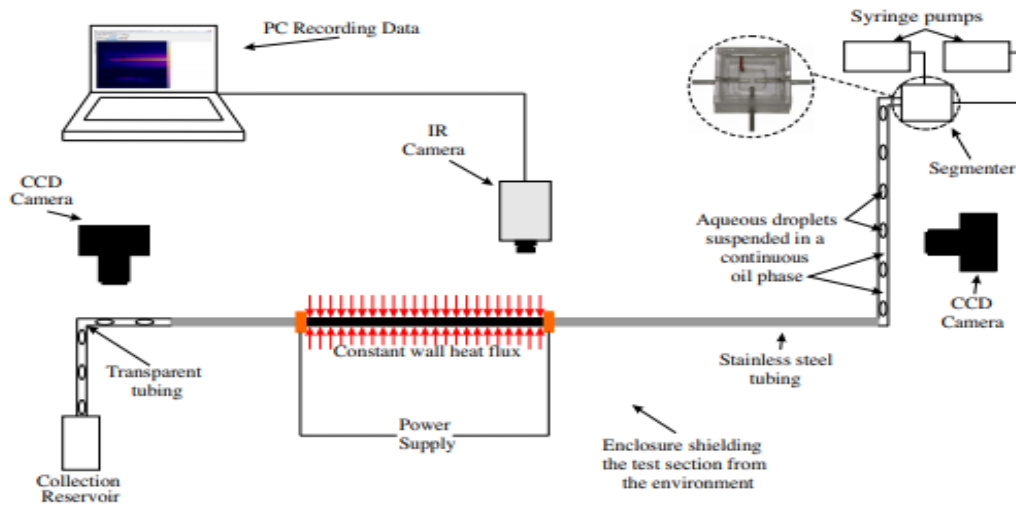


Figure 2.8 experimental setup of liquid-liquid Taylor flow [18]

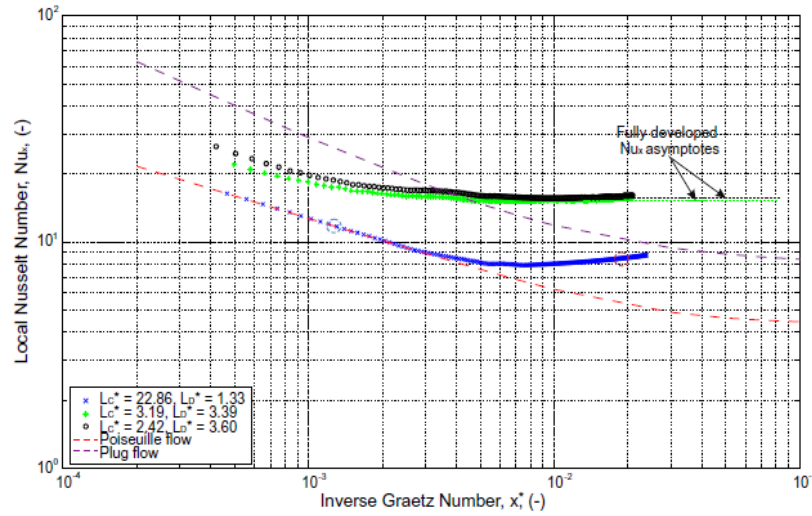


Figure 2.9 effect of slug lengths of liquid-liquid Taylor flow on local Nusselt number [18]

transfer enhancements up to 600 % over single phase flow. This study is valued because the obtained results provided a unique insight into the parameters that affect heat transfer enhancement in liquid–liquid Taylor flows under isothermal boundary condition.

Adrugi and Muzychka [17] carried out liquid-liquid heat transfer experiments under isothermal boundary conditions. They used a mini scale tube $D = 1.63$ mm with several tube lengths which ranged from 50 to 170 mm. A Taylor flow regime of liquid-liquid flows was obtained based on different flow modes of void fraction. The s Taylor / slug flows were created by introducing the two immiscible liquids (water – silicone oils) into a straight tube. They reported a heat transfer enhancement in the dimensionless form of heat flux when compared with a single phase flow model.

Asthana et al [19] experimentally examined the convective heat transfer of liquid-liquid Taylor flows using water and mineral oil droplets in microchannels of cross section $100 \mu\text{m}$ by $100 \mu\text{m}$ and using flow rates of up to $130 \mu\text{l/min}$. The segmented flows were subjected to a constant heat flux of 0.15 MW/m^2 . Fig. 2.10 shows the assembled experimental setup.

Throughout the study, temperature measurements were obtained using Laser Induced Fluorescence (LIF) as shown in Fig. 2.11. The micro-PIV measurements were conducted to determine the velocity field of the slug flows. Their findings showed that this concept significantly enhanced the Nusselt number up to four-fold when compared with single water flow.

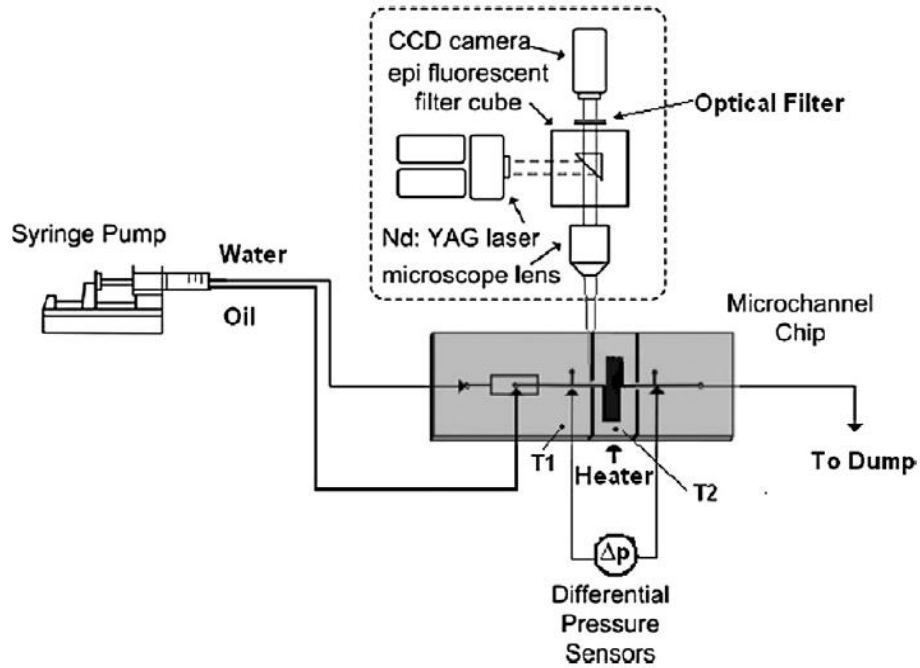


Figure 2.10 assembled experimental setup of liquid-liquid Taylor flow [19]

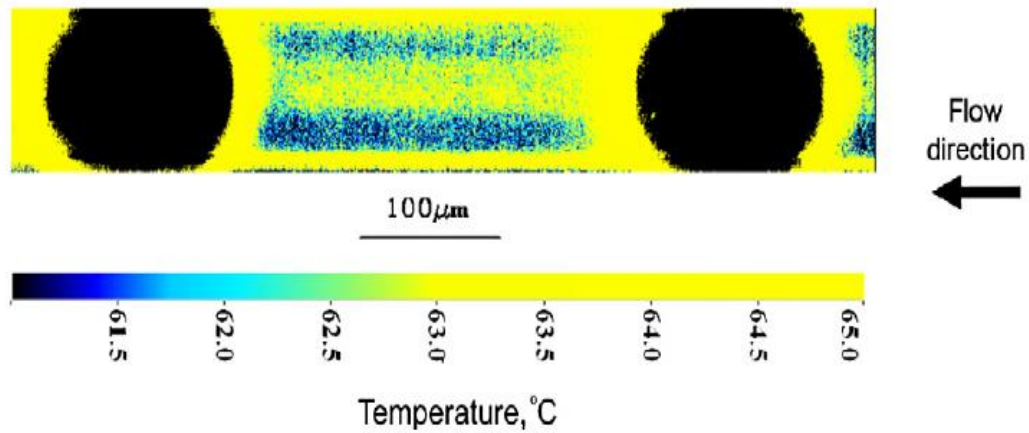


Figure 2.11 local temperature distribution between two slugs (water flow rate: 100 $\mu\text{l}/\text{min}$, oil flow rate: 30 $\mu\text{l}/\text{min}$) [19].

They concluded that the movement of oil droplets in Taylor flows of water-oil induced intensively the internal circulations within the carrier phase at the interfacial area. The fluid motion will disrupt the formation of the boundary layer and increases the radial mixing.

Table 2.2 summary of liquid-liquid Taylor flow studies in mini scale channels

Author	Condition	Geometries and Limits	Major Findings
A. Asthana [19]	Constant heat flux	Microchannel with two straight parts separated by a serpentine section with six turns. $W=H = 100 \mu\text{m}$ $Q = 130 \mu\text{l/min}$.	Oil slugs induces intensive circulation in the carrier water phase. For segmented flow, up to a four-fold increase of the Nusselt number compared to pure water flow was observed. The enhancement comes with a penalty of pressure drop,
W. M. Adrugi [17]	Constant temperature	Mini scale Curved tube, $L = 6.28, 9.42, 18.84 \text{ cm}$, $D = 1.63 \text{ mm}$ $R = (1, 2, 4, \text{ and } 8 \text{ cm})$	Better enhancement was achieved when compared with single phase flow in curved tubing. $Q = f(R, Pr, L)$
M. G. Eain, [18]	Constant heat flux	Mini scale straight tube, $L = 0.3 \text{ m}$, $D = 1.5 \text{ mm}$ Wall thickness = 0.25 mm $0.2 < L_c^* < 22.9$ $0.1 < L_D^* < 8.2$	Maximum enhancement was observed when Carrier slug length reached inside diameter of channel, Heat transfer: $Q \propto L_c$, $Q \propto 1/L_D$
W. M. Adrugi [20]	Constant temperature	Mini scale coiled tube, $L = 25.12, \text{ and } 50.24 \text{ cm}$, $D = 1.65 \text{ mm}$ $R = 1 \text{ cm}$, 4 Turns $R = 2 \text{ cm}$, 2 Turns $R = 4 \text{ cm}$, 1 Turn	Significant enhancement as result of Prandtl number tube curvature radii decrease, Nu_D for same curvatures was higher for short tubes. A new model was developed with less than 10% error.
Z. Dai [49]	Constant heat flux	Mini scale circular straight channel, $L = 266 \text{ mm}$ $D_h = 1.06 \text{ mm}$	A generalized model of heat transfer in gas-liquid and liquid-liquid Taylor flows is developed from a combination of resistances for wall-to-film, film-to-slug and film-to-bubble.

2.4 Nanofluid

Numerous studies have investigated the thermal characteristics and challenges of using nanofluid. Though, this investigation still faces a discrepancy when explaining the theories of heat transfer enhancement and nanoparticle stability. Kong, et al [21] mentioned two mechanisms of nanoparticles stability, steric and electrostatic repulsion.

Several types of surfactants were used to produce stabilized nanofluids such as sodium dodecyl benzene sulfonate (SDBS), Sodium Dodecyl Sulfate (SDS), sodium lauryl sulfate (SLS) and emulsifier. In contrast, Meibo, et al [22] reported that very little surfactant should be added to nanofluid to achieve acceptable stability to avoid affecting the thermal conductivity.

2.4.1 Thermal Conductivity of Nanofluids

Enhancement of thermal conductivity of conventional liquids is applicable by mixing with other substances, solids, or liquids. The inclusion of high thermal conductive material of nano scale size < 100 nm, metallic or non-metallic, causes an improvement in convection heat transfer.

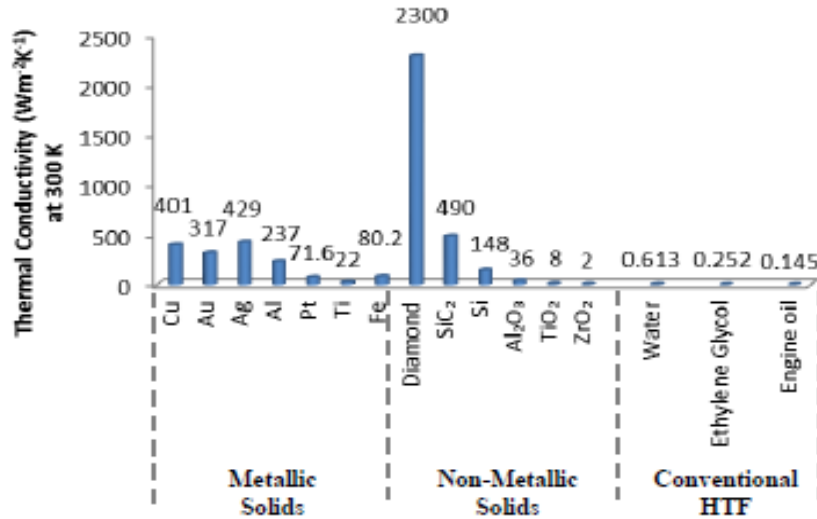


Figure 2.12 thermal conductivity values of materials [26]

Fig. 2.12 shows the thermal conductivity of pure materials. Recently, challenges of nanofluid stability still receives much interest as point of research. Theoretical modeling of the thermal conductivity of solid – liquid mixtures was considered by Hamilton and Crosser [23]; Bachelor and O'Brien [24]; followed by Choi and Eastman [25]. Table 2.3 contains commonly used models to predict the thermal conductivity.

Seok and Choi [27] investigated the effects of various parameters on the thermal conductivity of nanofluids and accurately concluded that (i) thermal conductivity directly is proportional to volumetric concentration (ii) thermal conductivity of nanoparticle materials is not a major factor in enhancing the thermal conductivity of nanofluids (iii) as the particle size decreases the Brownian motion of nanoparticles increases and then nano convection becomes more effective (iv) effective thermal conductivity of nanofluids dramatically increases with temperature which can be explained as a result of decreasing dynamic viscosity that leads to the increase in Brownian motion and then nano convection. Table 2. 3 contains the most used thermal conductive models.

Table 2.3 Common theoretical models of thermal conductivity of solid-liquid mixture

Author(s)	Expression	Applications
Maxwell [28]	$\frac{k_e}{k_f} = \frac{k_p + 2k_f - 2(k_f - k_p)\phi}{k_p + 2k_f - (k_f - k_p)\phi}$	Applied to homogeneous and low-volume fraction with randomly dispersed, uniformly sized, and non-interacting spherical particles:
Hamilton- Crosser [23]	$\frac{k_e}{k_f} = \frac{k_p + 2k_f - 2(k_f - k_p)\phi}{k_p + 2k_f + (k_f - k_p)\phi}$	Applied for non- spherical particles with specified n for each shape
Lu-Lin [30]	$\frac{k_e}{k_f} = 1 + \alpha\phi + b\phi^2$	Applied to both spherical and non-spherical particles
Petal [34]	$\frac{k_e}{k_f} = 1 + 0.135 \left(\frac{k_e}{k_f}\right)^{0.273} \phi^{0.467} \left(\frac{T}{20}\right)^{0.547} \left(\frac{100}{d_p}\right)^{0.234}$	The model accounting both particle size and nanofluid temperature
Bhattacharya [29]	$k_e = \phi k_p + (1 - \phi)k_f$	Brownian dynamics of spherical nano particles was considered in the model
Brugman [39]	$\phi \left(\frac{k_p - k_e}{k_p + 2k_e} \right) + (1 - \phi) \left(\frac{k_b - k_e}{k_b + 2k_e} \right) = 0$	Applied for spherical particle with no limit of nanoparticle concentration

2.4.2 Performance of Nanofluids

Nanofluids are promising to improve the thermal properties of cooling liquids. The thermal performance of the nanofluids depend on stability and dispersion of nanoparticles in the base fluid. The ultrasonication and use of the surfactants are used for proper dispersion of nanofluid with restriction of the negative effects on the thermal conductivity. The survey shows the important details on nanofluid performance and preparation as shown in Table 2.3.

Manaya and Sahin [31] experimentally investigated the upper limitations of nano particle volume concentrations on heat transfer and pressure drop of TiO₂–water nanofluids in a microchannel. The study covered a considerable range of concentration (0.25%, 0.5%, 1.0%, 1.5%, and 2.0%) without using dispersant. Their results showed that heat transfer was enhanced significantly over the range of Reynolds number from 100 to 750 with a slight sacrifice of pressure drop. Table [2.3] contains summery of recent publications that investigate the thermal performance of the nanofluid.

Table 2.1 preparation and thermal performance of nanofluids in mini- micro channels

Author(s)	Material and Concentration	Preparation	Remarks
Anbumeenak [32]	TiO ₂ , 0.25, 0.5, 1.0, 1.5, and 2.0 Vol.% and 25 nm size dispersed in di-water	6 h ultra-sonication, with no surfactant	Significant enhanced with no excessive pressure drop in MCS and 20day stabilized was observed.
Halelfadl [33]	MWCNT- 0.01 Wt. %	30 min stirring repeated after 24h, with no surfactant.	Temperature is significantly affected both ΔP & Q (- & +) respectively in MCS
Patrice [39]	CNTs, 0.005 - 0.55 vol % . and 9.2 nm size dispersed in di-water	Preparation process does not affect TC, SDBS, Lignin.	TC increased for low ϕ between (30-40)°C and presence of surfactant panelize TC
Xing [36]	CNTs, 0.1–1 wt.% or 0.05–0.48 vol.%, dispersed in di-water	120 min & Ultra - sonication 60 min, CTAB- 25% wt. of CNTs	CTAB do not effect TC, also TC increase with concentration over a temperatures (10-60)°C
Sahin [37]	CuO, 0.5, 1, 2, and 4 vol. % with 33 nm size, dispersed in di-water	20 h sonication, No dispersant	Heat transfer was enhanced in laminar flow & high concentration is not recommended.
Xing [43]	CuO, 0.5, 1, 2, and 4 vol. % with 33 nm size, dispersed in di-water	20 h sonication, Non-CTAB & SDBS	Stabilized for 28 days with or without surfactant
Kin [47]	CNTs, 0.01, 0.05, 0.1, 0.2, 0.3 wt.% & 30 nm size, E.G.- water (40+60) %	5 to 30 mins Ultra - sonication, Non-PVP, GA, CTAB	Better stability observed with surfactants & 25% max enhancement achieved with using AG
Sivakumar [40]	Al ₂ O ₃ & CuO , 0.01, 0.02, 0.03, 0.1, 0.2, 0.3 vol.% and dispersed in di-water	Ultra-sonication vibration bath, no surfactant.	CuO showed higher thermal performance than Al ₂ O ₃ and low ΔP at same volume fractions.
Mahbubul [42]	Al ₂ O ₃ (0.01, 0.1, 0.5, and 1 vol.%) with 13 nm size and 99.5% purity, dispersed in di-water	Ultrasonic for 1–5 h at two different amplitudes (25%-50%), No dispersant	Better stability at 3 to 5 h of ultra-sonication for the 50% and 25% of sonicator power amplitudes, respectively.
Pryazhnikov [44]	SiO ₂ , Al ₂ O ₃ , TiO ₂ , ZrO ₂ , CuO, (0.25 to 8 Vol. %) with size ranged (10 - 150 nm)	Mechanical Mixing 30 min ultra-sonication, Acrylic polymer (0.008 - 0.02 % wt.)	For all cases TC increases with increasing NP size and TC of base fluid significantly affected TC. Also NP material not effect TC
Zhang [41]	SiC and Al ₂ O ₃ , VI. 0.001% to 1%. (30 nm size supplier specifications), dispersed in water.	Ultrasonic vibration for 3–5 hrs, using CTAB.	Stable for two weeks. Nu_D enhanced by 85% with penalty of ΔP . nP size was measured to be (70-110nm)
Ho [45]	Al ₂ O ₃ , (1 - 2 vol.%), 33 nm and 99.95% purity, dispersed in pure water.	Ultrasonic vibration bath for 2 h. No dispersant	At max flow rate tested for the nanofluid of 1 vol.%, the average heat transfer coefficient increases by 70%
Singh [46]	Al ₂ O ₃ , (0.25 vol. %, 0.5 vol. %, and 1 vol.) % with 45 nm size, dispersed in water and EG	Sonicating for 5–6 h and Acid added to control PH of water	Alumina-water nanofluids showed higher Nu than that of alumina-EG nanofluids.

Vafaei S. and Wen [35] experimentally studied convective heat transfer of aqueous alumina nanofluids in a horizontal mini-channel which was subjected to a constant heat flux boundary condition as shown in Fig. 2.13.

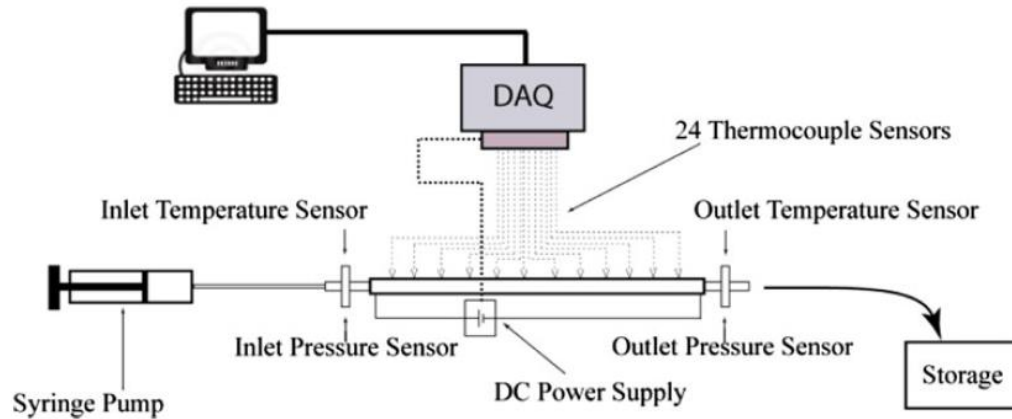


Figure 2.13 schematic of the experimental setup [35]

The experiments were run under laminar flow condition $40 < Re < 1000$. The observation showed that the heat transfer coefficient of nanofluids was a function of nanoparticle concentration and mass flow rate. The essential findings revealed that at higher flow rates, the enhancement was noticeable in the fully developed region and reached up to 40 % increase in local heat transfer coefficient.

2.5 Research Objectives

The main objectives of this dissertation focus on heat transfer enhancement in mini scale straight / coiled tubes using Taylor flows. This pattern of flow is characterized as a low laminar flow field which considers the same Reynolds number range of a single phase flow $Re_D < 2300$. The experimental work was performed under isothermal boundary conditions using several combinations of fluids gas-liquid and / or liquid-liquid of varied and fixed void fractions. These objectives will serve the development of the compact devices. Typically, these systems experience high thermal generation and then require further heat dissipation.

This study will be presented as a series of experimental and theoretical / empirical analyses of thermal enhancement challenges in mini scale channels. Briefly, the main objectives of this research are:

- Produce new experimental data using a gas-liquid Taylor flow in a straight tube and to examine effect of liquid slug length ratio. Verify the trends of the experimental data by comparison

with predictive models and published data from the literature to ensure reliability of the obtained results.

- Conduct liquid-liquid Taylor flow experiments in straight tubes using combinations of two immiscible liquids to examine the effect of slug ratio based on various liquid fractions.
- Predict the thermal behaviour of gas-liquid Taylor flow in curved / coiled tubes while keeping the void fraction constant. Influences of several parameters are considered: radius of curvature, Prandtl number, liquid slug ratio and tube length.
- The study also aims to develop a new model to predict Nusselt number as a function of slug ratio and tube curvatures. Several combinations of liquids are used to demonstrate effect of the Prandtl number on heat transfer enhancement of liquid-liquid Taylor flows.
- Produce nanofluids of different concentrations to conduct simple performance evaluation when considering heat transfer enhancement and pressure drop. Obtain results for continuous and segmented flows to show heat transfer enhancement due to nanofluid concentration and void fraction of the segmented flows.

The experimental results would be useful to understand and model the thermal behavior of Taylor flows in mini and micro scale tubes. These results will provide a reference line to additional investigations on heat transfer enhancement of continuous and segmented flows in small scale tube.

2.6 References

- [1] Tuckerman, Pease, "High-Performance Heat Sinking for VSLI," IEEE Electron Device Letters, Vol. EDL-2, pp. 126-129, (1981).
- [2] Y. S. Muzychka, Mehdi Ghobadi "Measurement and Analysis of Laminar Heat Transfer Coefficients in Micro and Mini-Scale Ducts and Channels", *Heat transfer engineering*, vol. 37 no. 11 2016.
- [3] Ghobadi M., Muzychka Y. S., "Effect of Entrance Region and Curvature on Heat Transfer in Mini Scale Curved Tubing at Constant Wall Temperature" *International Journal of Heat and Mass Transfer*, 65 (2013) 357–365.
- [4] Fairbrother F, Stubbs AE (1935) Studies in electro-endosmosis. Part VI. The "Bubble-tube" method of measurement", *Journal of Chemical Society* 1:527–529.
- [5] Taylor, "Deposition of a Viscous Fluid on the Wall of a Tube", *Journal of Fluid Mechanics*, 10(1961) 161–165.
- [6] Maddox D. E., Mudawar I., "Single- and Two-Phase Convective Heat Transfer from Smooth and Enhanced Microelectronic Heat Sources in a Rectangular Channel", *Journal of Heat Transfer*, ASME NOVEMBER 1989, Vol. 111 p. 1045.
- [7] A. Rachel Betz, D. Attinger, "Can Segmented Flow Enhance Heat Transfer in Microchannel Heat Sinks" *International Journal of Heat and Mass Transfer*, 53 (2010) 3683–3691.
- [8] S. Hase, "Characterisation of Gas-liquid Two-Phase Flow in Mini-Channels with co-flowing Fluid Injection inside the Channel, part II: gas bubble and liquid Slug Lengths, Film thickness, and Void Fraction Within Taylor Flow", *International Journal of Multiphase Flow*, 88, 2017, pp. 251–269.
- [9] Patrick A. Walsh, Edmond J. Walsh , Yuri S. Muzychka," Heat Transfer Model for Gas–Liquid Slug Flows under Constant Flux", *International Journal of Heat and Mass Transfer*, 53 (2010) 3193–3201.
- [10] Farzad Houshmand, Yoav Peles, "Heat Transfer Enhancement with Liquid–gas Flow in Microchannels and the Effect of Thermal Boundary Layer", *International Journal of Heat and Mass Transfer*, 70 (2014) 725–733.
- [11] Muzychka, Y.S., "Laminar Heat Transfer for Gas-Liquid Segmented Flows in Circular and Non-circular Ducts with Constant Wall Temperature" ASME, 2014.

- [12] Horvath, C., Solomon, B.A., Engasser, J.M., “Measurement of Radial Transport in Slug Flow Using Enzyme Tubes”, *Industrial and Engineering Chemistry, Fundamentals*, Vol. 12, no. 4, pp. 431-439, 1973.
- [13] Vrentas, J.S., Duda, J.L, and Lehmkuhl, G.D., “Characteristics of Radial Transport in Solid-Liquid Slug Flow”, *Industrial and Engineering Chemistry, Fundamentals*, Vol. 17, no. 1, pp. 39-45, 1978.
- [14] Howard A. and Walsh P. A., “Heat Transfer Characteristics of Liquid-Gas Taylor Flows incorporating Microencapsulated Phase Change Materials”, *Journal of Physics: Conference Series* 525 (2014) 012022.
- [15] W. M. Adrugi, Y. S. Muzychka and K. Pope, “Heat Transfer in Liquid-liquid Taylor Flow in Mini and Micro-scale tube with Constant Wall Temperature”, 2015 by ASME-ICNMM2015-48272.
- [16] M. Mac Giolla Eain , Vanessa E. , Jeff P. , “Local Nusselt Number Enhancement in Liquid-Liquid Taylor flow”. *International Journal of Heat and Mass Transfer*, 80,(2015) 85-97.
- [17] A. Asthana, Igor Zinovik, “Significant Nusselt Number Increase in Micro-channels with a Segmented Flow of Two Immiscible Liquids: An Experimental Study”, *International Journal of Heat and Mass Transfer*, 54 (2011) 1456–1464.
- [18] Adrugi, W., Muzychka, Y.S., and Pope, K., “Heat Transfer in Liquid-Liquid Taylor Flow in Mini-scale Curved Tubing for Constant Wall Temperature”, ASME-IMECE-67700, 2016.
- [19] L. Kong, J. Sun, and Y. Bao, “Preparation, Characterization and Tribological Mechanism of Nanofluids”, *RSC Adv.*, 2017, 7, 12599.
- [20] Meibo Xing, “Experimental Study on the Thermal Conductivity Enhancement of Water Based Nanofluids Using Different Types of Carbon Nanotubes”, *International Journal of Heat and Mass Transfer*, 88 (2015) 609–616.
- [21] Hamelton, Crosser, “Thermal Conductivity of Heterogeneous Two Component System, V O L. 1 N O 3 A gust 1 9 6 2 187.
- [22] G. K. Batchelor, F. R. S., R. W. O'Brien, “Thermal or Electrical Conduction Through a Granular Material”, *Proceedings of the Royal Society of London. Series A, Mathematical and Physical Sciences* Vol. 355, No. 1682 (Jul. 13, 1977), pp. 313-333.

- [23] S. U. S. Choi and J. A. Eastman , “Enhancing Thermal Conductivity of Fluids with Nanoparticles”, ASME International Mechanical Engineering Congress & Exposition, San Francisco, CA (1995).
- [24] D. H. Sukarnon D” Challenges for Nanofluid Applications in Heat Transfer Technology” *Journal of Physics: Conf. Series* 795 (2017) 012020.
- [25] Seok and Choi Seok Pil Jang, Stephen U. S. Choi, “Effects of Various Parameters on Nanofluid Thermal Conductivity ”, *Journal of Heat Transfer*, ASME MAY 2007, Vol. 129 / 617.
- [26] J.C. Maxwell, A Treatise on Electricity and Magnetism, Clarendon Press, 1873.
- [27] P. Bhattacharya, S. K. Saha, A. Yadav, Patrick Phelan, R. S. Prasher, “ Brownian Dynamics Simulation to Determine the Effective Thermal Conductivity of Nanofluids” *Journal of Applied Physics*, 95(11I), 6492-6494.
- [28] Lu, S. Y. H. C. Lin (19960 “ Effective Conductivity of Composites Containing Aligned Spherical Inclusions of Finite Conductivity “, *Journal of Applied. Physics.*, 79(19960) 6761-6769.
- [29] Eyuphan Manaya, Bayram Sahin” Heat Transfer and Pressure Drop of Nanofluids in a Microchannel Heat Sink”, *Heat Transfer Engineering*, 2017, volume, 38. No. 5, 510- 522.
- [30] C. Anbumeenakshi, P.I. Meenatchi Sunndhar, P.I. Kalyaahna Sundaram, M.R. Thansekhar, ” Experimental Investigation of Heat Transfer Study in Rectangle Type Straight and Oblique Finned Microchannel Heat Sink with Nanofluids”, *International Research Journal of Engineering and Technology (IRJET)*, 2017, Volume: 05 Issue: 12 ,621-634.
- [31] S. Halelfadl, A. M. Adham, ”Optimization of Thermal Performances and Pressure Drop of Rectangular Microchannel Heat Sink Using Aqueous Carbon Nanotubes Based Nanofluid”, *Applied Thermal Engineering*, 62(2014) 492- 499.
- [32] Hrishikesh E. Patel, T. Sundararajan, Sarit Kumar Das, “A cell Model Approach for Thermal Conductivity of Nanofluids”, *Journal of Nanoparticle Research*, 10(1):87-97.
- [33] S. Vafaei D. Wen” Convective Heat Transfer of Aqueous Alumina Nanosuspensions in a Horizontal Mini-channel”, *Heat Mass Transfer*, (2012) 48:349–357.
- [34] K. Y. Leong, N. M. Hanafi, “Thermal Effect of Surfactant on Stability and Thermal Conductivity of Carbon Nanotube Based Nanofluids” *Thermal Science*, Year 2016, Vol. 20, No. 2, pp. 429.

- [35] B. Sahin, E. Manay, E. F. Akyurek “An Experimental Study on Heat Transfer and Pressure Drop of CuO-Water Nanofluid” Hindawi Publishing Corporation, *Journal of Nanomaterials*, Volume 2015, Article ID 790839, 10 pages.
- [36] D. Bruggeman, “Berechnung verschiedener physikalischer Konstanten von heterogenen Substanzen”, *Ann. Phys. (Leipzig)* 24, 636-679 [1935].
- [37] Patrice Estellé, Salma Halelfadl, Thierry Maré, “Thermal Conductivity of CNT Water Based Nanofluids: Experimental Trends and Models Overview”, *Journal of thermal Energy* “ 2015, Volume 1, Issue 2, 381 – 390.
- [38] A. Sivakumar, A. Natarjan, “Experimental Investigation of Forced Convective Heat Transfer Performance in Nanofluids of Al₂O₃/Water and CuO/Water in a Serpentine Shaped Micro. Channel Heat Sink”, *Heat and Mass Transfer*, 2016, Volume 52, Issue 7, 1265–1274.
- [39] Ji Zhang, Y. Diao, Y. Zhao, ”Thermal-Hydraulic Performance of SiC-Water and Al₂O₃-Water Nanofluids in the Minichannel”, *Journal of Heat Transfer*, Feb 2016, 138(2): 021705 (9 pages).
- [40] I. M. Mahbubul, Tet Hien Chong “Effective Ultrasonication Process for Better Colloidal Dispersion of Nanofluid”, *Ultrasonics Sonochemistry*, 26 (2015) 361–369.
- [41] Xing, M., “Experimental Study on the Thermal Conductivity Enhancement of Water Based Nanofluids Using Different Types of Carbon Nanotubes”, *International Journal of Heat and Mass Transfer*, 88 (2015) 609-616.
- [42] Pryazhnikov, M.I. Minakov, A.V. Rudyak, “Thermal Conductivity Measurements of Nanofluids”, *International Journal of Heat Mass Transfer*, 2017, 104, 1275–1282.
- [43] C.J. Ho, L.C. Wei, Z.W. Li, ”An experimental investigation of forced convective cooling performance of a microchannel heat sink with Al₂O₃/water nanofluid” *Applied Thermal Engineering*, 30 (2010) 96–103.
- [44] P. K. Singh, P. V. Harikrishna, “Experimental and Numerical Investigation into the Heat Transfer Study of Nanofluids in Microchannel”, *Journal of Heat Transfer*, Dec 2011, 133(12): 121701.

- [45] Y. L. Kin , N. M. Hanafi, R. M. SOHAIMI, and N. H. AMER, “The effect of Surfactant on Stability and Conductivity of Carbon Nanotubes based nanofluid”, *Thermal Science*, Year 2016, Vol. 20, No. 2, 429-436.
- [46] Z. Che, T. N. Wong, N. Nguyen,” Heat Transfer Enhancement by Recirculating Flow within Liquid Plugs in Microchannels”, *International Journal of Heat and Mass Transfer*, 55 (2012) 1947–1956.
- [47] Z. Dai, Z. Guo, D. F. Fletcher n, B. S. Haynes,” Taylor Flow Heat Transfer in Microchannels-Unification of Liquid–liquid and Gas–liquid Results”, *Chemical Engineering Science*, 138 (2015) 140–152.
- [48] Betz A. R., Attinger D., “Can Segmented Flow Enhance Heat Transfer in Microchannel Heat Sinks”, *International Journal of Heat and Mass Transfer*, 53, pp. 3683-3691, 2010.
- [49] Oliver, D.R. and Wright, S.J., “Pressure Drop and Heat Transfer in Gas-Liquid Slug Flow in Horizontal Tubes”, *British Chemical Engineering*, Vol. 9, pp.590-596, 1964.

CHAPTER 3

LAMINAR HEAT TRANSFER OF GAS-LIQUID SEGMENTED FLOWS IN CIRCULAR DUCTS WITH CONSTANT WALL TEMPERATURE

3.1 Introduction

A simple model for heat transfer in gas-liquid Taylor flow is considered for flow in circular tubes. Studying two phase flow for gas-liquid Taylor flow was originally started by Fairbrother and Stubbs [1], followed by Taylor [2]. Oliver et al. [3], Horvath et al. [4] and Vrentas et al. [5]. Later, Maddox and Mudawar [6] investigated single and two-phase forced convection of a simulated microelectronic heat source to assess the feasibility of cooling. Betz and Attinger [7] performed experiments on a compact microchannel cooling system with both continuous and Taylor flows. They observed that segmented flow significantly enhanced heat transfer by up to 140 % in a microchannel heat sink as compared with single-phase flow at same liquid flow rate. Walsh et al. [11] measured the local Nusselt numbers using infrared thermography in both entrance and fully developed flow regions. Results indicate that optimized slug geometries can yield up to an order of magnitude heat transfer enhancement.

** The materials in this chapter were presented in ASME 2019 18th International Conference on Nanochannels, Microchannels, and Mini channels, June 24-26, 2019 in St John's, Canada.*

The primary benefit associated with Taylor flows is significantly enhanced transport phenomena [14]. Although segmented flows at micro and mini-scales have emerged as a fundamental research area in recent years [3-5,8] they are conceptually not new. The resurgence of research in non-boiling two phase plug flows has been motivated by the desire to increase heat transfer rates in compact liquid cooled systems. Early work in this area dates to the early 1960's and early 1970's, with a significant gap in major publication outputs until recent years. Muzychka [8] considered much of the early work in a journal publication along with new data obtained with his collaborators [9]. A significant observation of this work was the fact that heat transfer in segmented flow behaves in a manner like thermal boundary layer flow and that heat transfer scales with the liquid plug length. A re-analysis of the old data showed that much of the data could easily be predicted with a simple Leveque model [9] over most of the data range. What was not considered in this work was the phenomena of thermal saturation which occurs when short plugs have a long residence time, since much of the data did not display this characteristic. The present study addresses this issue. The current work presents the data of dimensionless mean wall heat flux, q^* , as a function of dimensionless plug length, L_s^* , and the plug to duct length ratio, L_s/L , see Fig. 3.1. The model which was developed by Muzychka [8] properly accounts for heat transfer behaviour for short and long plugs for long residence times. This model is validated with additional data not considered in [8]. The current work illustrates several additional important points related to the analysis of heat transfer in segmented flow, which include details on properly controlling plug length in experiments.

In many experiments the plug length to duct length ratio is not held constant while the Reynolds number is varied [10-14]. However, in some cases such as in Betz and Attinger [7] the ratio is approximately maintained such that a mean value may be used for comparison. Other issues pertaining to the use of the Nusselt number versus dimensionless mean wall flux will also be addressed. Nusselt number and dimensionless mean wall flux for Taylor gas-liquid Taylor flow will be considered in this paper. The actual wetted tube area along with maximum flow velocity are used to present heat transfer enhancement.

Some of the earliest studies examining the heat transfer rates in non-boiling Taylor / slug flows were those of Vrentas et al. [5] and Prothero and Burton [21]. In a one of a series of studies, they [21] compared the heat transfer rate of single phase Graetz flow with that of a segmented gas-

liquid stream. While Prothero and Burton [21] were able to show enhancement over the single phase flow, they did not assess the effect of slug length in a quantitative manner. In recent years, the experimental and theoretical analysis of heat transfer in gas-liquid Taylor/slug flow has received much attention with more aspects being investigated. Significant attempts were introduced by [8,9,11,15]. Furthermore, several studies aimed to achieve greater heat transfer enhancement by adding different materials such as nanoparticles or PCM's [14, 23]. Additional studies [7,10,13,22] were concerned with the potential of heat transfer enhancement using liquid-liquid Taylor flow.

Theoretical and experimental analysis of thermal behavior of laminar flow in small scale was provided in detail by Muzychka and Ghobadi [16]. Asymptotic models for entrance and fully developed regions were addressed. Hence, the aim of present study is to provide experimental data for a two phase flow rather than a single phase flow.

Oliver and Young [3] performed a study for controlling slug length. Later, the flow rates of both phases were increased to produce annular flow for comparison purposes. They aimed to investigate thermal and hydrodynamic behavior of gas liquid Taylor flow of non-Newtonian liquids under a constant wall temperature. They highlighted the importance of liquid slug lengths as a significant variable controlling heat transfer. Their results were benchmarked by carrying out measurements of single phase laminar flow. A non-dimensional analysis was used to present heat transfer data for Nusselt number as a function of Graetz number. Moreover, their study covered a wide range of Reynolds numbers including different flow regimes of gas liquid Taylor flow. Clearly, they reported an increase in heat transfer over the single phase flow for the slug flow regime, including different flow regimes of gas liquid Taylor flow.

Oliver and Wright [18] also conducted a series of measurements to investigate the effect of plug flow on heat transfer and friction in laminar flow. They surmised that the internal circulation would increase the heat transfer coefficient significantly, and therefore one would not be able to use Graetz -Leveque theory. They attributed the increase in heat transfer coefficient to both the effects of internal circulation and increased liquid velocity that results at constant mass flow rates due to the void fraction. They concluded that the effect due to void fraction is independent on plug length but that circulation effects would be strongest for shorter plugs. They reserved the assessment of plug length for a later study since the apparatus they used to collect data could not control liquid

plug lengths very well. As part of their study, Oliver and Wright [18] did develop simple correlations based upon their experimental data and modification of the Graetz-Leveque model.

Horvath et al. [4] highlighted the potential of radial transport of mass and heat within slug flow of gas-liquid. They obtained experimental data at high Prandtl number with constant liquid fractions of 0.5 throughout of their study. They reported their data as a Nusselt number for the liquid plug phase only versus slug aspect ratio (L_s/D) over a wide range of Reynolds from 20 to 300. The effect of slug velocity was studied by varying the Reynolds number of Taylor flow at same liquid fraction. They also concluded that liquid slugs become thermally saturated at lower aspect ratio (L_s/D). They conclude it is due to the high radial mixing of Taylor flow within short slugs.

Vrentas et al. [5] introduced a unique experimental study to assess radial transport of heat transfer enhancement of solid-liquid Taylor flow. Solid steel and plastic spheres were introduced into a stream of high viscosity silicone oils (100 cSt and 1000 cSt) with Reynolds numbers less than 1.5. Vrentas [5] suggested using steel spheres to avoid growing the liquid film on the tube wall with increasing viscosity [2]. They reported liquid phase Nusselt data three times greater than that of single phase flow at same Peclet number, and they covered a wide range of slug aspect ratios from 21 to 122. The results of single phase and segmented flows were presented as function of both Reynolds and Peclet numbers for three plug lengths. However, the primary distinguishing feature of this work is that the liquid plug ends cannot be assumed to be approximately adiabatic as in a gas-liquid flow, as the authors report that the steel spheres heat up to the wall temperature and thus provide another heat transfer path. This issue becomes more pronounced for shorter plugs.

Experimental data from [3,4,9] have been re-analyzed and then replotted using definitions for the Nusselt number and dimensionless heat flux q^* both as a function of dimensionless slug length L_s^* , tube length L^* , as well as Peclet number Pe . The details of each dataset are summarized in Table 1. These represent data for a circular tube except for the data from Betz and Attinger [7]. These data were also obtained for the isoflux condition but reduced using mean wall temperature consistent with the definitions used for constant wall temperature. In general, this is a reasonable approach, as integration of the Graetz-Leveque equation for isoflux conditions yields an expression that is within 7 percent of the result for an isothermal wall [13]. In conjugate heat transfer applications, the actual difference is much less when a highly conductive wall material is utilized.

Muzychka [8] provided an improvement on his previous analysis [9]. The new model properly considers effect of slug to tube lengths (L_s/L) on heat transfer as the boundary layer is dominant in shorter slugs. Hence one of important characteristic of this new model is that it shows how quick the short slugs are getting thermally saturated. Muzychka [8] used published experimental data from [3-5,7,9] to validate his model. In the present study a new experimental data are accurately obtained under constant wall temperature as an extra validation of this model.

S. Haase [12] developed a proper facility to study Taylor flow characterisation in mini scale channels using industrial fluids. The gas phase is introduced to the flow stream by injecting the gas phase through a capillary injector with variable inner diameter. Published experimental data with his own experimental data were used to develop a novel model to predict bubble and slug lengths of both phases. His study was motivated by early studies.

Howard and Walsh [14] investigated the potential of heat transfer enhancement associated with gas-liquid Taylor flows in mini sized channels incorporating microencapsulated phase change materials (MPCM) at a concentration up to 30%. However, they conclude the enhancement is due to the internal circulations within liquid slugs which was confirmed in [11] as well as increasing thermal capacity of the flow stream which is associated with adding PCM. An experimental test facility was developed which had a heated test section and allowed MPCM-air Taylor flows to be subjected to a constant heat flux boundary condition. Heat transfer enhancement was examined by changing liquid slug length and liquid fraction. The infrared thermography results demonstrated a significant reduction in experimental wall temperatures associated with MPCM-air Taylor flows when compared with the Graetz solution for conventional single phase coolants. Furthermore, the reduction in wall temperatures was observed even when data are not reduced to take account of the gaseous voids in the flow. Howard et al [14] confirmed that segmented MPCM flows provide further enhancement than that observed for MPCM Poiseuille flows.

Hughmark [19] proposed a simple correlation using a modified Graetz-Leveque theory. However, his modifications were based on the experimental observations of Oliver and Wright [18] and contained no new insights. Further, no rational basis was given for the proposed modification.

Eain et al. [22] investigated the potential of heat transfer enhancement of liquid–liquid Taylor flow. They use a segmented stream of water and oil which was heated under constant flux. However, the primary focus was to examine the influence of slug length and carrier phase variations on the local Nusselt numbers. Temperature measurement was carried out using infrared thermography system. Their experimental observations revealed that the greatest enhancements achieved in flows with carrier slug lengths approaching the channel diameter. The authors found that a liquid film separates the dispersed slugs from the heated capillary walls, which caused a reduction in the heat transfer rates. A similar study was performed in [13] using liquid-liquid Taylor flow. A scenario of variable void fraction was adopted throughout these experiments.

Alrbee and Muzychka [23] obtained new data to show additional heat transfer enhancement in mini scale channels. They considered nanofluids at various concentrations in the liquid phase. Nanofluids were prepared with several standard concentrations of 0.25, 0.5 and 1 vol %, using Aluminum Oxide Al_2O_3 and water as base fluid. They reported significant heat transfer enhancement when nanofluids were segmented by air bubbles to form a gas-liquid Taylor flow. The results showed that the enhancement was associated with nanofluid concentration as well as liquid slug length.

3.3 Theory of Data Analysis

This section provides the relevant theoretical expressions required to describe the thermal characteristics of single and two phase flows in both the developing and fully-developed regions for laminar flow in a tube, which utilizes the fundamental Graetz theory for both Poiseuille flow and slug flow under a constant wall temperature [17]. The mean Nusselt number for the tube is defined as:

$$\overline{Nu_D} = \frac{\bar{q}D}{k\Delta T_{LMTD}} \quad (3.1)$$

where

$$\Delta T_{LMTD} = \frac{(T_w - T_i) - (T_w - T_o)}{\ln\left(\frac{(T_w - T_i)}{(T_w - T_o)}\right)} \quad (3.2)$$

T_i and T_o are the inlet and outlet bulk temperatures, respectively, and T_w is the constant wall temperature. The dimensionless mean wall heat flux is defined as:

$$q^* = \frac{\bar{q}D}{k(T_w - T_i)} \quad (3.3)$$

The definition provided by Eq. (3.3) can be related to the definition in Eq. (3.1) by means of:

$$q^* = \frac{1}{4L^*} [1 - \exp(-4\overline{Nu}L^*)] \quad (3.4)$$

More details have been addressed in [16]. In the present work, we are interested in presenting new experimental data based on slug length L_S instead of the superficial duct length L . Finally, we also use the actual (maximum) local flow velocity rather than the superficial velocity, $U = U_b + U_s$, where U_b and U_s are the superficial velocities of each phase.

Muzychka [8] suggested using the wetted area instead of superficial tube area when reducing data of gas-liquid Taylor flow, as presented in definition (3.5):

$$q_s^* = \frac{QD}{k(\alpha_L A_w)(T_w - T_i)} \quad (3.5)$$

where $\alpha_L = L_S / (L_S + L_b)$ is liquid fraction as shown in Fig.3.1. In addition to this definition, the dimensionless slug length L_S^* will be used instead of the traditional dimensional tube length, which can be defined as:

$$L_S^* = \frac{L_S/D}{Pe_D} \quad (3.6)$$

Here the Peclet number Pe_D is defined using the maximum flow velocity U of both phases when the liquid phase superficial velocity u is divided by liquid fraction α_L :

$$Pe_D = \frac{UD}{\alpha} = Re_D Pr \quad (3.7)$$

In same manner, the Nusselt number for Taylor flow will be defined based on actual wetted tube area. Experimental data from several publications [3-5] and the new experimental data will be analysed accordingly using:

$$\overline{Nu}_D = \frac{QD}{k(\alpha_L A_w) \Delta T_{LMTD}} \quad (3.8)$$

The experimental data will be validated with a simple model which captures the expected behavior of segmented flow in gas-liquid flows. The model was first proposed by Muzychka [8]

based on earlier analysis by same author [20]. The model combines the two asymptotes for the entrance and fully developed regions:

$$q^* = \left(\left(\frac{1.614}{L_S^{*1/3}} \right)^{-3/2} + \left(\frac{L_S/L}{4L_S^*} \right)^{-3/2} \right)^{-2/3} \quad (3.9)$$

More details can be found in [8].

3.4 Experimental Setup

An experimental setup was assembled to measure heat transfer enhancement in mini scale tubes as shown in Fig. 3.2. The experimental setup has been equipped with two programmable syringe pumps (Harvard Apparatus) with a total capacity 200 ml each. The Harvard pumps are engineered to provide flow accuracy within 0.25 % and reproducibility within 0.05 %. A copper tube of mini-scale dimensions (1.63 mm ID) was kept horizontal to avoid gravity effect on the flow characteristics. A Fisher Scientific 3013 ISO-Temp thermal bath which is PID controlled has been used to provide constant temperature at 40 C° with stability of ± 1 % over a range of -30 to 200 °C

Two Omega T-type thermocouples are employed within T-junctions to measure inlet and outlet bulk temperatures of the flow. The thermocouples were carefully shielded to minimize heat transfer from other external sources such as the circulating bath. Flow patterns for the Taylor flow were captured using a high-speed camera (Phantom v611) as shown in Fig. 3.1. Since the present study requires running experiments at specified ratios of L_S/L over a range of slug regimes, this task needs to be conducted using varied sizes of junctions in order to obtain various slug lengths at the same running conditions. An accurate flow cell configuration measurement was performed using image processing software (ImageJ Software).

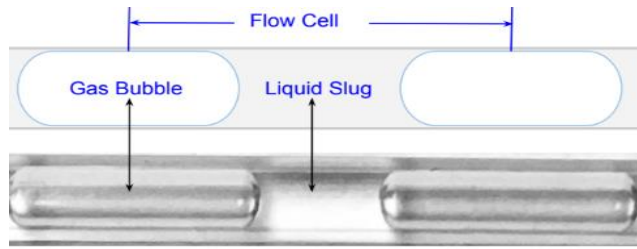


Figure 3.1 gas-liquid flow cell in a mini-scale tube

The experiments were run using 1 cSt silicone oil and air which forms the segmenting media to create a two phase Taylor flow. Low viscosity silicone oil was picked to obtain desired slug length ratios using several types of junctions.

Fig. 3.3 shows gas-liquid Taylor flow with various slug ratios. Furthermore, captured images show a very thin liquid film at the wall when using 1 cSt silicone oil as carrier phase, Fig. 3.1. The effect of liquid film on heat transfer becomes more pronounced in higher viscosity fluids [2,5, 22]. Careful design of the experiment was a priority to insure obtaining the desired results. Once benchmarked, we investigated experimentally the Taylor flow regime in a tube of 1.63 mm tube diameter using 1 cSt silicone oil segmented by air. With an stable slug and plug lengths, the desired slug regime was found to be over a range of Reynolds numbers from 50 to 312.

Heat transfer measurements were benchmarked by carrying out measurements of single phase flow under a constant wall temperature 40 °C. The tests covered a wide laminar flow range. Hence, the experimental data in Fig. 3.4 show results compared with the Graetz flow model. Agreement is within +/- 10 percent. A detailed uncertainty analysis is performed in the next section.

A straight copper tube of 1.63 mm ID with 50 and 100 mm lengths were employed for all the studies. Moreover, to keep the experimental data in the range of the asymptotic models, slug lengths were controlled to maintain the ratio of L_S/L approximately fixed while we varied the Reynolds number.

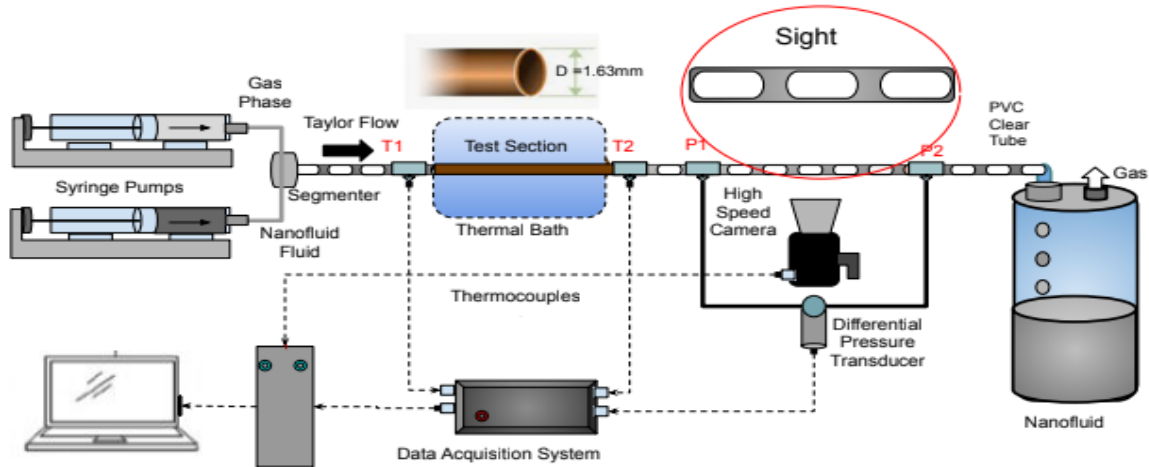


Figure 3.2 experimental setup for gas-liquid Taylor flow in straight tube subjected to isothermal condition

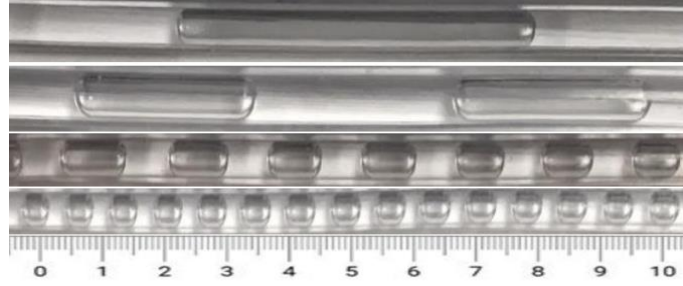


Fig. 3.3 high speed camera images for gas-liquid Taylor flow of void fraction $\alpha = 0.5$

In addition, the liquid fraction α_L throughout these experiments was maintained constant at 0.5. The results demonstrated more consistency with the asymptotic developed by Muzychka [8]. Additional experimental data from [4] and [5] have been re-analyzed for comparison and validation purposes. Table 3.1 contains some important experimental parameters which have been mentioned for comparison.

Kline & McClintock [19] has been used to predict experimental uncertainty. The root mean squared percentage error (RMSPE) has been employed to measure how well the data agree with Poiseuille theory. The uncertainties were found to be $\pm 1.75\%$ for L^* , while the uncertainty of the dimensionless heat transfer parameters was found to be ± 2.25 to 3.84% for Nusselt number and ± 1.54 to 1.91% for dimensionless heat flux q^* . The root-mean-square error (RMSPE) was used to estimate the error in the benchmark test of single phase flow over a range of Reynolds number from 20 to 1260. The results revealed low values of error for both parameters, 9.6% and 6.5% respectively.

Table 3.1 Summary of Published Experimental Data Compared with Present Data

Parameter	Oliver [3]	Horvath [4]	Vrentas[5]	Naraynan[19]	Present study
D	6.35	2.32 mm	9.5 mm	1 mm	1.63
L	914.4 mm	600.32 mm	1216 mm	40 mm	100, 50 mm
L/D	144	260	128	40	61, 30.5
Re_D	977-1362	30-220	0.7-15.8	1396-2135	50-312
Pr	10	1700	1000	5.5	16.5
α	0.61-0.85	0.5	0.913-0.984	0.205-0.480	0.5
L_S^*	0.07-0.47	0.03712 - 0.464	0.001-0.058	1.92-6.1	4 - 30.1
N	1-100	6.0-80	2.0-12	2.0-10	1.6 - 11
Type	Gas-liquid	Gas-liquid	Solid-liquid	Gas-liquid	Gas-liquid

3.5 Results and Discussion

This section presents the experimental results obtained for gas–liquid Taylor flows. The flows were subject to a constant wall temperature boundary condition using the experimental test facility presented in Fig. 3.2. The study provides an experimental data within thermally developing and developed regions of the test section. The discussion will address heat transfer enhancement of gas-liquid Taylor flow presented in dimensionless forms. Several junctions with different sizes and shapes have been used to create various slug ratio L_S/L and the new results were compared with published results from [4] and [5]. The new experimental data were validated by a comparison with predictive model has been developed by Muzychka [8].

Figs. 3.4 and 3.5 show three experimental data sets of dimensionless heat flux q^* as a function of dimensionless tube length L^* for the two tube lengths which were used. Reynolds numbers varied from 52 to 312 for each set of data. The wetted area of tube surface has been used to calculate heat transfer through the heated wall.

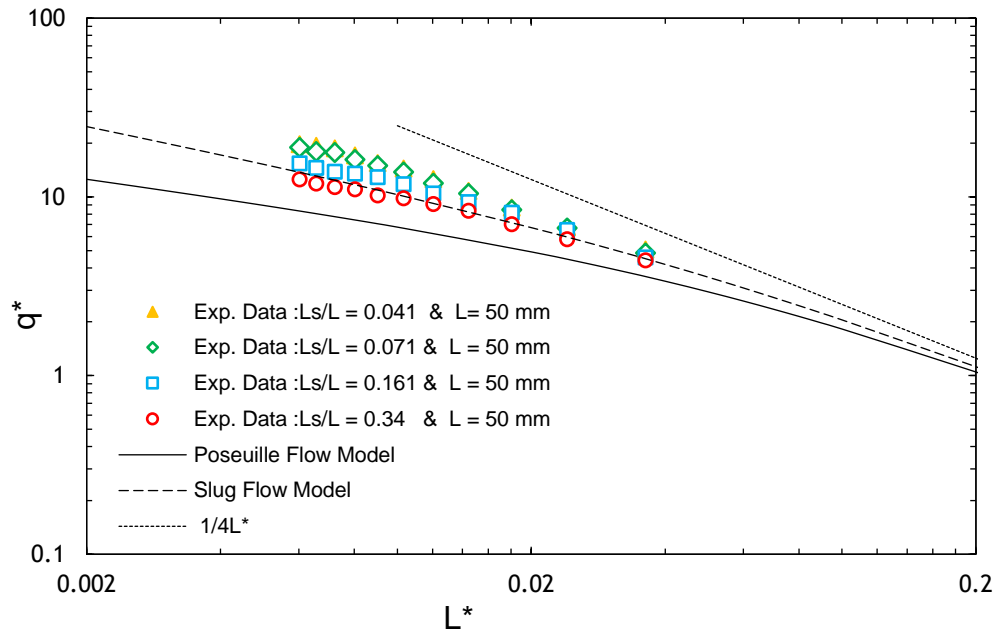


Figure 3.4 effect of slug length on dimensionless heat flux in a 50 mm tube length and varying Reynolds numbers.

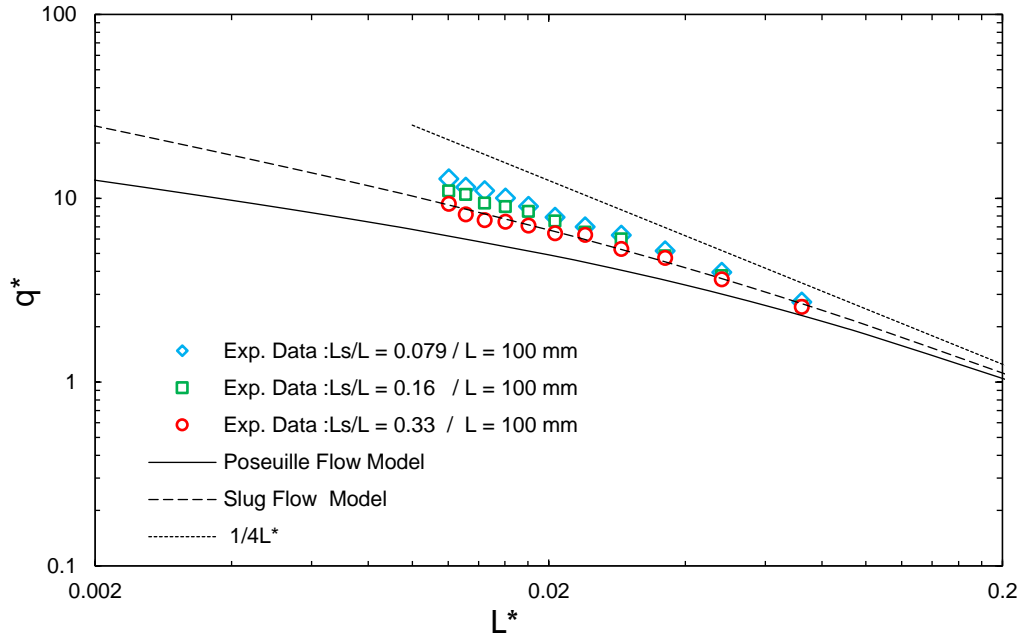


Figure 3.5 effect of slug lengths on dimensionless heat flux in a 100 mm tube length and varying Reynolds numbers.

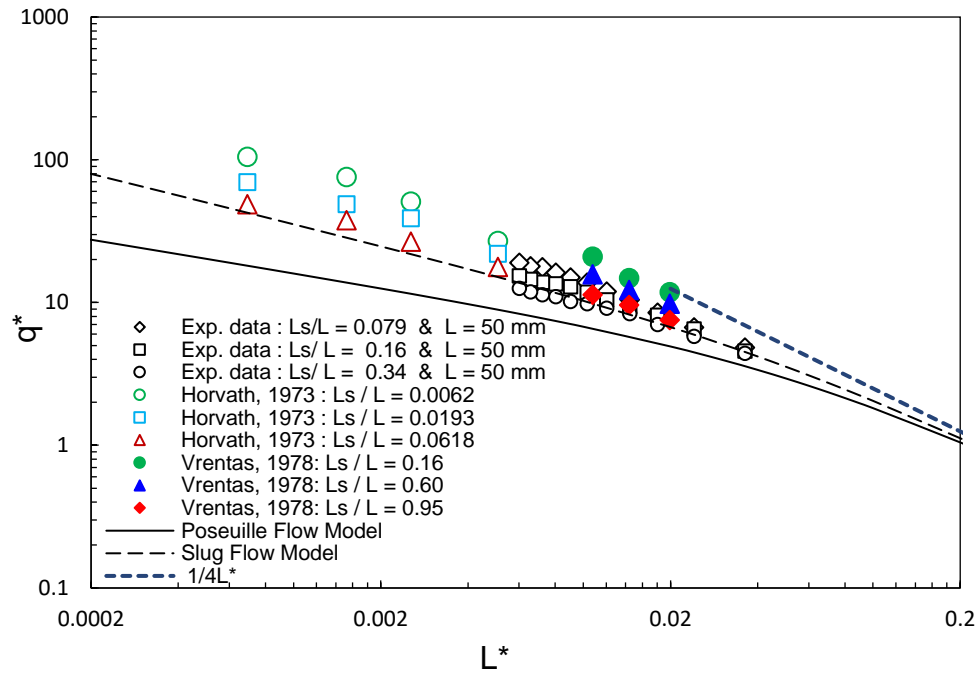


Figure 3.6 dimensionless heat flux data compared with published data [3,4] for varying Reynolds numbers.

Fig. 3.6 shows the new experimental data were compared with an experimental data of Horvath [4] and Vrentas [5]. It can be observed that reducing the data in this manner shows the effect of both increasing Reynolds number as well as slug length variation. To model this behavior a different way of data analysis is required to provide a better understanding to thermal performance of Taylor flow in mini / micro scale channels. Fig. 3.7 shows results for Nusselt number in our region of interest.

Figs. 3.8 and 3.9 present several data sets of Nu_D versus dimensionless tube length L^* . These data were obtained by changing liquid slug length and maintaining the Reynolds number constant. Obviously, heat transfer enhancement is obtained over a range of slug lengths varying from $0.04 < L_s/L < 0.33$. However, the experimental observations revealed that, heat transfer rates within liquid slugs are inversely proportional with slug length, while the wetted tube area $\alpha_L \pi DL$ is considered in calculating heat flux.

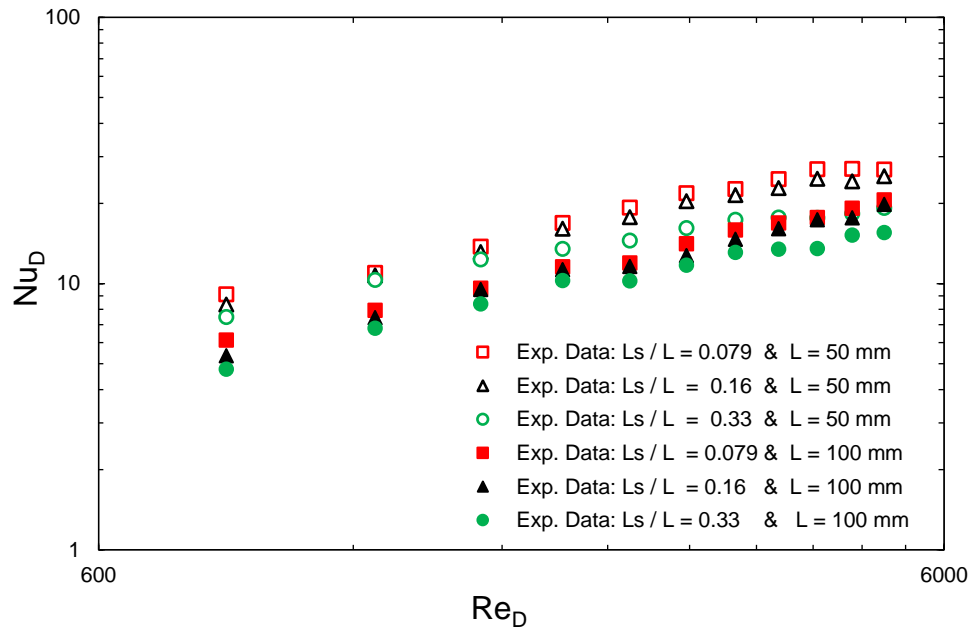


Figure 3.7 Nusselt number data of gas-liquid flow of various slug lengths plotted versus Figure 3.8 effect of slug lengths on Nusselt number data for a 50 mm tube length and constant Reynolds number.

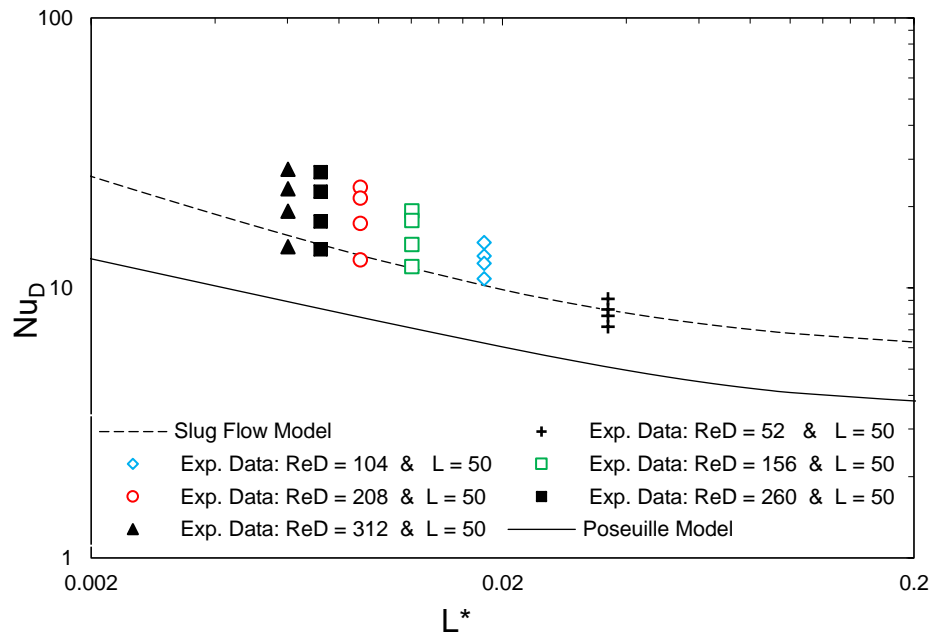
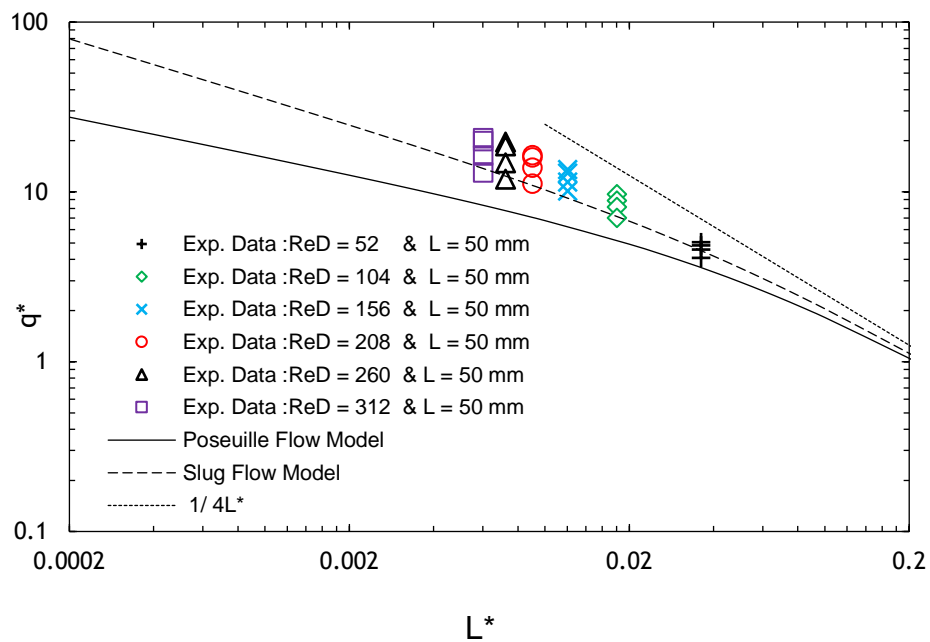


Figure 3.9 effect of slug length on Nusselt number data for a 100 mm tube length and constant Reynolds number for each set.



Figs. 3.10 and 3.11 show heat transfer data when dimensionless heat flux q^* is introduced to non-dimensionalized the data. The data were obtained by varying slug length and maintaining Reynolds number constant. This method of analysis has been shown to be better to demonstrate the effect of slug length variation on heat transfer rates. However, enhancement of heat transfer was consistently related with decreasing liquid slug length of gas-liquid Taylor flow.

Fig. 3.12 shows a dimensionless heat flux data q^* compared with published data from Horvath [4] and Vrentas [5]. The experiments were conducted using several junctions at constant Reynolds number for each set of data. Fig. 4.13 shows Nusselt number data as function of Peclet number when slug length is varying and maintain Reynold number constant.

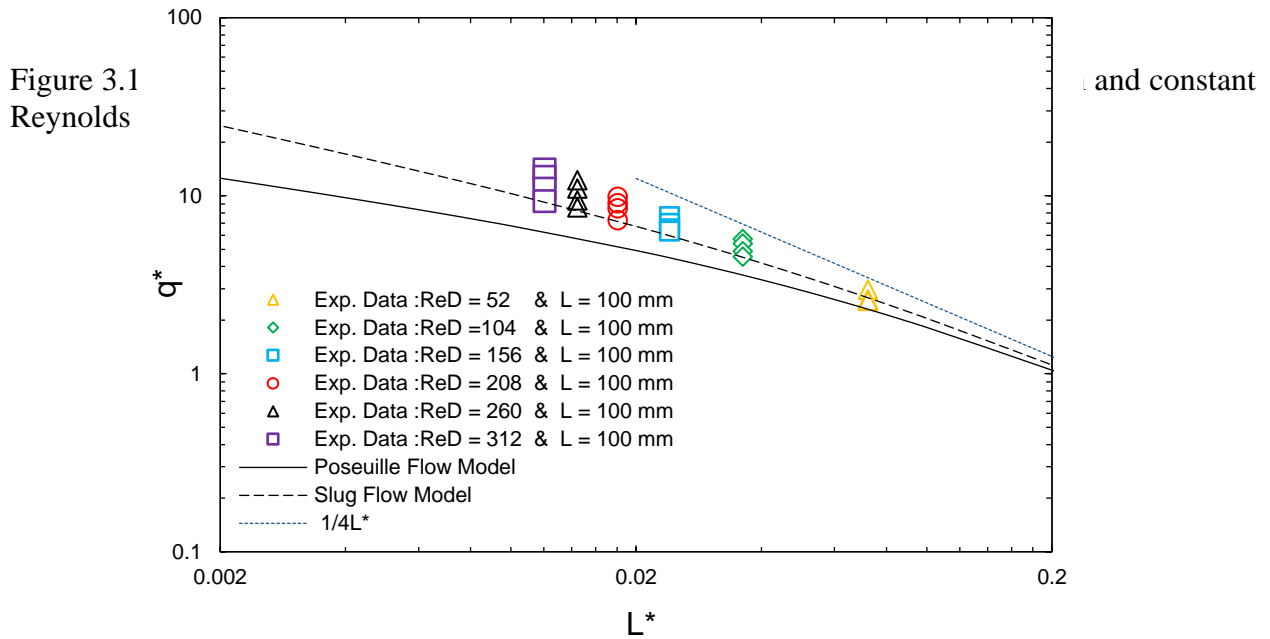


Figure 3.11 effect of slug length on dimensionless heat flux in a 100 mm tube length and constant Reynolds number.

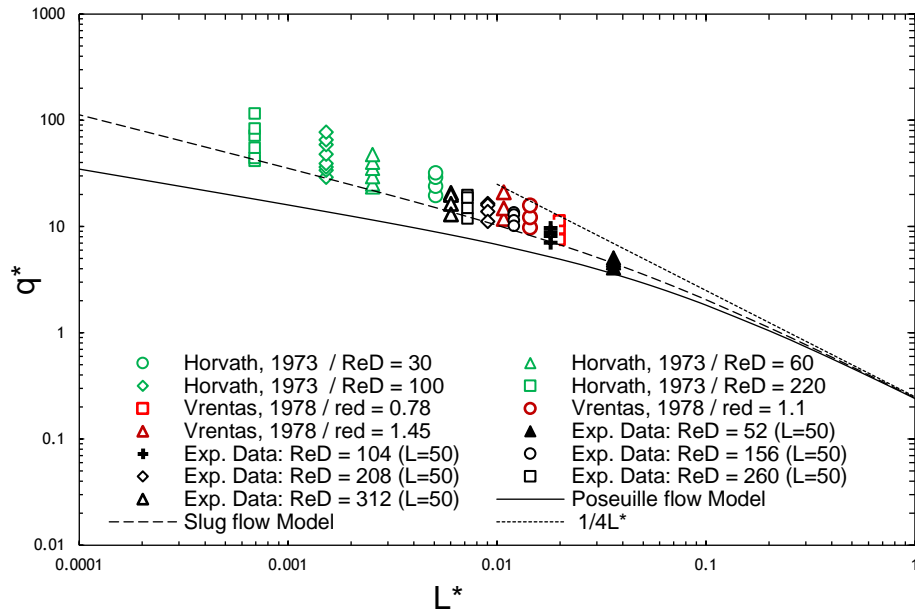


Figure 3.12 effect of slug length on dimensionless heat flux data in a 50 mm tube length and constant Reynolds number

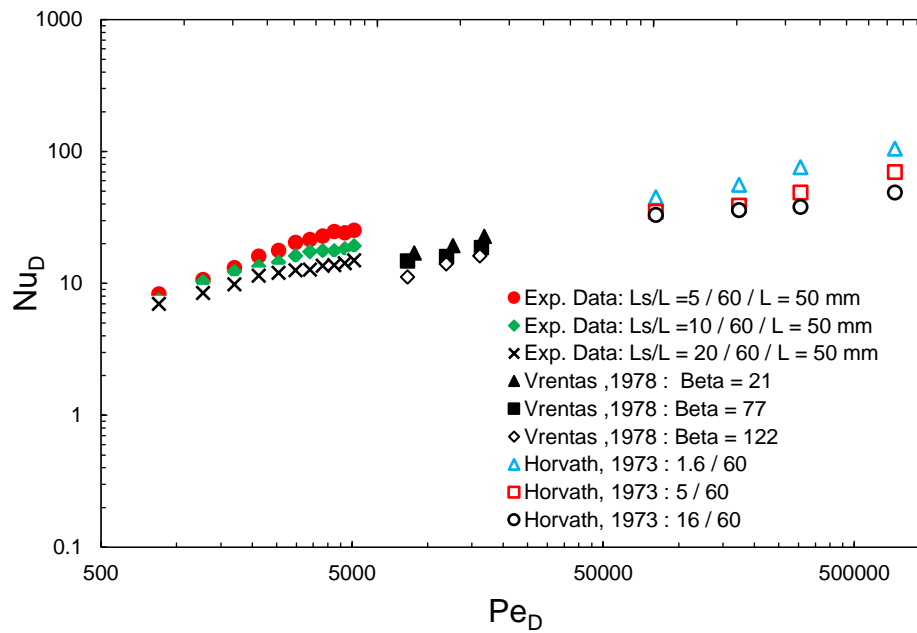


Figure 3.13 experimental data compared with published data from [4,5] for constant Reynolds numbers.

The new experimental data were compared with the Graetz slug flow model in Figs. 3.4 and 3.5 using the nominal dimensionless duct length L^* . The same data have been re-analysed by taking to account slug ratio L_s/L using the approach presented in [8]. The results in Figs. 3.14 and 3.15, are distributed nicely on the three asymptotes which maintain L_s/L constant. However, they are same data shown in Figs. 3.4 and 3.5. The data analysis demonstrates the level of thermal saturation, and hence their deviation from the Graetz-Leveque asymptote at smaller L_s^* . Slug lengths were controlled carefully to demonstrate this characteristic of Taylor flow over a wide range of Peclet number from 850 to 5100.

The experimental results reveal that liquid slugs become thermally saturated more quickly as slug length approaches the internal diameter of tube. This observation was confirmed earlier by Muzychka [8] and Howard [14]. In the present work, three slug ratios (L_s/L) were examined: 0.04, 0.079, and 0.16 under isothermal conditions. Full details of slug generation in mini scale tubes can be found in [12].

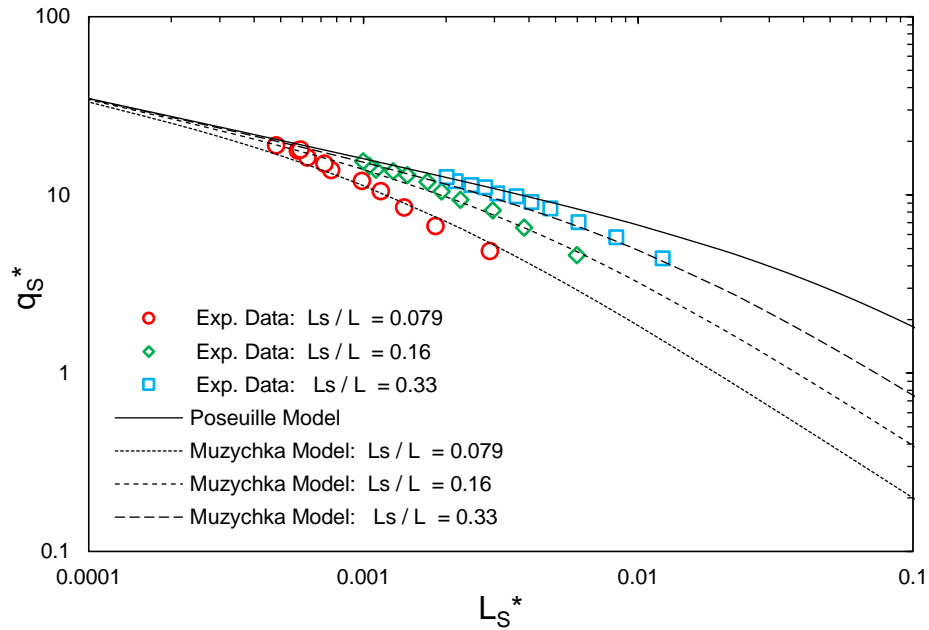


Figure 3.14 dimensionless mean wall heat flux data for various dimensionless slug lengths for a tube length of 50 mm compared with the model of Muzychka [8].

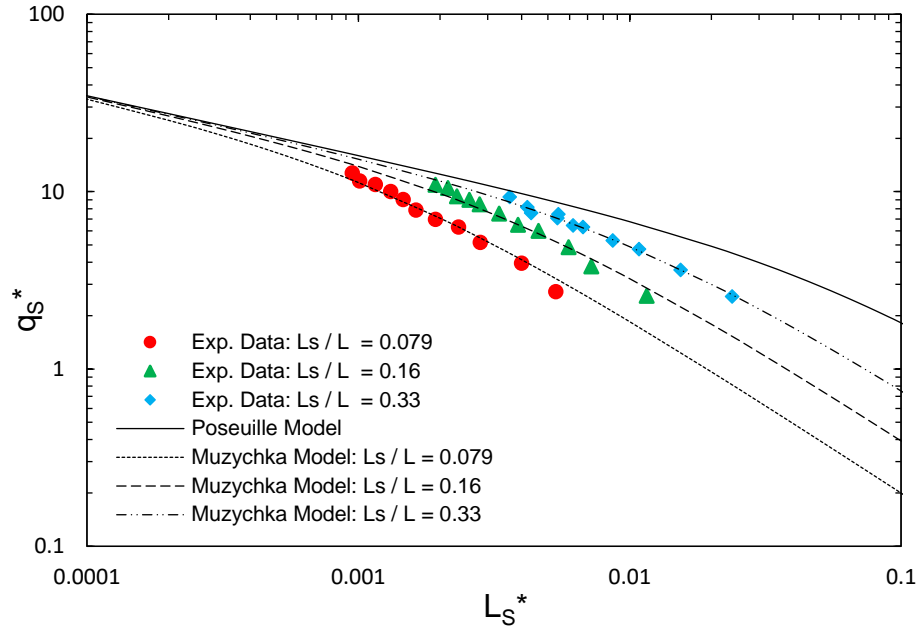


Figure 3.15 dimensionless mean wall heat flux data for various dimensionless slug lengths for a tube length of 100 mm compared with the model of Muzychka [8].

Finally, it is easy to conclude that shorter plugs which have stronger internal circulations and longer residence times, achieve thermal saturation quite quickly, since the parameter L_s/L causes the asymptote to move to the left as this ratio decreases. The parameter L_s/L was shown to be quite important to explain thermal behaviour of Taylor flow in [8].

3.6 SUMMARY AND CONCLUSIONS

Gas-liquid Taylor flow in mini scale tubes having a constant wall temperature was considered. New experimental data was carefully obtained using 1 cSt silicone oil and segmented by air with fixed liquid fraction $\alpha_L = 0.5$. The liquid slug ratio L_s/L showed significant effect on the thermal saturation of Taylor flow. The current data were compared with a model which considers both asymptotes of entrance and fully developed flow regions. Further Taylor flow data sets from the literature were also re-analyzed to cover both asymptotic regions. The thermal behavior of all gas-liquid Taylor flow data was presented in short and long residence times. Finally, this study with the new insights presents an archival content in heat transfer in mini scale tubes using gas-liquid Taylor flows.

3.6 References

- [1] Fairbrother F. and Stubbs, A.E., "Studies in Electro-endosmosis. Part VI. The Bubble-tube Method of Measurement", *Journal of the Chemical Society*, Vol. 1, pp.527-529, 1935
- [2] Taylor, "Deposition of a viscous fluid on the wall of a tube", *journal of Fluid Mechanics*. 10(1961) 161–165.
- [3] Oliver, D.R. and Young Hoon, A., "Two Phase Non-Newtonian Flow: Part 2 Heat Transfer", *Transactions of the Institution of Chemical Engineers*, Vol. 46, pp. 116-122, 1968.
- [4] Horvath, C., Solomon, B.A., Engasser, J.M., "Measurement of Radial Transport in Slug Flow Using Enzyme Tubes", *Industrial and Engineering Chemistry, Fundamentals*, Vol. 12, no. 4, pp. 431-439, 1973.
- [5] Vrentas, J.S., Duda, J.L, and Lehmkuhl, G.D., "Characteristics of Radial Transport in Solid-Liquid Slug Flow", *Industrial and Engineering Chemistry, Fundamentals*, Vol. 17, no. 1, pp. 39-45, 1978.
- [6] Maddox D. E., Mudawar I., "Single- and Two-Phase Convective Heat Transfer from Smooth and Enhanced Microelectronic Heat Sources in a Rectangular Channel", *Journal of Heat Transfer*, ASME NOVEMBER 1989, Vol. 111 p. 1045.
- [7] Betz A. R., Attinger D., "Can Segmented Flow Enhance Heat Transfer in Microchannel Heat Sinks", *International Journal of Heat and Mass Transfer*, 53, pp. 3683-3691, 2010.
- [8] Muzychka, Y.S., "Laminar Heat Transfer for Gas-Liquid Segmented Flows in Circular and Non-circular Ducts with Constant Wall Temperature" ASME, 2014.
- [9] Muzychka Y. S., Walish E., "Simple Models for Laminar Thermally Developing Slug Flow in Noncircular Ducts and Channels" *Journal of Heat Transfer*, ASME, November, 2010, Vol. 132 / 111702-1.
- [10] Muzychka Y. S., Walsh E. Walsh P. "Heat Transfer Enhancement Using Laminar Gas-Liquid Segmented Plug Flows" *Journal of Heat Transfer*, 2011 by ASME, APRIL 2011, Vol. 133 / 041902-1.
- [11] Walsh, P., Walsh, E., and Muzychka, Y.S., "Heat Transfer Model for Gas-Liquid Slug Flows Under Constant Flux", *International Journal of Heat and Mass Transfer*, Vol. 53 (15-16), pp. 3193-3201, 2010.

- [12] S. Hase, "Characterisation of Gas-liquid Two-phase Flow in Mini-channels with Co-flowing Fluid Injection inside the Channel, part II: Gas Bubble and Liquid Slug Lengths, Film Thickness, and Void Fraction within Taylor Flow", *International Journal of Multiphase Flow*, 88, 2017, pp. 251–269.
- [13] Adrugi, W., Muzychka, Y.S., and Pope, K., "Heat Transfer in Liquid-Liquid Taylor Flow in Mini-scale Curved Tubing for Constant Wall Temperature," ASME-IMECE-2015-67700, 2016.
- [14] J. Howard A. and Walsh P. A., "Heat Transfer Characteristics of Liquid-Gas Taylor Flows incorporating Microencapsulated Phase Change Materials" *Journal of Physics: Conference Series* 525 (2014) 012022.
- [15] Hughmark, G.A., "Holdup and Heat Transfer in Horizontal Slug Gas-Liquid Flow", *Chemical Engineering Science*, Vol. 20, pp. 1007-1010, 1965.
- [16] Talimi V., Muzychka Y. S., Kocabiyik S., "A Review on Numerical Studies of Slug Flow Hydrodynamics and Heat Transfer in Microtubes and Microchannels", *International Journal of Multiphase Flow*, 39, pp. 88-104, 2012.
- [17] Muzychka, Y.S. and Ghobadi, M. "Measurement of Laminar Heat Transfer Coefficients in Micro and Mini Scale Ducts and Channels", Proceedings of the 2014 IC-NMM, Chicago, IL, 2014.
- [18] Oliver, D.R. and Wright, S.J., "Pressure Drop and Heat Transfer in Gas-Liquid Slug Flow in Horizontal Tubes", *British Chemical Engineering*, Vol. 9, pp.590-596, 1964.
- [19] Kline, S. J., and F. A. McClintock. "Describing Uncertainties in Single-Sample Experiments." *Mechanical Engineering*, Vol. 75, No. 1, January 1953: 3-8.
- [20] Narayanan. C, Lakehal D., "Two-phase convective heat transfer in miniature pipes under normal and microgravity conditions", *ASME Journal of Heat Transfer*, 130 (2008) 074502-1–074502-5.
- [21] Muzychka, Y.S., "Generalized Models for Laminar Developing Flows in Heat Sinks and Heat Exchangers", *Heat Transfer Engineering*, vol. 34 (2-3), pp. 178-191, 2013.
- [22] Prothero, J. and Burton, A.C., "The Physics of Blood Flow in Capillaries: 1 The Nature of the Motion", *Bio-physical Journal*, Vol. 1, pp. 565-579, 1961.

- [23] Giolla M. M. Eain A., Vanessa E., Punch J., “Local Nusselt number enhancements in liquid–liquid Taylor flows”, *International Journal of Heat and Mass Transfer*, 80 (2015) 85–97.
- [24] K. Alrbee, Y.S. Muzychka and X. Duan, “Heat Transfer enhancement in laminar Graetz and Taylor Flows using nanofluids” ASME-ICNMM2018-7756.

CHAPTER 4

HEAT TRANSFER OF GAS-LIQUID TAYLOR FLOW IN COILED TUBE WITH CONSTANT WALL TEMPERATURE

4.1 Introduction

An experimental study on Taylor flow was conducted in mini scale tube that are subjected to a constant wall temperature. In particular, the study will investigate thermal characteristics of segmented slug / Taylor flows in coiled tube. Gas-liquid flow will be addressed in present study to highlight the effect of several parameters such as, effect of tube curvature R , liquid slug ratio L_s/L and Prandtl number Pr . Then, the experimental results will be employed to propose new predictive correlation. A survey on laminar flow in mini scale channels has revealed that two research areas require to be addressed as both relate to the present study. Effect of slug ratio γ on heat transfer augmentation in segmented slug / Taylor flows and curvature of the test section. In addition, development a new model to predict the thermal behavior of gas-liquid Taylor flow that responds to all required parameters for cooling system design.

Essentially, the fundamentals of current study have been obtained from early studies by Muzychka [1] and Ghobadi-Muzychka [2-6] for single phase in coiled tube.

**The materials in this chapter are intended to be submitted to Journal of Heat Transfer.*

Their experimental study showed an augmentation in heat transfer rates in coiled tube as a passive enhancement due to a secondary flow which is proportional to tube curvature $1/R$. Their study resulted in an asymptotic correlation valid up to Dean number $De = 700$. Besides to that, Muzychka [1] show heat transfer augmentation in segmented Taylor / slug flow as predictable based on liquid slug ratio L_S/L . His theoretical model was developed by combining two asymptotes of fully developed and entrance regions. The model demonstrated a potential of predicting heat transfer enhancement. Thus, liquid slug shortening leads to an increasing heat transfer rate as liquid slugs approaches tube diameter $L_S \sim D$. The boundary layer assumed to be dominant in shorter slugs and is one of the important characteristics of the proposed model to show that thermal saturation is reached more quickly for shorter liquid slugs.

The published literature has shown that Taylor flow remarkably enhances heat transfer [8-13,23]. Although, segmented flows at micro and mini-scales have emerged as a fundamental research area in recent years [13-17] they are conceptually not new. The resurgence of research in non-boiling two phase plug flows has been motivated by the desire to increase heat transfer rates in compact liquid cooled systems. One of the authors considered much of the early work in a recent journal publication along with new data obtained with his collaborators [11]. A significant observation of this work was the fact that heat transfer in segmented flow behaves in a manner like thermal boundary layer flow and that heat transfer scales with the liquid plug length. A re-analysis of the old data showed that much of the data could easily be predicted with a simple Leveque model [11] over most of the data range. What was not considered in this work was the phenomena of thermal saturation which occurs when short plugs have a long residence time, since much of the data did not display this characteristic.

In general, studying two phase segmented flow of gas-liquid components was originally started by Fairbrother and Stubbs, [18], followed by Taylor [19]. Oliver et al [2], Horvath et al [9] and Vrentas et al [10]. Later, Maddox and Mudawar [20] investigated single and two-phase forced convection of a simulated microelectronic heat source to assess the feasibility of cooling. Betz and Attinger [12] performed experiments on a compact microchannel cooling system with both single and two-phase flows. They observed that segmented flow significantly enhanced heat transfer, by up to 140 % in a microchannel heat sink as compared with single-phase flow at same liquid flow rate. Walsh et al [14] measured the local Nusselt numbers using infrared thermography in both

entrance and fully developed flow regions. The results indicate that optimized slug geometries can yield up to an order of magnitude heat transfer enhancement.

Additional studies examining heat transfer rates in non-boiling two-phase Taylor / slug flows were those of Vrentas et al [10] and Prothero and Burton [21]. In one of series of studies [21] they compared heat transfer rate of single phase Graetz flow with that of a segmented gas-liquid stream. While, Prothero and Burton [21]. were able to show enhancement over the single phase flow, they did not assess the effect of liquid slug length. In recent years, the experimental and theoretical analysis of heat transfer in gas-liquid Taylor/slug flow has received much attention. however, more aspects have been investigated. Several attempts were introduced by [1, 11, 14] to develop theoretical and experimental correlations. Furthermore, significant studies aimed to achieve greater heat transfer enhancement by adding different materials such as nanoparticles [22] or PCM [17]. Additional studies were concerned with the potential of heat transfer enhancement using liquid-liquid Taylor flow [5,7,31].

In many experiments the liquid slug ratio L_S/L is not held constant while the Reynolds number is varied [8-10]. However, in some cases such as in Betz and Attinger [12] the ratio is approximately maintained such that a mean value may be used for comparison. Other issues pertaining to the use of the Nusselt number versus dimensionless mean wall flux will also be addressed. Nusselt number and dimensionless mean wall flux for segmented gas-liquid Taylor flow will be considered in this paper. The actual wetted tube area along with maximum flow velocity are used to present heat transfer enhancement.

Oliver and Young [8] performed a study for controlling slug length. Later, the flow rates of both phases were increased to produce annular flow for comparison purposes. They aimed to investigate thermal and hydrodynamic behavior of gas liquid two phase flow of non-Newtonian liquids under a constant wall temperature. They highlighted the importance of liquid slug lengths as a significant variable controlling heat transfer. Their results were benchmarked by carrying out measurements of single phase laminar flow. A non-dimensional analysis was used to present heat transfer data for Nusselt number as a function of Graetz number. Moreover, their study covered a wide range of Reynolds numbers including different flow regimes of gas liquid two phase flow. Clearly, they reported an increase in heat transfer over the single phase flow for the slug flow regime including different flow regimes of gas liquid two phase flow.

Oliver and Wright [25] conducted a series of measurements to investigate the effect of plug flow on heat transfer and friction in laminar flow. They surmised that the internal circulation would increase the heat transfer coefficient significantly, and therefore one would not be able to use Graetz-Leveque theory. They attributed the increase in heat transfer coefficient to both the effects of internal circulation and increased liquid velocity that results at constant mass flow rates due to the void fraction. They concluded that the effect due to void fraction is independent on plug length but that circulation effects would be strongest for shorter plugs. They reserved the assessment of plug length for a later study since the apparatus they used to collect data could not control liquid plug lengths very well. As part of their study, Oliver and Wright [25] did develop simple correlations based upon their experimental data and modification of the Graetz-Leveque model.

Horvath et al. [9] examined the potential of heat within slug flow of gas-liquid. Their experiments were conducted using liquids having high Prandtl numbers and liquid fractions of 0.5. They presented their results as a Nusselt number for the liquid plugs as function of the aspect ratio L_S/D . The effect of slug velocity was studied by varying the two phase flow Reynolds number at same liquid fraction. They also reported that liquid slugs are getting thermally saturated at lower aspect L_S/D . They conclude that due to increase of radial mixing within short slugs.

Using the carved / coiled tube to achieve passive heat transfer enhancement in laminar flow was merged early by Dean [27, 28]. These were the first analytical studies of fully developed laminar flow in a curved tube of circular cross section. A series of theoretical solutions were developed for the Poiseuille flow in the straight tubes at low Dean number $De < 17$. The study established that, pressure gradient in curved circular tube independent of the curvature. To show the opposite, the analysis was modified by including the higher-order terms and was able to show that a reduction in flow due to curvature depends on a single variable named as the Dean number. Other authors have reported a different definition of the Dean number De for curved tube. For low Dean numbers, the axial-velocity profile was parabolic and unaltered from the fully developed straight tube flow. As the Dean number is increased, the maximum velocity begins to be skewed toward the outer periphery.

Alrbee and Muzychka [22] obtained new data to show additional heat transfer enhancement in mini scale channels. They considered nanofluids at various concentrations in the liquid phase. Nanofluids were prepared with several standard concentrations of 0.25, 0.5 and 1 vol %, using Aluminum Oxide Al_2O_3 and water as base fluid.

They reported significant heat transfer enhancement when nanofluids were segmented by air bubbles to form a gas-liquid Taylor flow. The results showed that the enhancement was associated with nanofluid concentration as well as liquid slug length. A similar attempt to enhance heat transfer rates was conducted by Howard and Walsh [17]. They investigated the potential of heat transfer enhancement associated with gas-liquid Taylor flows incorporating microencapsulated phase change materials. However, they conclude the enhancement is due to the internal circulations within liquid slugs as well as increasing thermal capacity of liquid which is due to adding PCM. An experimental test facility was developed which had a heated test section and allowed MPCM-air Taylor flows to be subjected to a constant heat flux boundary condition. Heat transfer enhancement was examined by changing liquid slug length and liquid fraction. The results revealed higher heat transfer rates when compared with the Graetz solution for conventional single phase coolants.

Additional studies were preformed by Adrugi and Muzychka [5] and [7] on segmented / Taylor flow of liquid-liquid using coiled tube. Their investigations considered the homogeneous approach to demonstrate heat transfer enhancement in mini scale coiled tubes subjected to a constant wall temperature. Thus, the experimental methods were employed to present an effect of several parameters like, tube curvatures and length beside to Prandtl number Pr for the flow mixture of the segmented liquid-liquid Taylor flow. Several experimental and theoretical studies were concerned with fundamentals of laminar flow in mini / micro channels [24, 32] and provided the base for the field of research.

4.2 Theory of Data Analysis

The collected data of inlet and outlet temperatures along with fluid flow rates have been used to demonstrate heat transfer of gas-liquid Taylor / slug flow in curved tubing, which utilizes the fundamentals of Graetz theory for slug flow under a constant wall temperature [32]. The convection heat transfer in flow direction can be obtained by conducting energy balance between inlet and outlet flow as:

$$\dot{Q} = \dot{m}cp(T_o - T_i) \quad (4.1)$$

Then, main wall heat flux can be determined as:

$$\bar{q} = \frac{Q}{\alpha_L A_w} \quad (4.2)$$

To non dimensionalize data when the wetted area is considered, Muzychka [1]. Then, dimensionless main wall heat flux q^* and Nusselt number Nu_D can be defined by (3) and (4);

$$q^* = \frac{QD}{k(\alpha_L A_w)(T_w - T_i)} \quad (4.3)$$

where $\alpha_L = Q_L / (Q_L + Q_G)$ presents the void fraction of Taylor flow. This assumption is valid for flow with unity slip ratio which has been verified over the range of the experiments Fig 4.1. Hence, liquid fraction $\alpha_L = \text{unity}$ for single phase flow calculations.

In the same manner, the Nusselt number for Taylor flow will be introduced based on actual wetted tube area. The experimental data will be analysed accordingly using:

$$\overline{Nu}_D = \frac{QD}{k(\alpha_L A_w)\Delta T_{LMTD}} \quad (4.4)$$



Figure 4.1 Shows flow segmentation of gas-liquid using 1 cSt oil and air bubbles. $\alpha_L = 0.5$ mm, and constant Reynolds number $Re_D = 104$ with liquid flow rate $Q = 8$ ml/min for tube radius 2cm.

The experimental results of single phase and gas-liquid Taylor flows in coiled tube were compared with an empirical correlation proposed for single phase flow in coiled tubes, Ghobadi and Muzychka [2]. The correlation was examined up to Dean number $De = 700$ including the developing and fully developed regions using the two asymptotes as:

$$Nu_D = \left[3.66^4 + \left(0.91375 \sqrt{De} Pr^{-0.1} \right)^4 \right]^{1/4} \quad (4.5)$$

The dimensionless heat transfer data of Nusselt number Nu_D and q^* were presented as a function of Dean number De . In some cases, the data were presented as function of L^* and Reynolds number Re_D . Dean number De is defined as:

$$De = Re_D \sqrt{\frac{D}{2R}} \quad (4.6)$$

where, R is radius of curvature, and D is the inside diameter of test section.

In general, the superficial flow velocity $U = U_L + U_G$ has been used here to calculate: the dimensionless tube lengths L^* , Reynolds number Re_D , and Dean number De as:

$$L^* = \frac{L/D}{Pe_D} \quad (4.7)$$

Peclet number Pe_D is calculated using maximum flow velocity along with the liquid phase properties as:

$$Pe_D = \frac{UD}{\alpha} \quad (4.8)$$

The formulation of laminar heat transfer of gas-liquid Taylor / slug flow in mini scale coiled tube was introduced by accounting for slug length in a proper way. This approach has been suggested by Muzychka [1] which provided a new insight on heat transfer analysis.

4.3 Experimental Setup and Procedure

The present study has been performed to demonstrate heat transfer augmentation due to flow segmentation and secondary flow in mini scale tubes. An experimental setup was assembled as shown in Fig. 4.3.

The experimental setup has been equipped with two programmable syringe pumps (Harvard Apparatus) with a total capacity of 200 ml each. The Harvard pumps are engineered to provide flow accuracy within 0.25 %. Several test sections of copper coiled tubing which have the same length were used to avoid effect of the entrance region on heat transfer rates, $L = 250$ mm and ID = 1.63 mm with different curvatures, $R = 10, 20$ and 40 mm, Fig. 4.2. The test section was kept horizontal to avoid the effects of gravity on the flow characteristics. A Fisher Scientific 3013 ISO-Temp thermal bath which is PID controlled has been used to provide constant temperature at 40 °C with stability of ± 1 % over a range of -30 to 200 °C. Ten temperature readings of each inlet

and outlet flows were received in data acquisition logger from two Omega T-type thermocouples were employed within T-junctions. Then, the average value was considered to reduce effect of errors.



Figure 4.2 Test sections of same length (250 mm) and three curvatures ($R= 10, 20$ and 40 mm)

Furthermore, thermocouples were carefully insulated to avoid being influenced by other sources. Flow patterns for the segmented flow were captured using a high-speed camera (Phantom v611) as shown in Fig. 4.1. Since the present study requires running experiments at several flow segmentations over a range of slug regime, this task needs to be conducted based on varied junction parameters (size, shape and flow direction) in order to obtain desired slug lengths at same running conditions Fig. 4.1. An accurate flow cell configuration measurement was available using image processing software (ImageJ Software). Furthermore, the segmented flows were monitored at inlet and outlet to ensure flow segmentation stability when passing through the coiled test section.

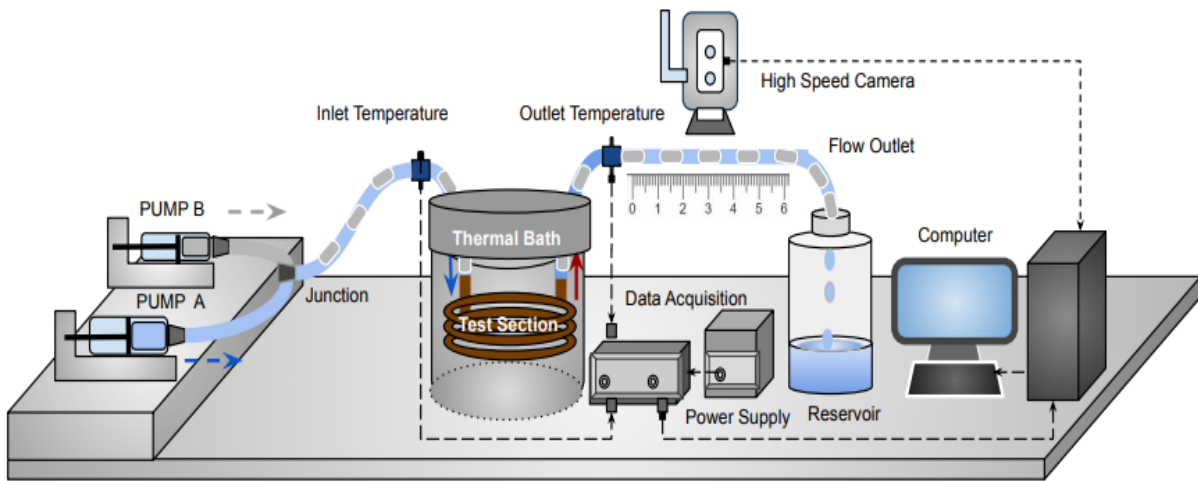


Figure 4.3 experimental set up of gas-liquid Taylor flow in mini scale curved tube

The experiments were run using two low viscosity silicone oils, 0.65, and 1 cSt. The flow was segmented regularly by air bubbles at fraction of $\alpha_L = 0.5$

The low viscosity liquids were picked to obtain desired slug length ratios L_S/L using several types of junctions presented in Fig. 4 2. Gas-liquid Taylor flow with various slug lengths L_S can be seen in Fig. 4.1. Furthermore, captured images show a very thin liquid film at the wall. The effect of liquid film on heat transfer becomes more pronounced for higher viscosity fluids [10, 19, 29]. Hence, the design of the experiment plays an important role to ensure obtaining the desired results. Taylor flow regime was experimentally applicable over a range of Reynolds numbers from 50 to 312 when using 1 cSt silicone oil.

Heat transfer measurements were benchmarked by carrying out measurements of single phase flow under a constant wall temperature $40C^o$. The tests covered a wide range of laminar flow. Hence, the experimental data in Fig. 4.4 show results compared with the Graetz flow model. Agreement is within +/- 10 percent or better. Uncertainty analysis root mean square percentage error of data will be addressed in next sections. The experimental observation using high speed camera images and image processing clearly showed very limited liquid film over the studied range of laminar gas-liquid Taylor flow. Consequently, the slip ratio β was verified to be near unity.

The uncertainty of gas-liquid Taylor flow measurements was estimated using the well-known methodology of Kline and McClintock [35]. The uncertainty of heat transfer measurements was estimated over a range of Reynolds numbers from 20 to 1265. The Kline and McClintock method [35] which requires first order derivatives in the root sum square method to estimate the experimental errors within the dimensionless parameters of interest. The uncertainties were found to be ± 1.75 % for L^* , while the uncertainty of the dimensionless heat transfer parameters was found to be ± 2.25 to 3.84 % for Nu_D and ± 1.54 to 1.85 % for q^* .

Root-mean-square percent error (*RMSPE*) has been employed to measure how well the proposed model is performing [36]. Typically, the difference between predicted and experimental data is measured. The root-mean-square percentage error (*RMSPE*) was determined based on predicted and observed data of Nusselt number Nu_D and dimensionless heat flux q^* [33]. Essentially, the results have been used as a benchmark test of the experimental setup of single phase flow using distilled water over a range of Reynolds number from 20 to 1265. The results revealed low values of error for both parameters, 9.6 % and 6.5 % respectively.

4.6 Results and Discussion

This section will be addressing the experimental results obtained in present study in distinguished manner takes the dimensionless form. Essentially, three main objectives next to the benchmark test will be in focus. The first objective to verify the base of heat transfer in coiled/curved tubes with single phase flow subjected to constant wall temperature. A comparison with a predictive model of Nusselt number Nu_D was developed early by Ghobadi-Muzychka [1]. Then, followed by obtained data for gas–liquid Taylor flows in coiled tube using the experimental facility presented in Fig. 4.2. The study provides data within thermally developing and developed regions of the laminar segmented flow using two low viscous fluids, 0.65 and 1 cSt silicone oils. The discussion will focus mainly on heat transfer augmentation due to: internal circulations within liquid slugs and effect of secondary flow as result of the tube curvature. Different methods of analysis have been considered to present heat transfer data in dimensionless forms.

As a part of this study to reference the possible ways to present heat transfer enhancement due to introducing gas bubbles to liquid flow stream in mini scale coiled tube. The study started with collecting results with single phase flows for comparison with Taylor flows. The study begins to investigate the main points: effect of curvature R , slug length L_s and Prandtl number Pr on heat transfer. Various curvatures and slug length ratios along with several types of liquids have been employed.

The results show that heat transfer enhancement is proportional to the ratio of slug length L_s/L and $1/R$. Several junctions have been used to create various slug lengths L_s as shown in Fig. 4.1. Besides this, three test sections having a different radius of curvatures 10, 20, and 40 mm were tested. A comparison has been made with predictive models for both single and slug flows.

Table 4. 1 summery of single phase experiments in coiled tube

Fluid cSt	Pr	ReD	R mm	L* *10-3	Ca *10-4	De
0.65 cSt	9.89	120-480	10	16-65	22-0.89	17-68
			20			24-97
			30			34-137
1 cSt	16.2	195-340	10	15-60	14-55	50-525
			20			37-371
			30			26-262

Fig. 4.4 shows a new experimental data of single phase using 1 cSt silicone oil was fed through three different curvatures, $R = 40, 20$ and 10 mm. Hence, the tube length L and diameter D were maintained constant at $L = 250$ mm and 0.00163 mm respectively, to avoid effects of the entrance region on heat transfer enhancement. Experimental data of Nusselt number Nu_D versus Dean number De have been compared with an experimental correlation which was developed by Ghobadi and Muzychka [1] for a spiral tube. The model was examined to up $De = 700$. Table 4.1 contains details on the experiments.

The results confirmed expanding the model [2] to be used for coiled tubes. $RMSPE$ was determined using predicted and observed data and the calculated error was: $RMSE = 9.2\%$. This finding can be observed in Fig. 4.4. Likewise, the same experimental data were presented in different manners as dimensionless heat flux q^* and Nu_D versus dimensionless tube length L^* and ReD , respectively. Figs. 4.5 - 4.6. show experimental data of single phase spread to demonstrate three levels of thermal enhancement which inversely proportional to radius of the coiled tubes R .

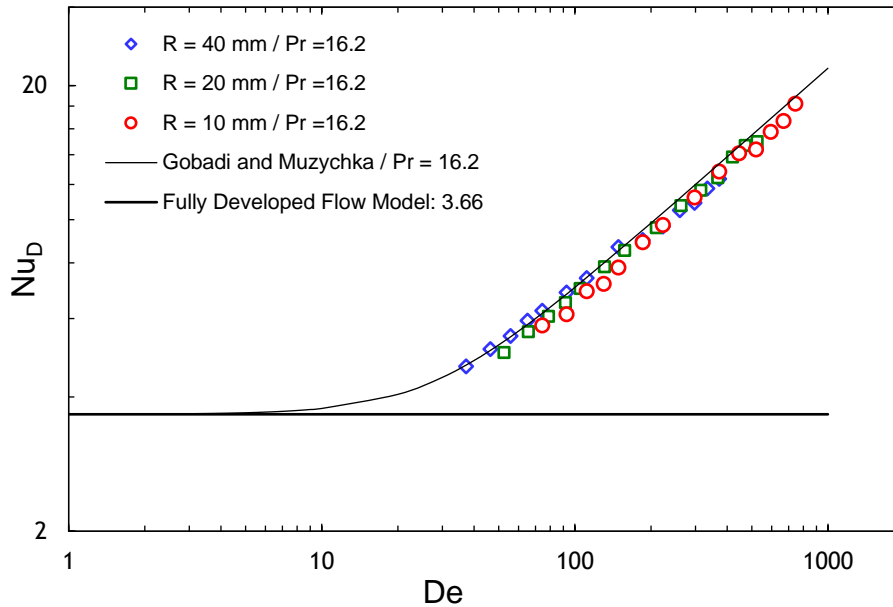


Figure 4.4 single phase data of 1 cSt oil compared with a model of Nusselt number for coiled tube developed by Ghobadi and Muzychka [2]

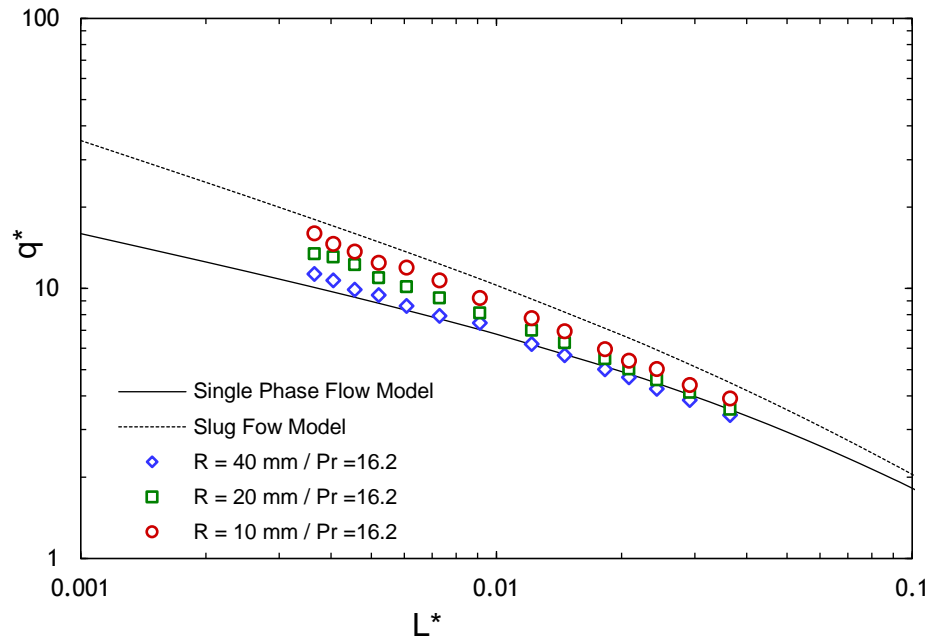


Figure 4.5 single phase data of 1 cSt oil compared with straight tube Graetz Poiseuille flow model to show the secondary flow effect.

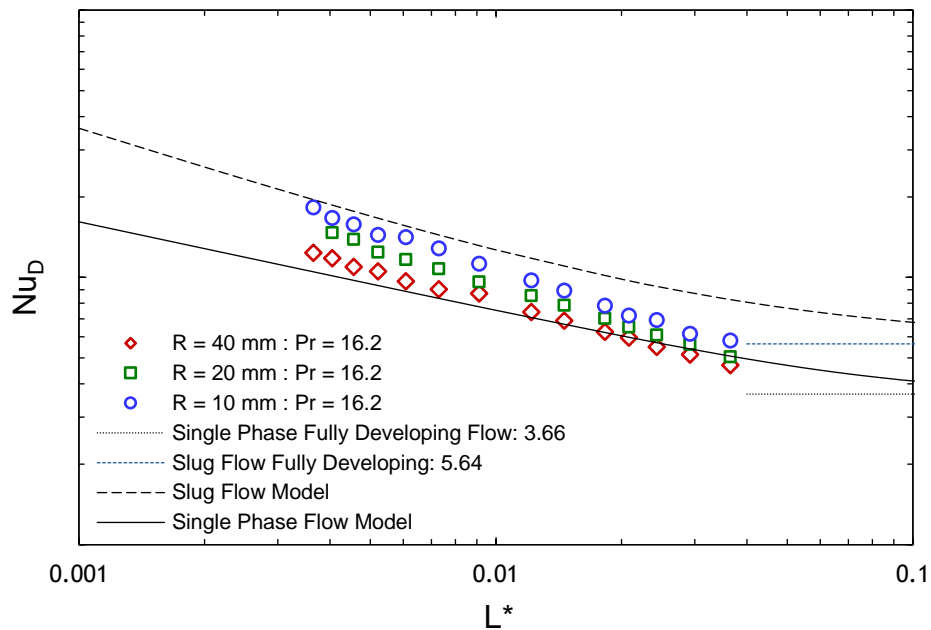


Figure 4.6 effect of tube curvatures on Nusselt number data of single phase using 1 cSt silicone oil, $L=250$ mm, $260 < Re_D < 2400$

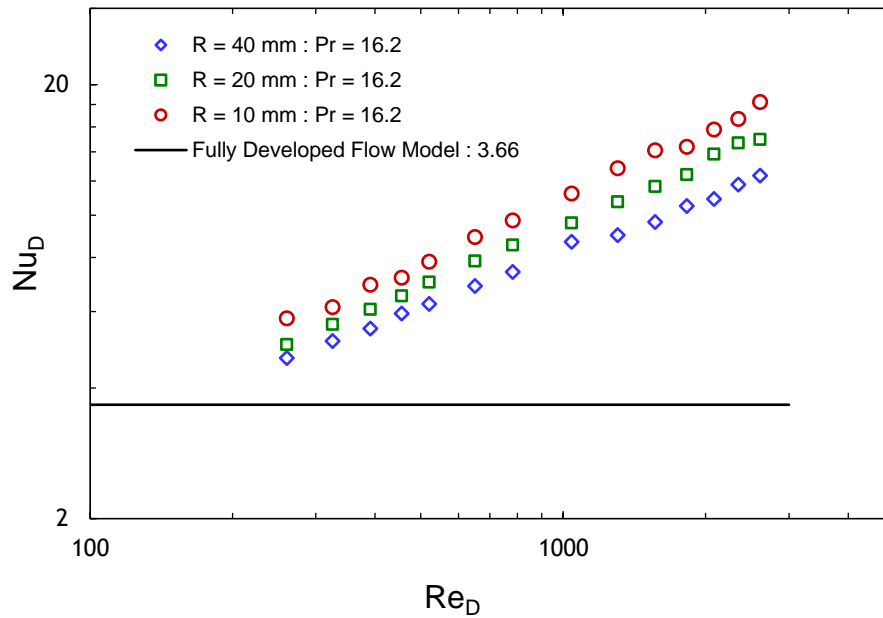


Figure 4.7 dimensionless heat transfer data of single phase flow with varied tube curvatures and fixed Prandtl number $Pr = 16.2$

The second purpose of the study is to obtain experimental data of segmented gas-liquid flow using various curvatures and constant liquid slug ratio γ . The discussion will be devoted to study the effect of tube curvature on heat transfer of gas-liquid / Taylor flow with constant wall temperature. Then, two phase Taylor flows with constant slug ratio γ were introduced to three different curvatures of coiled tubes, $R = 10, 20$ and 40 mm. The experimental data will be demonstrated in different dimensionless groups of Nusselt Nu_D and dimensionless mean wall heat flux q^* .

Later, the data of gas-liquid flow will be employed to develop a new empirical correlation of Nusselt number Nu_D to predict heat transfer of Taylor flow in coiled / curved tube with varying liquid slug ratio γ . Table 4.2 details of slug / Taylor flows of the new experiments.

Fig. 4.8 demonstrates the effect of varying tube curvatures on heat transfer of gas-liquid Taylor flow of fixed slug ratio $\gamma = 0.008$. The results represent data of Nusselt number Nu_D as function of Reynolds number Re_D when the radius of curvature is $10, 20$, and 40 mm. The experiments were conducted using low viscosity liquid 1 cSt silicone oil. Basically, the segmented flows were created by gas phase at liquid fraction $\alpha_L = 0.5$. Additional information was summarized in Table 4.2.

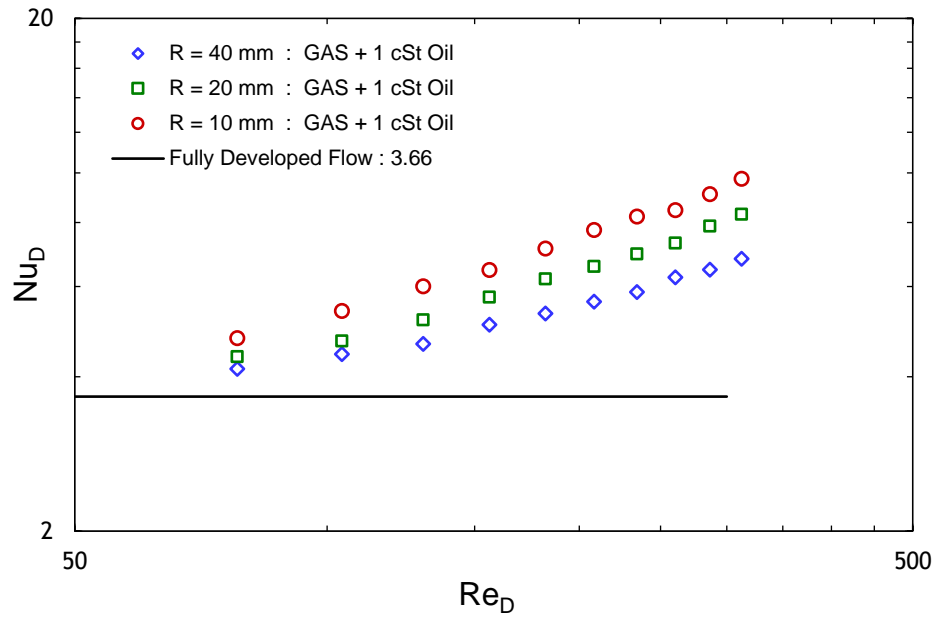


Figure 4.8 dimensionless heat transfer data of varied curvatures and fixed slug ratio of gas-liquid flow with $L_s/L = 0.008$.

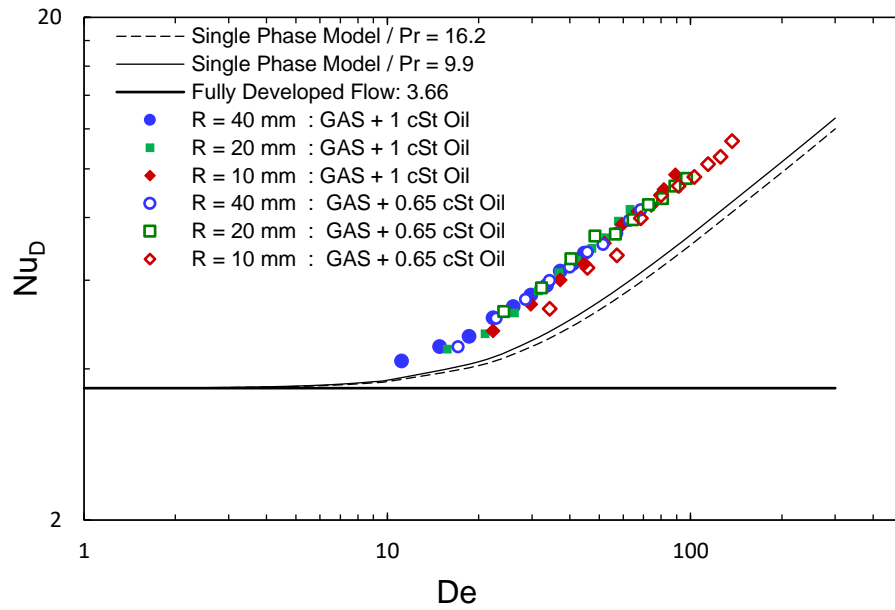


Figure 4.9 dimensionless heat transfer data of varied curvatures and fixed slug ratio of gas-liquid flow with $L_s/L = 0.008$. Compared with single phase model [2].

Fig. 4.9 shows heat transfer data of gas-liquid Taylor flow versus Dean number. Hence, Nusselt number Nu_D data were created using two low viscous silicone oils 0.65 and 1 cSt. The liquid flow was segmented by the gas phase flow which was introduced at the same volumetric flow rate where liquid fraction α_L maintained at 0.5. A consistent Taylor / slug flow was attainable with two silicone oils over a range of Capillary number $0.0022 < Ca < 0.0089$ and $0.0013 < Ca < 0.0054$ with tube diameter 0.00163 m.

The results of gas-liquid flow show an increasing heat transfer rate over a range of Dean number $10 < De < 200$. This increase is inversely proportional to slug length L_S and tube curvature R . The new data are not in agreement with an experimental correlation which was developed earlier by Ghobadi-Muzychka [2] for single phase data prediction. At this point a new correlation is required to predict such behavior where slug ratio and radius of curvature should be inexplicitly accounted for properly.

Slug / segmenting ratio γ of gas-liquid Taylor flow represents an important parameter in the present study. Hence, the mean value of the measured slug length is more relevant for use in the data analysis instead of the actual length to avoid data fluctuation. Fig. 4.10 demonstrates heat transfer enhancement due to liquid slug shortening. The results showed increasing heat transfer rates as the slug length reaches the low limit of the studied range which was found to be the internal diameter of the tube. This finding has been supported by the theory of internal circulation [1]. Fig. 4.1 demonstrated slug length variations which were created using several junctions and constant Reynolds number Re_D . Hence, Liquid slug length ratio lies in the range of $0.008 < \gamma < 0.06$. However, the experimental observations revealed that additional heat transfer enhancement can be attained when segmented flow is introduced to curved tubes. The experimental results verified that the amount of thermal enhancement relates inversely to slug length ratio L_S/L as well as radius of coiled tube R while the intrinsic wetted tube area $\alpha_L \pi DL$ is considered in the data analysis.

Table 4. 2 contains gas-liquid flow limits of present study

Liquid Phase	Pe_D	γ	L^*	$Ca (10^{-4})$
0.65 cSt oil	1188-4754	0.008	0.065-0.016	13-54
		0.032		
		0.060		
1 cSt oil	1268-5072	0.008	0.06-0.015	22-89
		0.032		
		0.060		

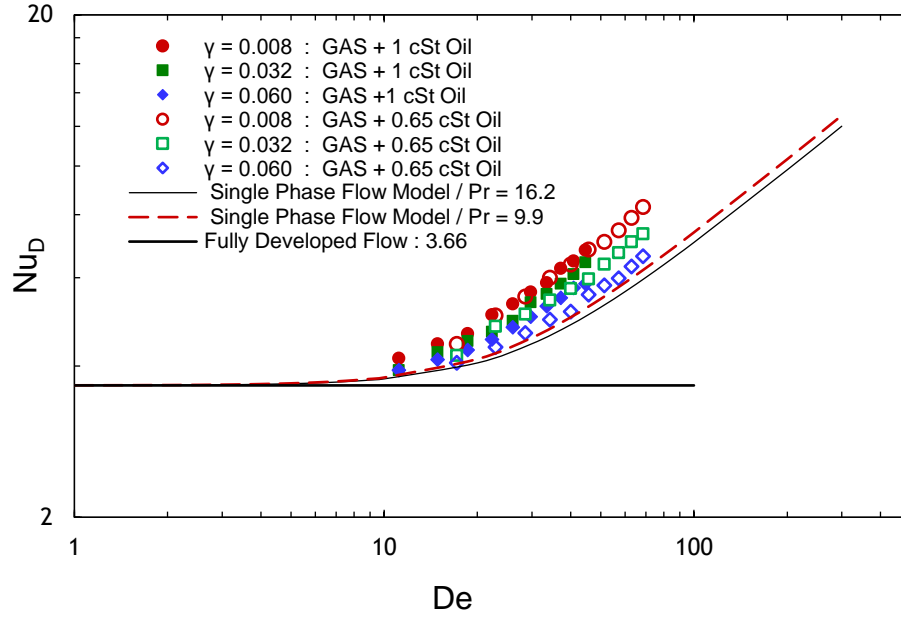


Figure 4.10 effect of liquid slug ratio γ and Prandtl number on Nusselt number data of gas-liquid flow with, $R=40$ mm.

Fig. 4. 10 demonstrate the experimental data using two silicone oils with three slug ratios. The results represent dimensionless heat transfer coefficient Nu_D versus Dean number De and compared with single phase model [2].

Clearly, the results show an augmentation are associated with varying the tube curvatures while the slug ratio was kept fixed $\gamma = 0.008$. These results are created by using two silicone oils, 0.65 and 1 cSt which have Prandtl numbers $Pr = 9.9$ and 16.2 . The continuous phases were segmented by gas phase at liquid fraction $\alpha_L = 0.5$. However, slug ratios were controlled by using varied junction parameters (size, shape, and flow direction). Theoretically, all the data in Fig. 4.9 – 4.10 were unpredictable when using models developed for single flow [1]. To predict the behavior of gas-liquid Taylor flow, developing a new correlation appeared to be very important as the literature never revealed any attempts for modeling that behavior. In the present study and based on the obtained results a new correlation will be developed to predict the thermal behavior of gas-liquid Taylor flow including three parameters: liquid slug ratio L_S/L of the Taylor flow, radii of curvature R , and Prandtl number Pr .

4.7 Modeling of Experimental Data

The experimental data of the present study were used to develop an empirical correlation to predict the effect of varying slug length ratio γ on heat transfer enhancement in coiled tubes under constant wall temperature. Enough sets of data have been employed to ensure validity of the new correlation. However, the study used two liquids having different Prandtl numbers: $Pr = 9.89$ and 16.2 . The gas phase was supplied at the same volumetric flow rates to create Taylor flow of three slug ratios $\gamma = 0.008, 0.032$ and 0.06 . Clear images were captured using a high speed Phantom camera as in Fig. 4.1.

Taylor flows were fed into a mini scale tube with three different radii of curvature: $R = 10, 20$ and 40 mm and fixed length $L = 250$ mm and diameter $D = 1.63$ mm. The change of the curvatures for the same tube length creates three coiled tubes with three numbers of turns: $N = 3, 2$ and 1 respectively. Fig. 4.2 shows the geometries of the test sections. Additional details regarding the flow conditions and limits can be found in Tables 4.1 and 4.2.

Developing an experimental correlation required employing enough sets of data by varying several parameters to ensure the high performance of the prediction, Table 4.2. However, to predict Nusselt number Nu_D of Taylor gas-liquid or liquid-liquid flows in coiled tube then the length of liquid slugs L_s needs to be considered, besides the tube curvature and Prandtl number.

A simple model was developed for Nusselt number Nu_D of the gas-liquid Taylor flows in coiled tubes which takes the algebraic form:

$$Nu_D = CDe^mPr^p\gamma^q \quad (4.9)$$

The experimental data of gas-liquid Taylor flow were used to determine the three coefficients: C , m , p , and q , which appeared in Eq. (4.9). Statistical modeling was employed where Nu_D is Nusselt number of gas-liquid Taylor flow in curved tubes. Consequently, the asymptotes within developing and fully developed regions take the form:

$$Nu_D = \begin{cases} 3.66 \\ CDe^mPr^p(\gamma)^q \end{cases} \quad \text{if } \begin{cases} De < 1 \\ De \geq 10 \end{cases} \quad (4.10)$$

where $Nu_D = 3.66$ for the fully developed flow in straight tube under the constant wall temperature boundary condition and small transition region $De < 10$. The two asymptotic limits were combined to take the form:

$$Nu_D = [3.66^n + (CDe^m Pr^p \gamma^q)^n]^{1/n} \quad (4.11)$$

The proposed correlations show that heat transfer is mainly affected by three parameters, tube curvature, liquid properties, and flow segmentations, in addition to four coefficients C , m , p and q . A Statistical analysis was employed to calculate the values of the coefficients in the model using the experimental data. Finally, the transitional flows were used to calculate the power $n \approx 5$.

$$Nu_D = [3.66^5 + (0.475De^{0.5} Pr^{0.1} \gamma^{-0.11})^5]^{1/5} \quad (4.12)$$

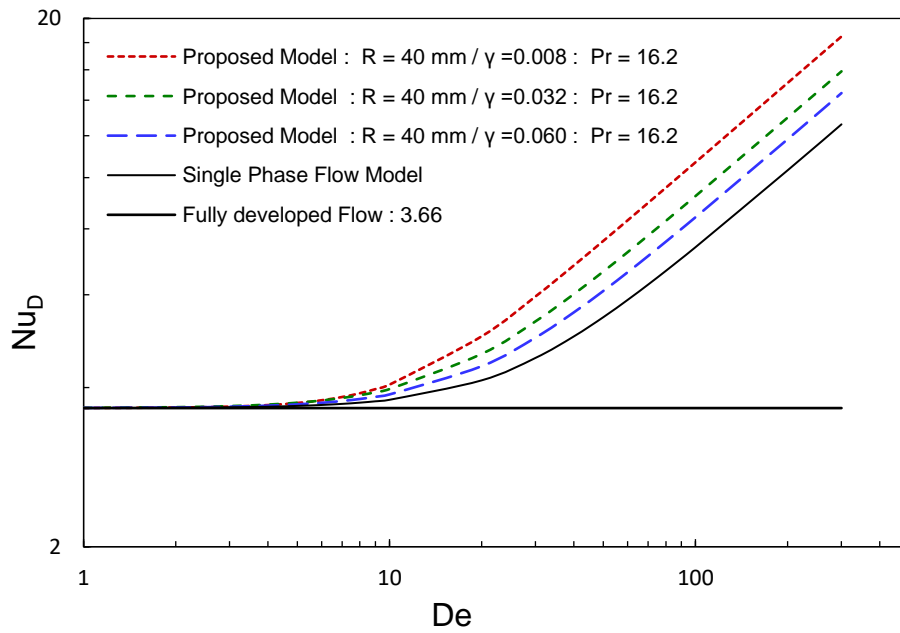


Figure 4.11 gas-liquid flow modeling based on liquid slug ratio γ for liquid fraction $\alpha = 0.5$ and $Pr = 16.2$

Fig. 4.11 demonstrates how the proposed correlation of Nusselt number Nu_D responds to the varying of the ratio γ for curved tubes of $R = 40$ mm using 1 cSt silicone oil. Hence, the carrier phase was segmented by gas phase at liquid fraction $\alpha = 0.5$. various junction parameters (shape, size and flow direction) were employed to create three slug ratios, $\gamma = 0.008$, 0.032 and 0.06 , which were plotted versus Dean number De and compared with single phase model was previously proposed by Ghobadi-Muzychka [2].

Figs. 4.12 - 4.16 demonstrate heat transfer data of Nusselt number Nu_D plotted as function of Dean number De . Tube curvature was varied to demonstrate the ability of the proposed correlation to predict the secondary flow effects on the thermal characteristics of gas-liquid Taylor flow. In general, good agreement with proposed correlation was observed. However, quantitative analysis was applied using root mean square percentage error (RMSPE) to support the experimental observations.

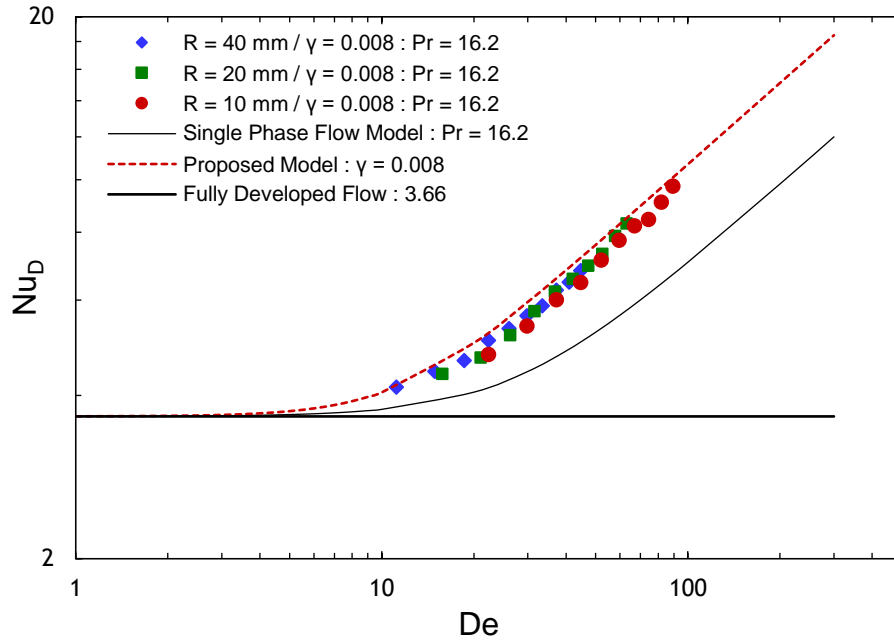


Figure 4.12 Nusselt number Nu_D data of different curvatures 10, 20 and 40 mm and fixed slug ratio $\gamma = 0.008$, $Pr = 16.2$.

Fig. 4.15, the proposed correlation (4.12) was examined with varying Prandtl number Pr and the tube curvature R with fixed liquid slug ratio $\gamma = 0.032$. However, such changes will reflect the impact of several parameters. One of these parameters are the dynamic viscosity μ which promotes the secondary flow and internal circulation within liquid slugs of Taylor flow in the coiled tubes.

The experimental results of gas-liquid flows of liquid fraction $\alpha = 0.5$ were analyzed based on the actual velocity of the flow along with witted tube area. The observation demonstrated higher enhancement with decreasing Pr . In general, the proposed model of Nusselt number Nu_D presented potential of predicting the experimental data of gas-liquid Taylor flows in coiled tubes.

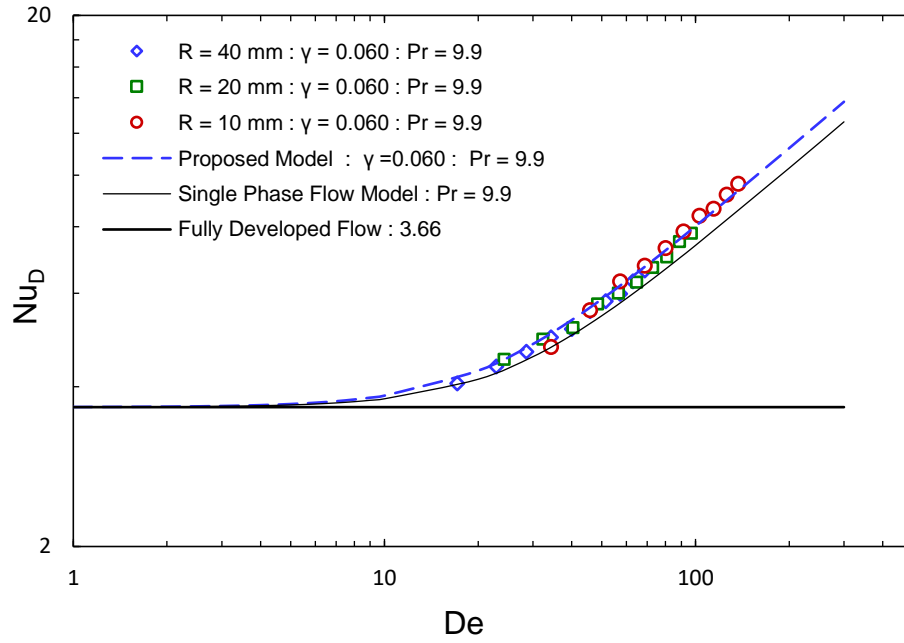


Figure 4.13 Nusselt number Nu_D data created with different curvatures 10, 20 and 40 mm and fixed slug ratio $\gamma = 0.060$, $Pr = 9.9$

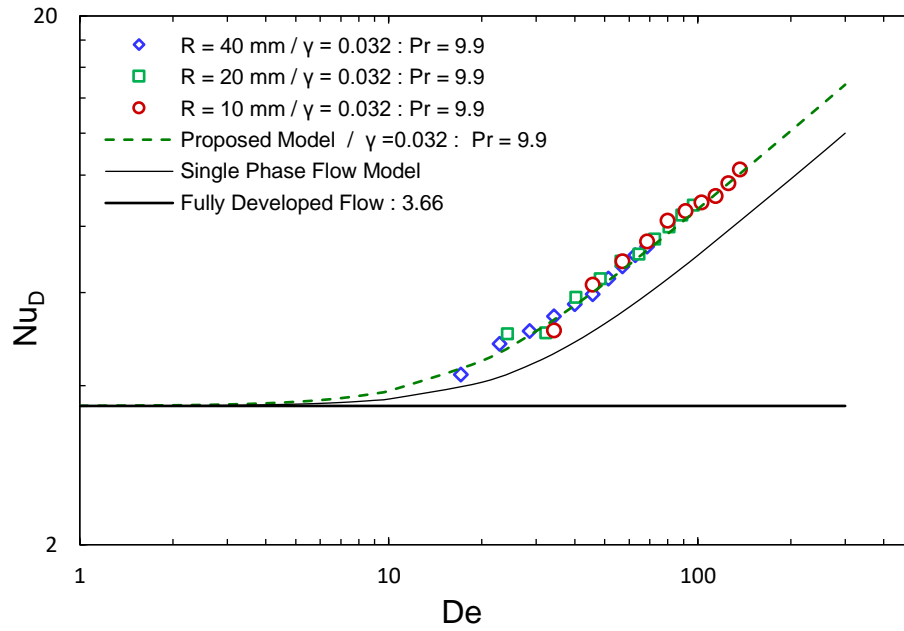


Figure 4.14 Nusselt number Nu_D data created with different curvatures 10, 20 and 40 mm and fixed slug ratio $\gamma = 0.032$, $Pr = 9.9$.

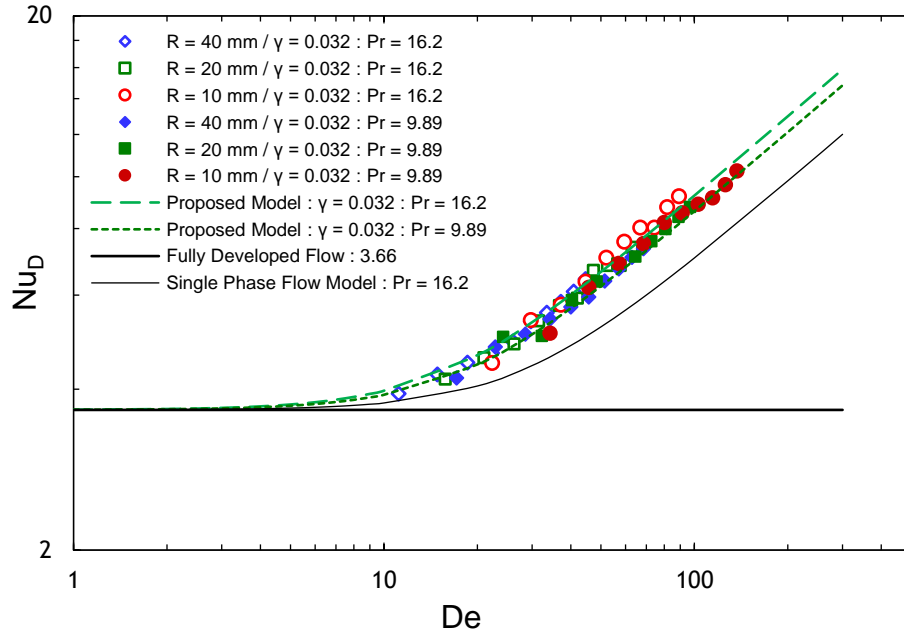


Figure 4.15 the proposed correlation when compared with Nusselt number Nu_D data created with different Prandtl numbers and fixed slug ratio $\gamma = 0.032$.

Figs. 4.16 - 4.17 demonstrate heat transfer augmentation due to liquid slug shortening of gas-liquid Taylor flow of in coiled tubes. Six sets of data were created using two viscous liquids which have Prandtl numbers $Pr = 9.89$ and 16.2 . However, the liquid slug ratio γ was controlled carefully and monitored using high speed Phantom camera to insure flow stability before and after the test section.

The root mean square percentage error (RMSPE) was estimated based on predicted and observed data sets [32]. The error analysis of the segmented flow covered performance of the proposed correlation over a range of Dean number $10 < De < 100$. The error analysis revealed 9.6 % as shown in Fig. 4.4 for single phase flow. In case of gas-liquid flow for tube curvature $R = 40$ mm in Fig. 4.17, the proposed model was able to predict the experimental data with RMSPE = 4.2, 7.02 and 6.89 % when the flow segmentations $\gamma = 0.08, 0.032$ and 0.06 .

Finally, the agreement for all the experimental results was observed with maximum RMSPE of 8.2 % when compared with proposed model of Nusselt number.

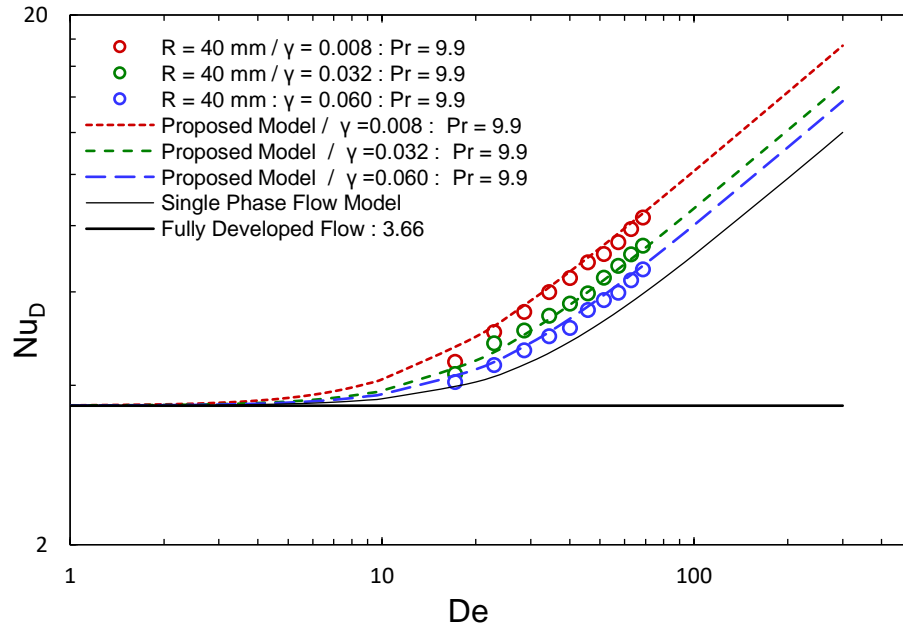


Figure 4.16 predictable behaviour of gas-liquid Taylor flow using 0.65 cSt silicone oil with varied flow segmentation γ and over a range of Dean number $De \cong (20 \text{ to } 70)$

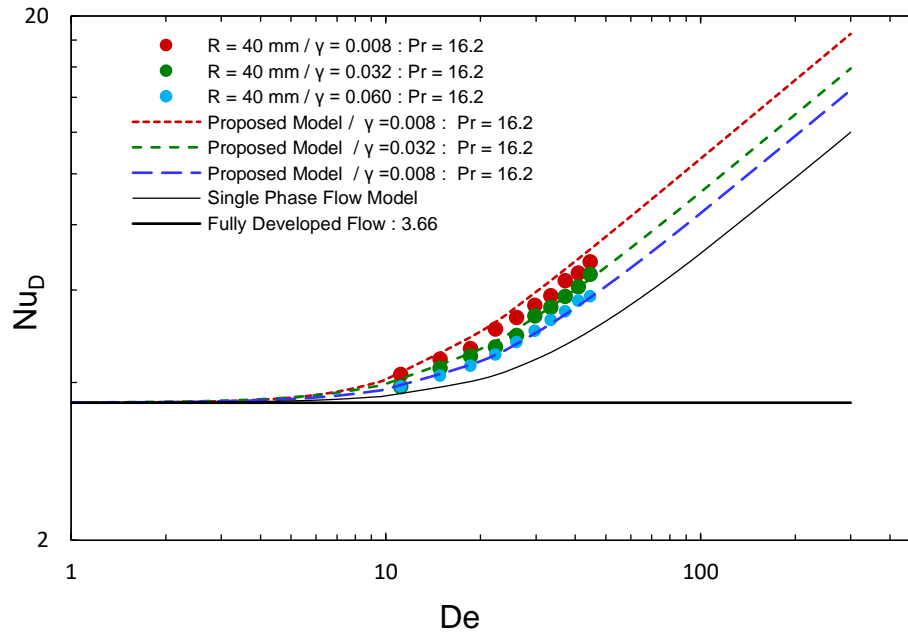


Figure 4.17 predictable behaviour of gas-liquid Taylor flow using 1 cSt silicone oil with varied flow segmentation γ and over a range of Dean number $De \cong (10 \text{ to } 40)$

4.8 Conclusion

Heat transfer in gas-liquid Taylor flow in coiled tubes showed an enhancement over the single phase flow model lay in the range from 10 to 35 % when considering the results on Fig. 4.12, where the slug ratio $\gamma = 0.008$ and the radii of curvature $R = 10$ mm geometries. These findings show the flow characteristics of Taylor flow, which are the boundary layer dominant due to internal circulation within liquid slugs. Clearly, the experimental data demonstrated a consistent relationship between heat transfer and liquid slug ratio L_S/L . In general, the gas-liquid Taylor flows in coiled tubes were characterized by three regions: low curvature region $De < 10$, where the heat transfer behaves as that of straight tubes. In contrast a high curvature region $De > 10$ and transitional region lies within the range of $1 < De < 10$. The proposed experimental correlation showed the potential of prediction for Nusselt number Nu_D when Dean number $De > 10$. The developed model showed successful prediction of the experimental data of gas-liquid flow of $10 < De < 100$ and $9 < Pr < 17$. Range of Dean number De of the experimental data is analogous to the range of gas-liquid Taylor flow in mini scale tubes.

4.9 References

- [1] Muzychka, Y.S., “Laminar Heat Transfer for Gas-Liquid Segmented Flows in Circular and Non-circular Ducts with Constant Wall Temperature” ASME, 2014.
- [2] Ghobadi M., Muzychka Y. S., 2014, “Fully Developed Heat Transfer in Mini Scale Coiled Tubing for Constant wall Temperature”, *Internal Journal of Heat and Mass Transfer*, 72, pp. 87–97.
- [3] Ghobadi M., Muzychka Y. S., “Effect of entrance region and curvature on heat transfer in mini scale curved tubing at constant wall temperature”, *International Journal of Heat and Mass Transfer* 65 (2013) 357–365.
- [4] Ghobadi M., Muzychka Y. S., 2014” Heat transfer and pressure drop in a spiral square channel” *Experimental Heat Transfer*, 28:546–563, 2015.
- [5] Adrugi, W., Muzychka, Y.S., and Pope, K., “Heat Transfer in Liquid-Liquid Taylor Flow in Mini-scale Curved Tubing for Constant Wall Temperature,” ASME-IMECE-2015-67700, 2016.
- [6] Ghobadi M., Muzychka Y. S.,” Heat Transfer in Spiral Channel Heat Sink”, ASME 2011 9th International Conference on Nanochannels, Microchannels, and Mini channels.
- [7] Adrugi, W., Muzychka, Y.S., and Pope, K.,” Heat Transfer Model for Liquid-liquid Taylor flow”, ASME 2018 16th
- [8] Oliver, D.R. and Young Hoon, A.,”Two Phase Non-Newtonian Flow: Part 2 Heat Transfer”, *Transactions of the Institution of Chemical Engineers*, Vol. 46, pp. 116-122, 1968.
- [9] Horvath, C., Solomon, B.A., Engasser, J.M., “Measurement of Radial Transport in Slug Flow Using Enzyme Tubes”, *Industrial and Engineering Chemistry, Fundamentals*, Vol. 12, no. 4, pp. 431-439, 1973.
- [10] Vrentas, J.S., Duda, J.L, and Lehmkuhl, G.D., “Characteristics of Radial Transport in Solid-Liquid Slug Flow”, *Industrial and Engineering Chemistry, Fundamentals*, Vol. 17, no. 1, pp. 39-45, 1978.
- [11] Muzychka Y. S., “Walish E., “Simple Models for Laminar Thermally Developing Slug Flow in Noncircular Ducts and Channels” *Journal of Heat Transfer*, ASME NOVEMBER 2010, Vol. 132 / 111702-1.

- [12] Betz A. R., Attinger D., “Can Segmented Flow Enhance Heat Transfer in Microchannel Heat Sinks”, *International Journal of Heat and Mass Transfer*, 53, pp. 3683-3691, 2010.
- [13] Muzychka Y. S., Walsh E. Walsh P. “Heat Transfer Enhancement Using Laminar Gas-Liquid Segmented Plug Flows”, *Journal of Heat Transfer*, 2011 by ASME, APRIL 2011, Vol. 133 / 041902-1.
- [14] Walsh, P., Walsh, E., and Muzychka, Y.S., “Heat Transfer Model for Gas-Liquid Slug Flows Under Constant Flux”, *International Journal of Heat and Mass Transfer*, Vol. 53 (15-16), pp. 3193-3201, 2010.
- [15] S. Haase, “Characterisation of gas-liquid two-phase flow in mini-channels with co-flowing fluid injection inside the channel, part II: gas bubble and liquid slug lengths, film thickness, and void fraction within Taylor flow” *International Journal of Multiphase Flow*, 88, 2017, pp. 251–269.
- [16] J Howard A. and Walsh P. A., “Heat Transfer Characteristics of Liquid-Gas Taylor Flows incorporating Microencapsulated Phase Change Materials”, *Journal of Physics: Conference Series* 525 (2014) 012022.
- [17] Fairbrother F. and Stubbs, A.E., “Studies in Electro-endosmosis. Part VI. The Bubble-tube Method of Measurement”, *Journal of the Chemical Society*, Vol. 1, pp.527-529, 1935
- [18] Taylor, Deposition of a viscous fluid on the wall of a tube, *Journal of Fluid Mechanics*. 10(1961) 161–165.
- [19] Maddox, D.E. and Mudawar, I., “Single- and Two-Phase Convective Heat Transfer from Smooth and Enhanced Microelectronic Heat Sources in a Rectangular Channel”, *Journal of Heat Transfer*, Vol. 111, pp. 1045-1052, 1989.
- [20] Prothero, J. and Burton, A.C., “The Physics of Blood Flow in Capillaries: 1 The Nature of the Motion”, *Bio-physical Journal*, Vol. 1, pp. 565-579, 1961.
- [21] K. Alrbee, Y.S. Muzychka and X. Duan, “Heat Transfer Enhancement in Laminar Graetz and Taylor Flows Using Nanofluids”, ASME-ICNMM2018-7756.
- [22] Hughmark, G.A., “Holdup and Heat Transfer in Horizontal Slug Gas-Liquid Flow”, *Chemical Engineering Science*, Vol. 20, 1007-1010, 1965.

- [23] Talimi V., Muzychka Y. S., Kocabiyik S., “A Review on Numerical Studies of Slug Flow Hydrodynamics and Heat Transfer in Microtubes and Microchannels”, *International Journal of Multiphase Flow*, 39, pp. 88-104, 2012.
- [24] Oliver, D.R. and Wright, S.J., “Pressure Drop and Heat Transfer in Gas-Liquid Slug Flow in Horizontal Tubes”, *British Chemical Engineering*, Vol. 9, pp.590-596, 1964.
- [25] Narayanan. C, Lakehal D., “Two-phase Convective Heat Transfer in Miniature Pipes Under Normal and Microgravity Conditions”, ASME, *Journal of Heat Transfer* 130 (2008) 074502-1–074502-5.
- [26] W. R. Dean, “Note on the Motion of Fluid in a Curved Pipe”, *London Edinburgh Dublin Philosophy Magazine and journal Science*, vol. 4, pp. 208–223, 1927.
- [27] W. R. Dean, “The Streamline Flow Through Curved Pipes”, *London Edinburgh Dublin Philosophy Magazine and journal Science*, vol. 5, pp. 673–695, 1928.
- [28] K. Alrbee, Y.S. Muzychka and X. Duan, “Laminar Heat Transfer of Gas-Liquid Segmented Flows in Circular Ducts with Constant Wall Temperature”, ASME 2019 17th International Conference on Nanochannels, Microchannels, and Minichannels.
- [29] K. Alrbee, Y.S. Muzychka and X. Duan, “An approximated method of Analysis for laminar Heat Transfer in liquid-liquid Taylor flow in mini scale tubing”, ASME 2019 17th International Conference on Nanochannels, Microchannels, and Minichannels.
- [30] Giolla M. M. Eain A., Vanessa E., Punch J., “Local Nusselt number enhancements in liquid–liquid Taylor flows”, *International Journal of Heat and Mass Transfer*, 80 (2015) 85–97.
- [31] Muzychka, Y.S. and Ghobadi, M., “Measurement of Laminar Heat Transfer Coefficients in Micro and Mini Scale Ducts and Channels”, Proceedings of the 2014 ICNMM, Chicago, IL, 2014.
- [32] Muzychka, Y.S., “Generalized Models for Laminar Developing Flows in Heat Sinks and Heat Exchangers”, *Heat Transfer Engineering*, vol. 34 (2-3), pp. 178-191, 2013.
- [33] Maxim V. S., Brebels, A., “A Survey of Forecast Error Measures”, World Applied Sciences Journal 24, *Information Technologies in Modern Industry*, Education & Society, 171-176, 2013.

- [34] Kline, S. J., and F. A. McClintock. "Describing Uncertainties in Single-Sample Experiments.", *Mechanical Engineering*, Vol. 75, No. 1, January 1953: 3-8.
- [35] Eduardo D. Glandt, T. Klein and E Edgar, "Optimization of Chemical Processes", Second edition, *McGraw-Hill Chemical Engineering Series*, 2001.

CHAPTER 5

AN APPROXIMATE METHOD OF ANALYSIS FOR LAMINAR HEAT TRANSFER IN LIQUID-LIQUID TAYLOR FLOWS IN MINI SCALE TUBING

5.1 Introduction

Enhancement of heat transfer when laminar flow is prescribed in mini / micro channels has received intensive investigation during the past few decades [1-6]. More recently, and due to increasing demands of the micro technology, it has been shown that introducing two immiscible fluids into the cooling stream can significantly enhance heat transfer as compared to a single phase flow of the same volume flow rate. This type of segmented flow is called a Taylor flow. Early work in this area dates to the 1960's and early 1970's. Taylor flow was first introduced by Taylor (1961) who studied the hydrodynamics. Several ways have been reported to create a uniform segmented slug flow [7-10]. For a purpose of enhancing heat transfer, early experimental studies were performed by Oliver et al. [7], Horvath, et al. [8] and Vrentas, et al. [9]. This field of research has evolved recently to applications in micro/mini scale cooling systems due to the ease of producing a Taylor flow in tubes of small diameter.

However, additional experimental and theoretical studies using different methods of analysis have shown that gas-liquid Taylor flow can enhance heat transfer in mini and micro channels with greater heat transfer rates achieved over single phase Graetz flow [11-16]. In particular, the

** The materials in this chapter was presented in ASME 2019 18th International Conference on Nanochannels, Microchannels, and Mini channels, June 24-27, 2019 in St John's, Canada.*

literature review revealed important attempts to predict thermal behavior of gas-liquid Taylor flow. Liquid properties and liquid slug length were the main parameters to be considered for prediction [11, 12, and 21].

Liquid-liquid Taylor flow at micro and mini-scales has emerged as a fundamental research area in recent years. Although, only a small number of studies have been reported with great heat transfer enhancement, [16 - 20]. Related studies will be considered with more details in later sections.

Theoretical and experimental analysis of thermal behavior of laminar flow in small scale tubes was considered in detail by Muzychka and Ghobadi [13]. Simple asymptotic limits for entrance and fully developed regions were considered and a simple model developed. Hence the aim of present study is to obtain new experimental data for a two fluid system rather than single phase flow and provide a means to model the results.

Oliver and Young [7] studied effect of liquid slug lengths on heat transfer rates in gas-liquid flows. The study aimed to investigate the thermal behavior of a gas liquid Taylor flow under an isothermal boundary condition. The results showed heat transfer enhancement when compared with single phase flow. Their investigation covered a wide range of Reynolds numbers including different flow regimes of gas liquid Taylor flow. They reported that decrease in heat transfer associated with wavy and annular flows due to boundary layer effects as the heat transfer in slug flow occurs in manner like that presented in single phase Graetz flow.

Horvath et al. [8] performed an important investigation on heat transfer in Taylor flow of gas-liquid flows. The segmented flows of 0.5 liquid fraction were fed into mini scale tube which was subjected to a constant heat flux boundary condition. They reported their data as a Nusselt number for the liquid plug phase only versus slug aspect ratio Ls/D over a high range of Reynolds from 20 to 300. The effect of plug velocity was studied by varying the two phase flow Reynolds number at same liquid fraction. The study revealed that higher heat transfer rate is obtained when liquid slug length equal to inner diameter of channel. This finding was referred to the high radial mixing in segmented flow within short liquid slugs.

Muzychka, [21] extended his earlier analysis of segmented gas-liquid flow [12] using the appropriate fully developed flow limit. The new model considers the effect of slug to tube length

(Ls/L) on heat transfer, Fig. 1 as the boundary layer renewal is most dominant in short slugs but becomes exhausted in long tubes. Hence, one of important characteristic of the new model is that shows how quickly short slugs become thermally saturated. Muzychka [21] used published experimental data from [2-4, and 6] to validate his model. One shortcoming of the published data was the fact that most data only showed early signs of fully developed flow being achieved. In the present study new experimental data are accurately obtained under constant wall temperature as further validation for liquid-liquid flows.

Adrugi and Muzychka, [16] carried out liquid-liquid heat transfer experiments. However, both liquids were fed through straight mini scale tubes under isothermal wall conditions. Experiments were conducted based on different flow modes of void fraction. The flow patterns were created by introducing two immiscible liquids (water – silicone oils) into mini scale tubes with straight and curved paths. The results showed a significant enhancement in heat transfer if compared with single phase flow models. More studies were published in this regard by Eain, et al. [18] to investigate heat transfer in mini scale tubes and channels.

Haase [23] produced a proper facility to study Taylor flow characterisation in mini scale channels using industrial fluids. The gas phase was introduced to the flow stream by injecting the gas phase through a capillary injector with variable inner diameter. Published experimental data along with his own experimental data were used to develop a novel model to predict bubble and slug lengths of both phases. His study was motivated by earlier studies [23].

Howard and Walsh [24] investigated the potential for heat transfer enhancement associated with gas-liquid Taylor flows in mini sized channels incorporating microencapsulated phase change materials (MPCM) at 30% concentration. However, they reported enhancement due to the internal circulations within liquid slugs which was confirmed in [8], as well as increasing thermal capacity of flow which is associated with addition of the MPCM. An experimental test facility was developed which had a heated test section and allowed MPCM gas-liquid Taylor flow to be subjected to a constant heat flux boundary condition. Heat transfer enhancement was examined by changing liquid slug length and liquid fractions. Infrared thermography results demonstrated a significant reduction in experimental wall temperatures associated with MPCM gas-liquid Taylor flow when compared with the Graetz solution for conventional single phase coolants. Furthermore, the reduction in wall temperature was observed even when data were not reduced to consider the

gaseous voids in the flow. Howard et al. [24] confirmed that segmented MPCM gas-liquid flows provided further enhancement than that observed for MPCM liquid only Poiseuille flows.

Alrbee and Muzychka [22] examined effect of nanoparticle inclusion in gas-liquid Taylor flow. The laminar Taylor flow was fed into a straight tube at mini scale size and was maintained at isothermal wall conditions. Several nanoparticle concentrations of Al_2O_3 were applied, 0.25%, 0.5% and 0.75%. A homogeneous analysis was considered to reduce the collected data. Heat transfer enhancement of nanofluid Taylor flow was compared with conventional flow at same flow conditions. They reported a significant enhancement by means of non-dimensional parameters, dimensionless heat transfer q^* and Nusselt number Nu_D .

Giolla et al. [18] investigated the potential of heat transfer enhancement in liquid-liquid Taylor flow. They used a Taylor flow of water-oil heated under constant flux. However, the primary focus was to examine the influence of slug length and carrier phase variations on the local Nusselt numbers. Temperature measurement was carried out using an infrared thermography system. Their experimental observations revealed that the greatest enhancement was achieved in flows with carrier slug lengths approaching the channel diameter.

The authors [18] found that the liquid film separates the dispersed slugs from the heated capillary walls, causing a reduction in the heat transfer rates. A similar study was performed in [17] using liquid-liquid Taylor flow. A scenario of variable void fraction was adopted throughout the experiments. However, the thermal enhancement under isothermal conditions was significantly greater with shorter slug lengths.

Adrugi and Muzychka [33] followed up their work in [16] with additional experiments on heat transfer enhancement using non-boiling liquid-liquid Taylor flow in mini scale coiled tubing for constant wall temperature conditions. A coiled copper tube with different radii of curvature and lengths were used as test sections. The study covered three low viscosity silicone oils (1 cSt, 3 cSt, 5 cSt) to examine the effect of Prandtl number on heat transfer rates in coiled tubing. They developed a new experimental model to predict heat transfer in coiled tubes. The new model provides useful insights into liquid-liquid Taylor flows in curved and coiled tubes at mini scale dimensions.

5.2 Separated Phase Modeling of Taylor Flow

This section presents the relevant analytical expressions required for describing thermal characteristics of Taylor flow in both developing and fully developed regions for internal flows. A new approach for liquid-liquid Taylor flow analysis will be introduced to show heat transfer enhancement. A separated phase analysis takes advantage of dealing with Taylor flow components as separate continuous phases when calculating heat transfer as:

$$Q_n = (\dot{m}c_p)_n(T_{o,n} - T_{i,n}) , \quad n = A, B \quad (5.1)$$

Where, Q_n is the bulk heat transfer achieved for each component, A and B, the subscript i and o, refers to tube inlet and outlet. We assume that the outlet temperatures of both flow components reach similar temperature at some point downstream, i.e. $T_{o,A} \sim T_{o,B}$. This assumption was verified in our experiments by measuring the bulk fluid locally with a thermocouple. In all our experiments both phases also had the same inlet temperature, i.e. $T_{i,A} \sim T_{i,B}$. Fig. 2 shows the basic liquid-liquid Taylor flow cell. The tube diameter is small and such the thermocouple junction occupies a significant portion of the tube cross section. Further, bulk fluid measurements made during benchmarking single phase flow further validate the experimental assumption.

Referring to gas-liquid Taylor flow modeling approach developed by Muzychka [21] the dimensionless mean wall flux is defined using the actual wetted duct area for each phase and the dimensionless slug length for each phase will be used instead of dimensionless tube length. This places the current analysis on a common basis with the gas-liquid model in [21] which assumes the gas phase does not participate significantly. This principle will be applied in present study for each component of the liquid-liquid Taylor flow as:

$$q_n^* = \frac{Q_n / (\pi D L \alpha_n) D}{k_n (T_w - T_{i,n})} \quad (5.2)$$

Where $A = PL_{S,n}$ and T_w is wall temperature and α_n referring to the fractions of both components A and B, which can be defined as:

$$\alpha_A = \frac{L_A}{L_A + L_B} , \quad \alpha_B = \frac{L_B}{L_A + L_B} \quad (5.3)$$

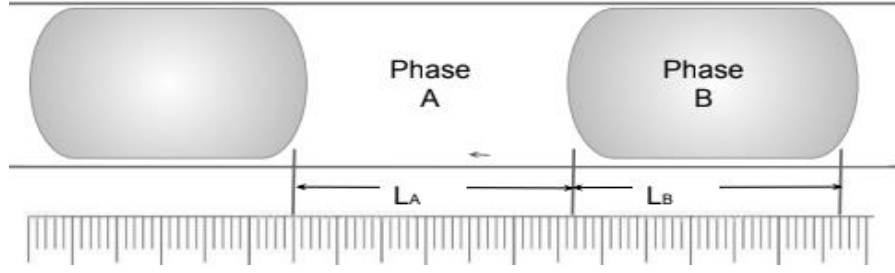


Figure 5.1 liquid-liquid Taylor flow cell configuration

Since, L_A and L_B refers to oil and water slug lengths of Taylor flow as shown in Fig 1.

In the present study, data is analyzed using the above definitions of liquid fraction α_A , and α_B but, we are also interested in presenting the experimental data using the dimensionless liquid slug length L_s^* for each phase component A and B instead of dimensionless tube length, L^* on the Graetz plot:

$$L_{S,n}^* = \frac{L_{s,n}/D}{Pe_{D,n}}, \quad n = A, B \quad (5.4)$$

where, Pe_D , is Peclet number for each component. Here the Peclet number Pe_D is defined as a function of maximum (combined) flow velocity when both components are taken to account. Thus, using the total superficial velocity that each phase experiences:

$$Pe_D = \frac{(U_A + U_B)D}{\left(\frac{k}{\rho c_p}\right)_n} \quad n = A, B \quad (5.5)$$

where U_A and U_B refer to superficial velocity of each phase. Further details of this approach may be found in [21].

Finally, experimental data were compared with a new general model which captures the expected behavior of Taylor flow for a gas-liquid stream (which ignores the gas phase). The model was proposed by Muzychka [21] to predict heat transfer data of segmented Taylor flow based on slug length instead of tube length. Theoretically, the model combines two asymptotes for the entrance region and fully developed regions which was expressed as:

$$q^* = \left[\left(\frac{1.614}{L_S^{*1/3}} \right)^{-3/2} + \left(\frac{L_S/L}{4L_S^*} \right)^{-3/2} \right]^{-2/3} \quad (5.6)$$

In the current approach we apply the above model for each phase using Eq. (2) for the dimensionless mean wall flux for each phase, and Eq. (3) for the dimensionless slug length for each phase. In this manner, the heat transfer data for each phase can be presented separately on the same Graetz plot. Conversely, when making predictions of heat transfer rate, the model is then applied separately for each phase using the expected slug lengths and flow fractions.

The uncertainty R within the experimental measurements has been estimated using the well-known methodology of Kline and McClintock [36]. The root mean squared percentage error (RMSPE) has been employed to measure how well the data agree with Poiseuille theory. Essentially, the predicted and measured data have been used with commonly used formula [36]

5.3 Experimental Setup and Procedure

An experimental study was undertaken to examine the effect of cell lengths (i.e. liquid fractions) on heat transfer in liquid-liquid Taylor flows in a mini scale tube. Fig. 5.2 shows the schematic of the experimental setup. To accomplish this task, heat transfer measurements of segmented flow were desired to be performed under a constant wall temperature to compare with the model proposed by Muzychka for a gas-liquid Taylor flow. The experimental setup has been equipped with two programmable syringe pumps (Harvard Apparatus) with a total capacity 200 ml each. The syringe pumps are engineered to provide a flow accuracy within 0.25 % and reproducibility within 0.05 %.

A copper tube of mini scale dimension (1.63 mm ID) was placed horizontally in a constant temperature thermal bath to avoid any gravity effects on flow. A Fisher Scientific 3013 Iso-temp thermal bath which is PID controlled has been utilized to provide constant temperature at 40 C° with a stability of ± 1 % over a range of -30 to 200 °C To measuring the inlet and outlet temperatures of the Taylor flow, two Omega T-type thermocouples were properly embedded within two T-junctions located at both ends of the test section. However, the thermocouples were carefully shielded against other external sources of heat transfer to ensure obtaining reliable experimental data.

Furthermore, the flow patterns of the liquid-liquid Taylor flow have been monitored continually using a data acquisition system connected with a high-speed camera (Phantom v611) as demonstrated in experiment setup, Fig. 5.2. The current study requires performing heat transfer experiments at designated slug ratios L_s/L over a range of Reynolds numbers. The flow cell dimensions were measured at each flow rate to ensure stability of the slug ratio. Accurate flow cell measurements were achieved using image processing software (Image J Software). Fig 5.1 shows liquid-liquid flow cell of 1 cSt silicone oil and water was taken at fraction of $\alpha_n = 0.5$. Table 5.1 Thermophysical properties of used liquids.

Table 5.1 Thermophysical Properties of Used Liquids

liquid	ρ	K	Cp	μ	$\alpha(10^8)$	Pr	$\nu(10^6)$
Water	996	0.6	4080	0.0009	10.5	6.05	0.89
1 Oil	815	0.1	2000	0.0008	6.1	16.2	1
3 Oil	895	0.12	1800	0.0027	7.4	40.3	3
5 Oil	918	0.117	1633	0.0046	7.8	64.1	5

In the present study, the experimental data were obtained using three low viscosity silicone oils having 1 cSt, 3 cSt, and 5 cSt viscosities, along with distilled water to create a liquid-liquid Taylor flow. However, those liquids were picked as they showed a flexibility to create desired cell lengths using the same junction, as the slugs length was controlled only by feeding both components at desired fractions α_A and α_B .

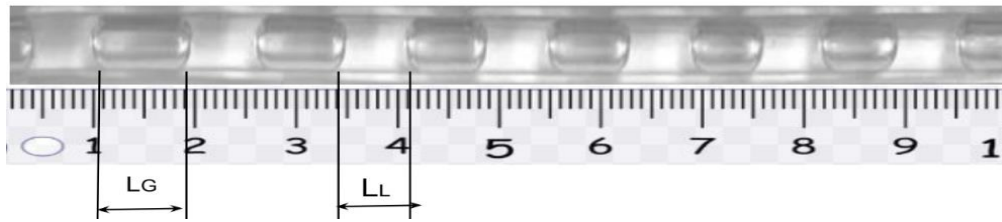


Figure 5.2 liquid-liquid Taylor flow cell with a liquid fraction $\alpha_n = 0.5$.

Furthermore, images were captured using a high-speed camera and show a very thin liquid film up to the wall. The effect of liquid film on heat transfer becomes more pronounced in higher viscosity fluids [5, 9, and 18].

The first step was designing the experiment to ensure obtaining accurate results. The range of Reynolds numbers needed to create liquid-liquid Taylor flow was investigated for the three combinations of liquids. Table 1 contains the thermophysical properties of the test liquids. For instance, the Reynolds number when $\alpha = 0.5$ is between three different ranges based on viscosity of flow components, from 65 to 182, 21 to 60 and 13 to 36. Furthermore, all the experiments have been performed over the same range of volumetric flow rates from 5 to 14 ml/s and three oil fractions 0.25, 0.5 and 0.75. Throughout the experiments it has been observed that both liquid slugs were moving at same velocity, i.e. unity slip ratio. A straight copper tube of size 1.63 mm ID with 100 mm length was employed as a heated test section with a constant wall temperature of 40 °C maintained in the bath.

Several T-junctions were used to create desired lengths of Taylor flow cells. Liquid-liquid Taylor flow formation and flow patterns can be found with more details in [33-35]. The main objective of the present work is to investigate the effect of length variations of the flow cells on heat transfer.

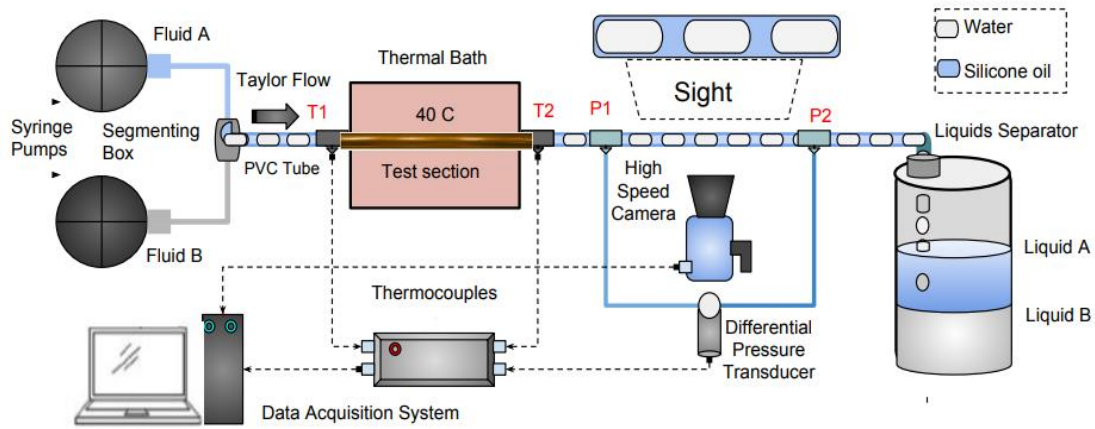


Figure 5.3 experimental setup to measure heat transfer in gas-liquid Taylor flow

The thermal performance of the experiment setup was benchmarked by carrying out measurements over a range of laminar flow Reynolds numbers. The benchmarking results were presented in dimensionless form of Nusselt number Nu_D and dimensionless mean heat flux q^* .

5.4 Results and Discussion

The estimation of uncertainty covered the whole range of Taylor flow in mini scale tubing. The uncertainties were found to be $\pm 1.92\%$ for L^* and the range of uncertainty in heat transfer dimensionless parameters were ± 1.54 to 1.91% for dimensionless heat flux q^* . The benchmarking results for single phase flow show that the method of measuring bulk temperature using a thermocouple and T junction before and after the tube appears to be sound.

The aim of study is presenting heat transfer of liquid –liquid Taylor flow as separate components in dimensionless form. The separated modeling of the two components is applied instead of homogeneous approach. But first we show the results in a manner consistent to show thermal enhancement. The main goal of producing separated modeling as a new approach is that effective properties of the mixture will no longer be used when reducing the data.

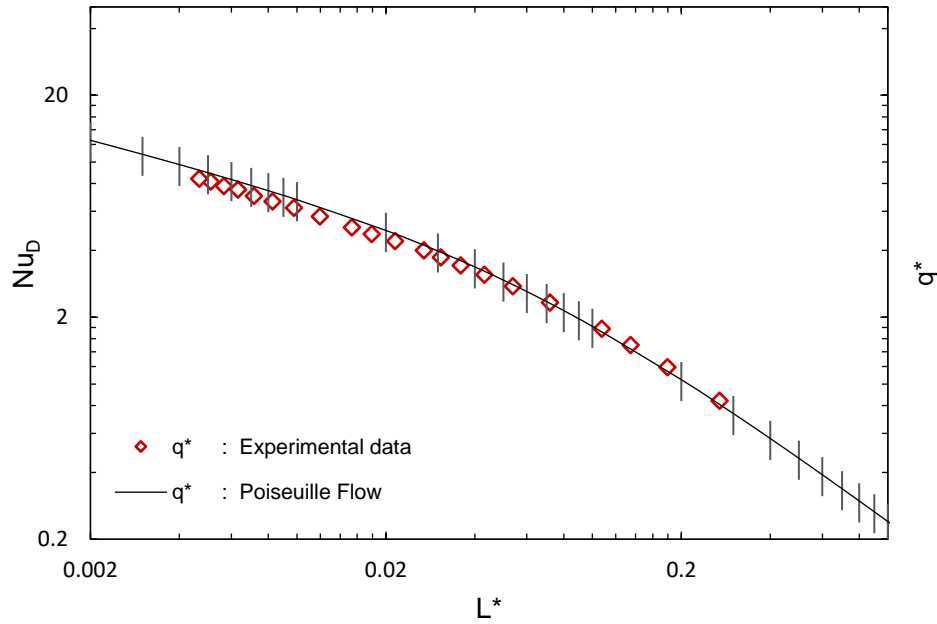


Figure 5.4 benchmarking results of heat transfer in single phase flow using distilled water.

Thus, a liquid-liquid Taylor flow can be modelled as two gas-liquid Taylor flows where the gas phase has generally been ignored relative to the contributions of the liquid phase. In particular, the effect of slug length to tube length Ls/L which was proposed from theory by Muzychka [21] as an important modelling parameter, will be shown to be important in liquid-liquid flows as well.

Figs. 5.5 and 6.6 show the heat transfer data of liquid-liquid Taylor using three silicone oils which have been segmented by water. The data have been reduced using the nominal tube lengths in the definitions of q^* and L^* along with effective thermal properties. The simple homogenous analysis has been presented to highlight some important points. First, for several liquid fractions the data do show that thermal enhancement is achieved over and above the Poiseuille flow Graetz theory. The analysis also shows that the data line up with the slug flow Graetz theory reasonably well, but this is purely a coincidence in this case, as other publications have shown greater deviations are possible [13,14].

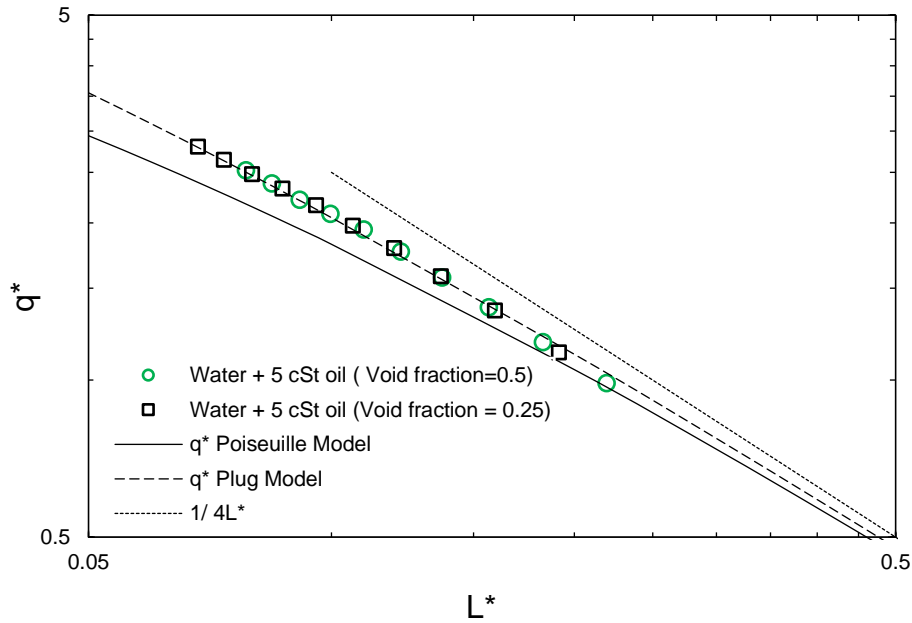


Figure 5.5 experimental data of homogeneous analysis using 5 cSt silicone oils were segmented by water at $\alpha_A = 0.25$ and 0.5.

Nonetheless, the use of effective properties does have some merit. Finally, despite the slug flow model showing some agreement with the data, they never explicitly show the effect of slug length variation on heat transfer. It is well established that slug length affects heat transfer rates [13].

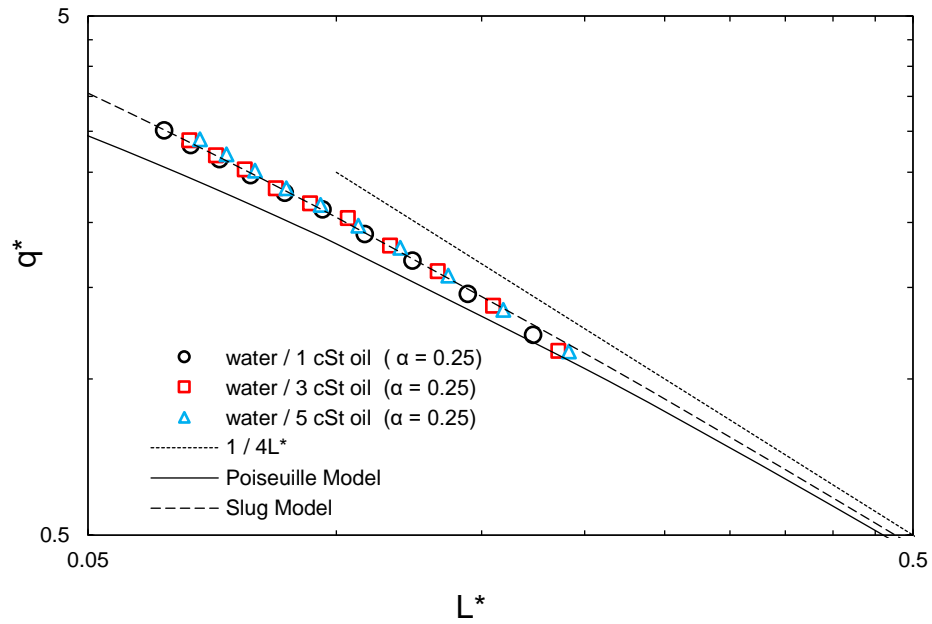


Figure 5.6 experimental data of homogeneous analysis using silicone oils segmented by water at same oil fraction $\alpha_A = 0.25$.

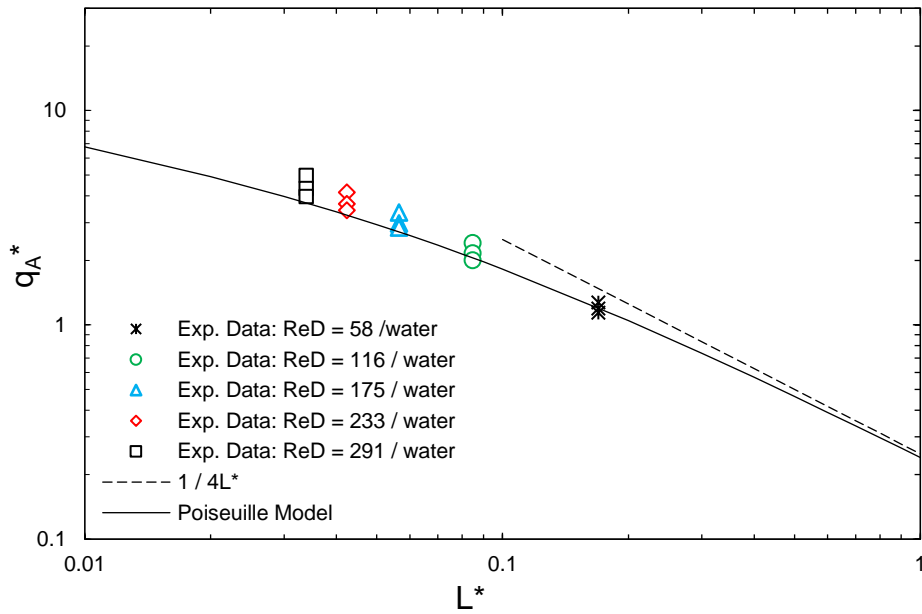


Figure 5.7 experimental data of water component plotted using superficial duct length and flow velocity at five values of Reynolds number with varying slug length.

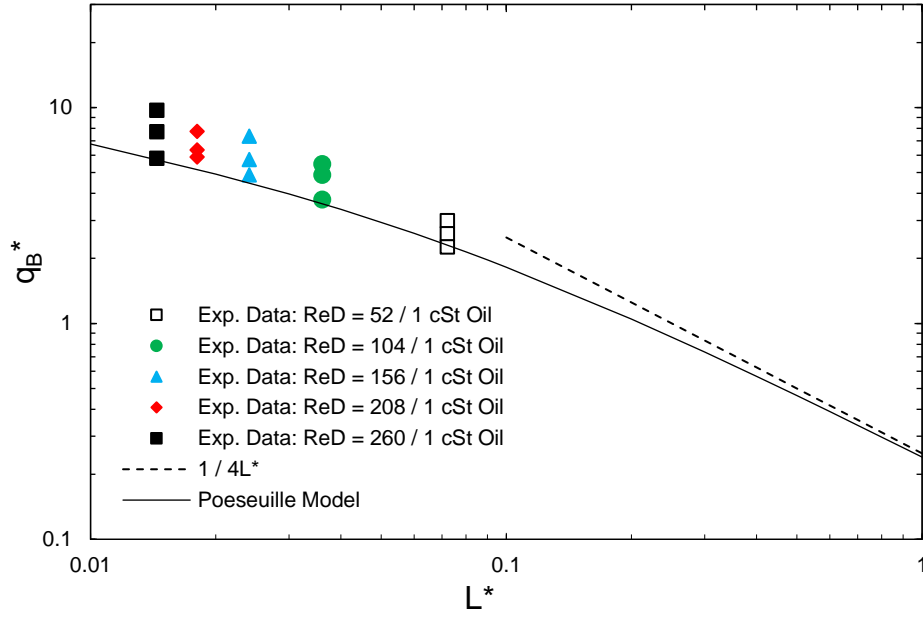


Figure 5.8 experimental data using actual wetted duct area of (for 1 cSt oil) component when applying separated phase modeling

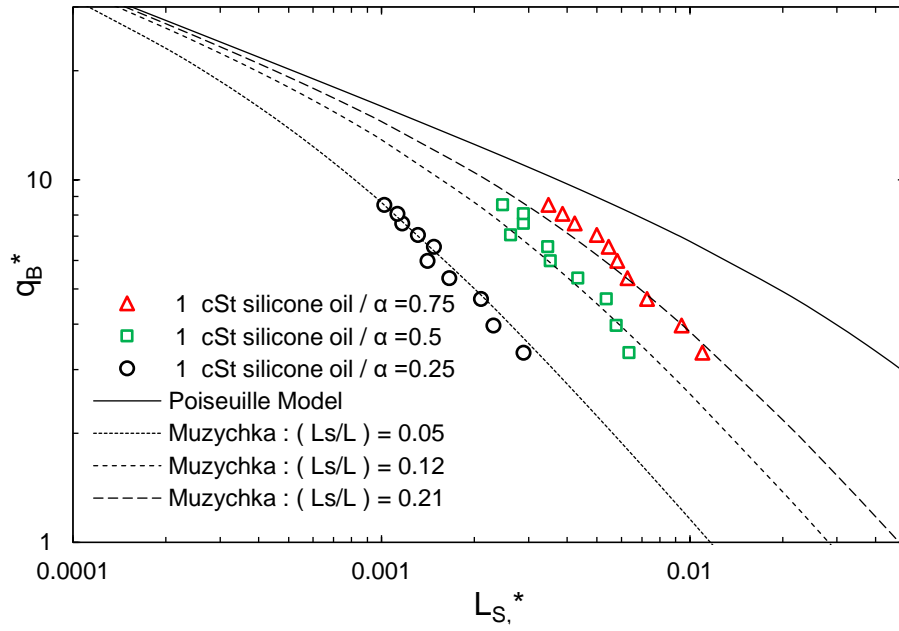


Figure 5.9 experimental data using actual wetted duct area of (for 1 cSt oil) component when applying separated phase modeling

Fig. 5.7 and 5.8 demonstrate heat transfer enhancement in 1 cSt oil and water experiments for each phase component when considering a separated approach, at various slug ratios $L_S/L = 0.05$, 0.12 and 0.21. The results show that heat transfer is clearly associated with slug length ratio in Taylor flow. The thermal enhancement occurs due to flow cell shortening which leads to more intense internal circulations within slugs. The length of liquid slugs has been carefully controlled by using three liquid fractions α in order to generate different slug ratios.

Figures 5.9 and 5.11 show the data presented according the scheme proposed by Muzychka [21]. Given that heat transfer enhancement is increasing consistently with decreasing slug length L_S , it makes more sense physically to use the slug length and not the tube length as the controlling parameter on a Graetz plot. The comparison between the new data and the single phase model (for one phase) supports the importance of using a separated model as a superior method in heat transfer analysis for segmented liquid-liquid Taylor flow. However, the actual (maximum) velocity of liquid slugs was used, i.e. the superficial velocity is divided by the liquid fraction.

Figs. 5.12 - 5.14 show that a consistent prediction of heat transfer performance for each phase is associated with slug length shortening. This alternative approach shows that a liquid-liquid Taylor flow can be predicted using a separated phase analysis and applying the gas-liquid model of Muzychka [21].

Finally, the experimental observations highlighted that maximum heat transfer rate can be reached when slug length getting close to tube diameter, i.e. $L_S \sim D$. This has been supported by the theory of internal circulation within liquid slugs, [11, 21]. However, the intensity of internal circulation within liquid slugs is proportional to $1/L_S$. Root mean square percentage error (RMSPE) for the three asymptotic models associated with slug ratios $L_S/L = 0.05$, 0.12 and 0.21 in Fig. 5.15 has been determined to be 6.8, 7.3 and 11.4 % respectively. These values demonstrate the model performance based on the present measurements. Hence, based on these findings it can be proved that the separated approach is more consistent method to be used for heat transfer modeling of Taylor flow in mini/micro channels.

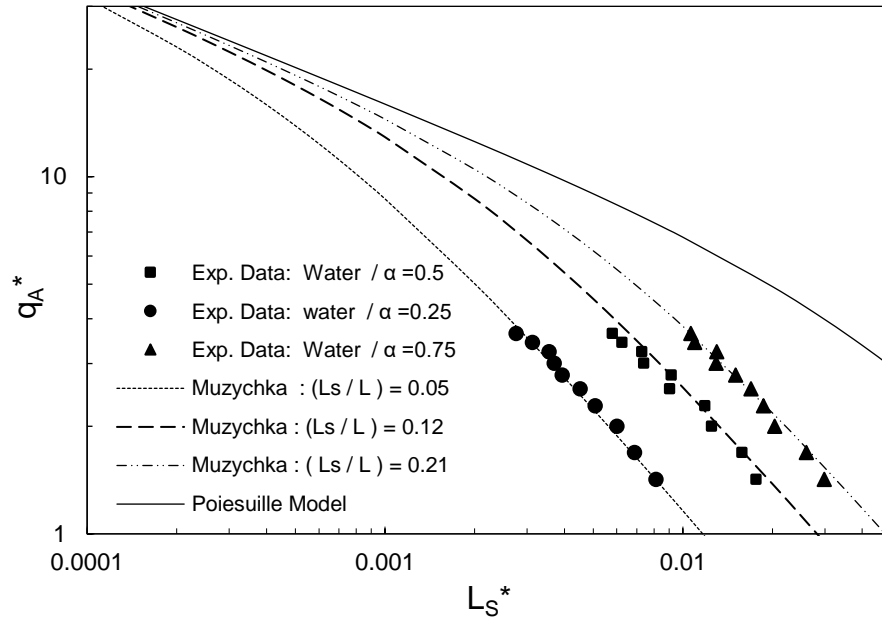


Figure 5.10 experimental data using actual wetted duct area of water component when applying separated phase modeling.

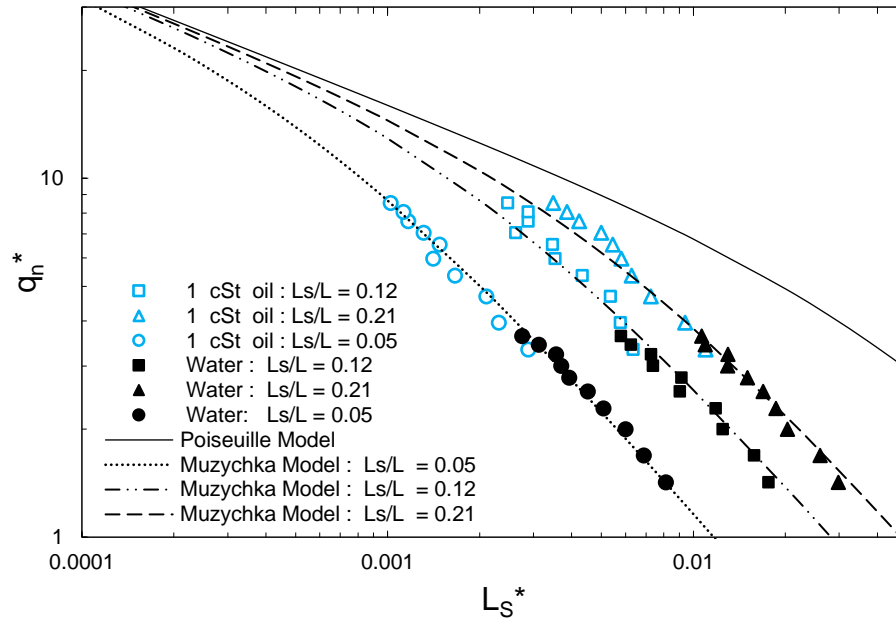


Figure 5.11 dimensionless heat flux data for the both components of segmented flow as compared with model predictions for three values of (L_S/L) .

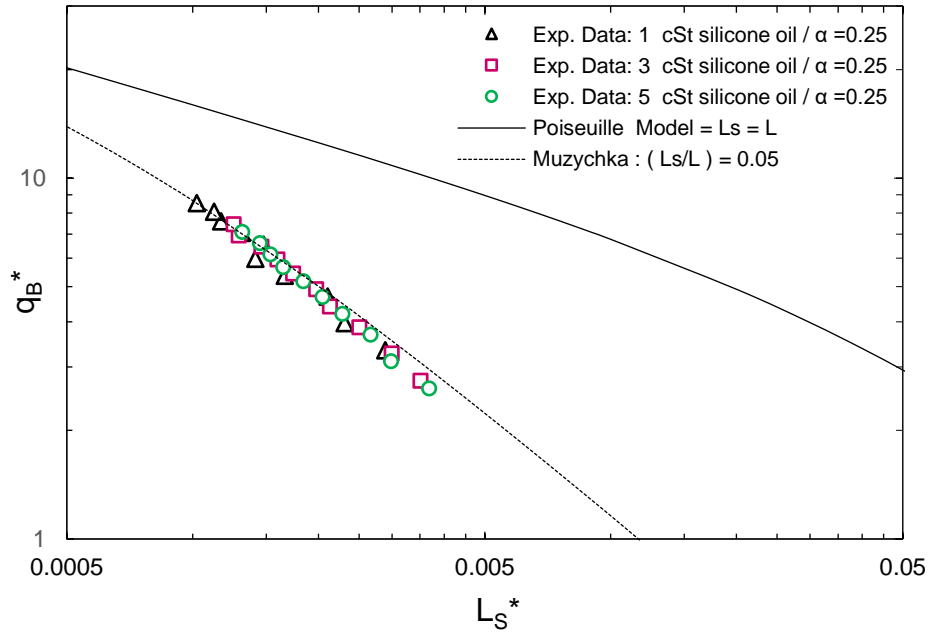


Figure 5.12 effect of liquid slug length ratio (L_s/L) on q^* for three silicone oil components in Taylor flow for $\alpha = 0.25$. RMSPE=6.8%

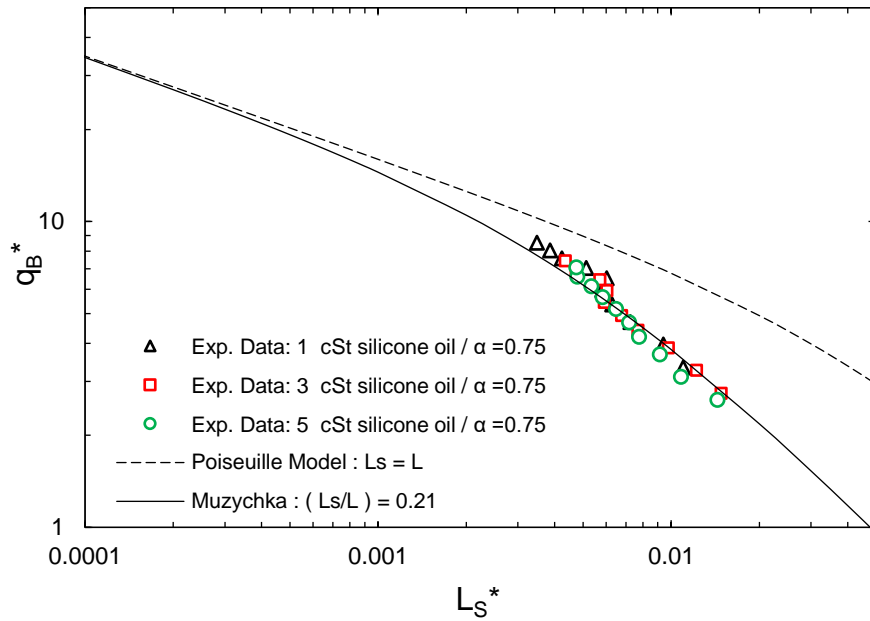


Figure 5.13 effect of liquid slug length ratio (L_s/L) on heat transfer for three silicone oil components in Taylor flow for $\alpha = 0.5$. RMSPE=7.3%

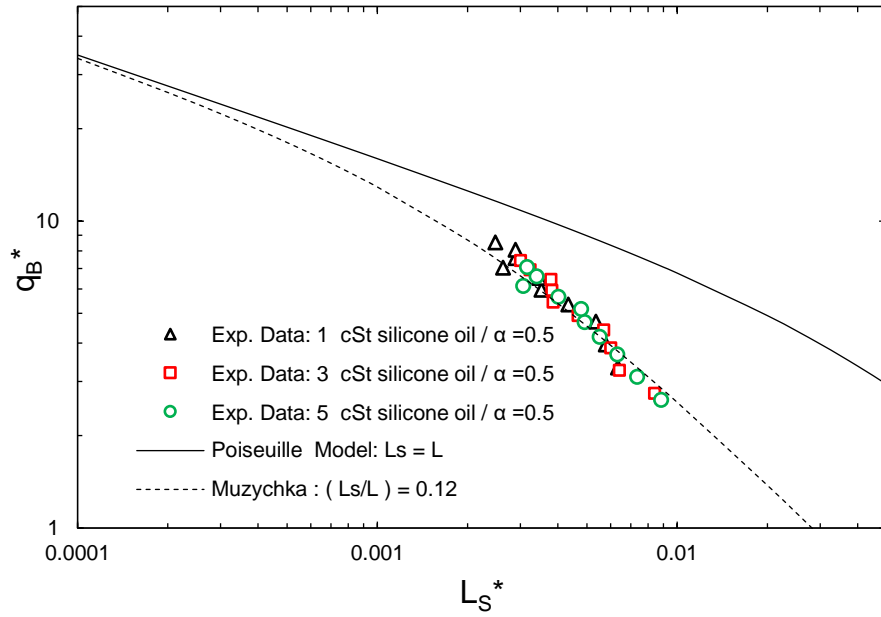


Figure 5.14 effect of liquid slug length ratio (L_S/L) on q^* for three silicone oil components in Taylor flow for $\alpha = 0.75$. RMSPE=11.4%

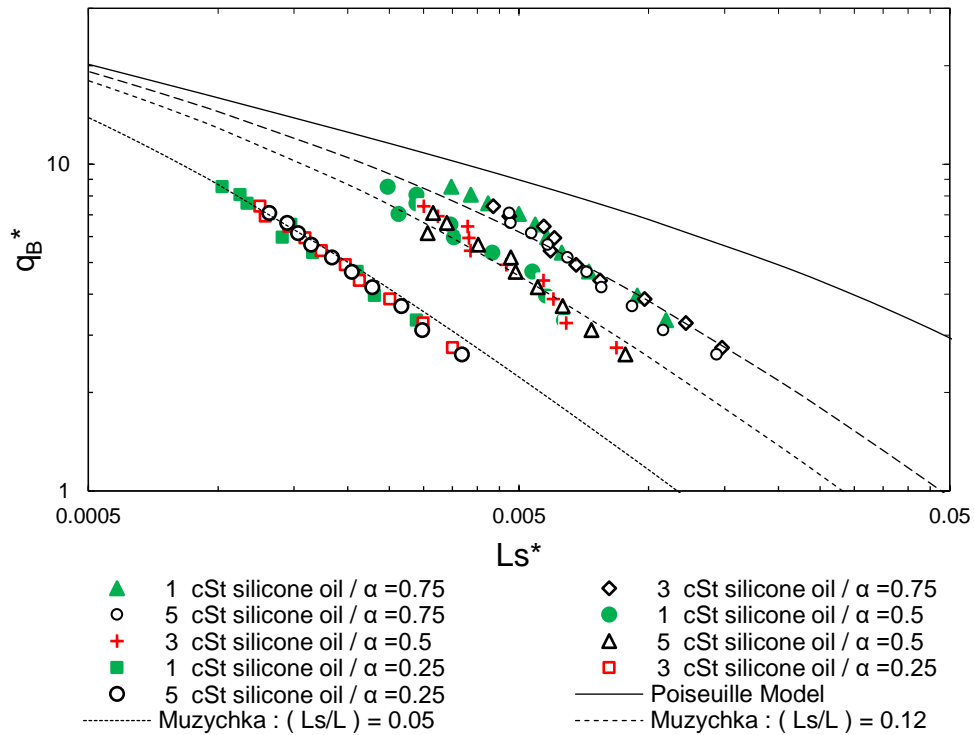


Figure 5.15 dimensionless heat flux data for all oil combinations as compared with model predictions for three values of (L_S/L) .

Fig. 5. 15 demonstrate an effect of slug shortening on heat transfer enhancement of Taylor flow. The short slugs were characterized by greater boundary layer renewal within each slug as compared with the longer slugs.

5.6 Conclusion

The present study provides important insights on heat transfer analysis for the segmented of liquid-liquid Taylor flow in mini scale tubes under a constant wall temperature. In this study, three silicone oils 1, 3 and 5 cSt were introduced with distilled water at different liquid fractions $\alpha = 0.25, 0.5$ and 0.75 . The slug length was experimentally varied to demonstrate the effect of slug length on heat transfer enhancement. Three slug ratios of $L_s/L = 0.05, 0.12$ and 0.2 were obtained for comparison of the proposed modelling approach.

The experimental observations using a separated phase modeling approach to demonstrate heat transfer enhancement within liquid-liquid Taylor flow, highlighted a new approach for two phase flow heat transfer analysis. Finally, heat transfer enhancement of liquid-liquid Taylor flows show a consistency with previous studies on gas-liquid flows and agreement with the published model of Muzychka [21] when applied to each liquid phase alone. Next study on liquid-liquid Taylor flow well be preformed in coiled tube by considering one value of fraction $\alpha = 0.5$ and slug ratio L_s/L will be controlled only by junction parameters (size, shape, and flow directions). Hence, extra heat transfer enhancement is expected due to secondary flow effect.

5.7 References

- [1] Muzychka, Y.S. and Ghobadi, M., "Measurement and Analysis of Laminar Heat Transfer Coefficients in Micro and Mini-Scale Ducts and Channels", *Heat Transfer Engineering*, Vol. 37, no. 11, pp. 938-946, 2016.
- [2] Tuckerman, D.B. and Pease, R.F., "High-Performance Heat Sinking for VSLI", *IEEE Electron Device Letters*, Vol. EDL-2, pp. 126-129, 1981.
- [3] Fairbrother F. and Stubbs, A.E., "Studies in Electro-endosmosis. Part VI. The Bubble-tube Method of Measurement", *Journal of the Chemical Society*, Vol. 1, pp.527-529, 1935.
- [4] Churchill, S. W., and Ozoe, H., "Correlations for Laminar Forced Convection in Flow Over an Isothermal Flat Plate and in Developing and Fully Developed Flow in an Isothermal Tube", *Journal of Heat Transfer*, Vol. 95, pp.416-419, 1973.
- [5] Taylor, G.I., "Deposition of a Viscous Fluid on the Wall of a Tube", *Journal of Fluid Mechanics*, Vol. 10, pp. 161-165, 1961.
- [6] Muzychka, Y.S. and Yovanovich, M.M., "Laminar Forced Convection Heat Transfer in the Combined Entry Region of Non-Circular Ducts", *Journal of Heat Transfer*, Vol. 126, pp. 54-61, 2004.
- [7] Oliver, D.R. and Young Hoon, A., "Two Phase Non-Newtonian Flow: Part 2 Heat Transfer", *Transactions of the Institution of Chemical Engineers*, Vol. 46, pp. 116-122, 1968.
- [8] Horvath, C., Solomon, B.A., Engasser, J.M., "Measurement of Radial Transport in Slug Flow Using Enzyme Tubes", *Industrial and Engineering Chemistry, Fundamentals*, Vol. 12, no. 4, pp. 431-439, 1973.
- [9] Vrentas, J.S., Duda, J.L, and Lehmkuhl, G.D., "Characteristics of Radial Transport in Solid-Liquid Slug Flow", *Industrial and Engineering Chemistry, Fundamentals*, Vol. 17, no. 1, pp. 39-45, 1978.
- [10] Maddox, D.E. and Mudawar, I., "Single- and Two-Phase Convective Heat Transfer from Smooth and Enhanced Microelectronic Heat Sources in a Rectangular Channel", *Journal of Heat Transfer*, Vol. 111, pp. 1045-1052, 1989.

- [11] Muzychka Y. S., “Walsh E., “Simple Models for Laminar Thermally Developing Slug Flow in Noncircular Ducts and Channels” *Journal of Heat Transfer*, ASME, 2010, Vol. 132 / 111702-1.
- [12] Walsh, P., Walsh, E., and Muzychka, Y.S., “Heat Transfer Model for Gas-Liquid Slug Flows Under Constant Flux”, *International Journal of Heat and Mass Transfer*, Vol. 53 (15-16), pp. 3193-3201, 2010.
- [13] Muzychka Y. S., Walsh E. Walsh P., “Heat Transfer Enhancement Using Laminar Gas-Liquid Segmented Plug Flows” *Journal of Heat Transfer*, 2011 by ASME, APRIL 2011, Vol. 133 / 041902-1.
- [14] Betz, A.R. and Attinger, D., “Can Segmented Flow Enhance Heat Transfer in Microchannel Heat Sinks”, *International Journal of Heat and Mass Transfer*, Vol. 53, pp. 3683-3691, 2010.
- [15] Asthana, A. and Zinovik, I., “Significant Nusselt Number Increase in Micro-channels with a Segmented Flow of Two Immiscible Liquids: An Experimental Study”, *International Journal of Heat and Mass Transfer*, Vol. 54, pp. 1456-1464, 2011.
- [16] Adrugi W. M., Muzychka Y.S., and K. Pope, “Heat Transfer in Liquid –Liquid Taylor Flow in Mini-Scale Tube with Constant Wall Temperature” ASME 2015.
- [17] Adrugi, W., Muzychka, Y.S., and Pope, K., “Heat Transfer in Liquid-Liquid Taylor Flow in Mini-scale Curved Tubing for Constant Wall Temperature,” ASME-IMECE-2015-67700.
- [18] Giolla M. M. Eain A. , Vanessa E., Punch J. , “Local Nusselt number enhancements in liquid–liquid Taylor flows”, *International Journal of Heat and Mass Transfer*, 80 (2015) 85–97.
- [19] Adrugi W. M, Muzychka Y.S. , and K. Pope,” Heat transfer in Liquid-Liquid Taylor Flow in a Minin-scale Tube with Constant Wall Temperature” ASME-ICNMM2015-48272.
- [20] Dai Z., Guo Z., David F, Brian S., “Taylor flow heat transfer in micro channels-Unification of liquid–liquid and gas–liquid results”, *Chemical Engineering Science*, 138(2015)140–152.
- [21] Muzychka, Y.S., “Laminar Heat Transfer for Gas-Liquid Segmented Flows in Circular and Non-circular Ducts with Constant Wall Temperature” ASME, 2014.

- [22] Alrbee, K., Muzychka Y.S. and X. Duan, “Heat Transfer enhancement in laminar Graetz and Taylor Flows using nanofluids” ASME-ICNMM2018-7756.
- [23] Haase, S., “Characterisation of gas-liquid two-phase flow in mini-channels with co-flowing fluid injection inside the channel, part II: gas bubble and liquid slug lengths, film thickness, and void fraction within Taylor flow”, *International Journal of Multiphase Flow*, 88 (2017) 251–269.
- [24] Howard A. and Walsh P. A., “Heat Transfer Characteristics of Liquid-Gas Taylor Flows incorporating Microencapsulated Phase Change Materials”, *Journal of Physics: Conference Series* 525 (2014) 012022.
- [25] Hughmark, G.A., “Holdup and Heat Transfer in Horizontal Slug Gas-Liquid Flow”, *Chemical Engineering Science*, Vol. 20, pp. 1007-1010, 1965.
- [26] Talimi V., Muzychka Y. S., Kocabiyik S., “A Review on Numerical Studies of Slug Flow Hydrodynamics and Heat Transfer in Microtubes and Microchannels”, *International Journal of Multiphase Flow*, 39, pp. 88-104, 2012.
- [27] Muzychka, Y.S. and Ghobadi, M. “Measurement of Laminar Heat Transfer Coefficients in Micro and Mini Scale Ducts and Channels”, Proceedings of the 2014 IC-NMM, Chicago, IL, 2014.
- [28] Oliver, D.R. and Wright, S.J., “Pressure Drop and Heat Transfer in Gas-Liquid Slug Flow in Horizontal Tubes”, *British Chemical Engineering*, Vol. 9, pp.590-596, 1964.
- [29] Kline, S. J., and F. A. McClintock. “Describing Uncertainties in Single-Sample Experiments.” *Mechanical Engineering*, Vol. 75, No. 1, January 1953: 3-8.
- [30] Narayanan. C, Lakehal D., “Two-phase convective heat transfer in miniature pipes under normal and microgravity conditions”, *ASME Journal of Heat Transfer*, 130 (2008) 074502-1–074502-5.
- [31] Muzychka, Y.S., “Generalized Models for Laminar Developing Flows in Heat Sinks and Heat Exchangers”, *Heat Transfer Engineering*, vol. 34 (2-3), pp. 178-191,2013.
- [32] Prothero, J. and Burton, A.C., “The Physics of Blood Flow in Capillaries: 1 The Nature of the Motion”, *Bio-physical Journal*, Vol. 1, pp. 565-579, 1961.
- [33] Adrugi, W. M. , Y. S. Muzychka and K. Pope, “Heat Transfer Model for Liquid-Liquid Taylor Flow in Mini-Scale Coiled Tubing”, ASME- ICNMM2018.

- [34] Svetlov S.D., R.Sh. Abiev, “Formation Mechanisms and Lengths of the Bubbles and Liquid Slugs in a Coaxial-spherical Micro Mixer in Taylor Flow Regime”, *Chemical Engineering Journal*, 354 (2018) 269–284.
- [35] Zan Wu, Zhen Cao, Bengt Sundén “Liquid-liquid Flow Patterns and Slug hydrodynamics in Square Microchannels of Cross-shaped Junctions”, *Chemical Engineering Science*, 174 (2017) 56–66.
- [36] Maxime, C., Eyangelia-Panagiota R., Panagiota A., “Studies of Plug Formation in Microchannel Liquid–liquid Flows Using Advanced Particle Image Velocimetry Techniques”, *Experimental Thermal and Fluid Science*, 69 (2015) 99–110.
- [37] Maxim Vladimirovich Shcherbakov, Brebels, A., “A Survey of Forecast Error Measures” *World Applied Sciences Journal*, (Information Technologies in Modern Industry, Education and Society): 171-176, 2013.

CHAPTER 6

HEAT TRANSFER IN LIQUID-LIQUID TAYLOR FLOW IN MINI SCALE COILED TUBES

6.1 Introduction

Enhancement of heat transfer using the curved / coiled tube to achieve passive heat transfer enhancement in laminar flow was considered early by Dean [1, 2]. These were the first analytical studies of fully developed laminar flow in a curved tube of circular cross section. Several theoretical solutions were developed for the Poiseuille flow in the straight tubes at low Dean number $De < 17$. Some authors have reported a definition of the Dean number De for curved tube. For low Dean numbers, the axial-velocity profile was parabolic and unaltered from the fully developed straight tube flow. As the Dean number is increased, the maximum velocity begins to be skewed toward the outer periphery which causes a secondary flow and increased heat transfer. Several experimental studies in literature were conducted in mini / micro scale coiled / spiral tubes using single phase flow. In general, heat transfer augmentation was reported and explained by increasing Dean number De which is inversely proportion to tube curvature $1/R$ [3-8].

**The materials in this chapter are intended to be submitted to International Journal of Heat Transfer*

Taylor flow was early named after Taylor [9] studied deposition of viscous liquids on the wall of tube. Taylor's study was followed by serious of studies which used two phase gas-liquid flows. Their results showed a remarkable heat transfer enhancement in small scale straight tubes using gas-liquid [10-15] [23,24] or liquid-liquid Taylor flows [6],[16-18] when compared with continuous Graetz flow. In particular, the literature review revealed important attempts to predict thermal behavior of gas-liquid Taylor flow. However, flow properties and liquid slug length were the main parameters of data prediction for the most proposed correlations [20-22].

Liquid-liquid Taylor flow at micro and mini-scales was the focus of recent publications. The experimental studies reported heat transfer augmentation over single phase flow. Although, only a small number of studies have been reported with great heat transfer enhancement, [16-20]. A survey on laminar heat transfer in mini / micro scale channels was performed to provide a research background and show the gap which needs to be investigated. Later sections will introduce the related theoretical and experimental studies considering continuous and segmented flows in small scale channels.

Experimental studies on laminar flow in small scale curved tubes were conducted earlier by W. R. Dean [1,2]. Muzychka and Ghobadi [3-5] reported heat transfer enhancement in coiled / spiral mini scale tubes. Their studies provided experimental data and predictive correlation was developed by considering two asymptotic limits for entrance and fully developed regions.

Alrbee and Muzychka [17] recently suggested a separated flow analysis as a new approach to demonstrate heat transfer of liquid-liquid Taylor flow in mini scale straight tubes. The new approach addressed the flow as two separate components which takes the advantage of actual flow velocity instead of the superficial one. The study was conducted using three silicone oils 1, 3 and 5 cSt which were segmented by distilled water at different liquid fractions $\alpha = 0.25, 0.5$ and 0.75 . The slug length was experimentally controlled to investigate the effect of slug length on heat transfer enhancement. Consequently, three segmentation ratios of $L_S/L = 0.05, 0.12$ and 0.2 were created for the three silicone oils. They report that heat transfer is significantly associated with liquid slug ratio L_S/L and the maximum heat transfer was observed as liquid slugs reached the inside diameter of the channels. Finally, the study concluded that heat transfer enhancement of liquid-liquid Taylor flows show a consistency with previous studies on gas-liquid flows and

agreement with the published model of Muzychka [21] when applied separately to the flow components.

Horvath et al. [11] studied heat within Taylor flow of gas-liquid in straight tubes of circular cross section. Their experimental results were obtained with constant liquid fractions of 0.5 throughout the study. The reported data of Nusselt number counted for liquid slug phase only versus slug aspect ratio $\beta = L_S/D$ over a range of the whole range of slug flow. The effect of slug velocity was studied by varying the two phase flow Reynolds number at the same liquid fraction. They also concluded that liquid slugs become thermally saturated at lower aspect ratio L_S/D . They explained their findings as result of the high radial mixing of segmented flow within short slugs. Additional studies by Oliver and Young [12] and Vrentas [13] were conducted using solid-liquid Taylor flow which considered liquid slug length as an important parameter on heat transfer rates.

Alrbee and Muzychka [10] examined potential of laminar heat transfer of gas-liquid Taylor flow in circular straight tubes. More specifically, the study demonstrated heat transfer enhancement due to the liquid slug shortening in a segmented flow and to further validate a model previously developed by the second author. New experimental data for gas-liquid Taylor flow in mini scale were carefully obtained using 1 cSt silicone oil which was segmented by air. The experiments were performed with a liquid fraction fixed at $\alpha = 0.5$. They observed that for constant wall temperature, the dimensionless mean wall flux and Nusselt number have been increased by a factor of two at the upper limit of laminar flow which was considered with $Re_D = 320$, when the slug aspect ratio L_S/D equal to 10. On other hand the enhancement became three times for the same limit of flow when slug aspect ratio has reduced to 1.25 which almost approaches the tube diameter.

Muzychka, [23] extended his earlier analysis of Taylor gas-liquid flow [20] using the appropriate fully developed flow limit. The new model considers the effect of slug to tube length (L_S/L) on heat transfer, Fig. 1 as the boundary layer renewal is most dominant in short slugs but becomes exhausted in long tubes. Hence, one of important characteristic of the new model is that it shows how quickly short slugs become thermally saturated. Muzychka [23] used published experimental data from [11-13] to validate his model. One shortcoming of the published data was the fact that most data only showed early signs of fully developed flow being achieved. In the present study new experimental data are accurately obtained under constant wall temperature as further validation for liquid-liquid flows.

Adrugi and Muzychka [16] studied heat transfer enhancement using liquid-liquid Taylor flows in mini scale coiled tubing which is subjected to isothermal conditions. Various geometries of mini scale tubes with different radii of curvature and lengths were tested. They used three low viscosity silicone oils (1 cSt, 3 cSt, 5 cSt) to examine the effect of Prandtl number on heat transfer enhancement. They developed a new experimental correlation to predict heat transfer in liquid-liquid Taylor flow within curved / coiled tubes.

Giolla et al. [19] investigated the potential of heat transfer enhancement in liquid-liquid Taylor flow in straight tubes. They used a Taylor flow of water-oil heated under constant flux. However, the primary focus was to examine the influence of slug length and carrier phase variations on the local Nusselt numbers. Temperature measurement was carried out using an infrared thermography system. Their experimental observations revealed that the greatest enhancement was achieved in flows with carrier slug lengths approaching the channel diameter. They found that the liquid film separates the dispersed slugs from the heated capillary walls, causing a reduction in the heat transfer rates. A similar study was performed in [17] using liquid-liquid Taylor flow. A scenario of variable void fraction was adopted throughout the experiments. However, the thermal enhancement under isothermal conditions was significantly greater with shorter slug lengths.

Adrugi and Muzychka, [26] carried out experimental study using liquid-liquid Taylor flow in mini scale tube under constant wall temperature. Both liquids were fed through straight test section. The experiments were conducted based on different flow modes of void fraction. The flow patterns were created by introducing two immiscible liquids (water – silicone oils) into mini scale tubes with straight and curved paths. The results showed a significant enhancement in heat transfer if compared with single phase flow models. More experimental studies were published in this regard by Eain, et al. [18] and Wei et al [19] to investigate heat transfer of liquid-liquid Taylor flow in mini scale tubes.

Howard and Walsh [24] studied heat transfer in Taylor flow of gas-liquid in mini scale tubes. They incorporated microencapsulated phase change materials into the liquid slugs. They reported heat transfer enhancement as result of the internal circulations within liquid slugs which was confirmed in [11-14], as well as increasing thermal capacity of flow which is associated with the MPCM. The experiments were conducted with a constant heat flux boundary condition. Heat transfer enhancement was examined by changing liquid slug length and liquid fractions. Infrared

thermography results demonstrated a significant reduction in the wall temperatures because of using MPCM gas-liquid Taylor flow as working fluid when compared with the conventional single phase coolants. Their study concluded that segmented MPCM gas-liquid Taylor flows provides further enhancement than that of MPCM single phase flows.

Alrbee and Muzychka [27] conducted experimental study to investigate the potential of increasing heat transfer rates by dispersing the nanoparticles in the gas-liquid Taylor flows. The dispersed Taylor flow was subjected to a constant wall temperature within mini scale straight tubes. Three concentrations of Al_2O_3 nanofluids were examined: 0.25 vol.%, 0.5 vol.% and 0.75 vol. %. They considered the homogeneous analysis for data reduction. Heat transfer enhancement of segmented nanofluids were compared with the conventional Taylor flows. The results showed a heat transfer enhancement associated with nanoparticle concentration as well as liquid fractions.

6.2 Taylor flow Modeling

Experimental data of liquid-liquid Taylor flow of two immiscible liquids were obtained. Heat transfer rates of flow components A and B were calculated as two separate flows Eq.(6.1). This analysis requires to determine heat transfer for each component. Ten temperature measurements of inlet and outlet flow were collected and averaged to reduce effect of errors. The same principle was introduced in [17 - 20] to demonstrate heat transfer enhancement of segmented flow as:

$$Q_n = (\dot{m}c_p)_n(T_o - T_i) , \quad n = A, B \quad (6.1)$$

$$Q_{Bulk} = Q_A + Q_B \quad (6.2)$$

where, Q_n is the bulk heat transfer achieved for each component, A and B, the subscript i and o, refers to tube inlet and outlet. Outlet temperature of flow was monitored to measure the fluctuation of the temperature measurements for flow components. The measurements revealed that the outlet temperatures of the two flow components which have the same slug length $L_{S,A} = L_{S,B}$ reach similar temperature at some point downstream, i.e. $T_{o,A} \sim T_{o,B}$. The two liquids were fed into the segmenting junction at the same temperature 24 °C, i.e. $T_{i,A} \sim T_{i,B}$. Fig.6.1 shows the basic liquid-liquid Taylor flow cell.

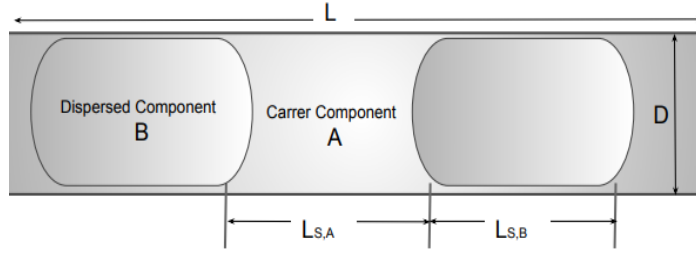


Figure 6.1 liquid-liquid Taylor flow cell configuration

Muzychka [20] defined the dimensionless mean wall heat flux q^* of the gas-liquid Taylor flow based on the actual wetted duct area for each component $\alpha_L A_w$ which has been used instead of hole tube area PL . In the present study, heat transfer Q for each component of the liquid-liquid Taylor flow in curved / coiled tubes was determined as two separate components Q_A and Q_B which is useful in order to reduce errors when using the averaged / homogenous correlations ($\bar{\rho}$, and \bar{c}_p). Finally, heat transfer rates of components A and B were added and converted to dimensionless forms of Nusselt number Nu_D and dimensionless heat flux q^* as:

$$\overline{Nu}_D = \frac{Q_{Bulk} D}{\bar{k} A_w \Delta T_{LMTD}} \quad (6.3)$$

Where ΔT_{LMTD} is log mean temperature difference which is defined as:

$$\Delta T_{LM} = \frac{(T_w - T_i) - (T_w - T_o)}{\ln \frac{(T_w - T_i)}{(T_w - T_o)}} \quad (6.4)$$

In same manner dimensionless heat flux q^* was determined using the principle as:

$$q_n^* = \frac{(Q_n / A_w) D}{k_n (T_w - T_i)} \quad (6.5)$$

where $A_w = PL$ and T_w and T_i are wall and inlet temperatures.

The experimental results are plotted as function of corresponding dimensionless parameters such as L^* , Re_D and Dean number De . The actual flow (maximum) velocity $U_m = U_A + U_B$ has been used instead of superficial velocity to reduce the experimental data [20]. The dimensionless groups were calculated as:

$$L^* = \frac{L/D}{Pe_D} \quad (6.6)$$

where the actual flow velocity and volume averaged flow properties [18,30] are considered to present the x-axis parameters as:

$$Pe_D = \frac{(U_A + U_B)D}{\left(\frac{k}{\rho c_p}\right)_{Ave}} \quad (6.7)$$

$$Re_D = \frac{\rho_{av} U_m D}{\mu_{av}} \quad (6.8)$$

The effective / averaged properties $E_{ave}(\rho, \mu, k \text{ and } C_P)$ of the liquid-liquid Taylor flow are determined based on liquid fraction α using the well known formulas [6,18,30] which take the general form:

$$E_{ave} = E_A(1 - \alpha_B) + E_B(\alpha_B) \quad (6.9)$$

$$\alpha_A = \frac{\dot{Q}_A}{\dot{Q}_A + \dot{Q}_B}, \quad \alpha_B = \frac{\dot{Q}_B}{\dot{Q}_A + \dot{Q}_B} \quad (6.10)$$

where \dot{Q}_A and \dot{Q}_B denotes to the volumetric flow rates of liquid components A and B of Taylor flow as shown in Fig. 6.1.

Heat transfer in curved tubes is affected by secondary flows which cause heat transfer augmentation proportional to tube curvature $1/R$. Fig. 6.2 demonstrates secondary flow intensity as function of Dean number De [33].

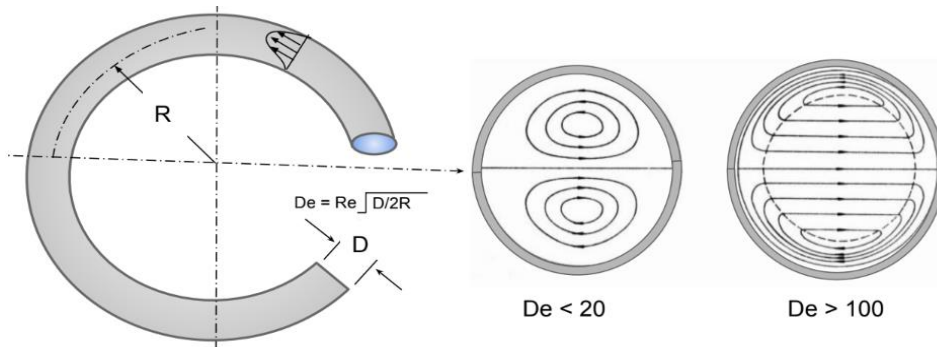


Figure 6.2 intensity of secondary flow of high and low Dean number (Dravid and., Smith, [8])

Dean number De of Taylor flow in coiled / curved tubes which is defined based on effective / averaged flow properties:

$$De = Re_D \sqrt{\frac{D}{2R}} \quad (6.11)$$

where, R and D are radius of the radius of curvature and the tube diameter, respectively. Reynolds number Re_D is determined using in Eq.(6.8) In general, the experimental results

The present study is also interested to present the experimental results of liquid-liquid Taylor flow using principle of flow separation. Nusselt number Nu_D and dimensionless heat flux q^* for each flow component A or B were plotted versus Dean number De of these components. The flow components A and B were treated as two separate flows exactly as gas-liquid flow. This approach uses the wetted tube area and actual (maximum) flow velocity. Detailed information can be found in [10,17,21].

The experimental results of single phase flow in straight tube were compared with Graetz-Poiseuille flow model in circular ducts: Nusselt number Nu_D and dimensionless mean wall heat flux q^* [21], these Models take the forms:

$$\overline{Nu}_D = \left(\left(\frac{1.614}{L^{*1/3}} \right)^5 + (3.65)^5 \right)^{1/5} \quad (6.12)$$

$$q^* = \left(\left(\frac{1.614}{L^{*1/3}} \right)^{-3/2} + \left(\frac{1}{4L^*} \right)^{-3/2} \right)^{-2/3} \quad (6.13)$$

The results of liquid-liquid Taylor flow in coiled / curved tubes were compared with single phase model which was developed by Ghobadi and Muzychka [3]. The comparison did not show any agreement over the examined range of Dean number De up to 100. The model takes the form:

$$Nu_D = \left[3.66^4 + \left(0.91375 \sqrt{De} Pr^{-0.1} \right)^4 \right]^{1/4} \quad (6.14)$$

The experimental results were also compared with liquid-liquid model. The model was developed by Adrugi and Muzychka [6]. Theoretically, this model combines the two asymptotes of the entrance and fully developed flow regions and takes the form:

$$Nu_D = \left[3.66^{15} + (0.75\sqrt{De}Pr^{-0.1})^{15} \right]^{1/15} \quad (6.15)$$

6.3 Methodology of Experimental Study

The study was performed to investigate the thermal characteristics of liquid-liquid Taylor flow in mini scale coiled / curved tubes which affected by isotherm condition. Fig. 6.4 shows the experimental setup. Mainly, the experimental setup was equipped with two programmable syringe pumps (Harvard Apparatus) of capacity 200 ml each. The syringe pumps are engineered to provide an accuracy of 0.25 %. A Fisher Scientific 3013 Iso-temp thermal bath which is PID controlled has been employed to provide constant temperature of 40 °C with a stability of ± 1 % over a range of -30 to 200 °C

Heat transfer of the liquid-liquid Taylor flow stream was calculated based on mass flow rate of two liquid components along with measured inlet and outlet temperatures. Two Omega T-type thermocouples were embedded within two T-junctions located at the both ends of test section. The thermocouples were carefully shielded to avoid effect of the external heat sources.

Liquid-liquid Taylor flow was created to investigate effect of slug ratio γ on heat transfer enhancement in coiled / curved tubes. In current study the experiments were performed by considering fixed fraction of $\alpha = 0.5$. To produce different slug ratio γ several flow segmenting junctions were employed. Fig. 6.3 shows schematic of liquid-liquid Taylor flow for various slug lengths L_S . The flow pattern of Taylor flow was monitored using data acquisition system connected to high-speed camera (Phantom v611) as demonstrated in experiment setup, Fig. 6 4. The flow cell dimensions were checked for each experiment at both sides of test section to ensure stability of

Table 6. 1 contains thermophysical properties of used liquids

liquid	ρ kg/m ³	K W/mK	Cp J/Kg.K	μ Ns/m ²	$\alpha(10^8)$ m ² /s	Pr	$\nu(10^6)$ m ² /s
Water	996	0.6	4080	0.0009	10.5	6.05	0.89
1 Oil	815	0.1	2000	0.0008	6.1	16.2	1
3 Oil	895	0.12	1800	0.0027	7.4	40.3	3
5 Oil	918	0.117	1633	0.0046	7.8	64.1	5

liquid slugs L_s . Length measurements were conducted using image processing software (Image J Software). The high speed camera images showed that the two flow components were moving at the same velocity, i.e. unity slip ratio.

The experimental data were obtained using two immiscible liquids: three low viscosity silicone oils: 1 cSt, 3 cSt, and 5 cSt and segmented by distilled water, Table 6.1. The liquids were picked as they showed a flexibility to create desired slug lengths.

Furthermore, images were captured using high-speed camera and show limited liquid film thickness up to the wall. However, the effect of liquid film on heat transfer becomes more pronounced for higher viscosity liquids [9, 10, and 13].

The design of the experiments was considered to obtain reasonable results. The range of Reynolds numbers was investigated for the three combinations of liquids. Table 6.1 contains summary of the properties of the used liquids. The slug flow regime of liquid-liquid Taylor flow using 1 cSt, 3 cSt and 5 cSt silicone oils with water for $\alpha = 0.5$ was fill within three ranges of Reynolds number Re_D , from 78 to 312, 41 to 165 and 30 to 120, respectively. Furthermore, the data sets have been collected over same range of volumetric flow rates from 4 to 20 ml/s.

Mini scale curved tubes (1.63 mm ID and 0.3 mm thick) made of copper material to achieve quick thermal stability. Three test coils of 250 mm length were formed to produce three coils of radius of curvature: 10, 20, and 40 mm. To apply isothermal conditions, the test section was immersed horizontally in thermal bath kept at 40 °C.

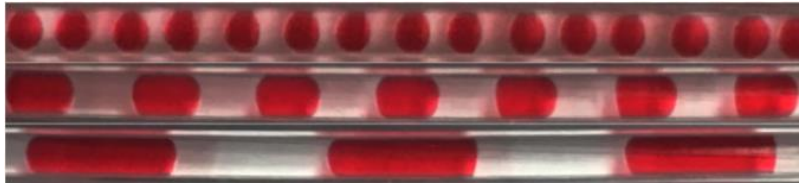


Figure 6.3 Water-1 cSt silicone oil Taylor flow segmentations of fraction $\alpha_n = 0.5$.

Several T-junctions were used to create three liquid slug ratio $\gamma = 0.008, 0.060$ and 0.100 . Liquid-liquid Taylor flow formation and flow patterns can be found with more details in [10][17]. Next section will address the experimental results and data modeling.

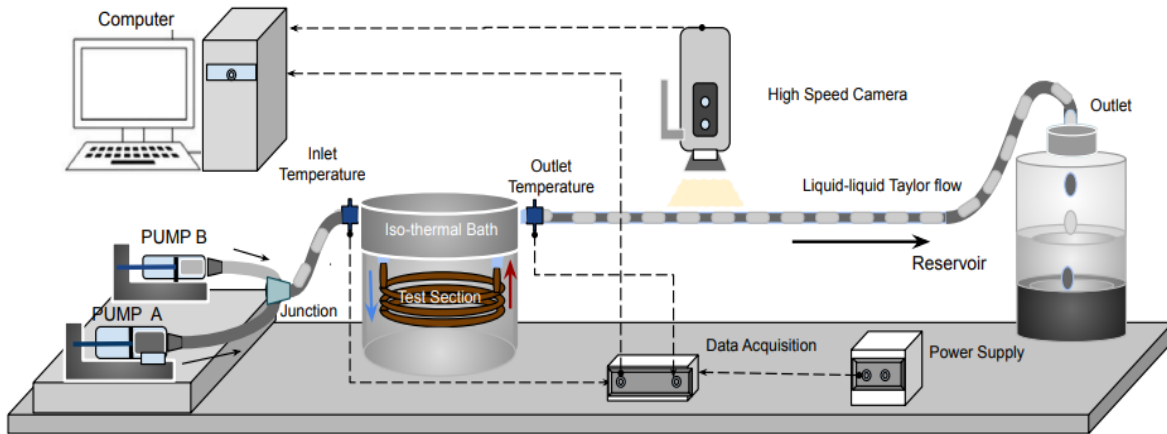


Figure 6.4 heat transfer experimental setup of liquid-liquid Taylor flow in curved/ coiled tube and under constant wall temperature.

6.4 Result and Discussion

Benchmarking results of single phase flow in dimensionless form of Nusselt number Nu_D and dimensionless mean heat flux q^* plotted versus dimensionless tube length L^* . Fig. 6.5 shows agreement between Poiseuille theory and the experimental data of water within a maximum 10% error with the Graetz flow theory for Poiseuille flows.

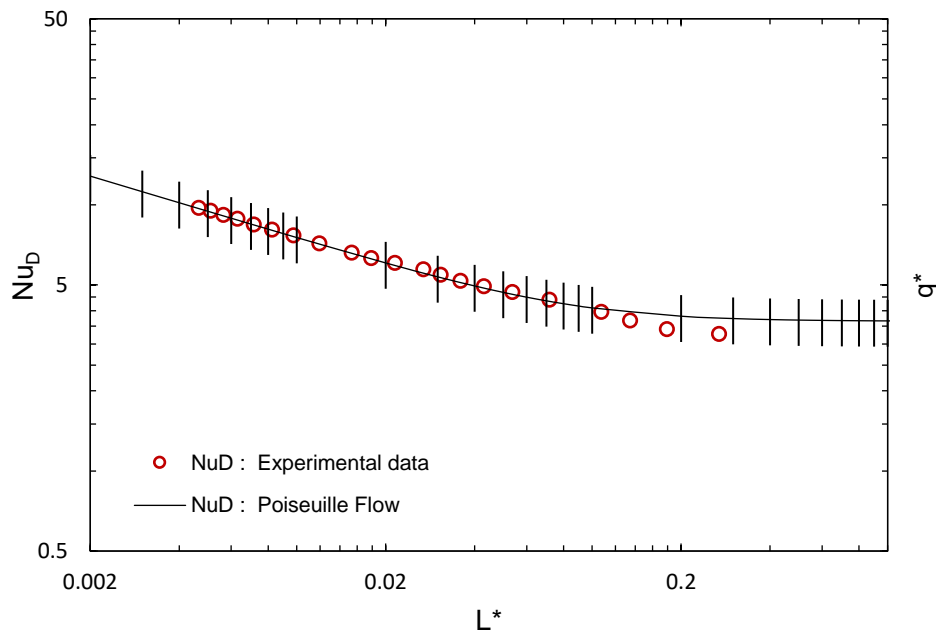


Figure 6.5 Benchmarking results of heat transfer in single phase flow using distilled water.

The well-known method of Kline and McClintock [31] was employed as quantitative analysis to estimate potential errors. The total uncertainty represents contribution of the used equipment in the experimental setup. The uncertainty was estimated over the whole range of ($20 < Re_D < 1260$). The uncertainties within experimental data were found to be ± 1.92 % for L^* . The range of uncertainty in heat transfer dimensionless parameters were ± 2.25 to 3.84 % for the Nusselt number. The benchmarking results for single phase flow showed that the method of measuring bulk temperature using a thermocouple and T junction at both sides of the test section appears to be sound.

Root mean squared percentage error (RMSPE) has been employed to measure how well the experimental data agree with theory. The commonly used formula [32] has the form. RMSPE was estimated for Nu_D and q^* using single phase as shown in Fig.6. 5. The test covered wide range of Reynolds number ($20 < Re_D < 1260$) to show RMSPE =9.6 % for Nu_D data when compared with theory.

The experimental data was presented in terms of Nusselt number Nu_D and q^* (y-axis) and Re_D , L^* and Dean number De (x-axis). Liquid –liquid Taylor flow in coiled tube was analysed based separated components when calculating Q . Thus, liquid-liquid Taylor flow was treated as two separated components. Bulk heat transfer rates Q was converted to dimensionless forms of Nu_D and q^* . Liquid slug ratio γ denotes to L_s / L , which was suggested by Muzychka [20] as an important heat transfer parameter for segmented flows.

The current study employed three low viscosity silicone oils 1, 3 and 5 cSt were segmented by distilled water at fixed fraction $\alpha = 0.5$. The segmented flows were fed into coiled tube of 250 mm length and 1.63 mm inside diameter and bended to form three test sections of 10 ,20 and 40 mm radius. The study considered 40 °C as fixed wall temperature to provide isothermal condition. The experimental data will be addressed in the next sections.

Fig. 6.6 shows dimensionless heat flux q^* of flow components of 1 cSt silicone oil and water. The results were presented as function of Reynolds number Re_D . The separated flow was considered to reduce data. Liquid-liquid Taylor flow was treated as two separate flows of gas-liquid flows [10,17]. This method of analysis counts only the wetted tube area as heat transfer surface.

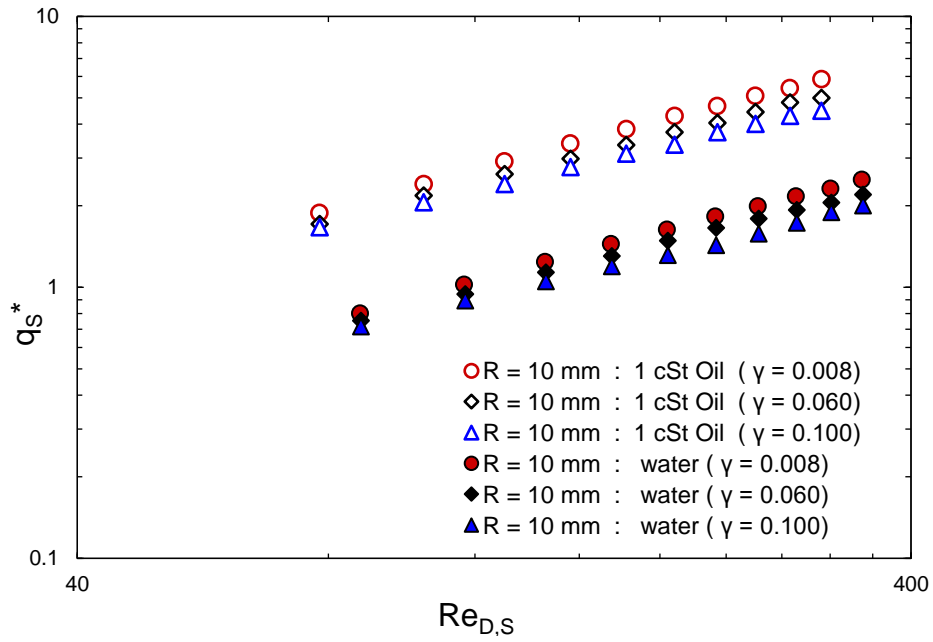


Figure 6.6 effect of slug ratio γ on dimensionless heat transfer data of silicone oils plotted as function of Reynolds number Re_D .

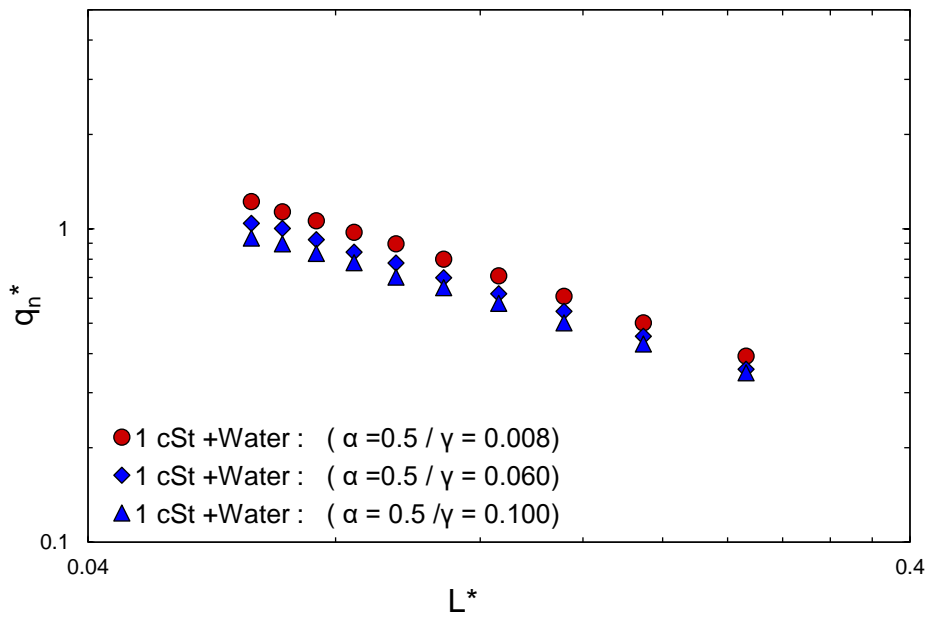


Figure 6.7 effect of slug ratio γ on dimensionless heat transfer data q^* plotted as function of Reynolds number Re_D .

Figure 6.8 effect of flow slug ratio γ on dimensionless heat transfer q_n^* plotted as function of invers Graetz number L^*

The actual / maximum flow velocity is also considered to take an advantage of higher Reynolds number Re_D . The results revealed a consistent level of heat transfer enhancement. However, heat transfer enhancement showed inverse behavior to liquid slug ratios. $\gamma = 0.008, 0.060$ and 0.100 . Fig. 6.7 demonstrates dimensionless heat flux q^* of liquid-liquid Taylor flow obtained using two silicone oils 1 and 3 cSt were fed into coiled tube $R = 10$ mm. The results presented effect of Prandtl number Pr and liquid slug ratio γ .

Figs. 6.8 and 6.9 demonstrate dimensionless heat transfer results of q^* and Nusselt number Nu_D of segmented liquid-liquid Taylor flow using 1 cSt silicone oil were segmented by distilled water at volume fraction $\alpha = 0.5$. The results showed heat transfer enhancement proportional to liquid slug ratio γ . Fig. 6.10 shows an effect Prandtl number Pr change was presented as a function of dimensionless thermal tube length L^* . As mentioned earlier x -axis parameters: Re_D , L^* and Dean number De were calculated based on homogeneous properties using volume average property models of k , μ and ρ [18,30]. This approach has been used in current study to present heat transfer of liquid-liquid Taylor flow.

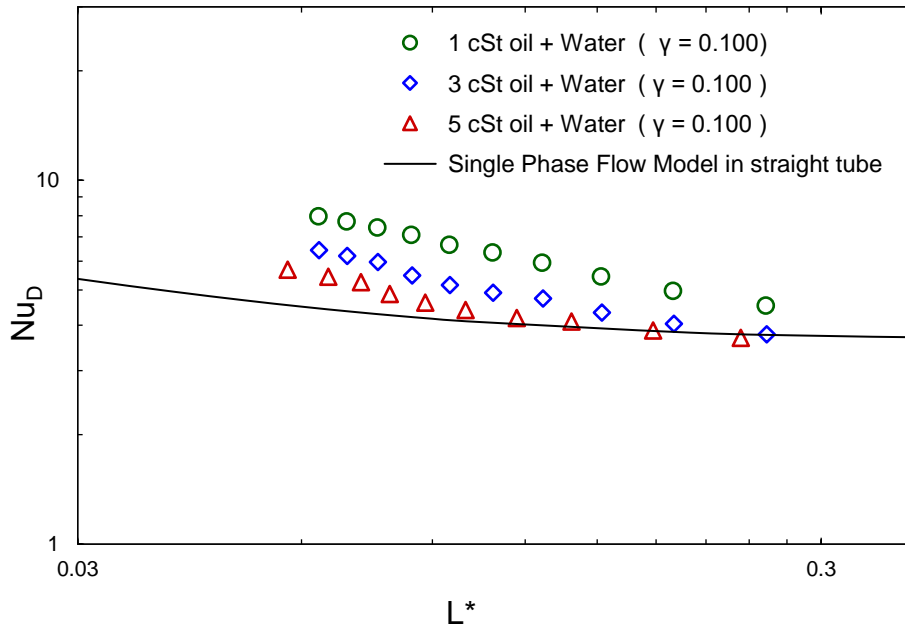


Figure 6.9 effect of Prandtl number Pr change on Nusselt number data Nu_D of Taylor flow as a function of invers Graetz number L^* ($D = 10$ mm).

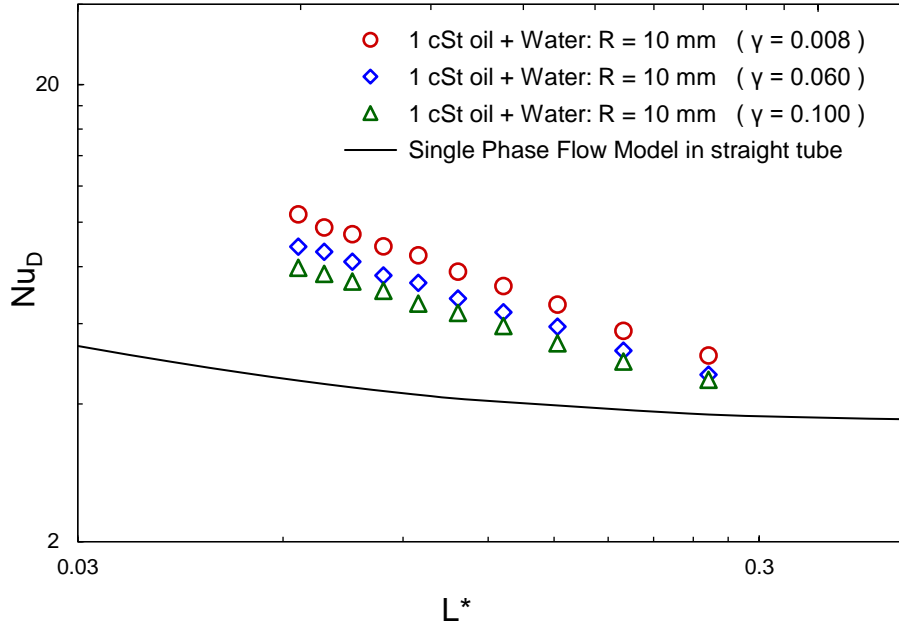


Figure 6.10 effect of slug ratio γ on Nusselt number Nu_D of Taylor flow plotted versus invers Graetz number L^* ($R=10$ mm).

Fig. 6.11 presents an effect of test section radius $R = 10, 20$ and 40 mm on heat transfer parameter Nu_D . A combination of 1 cSt silicone oil and water was created with fraction $\gamma = 0.008$ and fed at same volumetric flow rates of $\alpha = 0.5$. The results were compared with single phase model for straight tube to show heat transfer augmentation as result of curvature radius R .

Figs. 6.12 and 6.13 demonstrate heat transfer data of liquid-liquid Taylor flow using 1 and 5 cSt silicone oil. The flow was segmented by distilled water and fed into coiled tube of 10 mm inside diameter. The bulk heat transfer was determined for each component: water and oil using Eq. (6.1). The experimental data were plotted as a function of Dean number De which was calculated based on volume average property models. Fig. 13 shows the experimental of liquid-liquid Taylor flow as function of Dean number De . Heat transfer of Taylor flows of three liquid slug ratio $\gamma = 0.008, 0.060$ and 0.100 was plotted to present heat transfer augmentation as function of dean number De . The results revealed a maximum heat transfer enhancement when liquid slugs L_s became close to inside diameter of test section D . The thermal enhancement in Taylor flow was theoretically and experimentally addressed in [11],[21] which is referred to the internal circulation within liquid slugs.

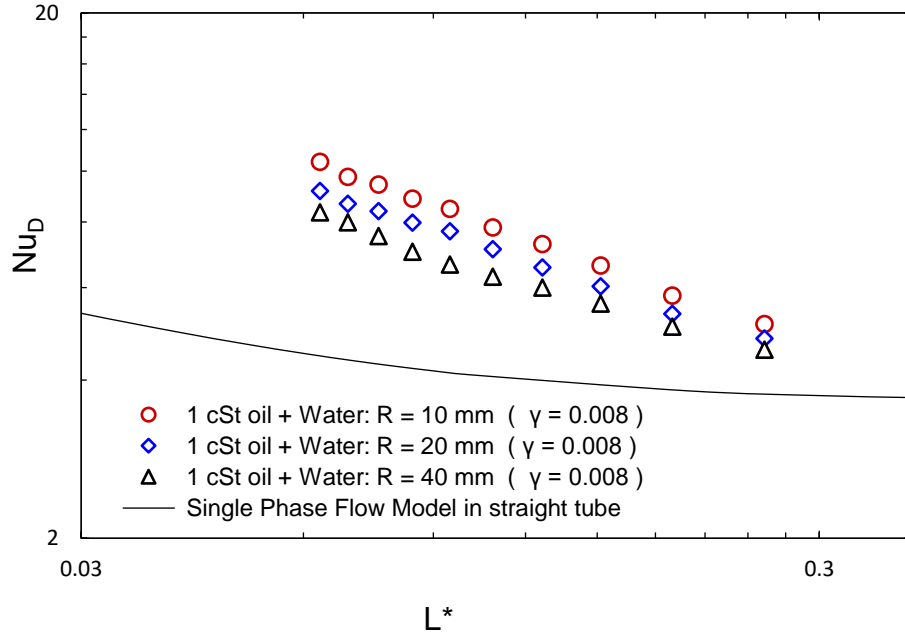


Figure 6.11 effect of tube curvature radius R on Nusselt number Nu_D , of liquid-liquid Taylor flow versus invers Graetz number L^* .

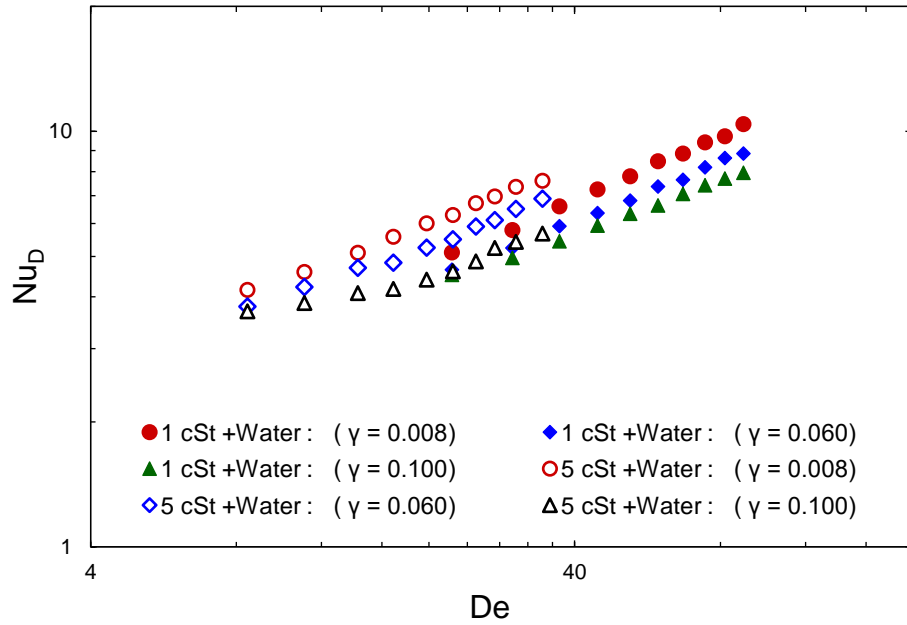


Figure 6.12 effect of slug ratio γ on Nusselt number data Nu_D of Taylor flow as function of Dean number De ($R=10$ mm)

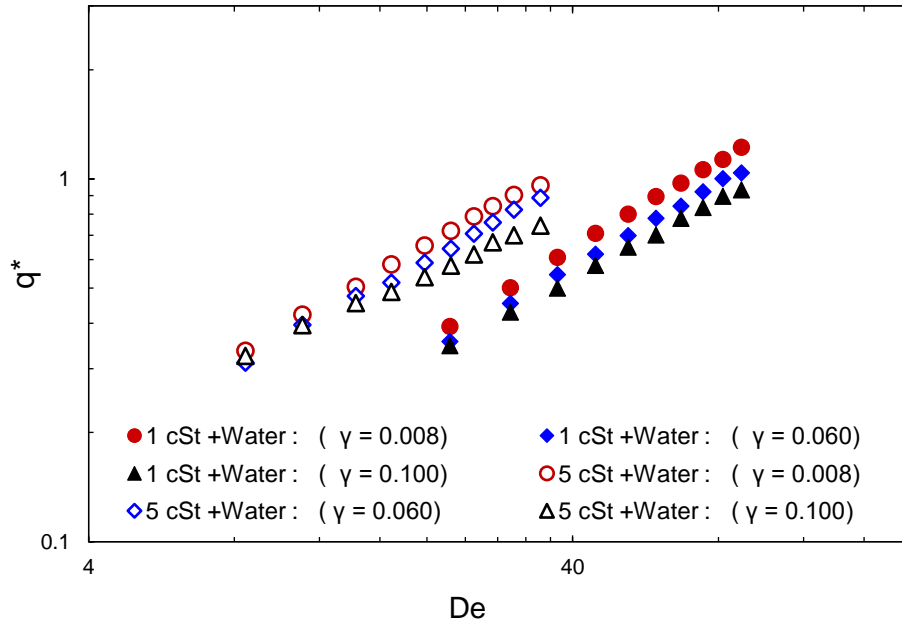


Figure 6.13 effect of slug ratio γ on dimensionless heat transfer of Taylor flow as function of Dean number De for ($R = 10$ mm).

6.5 Modeling of Experimental Data

The experimental data of liquid-liquid Taylor flow were collected to demonstrate different aspects of heat transfer in mini scale coiled tubes. Three parameters were in focus: effect of Prandtl number Pr , curvature radius of test section R , varying liquid slug ratio γ . The results were used to develop an empirical correlation to predict heat transfer enhancement in coiled tubes affected by constant wall temperature. Enough sets of data have been employed to insure validity of the new correlation. Experimental results were obtained using three combinations of silicone oils segmented by distilled water to produce three mixtures of immiscible liquids of Prandtl numbers: $Pr = 17, 27.45$ and 41.35 . The flows were created with fixed liquid fraction $\alpha = 0.5$. Three liquid slug ratios $\gamma = 0.008, 0.060$ and 0.100 were obtained using several T-junctions.

Test sections of 250 mm length in mini scale coiled tubes were bent to form three radii of curvature: $R = 10, 20$ and 40 mm. The change of the curvatures for the same tube length creates three coiled tubes with three numbers of turns: $N = 3, 2$ and 1 respectively.

Based on the experimental results, a simple empirical correlation was developed to predict Nusselt number Nu_D in mini scale coiled tubes MSCT which takes to account the change of: radius of curvature R , Prandtl number Pr which presents the effective flow properties ($\bar{\rho}$, $\bar{\mu}$, and \bar{k}) as well as liquid slug ratio γ . Employing the empirical approach for the curvature region which prescribed by higher Nu_D . The following correlation is valid for $De \geq 5$ and takes the form:

$$Nu_D = CDe^m Pr^p \gamma^q \quad (6.18)$$

The experimental approach with obtained results of LLTF were used to determine the three coefficients C , m , p and q which appeared in Eq. 18. The proposed model presents two asymptotes of high curvature region, Eq.18 and $Nu_D = 3.66$ of fully developed region in straight tube to take the forms:

$$Nu_D = \begin{cases} 3.66 \\ CDe^m Pr^p \gamma^q \end{cases} \text{ if } \begin{cases} De < 5 \\ De \geq 5 \end{cases} \quad (6.19)$$

The two asymptotes of both regions were combined to cover whole range of laminar flow in mini scale tube. The model takes the general form:

$$Nu_D = [3.66^n + (CDe^m Pr^p \gamma^q)^n]^{1/n} \quad (6.20)$$

The experimental results in coiled tubes showed that heat transfer enhancement was proportional to the investigated parameters, R , Pr and γ . The coefficients C , m , p and q were determined based on collected results. Finally, data of transitional flow were used to determine the power $n = 4$.

$$Nu_D = [3.66^4 + (0.6252De^{0.5} Pr^{0.1} \gamma^{-0.13})^4]^{1/4} \quad (6.21)$$

The proposed model has been examined over the range of Dean number De up to 100. As mentioned, the volume average property models were employed to calculate the effective properties of flow mixture. Fig. 14 shows how the proposed model responds to liquid slug ratio γ (Ls/L). The observation showed that sensitivity of the proposed model decreases with increasing γ . This finding is reasonable as internal circulation or radial transfer of heat and mass decreases for long liquid slug [11,21].

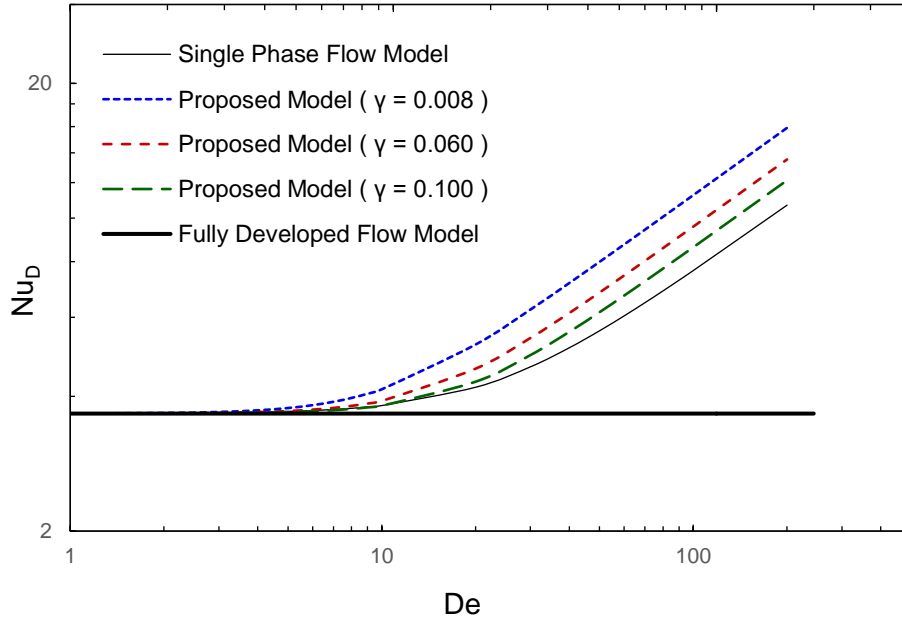


Figure 6.14 effect of liquid slug ratio γ (L_s / L) variation on proposed model of Nusselt number Nu_D of liquid-liquid Taylor flow.

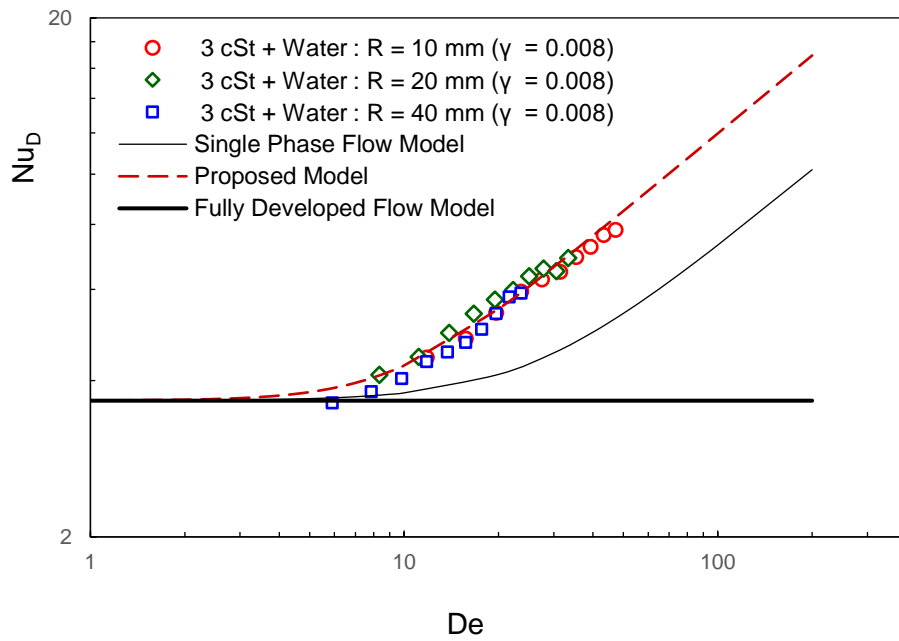


Figure 6.15 heat transfer of liquid-liquid flow with varied curvatures plotted versus De and compared with proposed model.

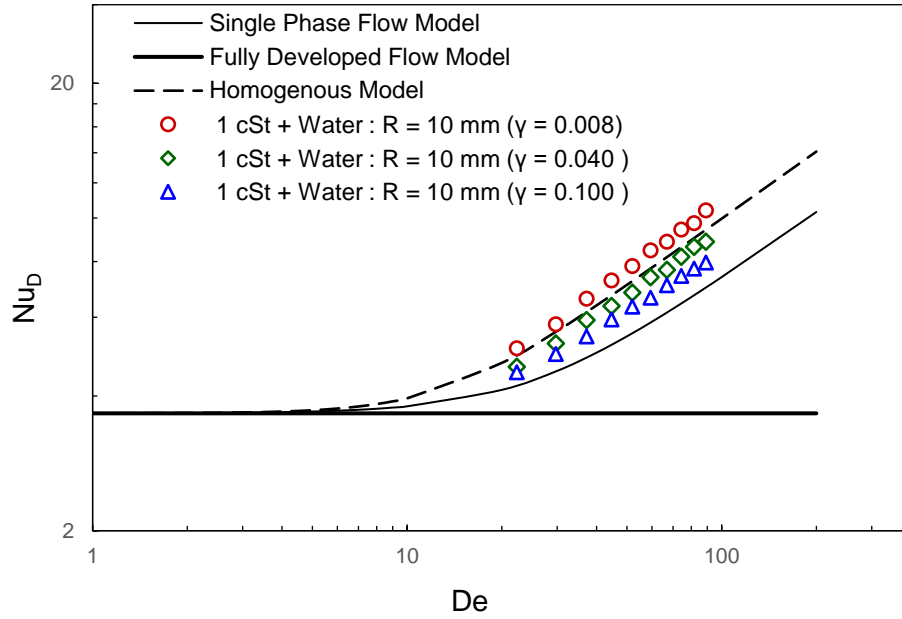


Figure 6.16 Taylor flow data (1 cSt oil + water) of varied slug ratio L_S/L compared with homogenous model [6].

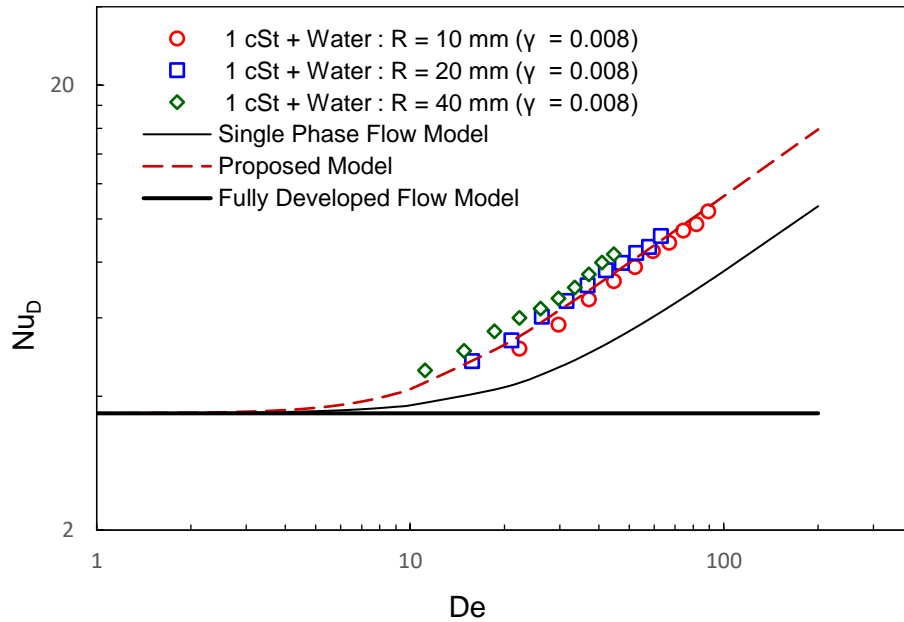


Figure 6.17 heat transfer of liquid-liquid flow with varied Prandtl number plotted against De and compared with proposed model.

Fig. 6.15 and 6.16 show the predictable behavior of the experimental data of liquid-liquid Taylor flow when compared with the proposed model Eq. (6.21). The data were created using 1 and 3 cSt silicone oil and segmented by water at constant fraction $\alpha = 0.5$. Prandtl numbers of flow mixtures were determined on base of volume average property models Eq. (6.9). The flow segmentation ratio was kept constant at $\gamma = 0.008$. To some extent the proposed model presents an ability for predicting the heat transfer rates for varied tube curvature $R = 10, 20$ and 40 mm over the studied range of Prandtl number Pr corresponds to the flow components in the present study. However, the experimental data spread around the model line to demonstrate effect of tube curvature on heat transfer due to increase of secondary flow, see Figs [6-15] and [6-16].

Fig. 6.17 shows liquid-liquid Taylor flow data of 1 cSt silicone oil and water were compared with homogenous model Eq. (6.15). Heat transfer enhancement due to effect of slug ratio L_S / L on heat transfer was not predictable as the model only consider effect of Prandtl number Pr and radius of curvature R .

Figs. 6.18 and 6.19 show the proposed model of varied Prandtl number $Pr = 17, 27.45$ and 41.35 examined with experimental data of liquid-liquid Taylor flow. Tube radius and liquid slug ratio γ were kept constant to demonstrate how the model responds to the change of liquid combinations of the water with three silicone oils 1, 3 and 5 cSt. Nine sets of data demonstrated the predictable behavior of the proposed model with an acceptable error of $RMSPE = 11.6 \%$

Figs. 6.20 - 6.22 show experimental data of three silicone oils 1, 3 and 5 cst with water. The results were collected using $R = 10$ mm test section radius of $L = 250$ mm. liquid slug lengths were controlled to obtain three values of flow segmentation ratios $= 1.22, 3.9$ and 8.4 . The variation of slug ratio γ cause heat transfer rates of liquid-liquid Taylor flow to show different levels of thermal enhancement. The enhancement has an inverse proportional to liquid slug length L_S as demonstrated in Fig. 6.20. This finding was supported by the theory of internal circulation [20,21] and earlier publications for gas-liquid and liquid-liquid Taylor flow in straight [10,17,26].

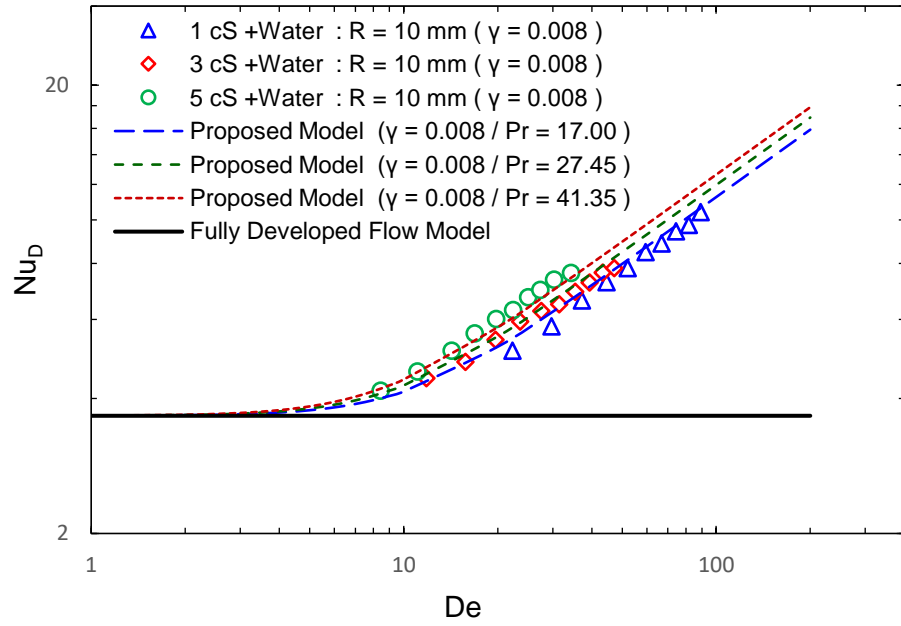


Figure 6.18 Nusselt Number of Taylor flow of various Prandtl number Pr compared with the proposed model.

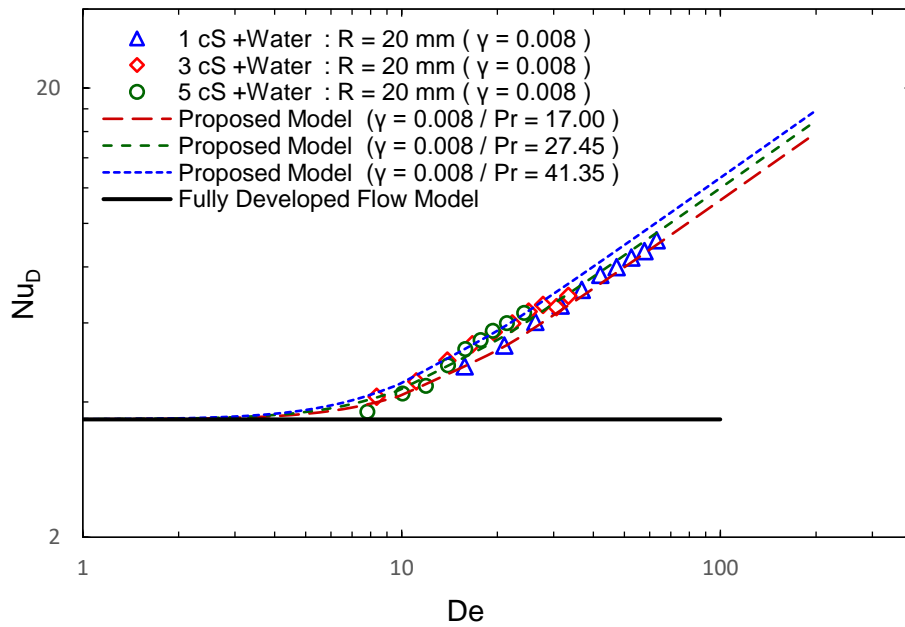


Figure 6.19 Nusselt Number of Taylor flow with varied Prandtl number Pr compared with the proposed model.

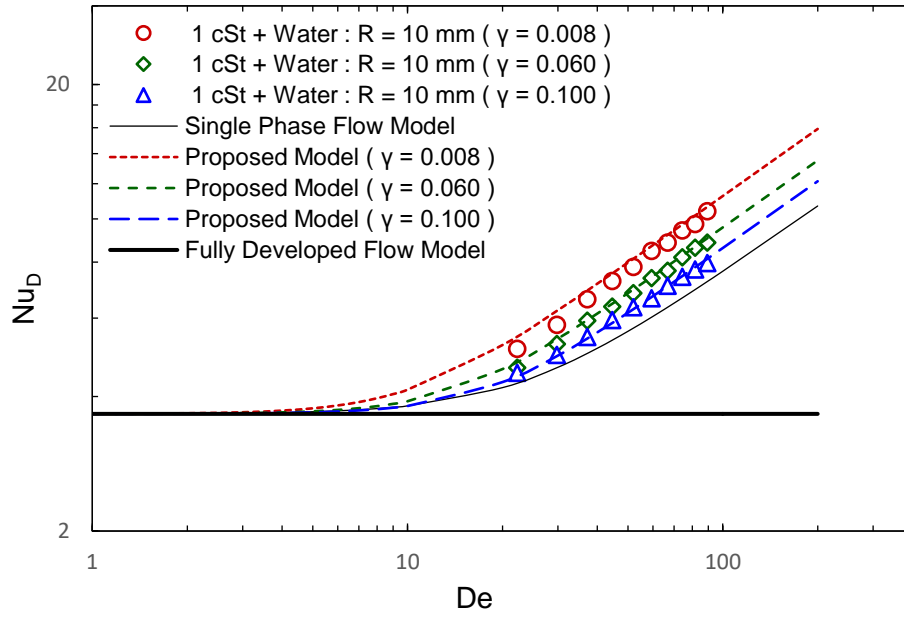


Figure 6.20 Nusselt Number of Taylor flow with various γ compared with proposed model.

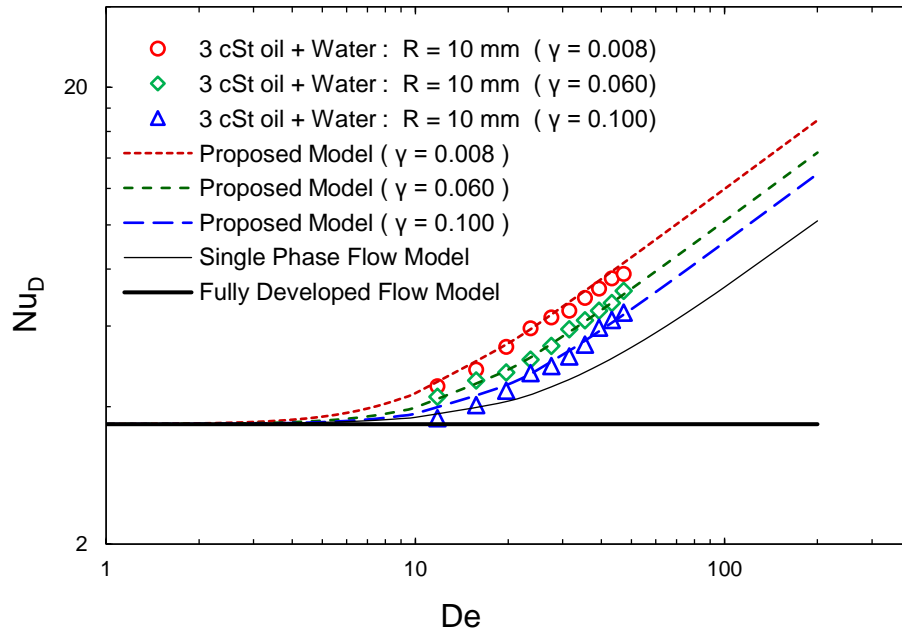


Figure 6.21 Nusselt number of liquid-liquid Taylor flow of various γ compared with the proposed model.

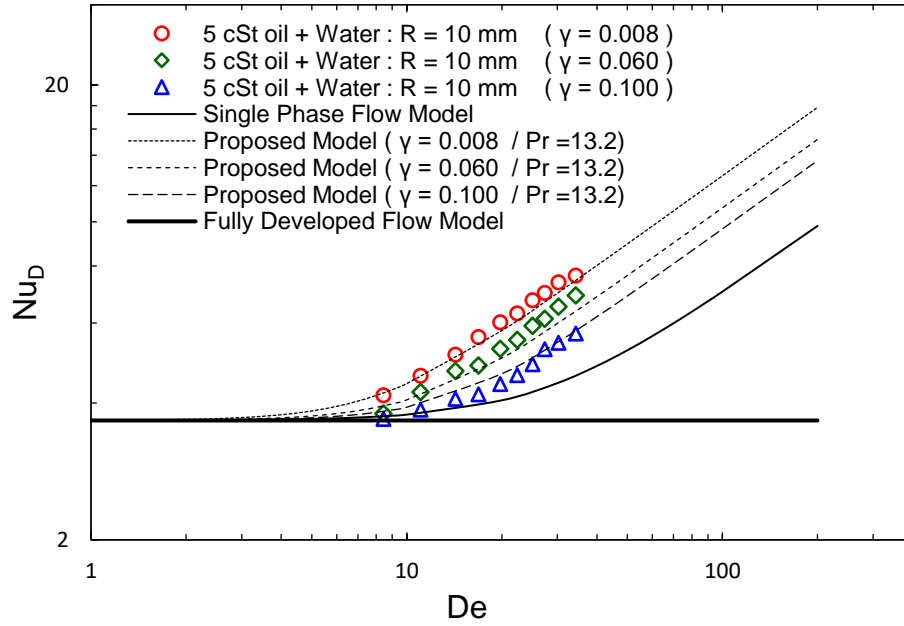


Figure 6.22 Nusselt Number of liquid-liquid Taylor flow of various γ compared with the proposed model.

6.6 Conclusion

Heat transfer in liquid-liquid Taylor flow in coiled tubes showed an enhancement when compared with single phase flow model [14]. The enhancement was proportional to the three parameters: radius of curvature R , liquid slug ratio γ and Prandtl number Pr . Maximum heat transfer enhancement over single when $\gamma = 0.008$ was from 16.54 to 31.33 % when considering the results on Fig. 6.20, and radii of curvature $R = 10$ mm. These findings referred to the secondary flow effect and Taylor flow characteristics. The proposed model Eq. (6.21) demonstrated a consistent response to the considered parameters γ , Pr and R . Three regions can be characterized in the proposed model: low curvature region $De < 5$, where the behaves as that of straight tubes. In contrast a high curvature region $De > 10$ and transitional region of $5 < De < 10$. Most of the obtained experimental of liquid-liquid Taylor flow scattered around the proposed model in high curvature region $De < 10$. The developed model demonstrated successful prediction of liquid-liquid Taylor flow data for $10 < De < 100$ and $17 < Pr < 43$. An agreement was determined using RMSPE, Eq. (6.17) to examine ability of data prediction. RMSPE was calculated for 27 data set to show that $6.11 < RMSPE < 14.8$. The obtained results and proposed model will provide a useful guideline for predicting heat transfer in mini / micro scales.

6.7 References

- [1] W. R. Dean, Note on the Motion of Fluid in a Curved Pipe, London Edinburgh Dublin Philosophy Mag. J. Sci., vol. 4, pp. 208–223, 1927.
- [2] W. R. Dean, “The Streamline Flow Through Curved Pipes”, London Edinburgh Dublin Philosophy Mag. J. Sci., vol. 5, pp. 673–695, 1928.
- [3] Ghobadi M., Muzychka Y. S., 2014, “Fully Developed Heat Transfer in Mini Scale Coiled Tubing for Constant Wall Temperature”, *International Journal of Heat and Mass Transfer*, 72, pp. 87–97.
- [4] Ghobadi M., Muzychka Y. S., “Effect of Entrance Region and Curvature on Heat Transfer in Mini Scale Curved Tubing at Constant Wall Temperature”, *International Journal of Heat and Mass Transfer*, 65 (2013) 357–365.
- [5] Ghobadi M., Muzychka Y. S., 2014” Heat Transfer and Pressure Drop in a Spiral Square Channel”, *Experimental Heat Transfer*, 28:546–563, 2015.
- [6] Adrugi, W., Muzychka, Y.S., and Pope, K., “Heat Transfer in Liquid-Liquid Taylor Flow in Mini-scale Curved Tubing for Constant Wall Temperature,” ASME-IMECE-2015-67700, 2016.
- [7] Ghobadi M., Muzychka Y. S.,” Heat Transfer in Spiral Channel Heat Sink”, ASME 2011 9th International Conference on Nanochannels, Microchannels, and Mini channels
- [8] Dravid, A. N., Smith, K. A., Merrill, E. W., Brian, P. L. T., 1971, “Effect of Secondary Fluid Motion on Laminar Flow Heat Transfer in Helically Coiled Tubes”, American Institution of Chemical Engineers, Vol. 17, no. 5, pp. 1114-1122.
- [9] Taylor, Deposition of a Viscous Fluid on the Wall of a Tube, *Journal of Fluid Mechanics*. 10(1961) 161–165.
- [10] K. Alrbee, Y.S. Muzychka and X. Duan, “Laminar Heat Transfer of Gas-Liquid Segmented Flows in Circular Ducts with Constant Wall Temperature”, ASME 2019 17th International Conference on Nanochannels, Microchannels, and Mini channels.
- [11] Horvath, C., Solomon, B.A., Engasser, J.M., “Measurement of Radial Transport in Slug Flow Using Enzyme Tubes”, *Industrial and Engineering Chemistry, Fundamentals*, Vol. 12, no. 4, pp. 431-439, 1973.

- [12] Oliver, D.R. and Young Hoon, A., "Two Phase Non-Newtonian Flow: Part 2 Heat Transfer", Transactions of the Institution of Chemical Engineers, Vol. 46, pp. 116-122, 1968.
- [13] Vrentas, J.S., Duda, J.L, and Lehmkuhl, G.D., "Characteristics of Radial Transport in Solid-Liquid Slug Flow", *Industrial and Engineering Chemistry, Fundamentals*, Vol. 17, no. 1, pp. 39-45, 1978.
- [14] Betz A. R., Attinger D., "Can Segmented Flow Enhance Heat Transfer in Microchannel Heat Sinks", *International Journal of Heat and Mass Transfer*, 53, pp. 3683-3691, 2010.
- [15] Muzychka Y. S., Walsh E. Walsh P. "Heat Transfer Enhancement Using Laminar Gas-Liquid Segmented Plug Flows" *Journal of Heat Transfer*, 2011 by ASME, APRIL 2011, Vol. 133 / 041902-1.
- [16] Adrugi, W., Muzychka, Y.S., and Pope, K., "Heat Transfer Model for Liquid-liquid Taylor flow", ASME 2018 16th.
- [17] K. Alrbee, Y.S. Muzychka and X. Duan, "An approximated method of Analysis for laminar Heat Transfer in liquid-liquid Taylor flow in mini scale tubing" ASME 2019 17th International Conference on Nanochannels, Microchannels, and Minichannels.
- [18] Wei Xing and Joel Plawsky "Liquid-liquid phase separation heat transfer in advanced microstructure" *International Journal of Heat and Mass Transfer* 127 (2018) 989–1000.
- [19] Giolla M. M. Eain A., Vanessa E., Punch J., "Local Nusselt number enhancements in liquid-liquid Taylor flows" *International Journal of Heat and Mass Transfer*, 80 (2015) 85–97.
- [20] Muzychka Y. S., "Walish E., "Simple Models for Laminar Thermally Developing Slug Flow in Noncircular Ducts and Channels", *Journal of Heat Transfer*, ASME NOVEMBER 2010, Vol. 132 / 111702-1.
- [21] Muzychka, Y.S., "Generalized Models for Laminar Developing Flows in Heat Sinks and Heat Exchangers", *Heat Transfer Engineering*, vol. 34 (2-3), pp. 178-191, 2013.
- [22] Walsh, P., Walsh, E., and Muzychka, Y.S., "Heat Transfer Model for Gas-Liquid Slug Flows Under Constant Flux", *International Journal of Heat and Mass Transfer*, Vol. 53 (15-16), pp. 3193-3201, 2010.

- [23] Muzychka, Y.S., “Laminar Heat Transfer for Gas-Liquid Segmented Flows in Circular and Non-circular Ducts with Constant Wall Temperature” ASME, 2014.
- [24] J. Howard A. and Walsh P. A., “Heat Transfer Characteristics of Liquid-Gas Taylor Flows incorporating Microencapsulated Phase Change Materials”, *Journal of Physics: Conference Series* 525 (2014) 012022.
- [25] Maddox, D.E. and Mudawar, I., “Single- and Two-Phase Convective Heat Transfer from Smooth and Enhanced Microelectronic Heat Sources in a Rectangular Channel”, *Journal of Heat Transfer*, Vol. 111, pp. 1045-1052, 1989.
- [26] Adrugi W. M., Muzychka Y.S., and K. Pope, “Heat Transfer in Liquid –Liquid Taylor Flow in Mini-Scale Tube with Constant Wall Temperature” ASME 2015.
- [27] K. Alrbee, Y.S. Muzychka and X. Duan, “Heat Transfer Enhancement in Laminar Graetz and Taylor Flows Using Nanofluids”, ASME-ICNMM2018-7756.
- [28] S. Haase, “Characterisation of gas-liquid two-phase flow in mini-channels with co-flowing fluid injection inside the channel, part II: gas Bubble and Liquid Slug Lengths, Film Thickness, and Void Fraction Within Taylor Flow”, *International Journal of Multiphase Flow*, 88, 2017, pp. 251–269.
- [29] Hughmark, G.A., “Holdup and Heat Transfer in Horizontal Slug Gas-Liquid Flow”, *Chemical Engineering Science*, Vol. 20, 1007-1010, 1965.
- [30] Maxim Vladimirovich Shcherbakov, Brebels, A. “A Survey of Forecast Error Measures” *World Applied Sciences Journal* (Information Technologies in Modern Industry, Education & Society): 171-176, 2013.
- [31] M.M. Awad, Y.S. Muzychka “Effective Property Models for Homogeneous Two-phase flows”, *Experimental Thermal and Fluid Science* , Vol. 33 (2008) 106–113
- [32] Kline, S. J., and F. A. McClintock. “Describing Uncertainties in Single-Sample Experiments.” *Mechanical Engineering*, Vol. 75, No. 1, January 1953: 3-8.
- [33] Eduardo D. Glandt, T. Klein and E Edgar, “Optimization of Chemical Processes”, Second edition, *McGraw-Hill Chemical Engineering Series*, 2001.

CHAPTER 7

HEAT TRANSFER ENHANCEMENT IN LAMINAR GRAETZ AND TAYLOR FLOWS USING NANOFLUIDS

7.1 Introduction

Heat transfer enhancement offers considerable opportunity to increase heat transfer coefficients and/or decrease operating temperatures. In laminar ow, heat transfer enhancement is significantly more advantageous given the lower heat transfer coefficients as compared with turbulent flows of a similar fluid. In this paper we examine the use of nanofluids for enhancing heat transfer in laminar developing flows and their use in Taylor flow using both air and oil as segmenting fluid.

The application of nanofluids as an enhancement mechanism is quite well established, though some gaps in understanding and modelling are still present. The use of segmented flows has also been pursued over the past ten years, though it too is not a new concept. The combination of nanofluids and Taylor flow has been sparingly studied and will be discussed in more detail in the next section. In this work, new experimental data are obtained using mini-scale tubing under constant wall temperature conditions. These data are carefully analyzed with respect to their performance relative to the classic Graetz theory predictions. Additionally, we also consider the

** The materials in this chapter were presented in ASME 2018 16th International Conference on Nanochannels, Microchannels, and Mini channels, June 10-13, 2018 in Dubrovnik, Croatia.*

presentation of data as both a Nusselt number and dimensionless mean wall heat flux. The latter is offers number of advantages, especially for assessing the accuracy of measured data [1].

These new insights offer new potential for both methods to be combined as a method of improving thermal performance in compact systems where laminar flow prevails.

7.2 Literature Review

Hydrodynamics and heat transfer of two phase flows contains a large variety of points of research which are currently receiving more attention. In small size tubes, Taylor flow, and nanofluids. This attention is a result of the increased demand for cooling compact electronic devices. This survey comprises of previous experimental and CFD simulations that address heat transfer conditions and pressure drop in mini - micro scale tubes. Use of micro and mini scale tubes to increase surface area and reduce thermal resistance was first considered nearly forty years ago. Tuckerman and Pease [2] experimentally tested compact designs of heat sinks under a constant heat flux of 790 W/cm^2 . Their result showed that heat removal significantly sacrificed the pumping power. Since this study, countless studies in the field of micro channel heat sinks have been published.

Muzychka and Ghobadi [1] carried out experimental and theoretical study on single phase ow in mini- and micro-scale to show the significance of thermally developing flows in small systems. Experiments were conducted under isothermal wall conditions. They reported that in most cases that to reach fully developed heat transfer, a significant tube length is required for higher Reynolds numbers. Such dimensions not typically found in compact systems.

Gas-liquid Taylor flow was considered very early by Fairbrother and Stubbs [3], followed by Taylor [4]. Churchill and Ozoe [5] and Muzychka and Yovanovich [6] considered models for thermally developing flow in tubes. Later, Maddox and Mudawar [7] investigated forced convection of a simulated microelectronic heat source to assess the feasibility of cooling. Betz and Attinger [8] preformed experiments on compact micro cooling systems with both continuous and Taylor flow and highlighted that segmented flow significantly enhances heat transfer by up to 140 % in a microchannel heat sink when compared with single phase flow at same liquid flow rate. Asthana et al [9] experimentally examined convective heat transfer of liquid-liquid Taylor flow in microchannel maintained under constant heat flux of of 15 MW/m^2 . Laser Induced Fluorescence

(LFF) was used to visualize the temperature distribution. They reported that this concept significantly enhanced the Nusselt number in microchannel heat sinks by up to four-fold compared to pure water flow, and this enhancement came with penalty of pressure drop as they reported.

Muzychka et al [10] examined potential of heat transfer enhancement using uniformly segmented flows. They proposed a useful predictive model for gas-liquid Taylor flow in small scale tube. Experimental data for small mini scale tubes under isothermal conditions were considered. Janes et al [11] considered Taylor flow in mini-scale heat sinks. Houshmand and Peles [12] conducted an experimental study using gas-liquid Taylor flow in microchannel. The mixing effect of bubbles and interaction with thermal boundary layer were studied over a range of flow rates. They revealed that enhancement of heat transfer up to 100 % as compared to continuous flow, and that the enhancement for thermally developed flow positively scaled to boundary layer thickness. Eain et al [13] experimentally considered liquid-liquid Taylor flow in tubes and its enhancement on the local Nusselt number.

Recently, Adrugi and Muzychka [14] carried out liquid-liquid Taylor flow heat transfer experiments under a constant wall temperature condition. Experiments were conducted for different flow modes and liquid fractions. The flow patterns were created by introducing two immiscible liquids (water and silicone oils) into miniscale tubes with straight and curved paths. The results showed a significant enhancement in heat transfer when compared with single phase model. Pressure drop in two phase plug flows has been considered by a few researchers. The key studies are those of Walsh et al. [15], Heravi and Torabi [16], Adrugi et al [17], and Karimzadehkhoeie and Yalcin [18]. The more promising study for liquid-liquid flow is the work of Adrugi et al [17] who proposed a simple model based on a force balance across a Taylor flow cell.

Numerous studies have investigated characteristics and challenges of nanofluids. Kong, et al. [19] discussed two mechanisms of nanoparticles stability, steric and electrostatic repulsion. Several types of surfactants were used to produce stabilized nanofluids such as: sodium dodecyl benzene sulfonate (SDBS), sodium dodecyl sulfate (SDS), sodium lauryl sulfate (SLS), and an emulsion. In contrast, Xing [20] reported that adding surfactants to nanofluids to achieve acceptable stability should be done as little as possible to avoid affecting the thermal conductivity of nanofluid.

Thermal conductivity is most significant property in a nanofluid. Theoretical modeling of thermal conductivity of suspensions has been considered by Hamilton and Crossar [21], Bachelor and O'Brien [22], Awad and Muzychka [23], and Choi and Eastman [24] among others.

Seok and Choi [25] investigated the effect of various parameters and accurately concluded that: (i) thermal conductivity is directly proportional to volumetric concentration (ii) thermal conductivity of nanoparticle material is not a major factor to enhance thermal conductivity of nanofluids (iii) as the particle size decreases the Brownian motion of nanoparticles increases and nanoscale convection becomes more effective (iv) effective thermal conductivity of nanofluids dramatically increases with temperature, which can be explained as a result of decreasing dynamic viscosity that leads to increased Brownian motion and then nanoscale convection. Manaya and Sahin [26] experimentally investigated upper limitations of particle volume fraction on heat transfer and pressure drop of TiO₂ water nanofluids in microchannel. The study covered a considerable range of concentrations 0.25 %, 0.5%, 1.0%, 1.5%, and 2.0% under laminar flow conditions with Reynolds numbers between (100-750). The results highlighted heat transfer enhancement with no significant increase in pressure drop when compared with pure water. Several studies on nanofluid performance and applications can be found in the published literature [26-32]. Additional studies on nanofluid stability and preparation are available [33-35].

7.3 Fundamental of Graetz Theory

Given that we are examining laminar developing flow in a tube, it is appropriate to provide a reference to the fundamental Graetz theory for both Poiseuille and Slug flow for constant wall temperature. The following fundamental results are applicable [36, 37]. The mean Nusselt number for the tube is defined as:

$$\overline{Nu}_D = \frac{\overline{q}D}{k\Delta T_{LMTD}} \quad (7.1)$$

where

$$\Delta T = \frac{(T_w - T_i) - (T_w - T_o)}{\ln\left(\frac{(T_w - T_i)}{(T_w - T_o)}\right)} \quad (7.2)$$

where T_i and T_o are the inlet and outlet bulk temperatures, respectively, and T_w is the constant wall temperature. The dimensionless mean wall heat flux is defined as:

$$q^* = \frac{\bar{q}D}{\bar{k}(T_w - T_i)} \quad (7.3)$$

In both cases, each parameter is a function of $L^* = (L/D) / PeD$. The mean Nusselt number and dimensionless mean wall heat flux are related through the following expression [37]:

$$q^* = \frac{1}{4L^*} (1 - 4Nu_D L^*) \quad (7.4)$$

Poiseuille Flow In the case of the Nusselt number the following model proposed by Muzychka [36] for thermally developing Poiseuille flows:

$$\overline{Nu}_D = \left(\left(\frac{1.614}{L^{*1/3}} \right)^5 + (3.65)^5 \right)^{1/5} \quad (7.5)$$

More appropriately when dealing with a single fluid heat transfer device we may also wish to characterize heat transfer rates using a dimensionless mean wall heat flux defined as [36]:

$$q_{Pois}^* = \left(\left(\frac{1.614}{L^{*1/3}} \right)^{-3/2} + \left(\frac{1}{4L^*} \right)^{-3/2} \right)^{-2/3} \quad (7.6)$$

Taylor Flow In the case of the Nusselt number the following model proposed by Muzychka et al. [37] for thermally developing Slug flows:

$$\overline{Nu}_D = \left(\left(\frac{1.128}{L^{*1/2}} \right)^2 + (5.78)^2 \right)^{-1/2} \quad (7.7)$$

Finally, the dimensionless mean wall heat flux for Slug flow is defined as [37]:

$$q_{Plug}^* = \left(\left(\frac{1.128}{L^{*1/2}} \right)^{-2} + \left(\frac{1}{4L^*} \right)^{-2} \right)^{-1/2} \quad (7.8)$$

Both special cases provide a convenient nondimensional reference to measure heat transfer enhancement against. In Eq. (7.6) or (7.8), the limit of $q^* \rightarrow 1/4L^*$ must be achieved regardless of the type of flow or fluid makeup. As a fundamental limit it is a result which no data points can or should exceed. Finally, the widely accepted entrance lengths for laminar flow in circular tubes were used to assess the flows measured in the experiments reported later. These are:

$$\frac{L_{hy}}{D} = \frac{0.60}{0.035Re_D+1} + 0.056Re_D \quad (7.9)$$

$$\frac{L_{hy}}{D} = 0.0335Re_DPr \quad (7.10)$$

The Reynolds numbers in our experiments were between 30 to 150 in a tube of length 200 mm and diameter 1.63 mm, which indicates that the hydrodynamic entrance length in used tubes is of the order of 10 mm ensuring hydrodynamic fully developed flow over 90 percent of the tube thus ensuring that thermally developing Graetz flow is the base line for our comparison. Further benchmarking studies validate that we are achieving thermally developing flow and hydrodynamical fully developed flows. Finally, in the case of gas-liquid Taylor flows Muzychka et al. [10] show that comparison of Taylor flow should be made considering the liquid fraction α_L in the non-dimensional parameters of Nu , q^* and L^* .

7.4 Experimental Setup

A simple experimental setup has been assembled to measure heat transfer enhancement. For pressure drop measurements, thick-walled PVC tubing and a differential pressure sensor with range from 0 psi to 1 psi were used to conduct pressure drop measurements with minimum level of uncertainty. The experimental setup has been equipped with two syringe pumps (Harvard Apparatus) with a total capacity 200 ml each Figs. 1. The Harvard pumps are engineered to provide flow accuracy within 0.25 % and reproducibility within 0.05 %. However, the maximum volumetric flow rate is proportion to hydrodynamic resistance of system setup.

Flow patterns for the segmented flow studies were captured using a high-speed camera (Phantom v611) as demonstrated in Fig. 7.2. Since the main part of study requires preforming heat transfer experiments at same scale of pressure drop experiments, we use copper tubing of similar diameter placed in an isothermal bath.

The experiments are conducted under these conditions using different aspect ratios of L/D of the test sections. A Fisher Scientific 3013 Isotemp thermal bath which is PID controlled, provides temperature stability of ± 1 % over a range of -30 to 200 °C. Two Omega T-type thermocouples are employed to measure inlet and outlet bulk temperatures of the flow. A simple T-junction with thermocouple imbedded in flow stream is used. Fig. 7.1 illustrates heat transfer experiment setups.

The uncertainty of pressure drops and heat transfer measurements was evaluated using the popular Kline and McClinton [38, 39] method. Uncertainties of the measuring equipment used in the experiment setup which are specified by manufacturer. These include the uncertainties of measuring equipment, such as temperature, mass flow rate, pressure, etc. Estimating uncertainty of experimental results of single phase and two phase flows were performed for both hydrodynamic and thermal parameters, f , q^* , L^* , and Nu_D using Kline and McClinton [38] method. The uncertainty in these dimensionless parameters represents all contributions of the uncertainties of the sensors. Generally, the results show increasing uncertainties in q^* and Nu_D . The uncertainty of the experimental data was considered for the range of Reynolds number from 100 to 250 which was our flow range for most of the experiments .

The uncertainties are estimated to be $\pm 1.75\%$ for L^* ± 2.65 for f and the ranges of uncertainty of heat transfer dimensionless parameters were ± 2.25 to 3.84% for Nusselt number and ± 1.54 to 1.91% for dimensionless heat flux q^* .

Data for water and silicone oils were obtained to benchmark the facility used in the present study. Figs. 7.3 and 7.4, show the results of friction factor and Nusselt number in a straight tube are in excellent agreement with theory. Additional results for various L/D ratios including varying tube length and /or diameter were obtained. All are in excellent agreement with Graetz and Fanning theory. In the later sections will discuss results and trends observed in both continuous and Taylor

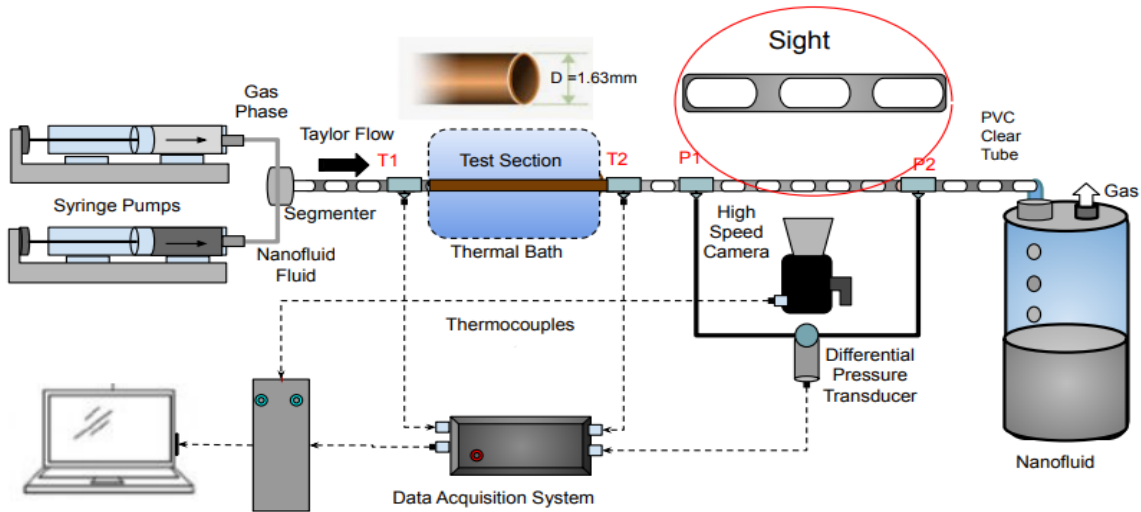


Figure 7.1 schematic of experimental setup of segmented flow

nanofluid streams using the same facility. Care was taken to ensure that data for larger values of L^* are measured appropriately. Table [7.1] contains experimental data of friction factor and limits using three liquids.

Table 7.1 friction factor benchmark test limits and results

Test fluid	ID (mm)	L (mm)	Re_D	f		Max error %
				min	max	
Water	1.63	500	66-2120	0.009	0.23	8
3 cst oil	1.63	500	17 - 216	0.081	0.95	6
5 cst oil	1.63	500	13 - 365	0.045	1.15	7

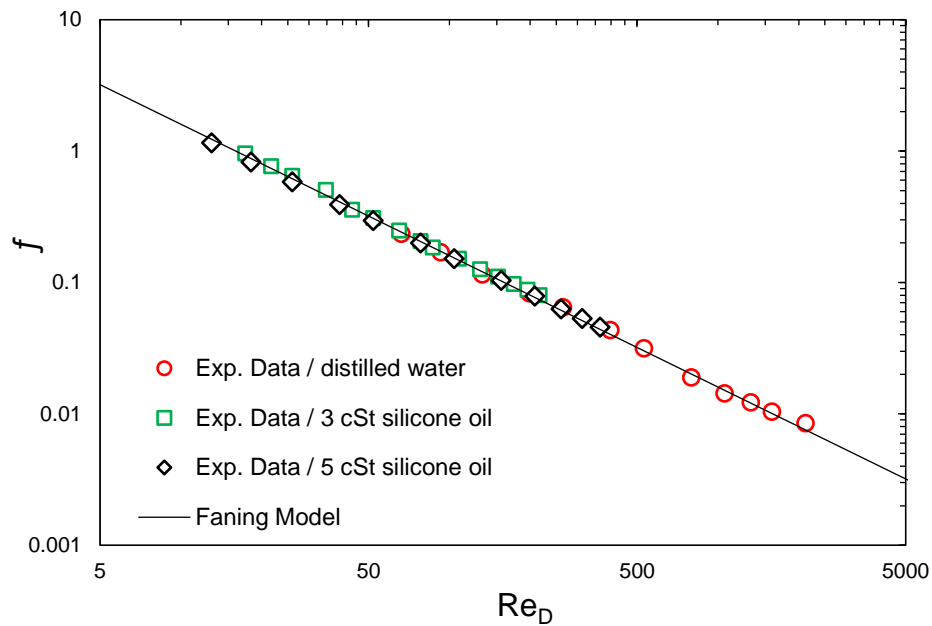


Figure 7.2 laminar friction factor benchmark test for a straight tube using different fluids with maximum error of 5 -7 percent

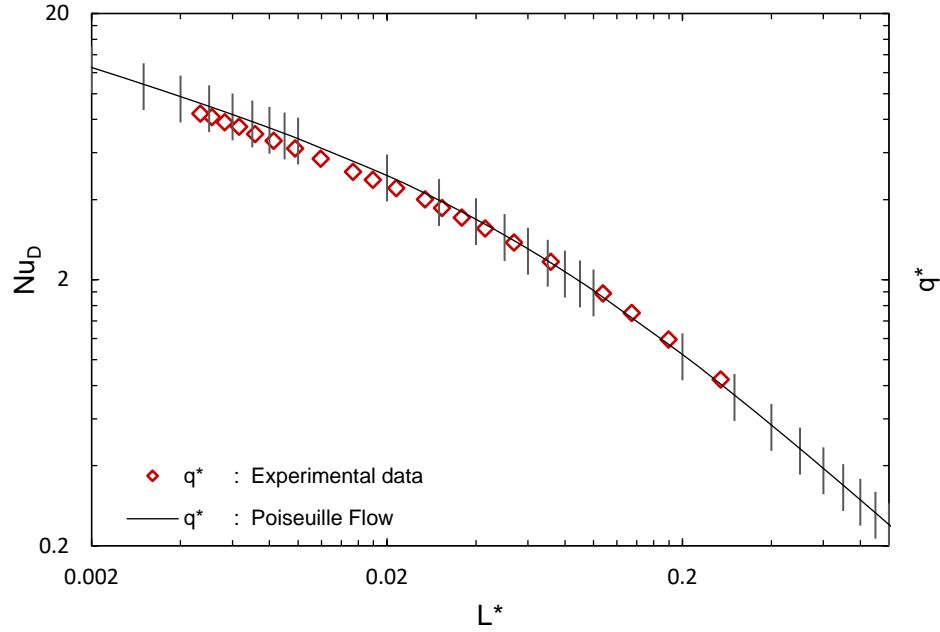


Figure 7.3 benchmarking results of heat transfer using distilled water in 150 mm tube length



Figure 7.4 segmented flow of gas-liquid in mini scale tube with $\alpha L = 0.5$

7.5 Nanofluid Preparation and Modeling

Data for several concentrations of Al_2O_3 nanofluid were obtained for continuous and segmented flows. Several concentrations of nanofluid were prepared and thoroughly dispersed before use.

The two-step method was used to produce three samples of 500 ml each using aluminum oxide Al_2O_3 , ($D < 40\text{nm}$) with volumetric concentrations (0.25, 0.5, and 1 Vol. %) as shown in Fig. 7.5. The nano powders were dispersed in distilled water with no dispersant to avoid the negative effects of these additives on the thermal conductivity of nanofluid.

The preparation process started by applying mechanical stirring for 1 hour as initial suspension. To ensure the uniform distribution of nanoparticle within the base fluid, 3 hours of ultra-sonication (Digital Sonicator) at 30 % amplitude was applied, followed by sonication in an ultra-sonication bath for 1 hour before each experiment. The entire preparation process was performed without applying heat to the samples. Samples of both dry nanoparticles before mixing solutions and after mixing solutions were analyzed using a scanning electron microscope (SEM). Mean particle size was found to be on the order of 64 nm as shown in Fig. 7.6. Composition and purity of Al_2O_3 Nano powders was analyzed using (SEM) as shown in Fig. 7.7.

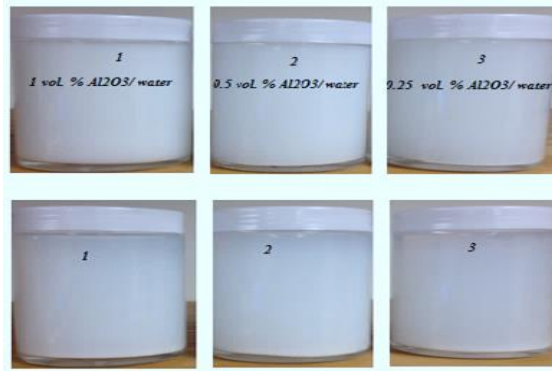


Figure 7.5 shows three samples of Al_2O_3 with different concentrations, second row shows stability of samples after a week

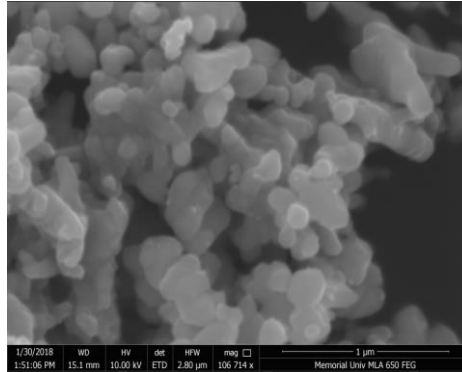


Figure 7.6 (SEM) image shows the microstructure of Al_2O_3 Nano powders with micro scale

Homogeneous or effective single-phase modeling assumes that base fluid and nanoparticles have the same temperature and velocity field. Therefore, models of the effective properties are used in both thermal and hydro- dynamic analysis. In the present study the volume concentration was determined from the mass concentration of the dispersed fluid using Eq. (7.11).

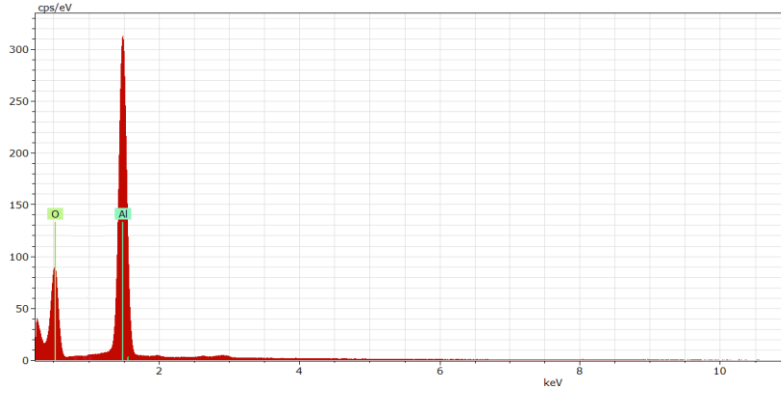


Figure 7.7 shows composition and purity analysis of Al₂O₃ Nano powders using (SEM)

$$\phi = \frac{1}{1 + \left[\left(\frac{100}{\phi_m} \right) \times \left(\frac{\rho_p}{\rho_f} \right) \right]} \times 100\% \quad (7.11)$$

Where ϕ_m denotes to the mass concentration of nanofluid (m_{np}/m_{nf}).

Thermal conductivity k_{nf} can be determined using a well-known predictable formula and most widely used in recent studies. The correlation was suggested by Batchelor [22] which is an extension to Einstein's equation as:

$$k_{nf} = \phi k_p + (1 + \phi) k_{bf} \quad (7.12)$$

Another useful model is the Buongiorno [40] model given by:

$$k_{nf} = k_{bf} (T) (1 + 4.5503\phi) \quad (7.13)$$

The most common classical models for predicting the effective viscosity of nanofluids is the Einstein formula presented the dynamic viscosity expression as Einstein's formula:

$$\mu_{nf} = (1 + 2.5\phi) \mu_{bf} \quad (7.14)$$

The density of nanofluid was determined based on nanoparticle concentration, ϕ using the Pak and Cho correlation of dispersed liquid:

$$\rho_{nf} = (1 + \phi) \rho_{bf} + \phi \rho_{np} \quad (7.15)$$

Finally, for the synthesized nanoparticle liquid suspension, the parameter $(\rho C_p)_{nf}$ of the nanofluid is expressed as:

$$(\rho C_p)_{nf} = (1 - \phi)(\rho C_p)_{bf} + \phi(\rho C_p)_{np} \quad (7.16)$$

The effective thermal conductivity of the nanofluid was characterized using the thermal property analyzer KD2 ProTM. Ten measurements were averaged at each nanofluid concentration to reduce possible measurement error. An experimental measurement in Fig. 7.8 shows the thermal conductivity enhancement of nanofluids as compared with base fluid and can be reasonably correlated by the Williams et al. model [40] at the ambient temperature of nanofluid, which was 25 °C. Excellent agreement between Eq. (7.13) and the measured data was obtained as shown in Fig. 7.8. Comparisons with other models [41] is also made. In the subsequent data reduction, we use the actual measured k-values of the fluid samples but use volume averaged predicted values for the heat capacity, density, and viscosity.

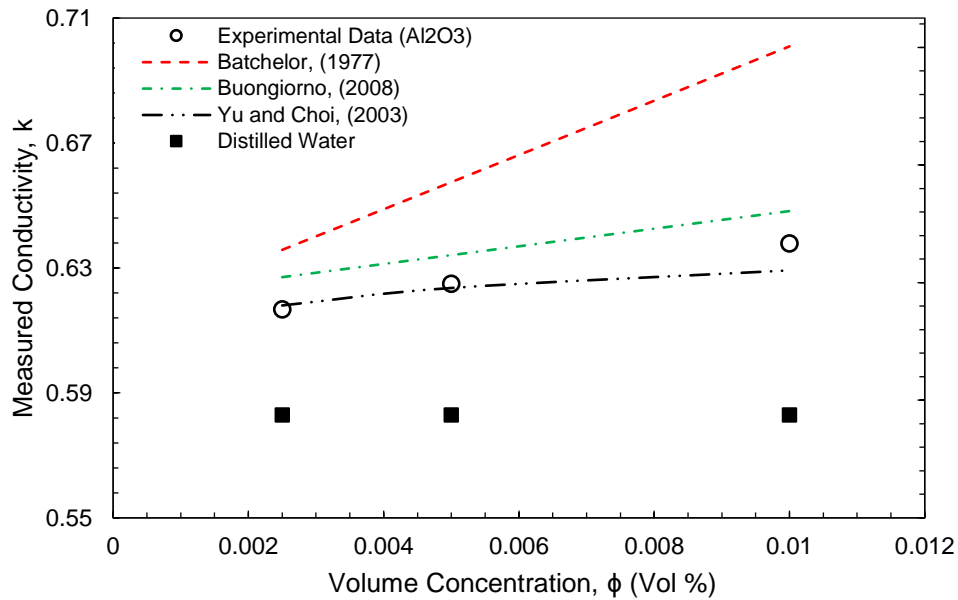


Figure 7.8 thermal conductivity measurements compared with published predictive models

7.6 Result and Discussion

Two sets of experiments were conducted with three nanofluid concentrations and distilled water: continuous flow and Taylor flow. Each set of experiments are discussed in separate sections.

In both cases the single phase Graetz flow is considered the baseline for comparison of the continuous and segmented flows.

For continuous flow, the thermal enhancement of both q^* and Nu_D are measured and plotted versus the inverse Graetz parameter L^* for distilled water and three nanofluid suspensions. As can be seen in Figs. 7.9 and 7.10, excellent agreement with past trends is observed. i.e increasing nanoparticle concentration leads to higher Nusselt numbers. Thermal enhancement on the fundamental Graetz plot is observed for all three nanofluid suspensions. Fig. 7.11 shows Nusselt number data as function of Reynolds number .

The rationale behind considering q^* is that regardless of nanofluid concentration, all data must converge to the asymptote $1/4L^*$. This limit represents the limit of maximum heat transfer calculated from the enthalpy balance when outlet temperature approaches the wall temperature. In a Poiseuille or Taylor flow, while Nusselt numbers approach different fully developed flow asymptotes, they must both approach the same q^* limit for long tubes. This behaviour must also be observed for the nanofluid suspensions and can be seen to do so in Fig. 7.9. This is a good indicator that experiments in miniscale systems are being conducted accurately. As shown by Muzychka and Ghobadi [1], significant errors can result when measuring Nusselt numbers in min-scale systems.

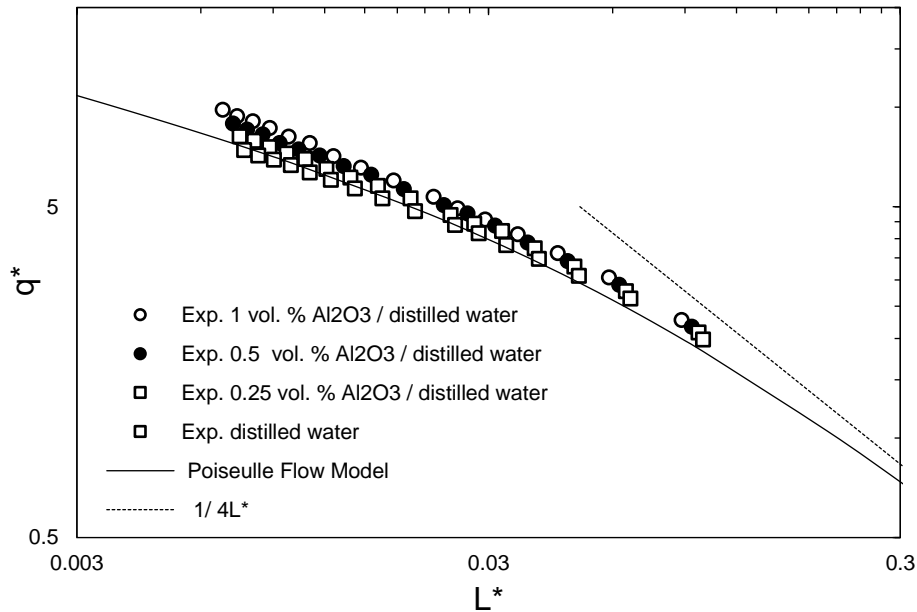


Figure 7.9 effect of nanofluid concentration on dimensionless heat flux plotted versus inverse Graetz number.

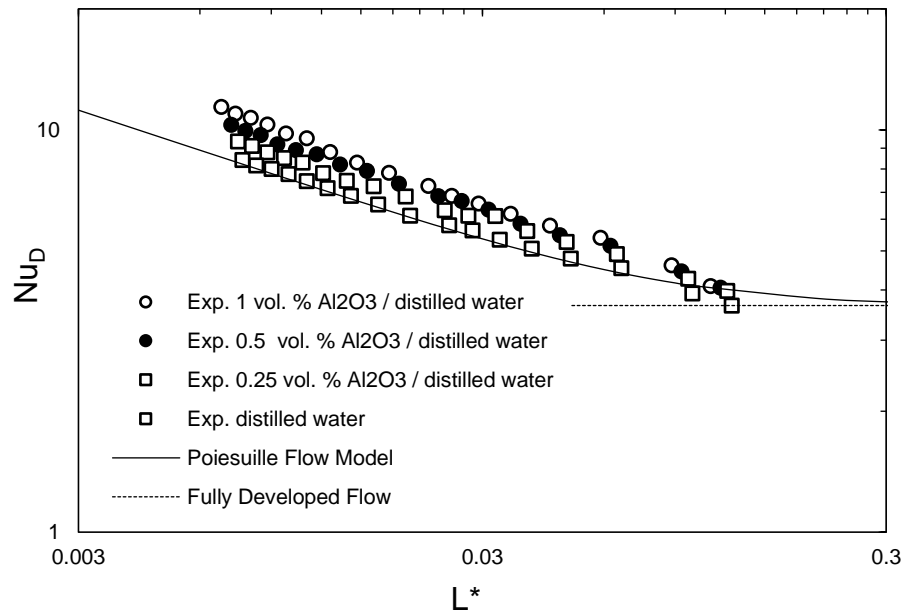


Figure 7.10 effect of nanofluid concentration on Nusselt number plotted versus inverse Graetz number

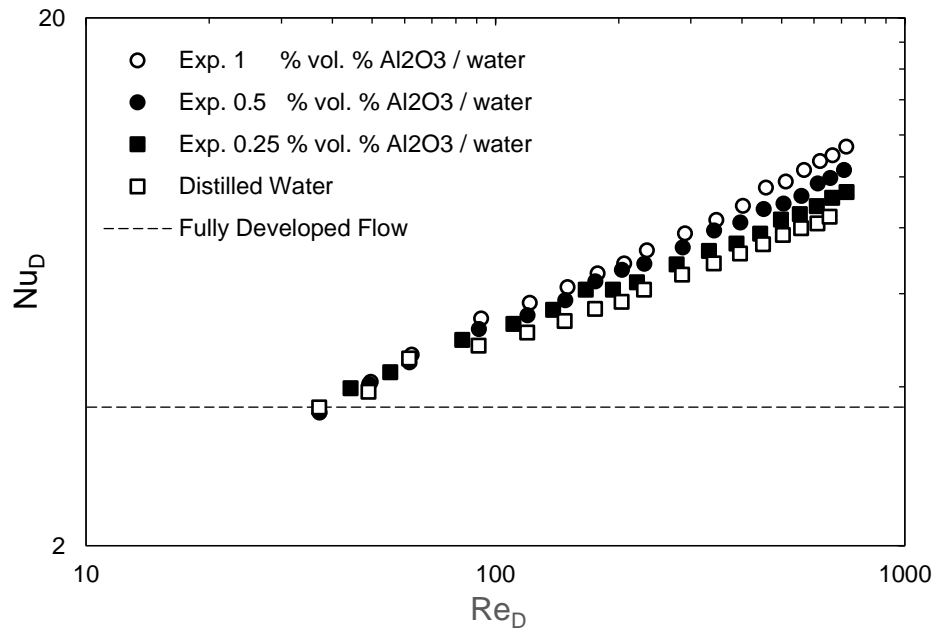


Figure 7.11 Nusselt number data of water and three nanofluid concentrations plotted versus Reynolds number

The penalty in pressure drop can be assessed by considering the friction factor versus Reynolds plot of the nanofluids used in the present study. Fig. 7.12 compares the predicted values of the friction factor. Excellent agreement with classical friction prediction is achieved. Data are reduced using volume averaged density and viscosity predicted using the Einstein viscosity model Eq. (7.12). And agree within 5 percent of the classical Fanning friction equation.

Simple performance evaluation criteria (PEC) was applied to the data in the Figs. 7.10 and 7.12 to properly account for the increased viscosity of the nanofluid. Using the following equation based on the constant pumping power criterion:

$$PEC = \frac{Nu_{nf}/Nu_{bf}}{(f_{nf}/f_{bf})^{1/3}} \quad (7.15)$$

The results of PEC analysis are summarized in Fig. 7.13 also agree with similar data reported in [42] using a similar approach. Even though greater non-dimensional heat transfer rates are obtained for higher nanofluid concentrations, the increased viscosity leads to poorer performance under the constant pumping power constraint.

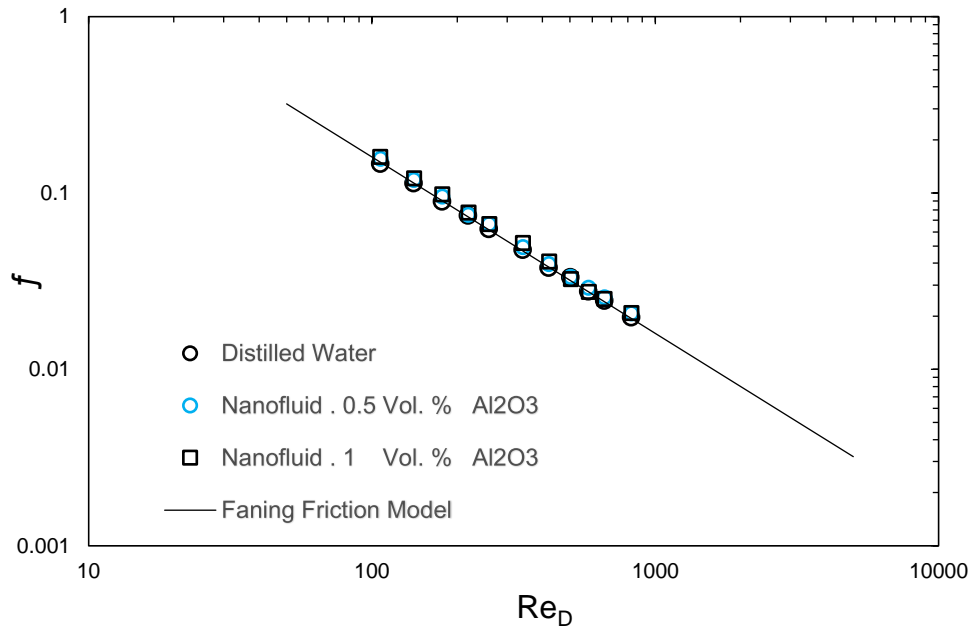


Figure 7.12 effect of nanofluid concentration on friction factor versus Reynolds number

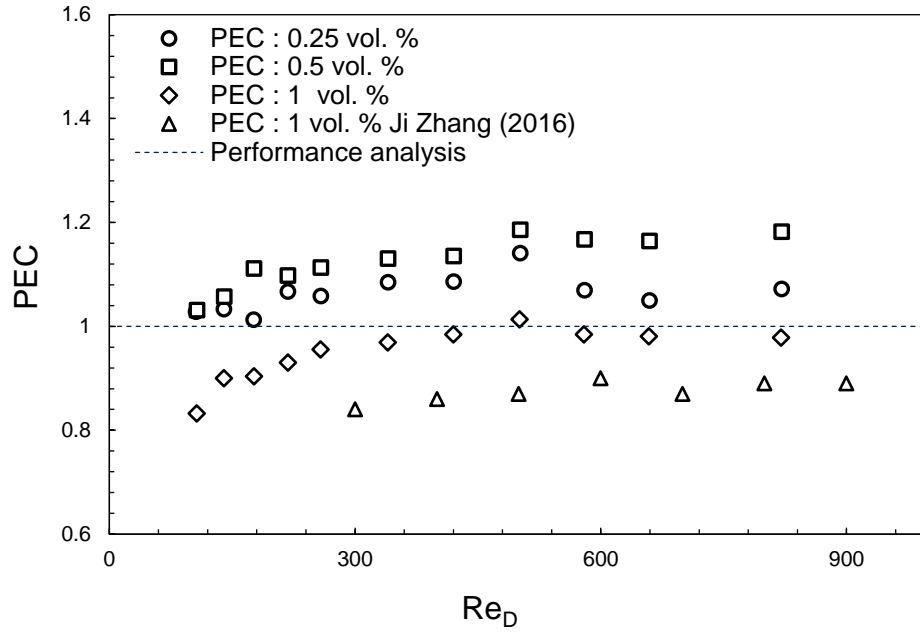


Figure 7.13 performance analysis of Aluminum oxide nanofluid of different concentrations

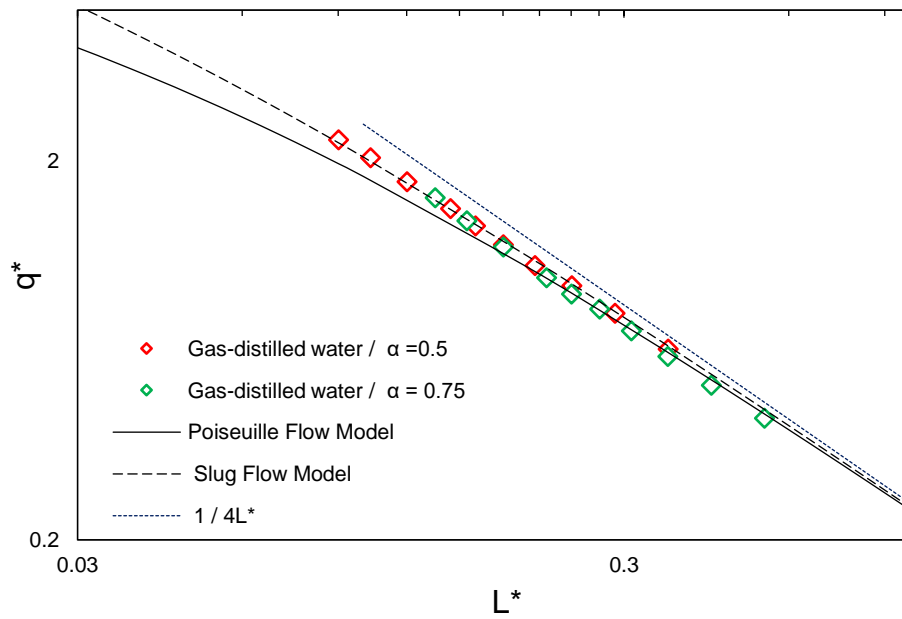


Figure 7.14 dimensionless heat flux data of gas-liquid flow with liquid fraction 0.5 and 0.75 plotted versus invers Graetz number

Taylor flow analysis considers the effect of fluid stream segmentation on the heat transfer when a nanofluid is used. Fig. 7.4 illustrates a gas-liquid cell for a Taylor flow having a liquid fraction of 50 %, i.e equal volumetric gas and liquid flow rates. In the present study we consider liquid fractions of 0.5 and 0.75. We examined the effect of segmentation using gas as a segmenting medium as can be seen in Fig. 7.14. Results were obtained for the two liquid fractions over a small range of Reynolds numbers. Data are reduced considering the liquid fraction in the surface area and the effective liquid velocity in the Reynolds number for the liquid phase only. This is in keeping with the approach outlined in Muzychka et al. [10] who showed that thermal enhancement on the Graetz plot is appropriately shown using this approach. Figs. 7.13 - 7.16 present data for a segmented flow nanofluid as compared with distilled water for the same segmentation process. It has been well established that fluid segmentation can provide significant thermal enhancement [8,10], but additional gains can be achieved when a nanofluid is used.

The result showed that the dimensionless heat transfer rate is increased above the Graetz Poiseuille and Taylor flow theory in the Figs. 13 -16. Thermal enhancement using nanofluids in a Taylor flow is quite promising. In future studies additional data are being collected for smaller L^* values corresponding to ducts with smaller $L = D$ values as well as examining the effects of liquid slug length. A comparison of the minimum and maximum ratios of both Nu and q^* as compared with water alone are shown in the Table 7.1.

The present study shows promising thermal enhancement may be obtained using both continuous and gas- liquid Taylor flows with nanofluids for thermally developing laminar flows. Heat transfer enhancement is greater in gas-liquid Taylor flows due to having a secondary mixing mechanism present in the liquid slugs.

Table 7.1 heat transfer enhancement in different flow regimes with/without nanoparticles

Flow regime	αL	$\emptyset \%$	Re_D	q^*/q^*_{bf}		Nu_D/Nu_{bf}	
				min	max	min	max
Cont. phase	1	0.25	34 -131	1.05	1.10	1.11	1.12
Cont. phase	1	0.5	33 -130	1.10	1.24	1.21	1.29
Cont. phase	1	1	32 -129	1.14	1.33	1.16	1.35
Gas-liquid	0.75	00	45-180	1.05	1.13	1.13	1.24
Gas-liquid	0.5	00	68-271	1.04	1.15	1.40	1.36
Gas-liquid	0.75	1	43 -172	1.06	1.17	1.15	1.41
Gas-liquid	0.5	1	66-264	1.08	1.2	1.23	1.65

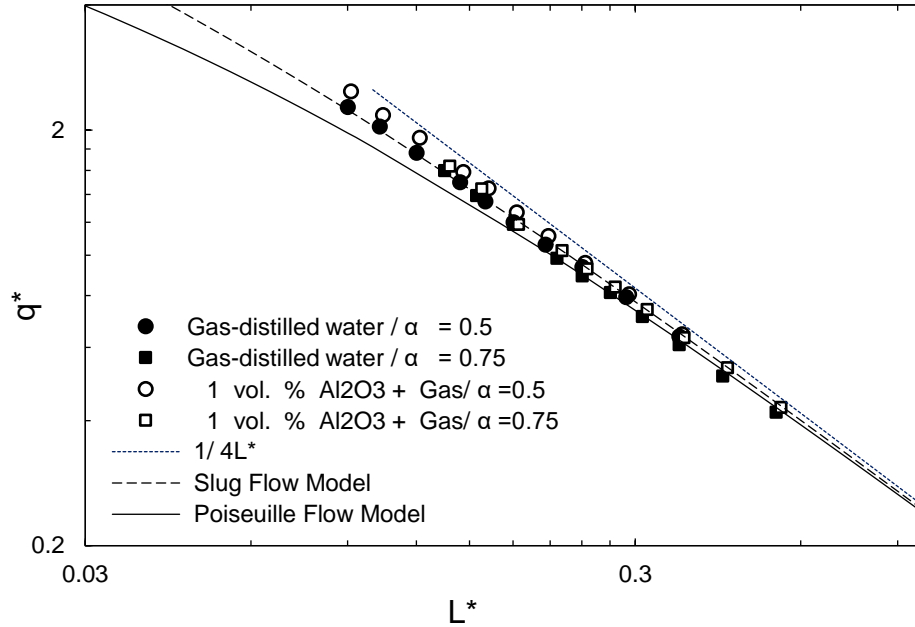


Figure 7.15 segmented nanofluid data of 1 vol. % concentration plotted versus inverse Graetz number.

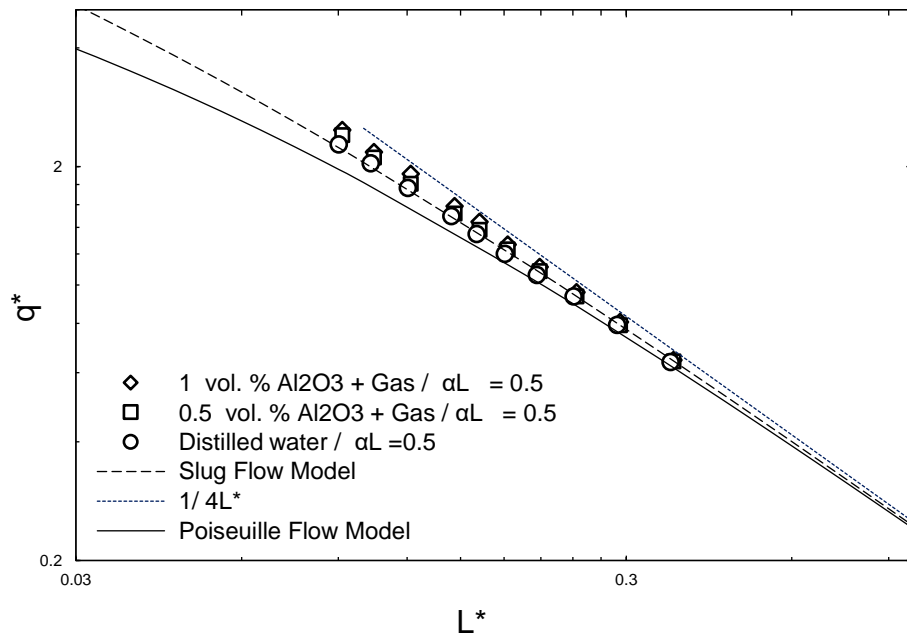


Figure 7.16 effect of the nanofluids concentration on heat transfer of Taylor / slug flows

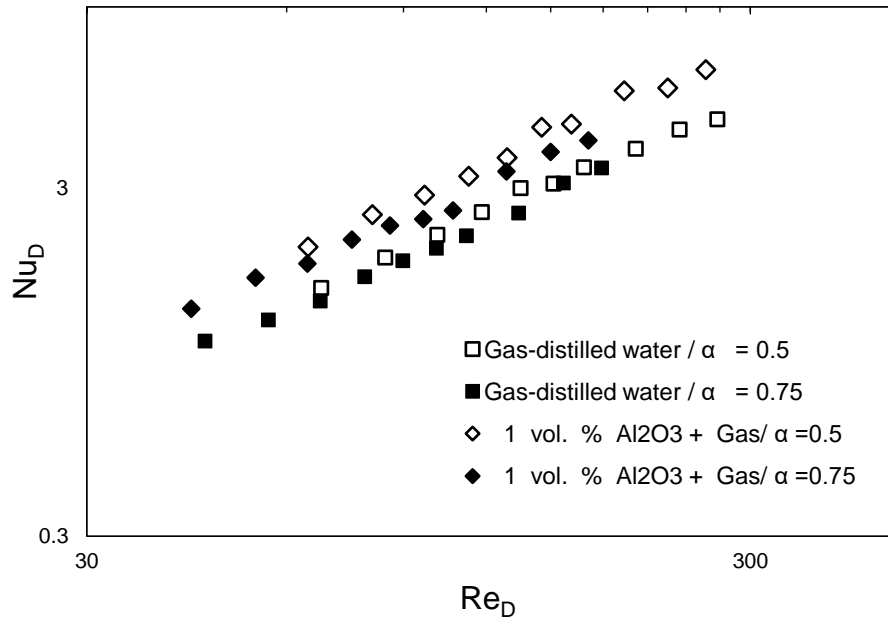


Figure 7.17 Nusselt number of dispersed gas-liquid Taylor flows with different concentrations plotted versus Reynolds number

7.7 Summary and Conclusion

This study carefully considered the flow of nanofluids in continuous and Taylor flows using nanofluids in a mini-scale tube. The flows were laminar and demonstrated significant heat transfer enhancement over their single phase (Graetz) flow reference points.

Both fully developed and thermally developing flows were considered. Results were compared with classical single phase Graetz flows and show great potential for enhancing heat transfer. However, appropriate performance enhancement criteria must be considered since merely increasing Nusselt number is not strictly an appropriate indicator.

7.8 References

- [1] Muzychka, Y.S. and Ghobadi, M., "Measurement and Analysis of Laminar Heat Transfer Coefficients in Micro and Mini-Scale Ducts and Channels", *Heat Transfer Engineering*, Vol. 37, no. 11, pp. 938-946, 2016.
- [2] Tuckerman, D.B. and Pease, R.F., "High-Performance Heat Sinking for VSLI," IEEE Electron Device Letters, Vol. EDL-2, pp. 126-129, 1981.
- [3] Fairbrother F. and Stubbs, A.E., "Studies in Electro-endosmosis. Part VI. The Bubble-tube Method of Measurement", *Journal of the Chemical Society*, Vol. 1, pp.527-529, 1935.
- [4] Taylor, G.I., "Deposition of a Viscous Fluid on the Wall of a Tube", *Journal of Fluid Mechanics*, Vol. 10 pp. 161-165, 1961.
- [5] Churchill, S. W., and Ozoe, H., "Correlations for Laminar Forced Convection in Flow Over an Isothermal Flat Plate and in Developing and Fully Developed Flow in an Isothermal Tube", *Journal of Heat Transfer*, Vol. 95, pp.416-419, 1973.
- [6] Muzychka, Y.S. and Yovanovich, M.M., "Laminar Forced Convection Heat Transfer in the Combined Entry Region of Non-Circular Ducts", *Journal of Heat Transfer*, Vol. 126, pp. 54-61, 2004.
- [7] Maddox, D.E. and Mudawar, I., "Single- and Two- Phase Convective Heat Transfer From Smooth and Enhanced Microelectronic Heat Sources in a Rectangular Channel", *Journal of Heat Transfer*, Vol. 111, pp. 1045-1052, 1989.
- [8] Betz, A.R. and Attinger, D., "Can Segmented Flow Enhance Heat Transfer in Microchannel Heat Sinks", *International Journal of Heat and Mass Transfer*, Vol. 53, pp. 3683-3691, 2010.
- [9] Asthana, A. and Zinovik, I., "Significant Nusselt Number Increase in Micro-channels with a Segmented Flow of Two Immiscible Liquids: An Experimental Study", *International Journal of Heat and Mass Transfer*, Vol. 54, pp. 1456-1464, 2011.
- [10] Muzychka, Y.S., Walsh, E., and Walsh, P., "Heat Transfer Enhancement Using Laminar Gas-Liquid Segmented Plug Flows", *Journal of Heat Transfer*, Vol. 133, pp. 041902.1-041902.9, 2011.
- [11] Janes, N., Muzychka, Y.S., Guy, B., Walsh, E., and Walsh, P., "Heat Transfer in Gas-Liquid and Liquid- Liquid Two Phase Plug Flow System", Proceedings of the 12th IEEE

- Intersociety Conference on Thermal and Thermomechanical Phenomena in Electronic Systems, pp. 1-11, 2010.
- [12] Houshmand, F. and Peles, Y., “Heat Transfer Enhancement with Liquid Gas Flow in Microchannel and the Effect of Thermal Boundary Layer”, *International Journal of Heat and Mass Transfer*, Vol. 70, pp. 725-733, 2014.
- [13] Mac Giolla Eain, M., Egan, V., and Punch, J., “Local Nusselt Number Enhancement in Liquid-Liquid Taylor Flow”, *International Journal of Heat and Mass Transfer*, Vol. 80, pp. 85-97, 2015.
- [14] Adrugi, W., Muzychka, Y.S., and Pope, K., “Heat Transfer in Liquid-Liquid Taylor Flow in Mini-scale Curved Tubing for Constant Wall Temperature”, ASME-IMECE-2015-67700, 2016.
- [15] Walsh E., Muzychka, Y.S., Walsh, P., Egan, V., and Punch, J., “Pressure Drop in Two Phase Slug/Bubble Flows in Miniscale Capillaries”, *International Journal of Multiphase Flow*, Vol. 35, pp. 879-884, 2009. [16] Heravi, P. and Torabi, F., “A Mathematical Model for Pressure Drop of Two Phase Dry Plug Flow in Circular Mini/Micro Channels”, *International Journal of Multi-phase Flow*, Vol. 87, pp. 9-15, 2016.
- [16] Adrugi, W., Muzychka, Y.S., and Pope, K., “Pressure Drop of Liquid-Liquid Taylor Flow in Mini-scale Tubing”, ASME-IMECE-2015-67736, 2016.
- [17] Karimzadehkhoei, M. and Yalcin, S., “Pressure Drop and Heat Transfer Characteristics of Nanofluids in Horizontal Microtubes Under Thermally Developing Flow Conditions”, *Experimental Thermal and Fluid Science*, Vol. 67, pp. 37-47, 2015.
- [18] Kong, L., Sun, J., and Bao, Y., “Preparation Characterization and Tribological Mechanism of Nanofluids”, RSC Advances, Vol. 7, pp. 12599 - 12609, 2017.
- [19] Xing, M., “Experimental Study on the Thermal Conductivity Enhancement of Water Based Nanofluids Using Different Types of Carbon Nanotubes”, *International Journal of Heat and Mass Transfer*, Vol. 88, pp. 609-616, 2015.
- [20] Hamilton, R.L. and Crosser, O.K., “Thermal Conductivity of Heterogeneous Two Component System”, *Ind. Eng. Chem. Fundamental*, Vol. 1, No. 3, pp. 187-191, 1962.

- [21] Batchelor, G.K. and O'Brien, R.W., "Thermal or Electrical Conduction Through a Granular Material", Proceedings of the Royal Society of London. Series A, Mathematical and Physical Sciences, Vol. 355, No. 1682, pp. 313-333, 1977.
- [22] Awad, M. and Muzychka, Y.S., "Effective Property Models for Homogeneous Two Phase Flows", Experimental Thermal and Fluid Science, Vol. X, pp. 106-113, 2008.
- [23] Choi, S. U. S. and Eastman, J.A., "Enhancing Thermal Conductivity of Fluids with Nanoparticles", ASME, International Mechanical Engineering Congress and Exposition, San Francisco, CA, 1995.
- [24] Seok, P. J. and Choi, S.U.S., "Effects of Various Parameters on Nanofluid Thermal Conductivity", *Journal of Heat Transfer*, Vol. 129, pp. 617 - 623, 2007.
- [25] Manaya, E. and Sahin, B., "Heat Transfer and Pressure Drop of Nanofluids in a Microchannel Heat Sink", *Heat Transfer Engineering*, Vol. 38, No. 5, pp. 510- 522, 2017.
- [26] Estell, P. and Halelfadl, S., "Thermal Conductivity of CNT Water Based Nanofluid: Experimental Trend and Models Overview", *Journal of Thermal Engineering*, Yildiz Technical University Press, Istanbul, Turkey, Vol. 1, No. 2, pp. 381-390, 2015.
- [27] Hossein S., Mohammad G., "Performance Analysis of Using Nanofluids in Microchannel Heat Sink in different Flow Regimes and its Simulation Using Artificial Neural Network", Proceedings of the World Congress on Engineering, Vol. III, pp. 978-988, 2008.
- [28] Sivakumar, A. Alagumurthi, N., and Senthilvelan, T." Experimental Investigation of Forced Convective Heat Transfer Performance in Nanofluids of Al₂O₃/Water and CuO/Water in a Serpentine Shaped Microchannel Heat Sink", *Heat Mass Transfer*, Vol. 52, pp. 1265-1274, DOI 10.1007/s00231-015-1649-5, 2016.
- [29] Anbumeenakshi, T., "On the Effectiveness of a Nanofluid Cooled Microchannel Heat Sink Under Non-Uniform Heating Condition", *Applied Thermal Engineering*, Vol. 113, pp. 1437-1443, 2017.
- [31] Sukarno, D. H., "Challenges for Nanofluid Applications in Heat Transfer Technology", IOP Conference Series: *Journal of Physics*, Vol. 795, No. 1, article id. 012020, 2017.

- [32] Sahin, B., Manay, E., and Akyurek, E.F., "An Experimental Study on Heat Transfer and Pressure Drop of CuO-Water Nanofluid", *Journal of Nanomaterials*, Vol. X, Article ID 790839, 10 pages, 2015.
- [33] Mahbubul, I.M. and Chong, T.H., "Effective Ul-trasonication Process for Better Colloidal Dispersion of Nanofluid Ultrasonics", *Sonochemistry*, Vol. 26 , pp. 361-369, 2013.
- [34] Leong, K. Y. and Hana_, N.M., "Thermal Effect of Surfactant on Stability and Thermal Conductivity of Carbon Nanotube Based Nanofluids", *Thermal Science*, Vol. 20, No. 2, pp. 429-441, 2016.
- [35] Subramaniyan, A.L and Kumar, A., "Preparation and Stability Characterization of Copper Oxide Nanofluid by Two Step Method", *Material Science Forum*, Vol. 832, pp. 139-143, Trans Tech Publications, Switzerland, 2015.
- [36] Muzychka, Y.S., "Generalized Models for Laminar Developing Flows in Heat Sinks and Heat Exchangers", *Heat Transfer Engineering*, Vol. 34 (2-3), pp. 178-191, 2013.
- [37] Muzychka, Y.S., Walsh, E., and Walsh, P., "Simple Models for Laminar Thermally Developing Slug Flow in Noncircular Ducts and Channels", *Journal of Heat Transfer*, Vol. 132 / 111702-1, 2010.
- [38] Kline, S. J., and McClintock, F. A., "Describing Uncertainties in Single-Sample Experiments", *Mechanical Engineering*, Vol. 75, No. 1, pp. 3-8, 1953.
- [39] Holman, J.P., *Experimental Methods for Engineers*, 4th Edition, McGraw-Hill, New York, NY 10020, 1989.
- [40] Williams, W., Buongiorno, J., and Hu, L. W., "Experimental Investigation of Turbulent Convective Heat Transfer and Pressure Loss of Alumina/ Water and Zirconia/Water Nanoparticle Colloids in Horizontal Tubes," *Journal of Heat Transfer*, Vol. 130, pp. 042412, 2008.
- [41] W. Yu, and S. U. S. Choi, "The Role of Interfacial Layers in the Enhanced Thermal Conductivity of Nanofluids: A Renovated Maxwell Model", *Journal of Nanoparticle Research*, Vol. 5, no. 1, pp. 167-171, 2003.
- [42] Zhang, J., Diao, Y., and Zhao, Y., "Thermal- Hydraulic Performance of SiC-Water and Al₂O₃-Water Nanofluids in the Mini channel", *Journal of Heat Transfer*, Vol. 138, pp. 021705-1, 2016.

CHAPTER 8

CONCLUSION AND RECOMENDATIONS

To improve the value of scientific research based on reliable findings, this chapter will provide summarized conclusions and address significant recommendations and guidelines for future studies in the field of the present study.

8.1 Summary and Conclusions

The dissertation mainly focused on heat transfer enhancement in mini scale channels subjected to constant wall temperature. Several parameters were employed over five chapters: flow segmentation, tube geometries, and the inclusion of nanoparticles to conventional fluids. Chapter three was devoted to investigating the heat transfer of gas-liquid Taylor flow in straight tubes. The results showed the significant effect of liquid slug length on heat transfer. A unique analysis was employed which considers the actual flow velocity and only the wetted tube area [1]. The results in the fully developed region were compared with a model that was developed by Muzychka [1]. The study concluded that the thermal saturation can be reached more quickly with decreasing liquid slug lengths. Chapter four addresses a new method of analysis which consider separated analysis of liquid-liquid Taylor flow for various liquid fractions. The analysis treats both flow components as two separate flows of gas-liquid Taylor flow. Hence, the benefits of the actual flow velocity and wetted tube area are considered. The conclusions highlighted effects of liquid slug

length on heat transfer enhancement over single phase flow. Considerable publications have employed the homogenous liquid-liquid Taylor flow to demonstrate the effect of the liquid slug lengths [1,2]. In chapter five and six another parameter was added to promote heat transfer enhancement of liquid-liquid or gas-liquid Taylor flows in mini scale tube. The effect of curved tube geometries was investigated using various tube curvatures. A quantitative analysis revealed that heat transfer enhancement reached 50 % over a single phase flow for the same tube geometries. Experimental correlations were developed with good accuracy to predict heat transfer in Taylor flow in mini scale curved tubes when isothermal boundary conditions are applied. Finally, chapter seven investigated the inclusion of nanoparticles in conventional liquids to improve their thermal properties. Through out the study different experimental measurements were performed which included: measuring thermal conductivity of conventional and nanofluids and nanoparticle size and distributions using scanning electron microscopy (SEM) which was available in the laboratory facilities of Memorial University. An increase in heat transfer was observed when dispersing nanoparticles of Aluminum Oxide to distilled water which added a promising potential of thermal enhancement in mini scale channels.

8.2 Recommendation for Future Studies

Heat transfer of Taylor gas-liquid or liquid Taylor flows in mini / micro scale channels has received intensive investigation including flow segmentation techniques in various channel geometries. However, there are several aspects which affect heat transfer that require additional theoretical and experimental studies. Based on the present results, there are still many open questions and discussions on heat transfer in two phase slug flows in small scale geometries. The following are the most important questions which can be considered and addressed in future studies.

8.2.1 Particle Motion in Taylor Flow

Perform experimental and CFD analysis to understand the hydrodynamic nature of the fluid particle in the segmented flows in straight and curved channels. Micro-PIV observation is also required to determine Taylor flow field changes in the interfacial region for different flow segmentation and channel geometries. This type of analysis will help understand heat transfer enhancement in Taylor flows in mini / micro scale channels.

8.2.2 Micro Scale Geometries

The proposed models in the present study regarding mini scale channels can be employed to predict heat transfer in microscale channels. These models will provide an evaluation for heat transfer rates within micro electronics which requires minimum size and high performance. Perform additional investigation on Taylor flows in mini and micro channels using different channel cross sections and different boundary conditions.

8.2.3 Fluid Engineering

One of the passive techniques to enhance heat transfer is the inclusion of several additives which improve the thermal properties of the liquids. Considerable studies have examined the effect of these materials on heat transfer. Micro encapsulated phase change material and nanoparticles are common examples of these additives [3,4]. In Taylor flow this technique still needs more study , although a few studies reported promising results of heat transfer enhancement [5]. Effect of these additives on hydrodynamics of Taylor flows needs to be investigated.

8.2.4 Film Thickness

The inner surface of a channel is surrounded by a liquid layer / film as the result of the no slip conditions of the viscous flows. The influence of the liquid layer on heat transfer becomes important for high viscosity fluids [6,7]. The liquid film around slugs isolates liquid slugs from contact with the wall of heat transfer. Predicting liquid film thickness and the associated impact on heat transfer is necessary for accurate modeling and prediction.

8.3 References

- [1] Muzychka, Y.S., “Laminar Heat Transfer for Gas-Liquid Segmented Flows in Circular and Non-circular Ducts with Constant Wall Temperature” ASME, 2014.
- [2] Patrick A. Walsh a, Edmond J. Walsh , Yuri S. Muzychka,” Heat transfer model for gas–liquid slug flows under constant flux”, *International Journal of Heat and Mass Transfer*, 53 (2010) 3193–3201.
- [3] C.J. Ho, L.C. Wei, Z.W. Li,” An Experimental Investigation of Forced Convective Cooling Performance of a Microchannel Heat Sink with Al₂O₃/water Nanofluid”, *Applied Thermal Engineering*, 30 (2010) 96–103
- [4] P. K. Singh,P. V. Harikrishna, “Experimental and Numerical Investigation into The Heat Transfer Study of Nanofluids in Microchannel”, *Journal of Heat Transfer*. Dec 2011, 133(12): 121701.
- [5] Howard A. and Walsh P. A., “Heat Transfer Characteristics of Liquid-Gas Taylor Flows incorporating Microencapsulated Phase Change Materials”, *Journal of Physics: Conference Series* 525 (2014) 012022.
- [6] Zhang, J., Fletcher, D. F., and Li, W., 2016, “Heat Transfer and Pressure Drop Characteristics of Gas-Liquid Taylor Flow in Mini Ducts of Square and Rectangular Cross-Sections”, *International Journal of Heat Mass Transfer*, 103, pp. 45–56.
- [7] Jovanović, J., Zhou, W., Rebrov, E. V., Nijhuis, T. A., Hessel, V., and Schouten, J. C., 2011, “Liquid-Liquid Slug Flow: Hydrodynamics and Pressure Drop”, *Chemical Engineering Society.*, 66(1), pp. 42–54.